RHEOLOGICAL CHARACTERISATION OF LOW-RANK COAL ASH AT HIGH TEMPERATURES

A Thesis Submitted for the Degree of Doctor of Philosophy

By

Narongsak Tonmukayakul (M.Eng)

June 30th, 2004

School of Chemical Engineering
The University of Adelaide
Australia

DECLARATION

This thesis contains no material that has been accepted for the award of any other degree or diploma in any university or other tertiary institution and, to the best of my knowledge and believe, contains no material previously published or written by another person expect when due to reference has been made in the text.

I give consent of this copy of my thesis, when deposited in the University Library, to be available for loan and photocopying

Narongsak Tonmukayakul
Worcester, MA
June 30th, 2004

ACKNOWLEDGEMENTS

In the past five years, my Ph.D. candidature was very much up and down. During these times, I have received the help, support and friendships of so many people and I would like to take this opportunity to express my sincere gratitude to them.

First and foremost is my supervisor, Associate Professor Quoc Dzuy Nguyen, who gave me a splendid start into the subject of rheology, from whom I have learned much about rheology and many aspects of life. It was my great pleasure to work with him. Over the years, he has displayed a great deal of patience and tolerance for my behaviour. I am deeply indebted for his patient guidance, confidence and encouragement throughout the entire project. **Dzuy-Thank you!**

I am thankful for the financial and other support received for this research from the Cooperative Research Centre for Clean Power from Lignite, which is established and supported under the Australian Government's Cooperative Research Centres Program (CRC). Without CRC scholarship, I would not able to pay my tuition fee charged by The University of Adelaide and to survive during my Ph.D. candidature. Assistance from Drs. David Brockway, Peter Jackson and Mr. Howard Mitchell are gratefully acknowledged.

I would also like to acknowledge the academic and staff of the School of Chemical Engineering, The University of Adelaide, for their assistance and friendship- particularly Brian Mulcahy, Jason Peak and Peter Kay for their friendship and expert advice. They made my time in Adelaide unforgettable. I wish to thank Mrs. Mary Barrow, Elaine Minerds, Lynette Kelly and Terri Whitworth for their help and support.

Thanks are also extended to Tim Akroyd for his friendship, proof reading this thesis and his comic relief in the last four years; and Michael Brauer for helping with proof reading. Ben Daughtry, thank you for your expert advice on statistic and analyses.

My very special thanks to my better other half, Charm, for her encouragement, companionship and constant love. Over the years, we shared the emotions, hardships and the happiness of my progress.

I am deeply indebted my parents for all the support they have given me throughout my life; without their sacrifices and devotion, I could never have achieved so much. Mum

and Dad thank you for help me buying this degree. ***To my parents, I sincerely dedicate this degree.***

"Go confidently in the direction of your dreams! Live the life you've imagined"

Henry David Thoreau
1817-1862, American Writer

SUMMARY

Ash deposition is a problem in power generation when coal with high ash and alkali contents are utilised. The problem is more severe in fluidised bed combustion where the ash deposition can causes agglomeration of the bed material, and may lead to defluidisation of the unit. The successful operation of fluid bed combustion with coal high in ash and alkali content will depend on the ability to control ash deposition. The rheological properties of coal ash under furnace conditions are important in controlling the stickiness and mobility of the molten ash deposition. Therefore, a good knowledge of the rheological properties of coal ash will improve the understanding of the mechanisms associated with ash deposition, and may assist in controlling the deposition and agglomeration of fluid bed material.

At present, a good deal of information about coal ash rheology under conditions similar to those found in fluidised bed combustion is not known, and greater understanding is required. This is primarily due to a lack of reliable instruments and measurement techniques. In this work, a new high temperature rheometer has been developed based on the principle concepts of viscometric flow. The developed rheometer allows fundamental rheological properties, such as shear stress and shear rate, to be obtained without relying on calibrations with materials of known properties. With this instrument the flow characteristics of the tested samples can be determined directly without assuming a particular fluid model. The new rheometer has the capability to measure the rheological properties of materials at temperatures ranging from 500°C to 1300°C and under different processing conditions.

Rheological characteristics and properties of a range of low rank Australian coal ashes have been carried out using the newly developed high temperature rheometer, equipped with a cone and plate measuring geometry. It has been found that coal ash samples exhibit thixotropic and viscoplastic flow behaviours. SEM and XRD analyses have revealed that during high temperature rheological measurements the coal ash sample is basically a suspension of colloidal mineral solids in a molten eutectic liquid. The solid phase is mainly silica (SiO_2), and the liquid phase is a mixture of alkali sulphates mainly $CaSO_4$, $MgSO_4$ and Na_2SO_4 compounds. The equilibrium viscometric data of coal ash samples is found to be satisfactorily described using the Herschel-Bulkley model. The equilibrium rheological properties are strongly affected by the concentration levels of $CaSO_4$, $MgSO_4$ and Na_2SO_4. The operating temperature and chemical composition of the

surrounding gas phase were also found to affect the rheological properties of the coal ash samples.

In order to obtain a better understanding and to model the rheological properties of the coal ashes, a series of synthetic ash mixtures were examined. The synthetic mixtures contained the key chemical components that represent the solid and the liquid phases. The solid phase is represented by silica (SiO_2), while a mixture of $CaSO_4$, $MgSO_4$ and Na_2SO_4 compounds represented the liquid phase. In this work, the rheological characteristics of mixtures of synthetic ash were investigated using a factorial experimental design. Using the synthetic ash mixtures together with the statistical design experiment, the effect of key chemical compounds on the rheological properties could be systematically investigated. The rheological results showed that the synthetic mixtures exhibited thixotropic and viscoplastic behaviours. It was also found that mixtures predominantly high in $CaSO_4$, and $MgSO_4$ had a high degree of thixotropy behaviour, while those mixtures predominantly high in Na_2SO_4 showed a lower degree of thixotropy behaviour. The statistical analysis also showed that Na_2SO_4 is the most significant chemical compound causes a high yield stress and high viscosity. In contrast, $CaSO_4$ and $MgSO_4$ were found to decrease the value of the yield stress and the viscosity. The rheological behaviour of the synthetic ash mixtures can be used to describe rheological behaviour of the coal ash samples.

Relationships between the equilibrium flow properties and chemical compounds, and temperatures are developed using a linear regression method. The statistical analysis has shown that $CaSO_4$, $MgSO_4$ and Na_2SO_4, and their interactions are all significant compounds that have effects on the yield stress and viscosity of the synthetic mixtures. It was also found that the yield stress and viscosity decreased with increasing concentration level of either $CaSO_4$ or $MgSO_4$. Yield stress and viscosity are increased with increases in the concentration of Na_2SO_4. The statistical models can successfully predict rheological properties of ash with high concentrations of $CaSO_4$, $MgSO_4$ and Na_2SO_4, but it fails to predict the rheological properties of ashes that also high in concentrations of either Fe_2O_3 or Al_2O_3, or a combination of both.

The relationship between ash rheology and fluidised bed agglomeration has been established. The yield stress of a coal ash may be used to describe the tendency of the molten ash to deposit on surface of the fluid bed particles. Yield stress also determines the tendency of stickiness of the molten ash deposit to adhere the fluid bed particles during fluidised bed combustion process. The viscosity of the molten ash describes the

ability of the molten ash layer to adhere the fluid bed particles after a collision. High viscosity ash tend to hold the colliding particles together longer than a low viscosity ash. Shear thinning behaviour of the ash samples (decreasing viscosity with increasing shear rate) suggests that the operating conditions could be arranged so as to minimise the chance of agglomeration. For example, in order to avoid agglomeration a high viscosity coal ash would benefit from operating the fluidised bed combustion at a high velocity, this is because a high velocity means a higher shear rate and this causes a reduction in the viscosity of the molten ash. Thus, particles agglomerated by a low viscosity ash would be easily broken by the hydrodynamic forces present during the fluidised bed process. Finally, information about ash rheology has formed a basic knowledge for estimating tendency of fluid bed agglomeration when coal obtained from different source is being used.

PUBLICATIONS

1. **N. Tonmukayakul** and Q.D. Nguyen., "A high temperature viscometer unit designed for direct rheological measurement of low rank Australian coal ash", *Fuel* (2001), 81(4) 397-404.

2. **N. Tonmukayakul** and Q.D. Nguyen., "Flow properties of low rank coal ashes at high temperature" IVth International Congress on Rheology, Soul, Korea, 2004.

3. **N. Tonmukayakul** and Q.D. Nguyen., "Flow Characteristic of Molten Alkali Sulphate Mixture Includes Silicate at High Temperature" *18th Annual Pittsburgh Coal conference*, Newcastle, December, Australia, 2001.

4. **N. Tonmukayakul** and Q.D. Nguyen., "Modelling the rheology of coal ash at high temperatures", *Proc 6th World Congress Chemical Engineering*, Melbourne, September 2001.

5. **N. Tonmukayakul** and Q.D. Nguyen., "Rheological Study of Alkali Sulphate Eutectic Mixtures as Related to Agglomeration problems", *Proc. CHEMECA' 2000*, Perth, July 2000.

6. **N. Tonmukayakul** and Q.D. Nguyen., "Rheological Characterisation of Coal Ash at High Temperatures", *Proc. XIII Int. Congr. Rheology*, Cambridge, August 2000. Vol. 2, p.401-403.

7. **N. Tonmukayakul** and Q.D. Nguyen., "Rheological Characterisation of Coal Ash at High Temperatures", *Proc. CHEMECA' 99*, Newcastle, September 1999. p. 59.

TABLE OF CONTENTS

CHAPTER THREE: EXPERIMENTAL EQUIPMENT AND TECHNIQUES

CHAPTER FOUR: RHEOLOGICAL PROPERTIES OF AUSTRALIAN LOW-RANK COAL ASH

CHAPTER FIVE: RHEOLOGICAL STUDY OF SYNTHETIC ASH MIXTURES

CHAPTER SIX: MODELLING THE RHEOLOGICAL BEHAVIOUR OF LOW-RANK COAL ASH

LIST OF FIGURES

LIST OF TABLES

NOMENCLATURE

Symbol	Quantity	Units
A	Pre-exponent ional parameter in Arrhenius equation	
Ea	The activation energy in Arrhenius equation	
R	The gas constant	
μ	Newtonian viscosity	Pa.s
K	Consistency index	$Pa.s^n$
n	Flow behaviour index	
τ_y^B	The Bingham yield stress	Pa
μ_B	Bingham viscosity	Pa.s
τ_y^{H-B}	The Herschel & Bulkley yield stress	Pa.s
η_c	Casson viscosity	Pa.s
τ_c	Casson yield stress	Pa.s
T	Torque on the cone	N.m
R	The cone radius	mm
Ω	The angular velocity of the rotating cone	Rad/s
θ	The cone angle	^{o}
ψ	A dimensionless unit of thixotropic material	
t	Shearing time	min
k	The rate of structure breakdown	s^{-1}
m	An arbitrary order of the irreversible reaction	

Symbol	Quantity	Units
η_0	The initial viscosity (or structured state)	Pa.s
η_α	The equilibrium viscosity	Pa.s
$\dot{\gamma}$	Shear rate	s^{-1}
SS	Sum of square	
df	Degree of freedom	
MS	Mean square	
β_i	The regression coefficient for the yield stress	
α_i	The regression coefficient for the consistency index	
χ_i	The regression coefficients for the flow behaviour index	
x_A	The code factor representing relative concentration of $CaSO_4$	
x_B	The code factor representing relative concentration of $MgSO_4$	
x_C	The code factors representing relative concentrations of Na_2SO_4	
R	The radius of contact area in equation 7.1	
v_s	Separation velocity in equation 7.1	
h_o	A minimum separation distance in equation 7.1	

CHAPTER ONE

Introduction

1.1 BACKGROUND

Australia has vast deposits (more than 500,000 million tones) of low-rank coal (brown, lignite and sub-bituminous coals), primarily in Victoria and South Australia (Durie, 1991). These low-rank Australian coals make up about one third of the total energy reserves in Victoria and South Australia (Durie, 1991; Brockway, 2001). Low-rank Australian coals are typically present in thick seams with less overburden than bituminous coals. This means that Australian low-rank coals are easily excavated by using a low cost strip mining method.

At present, especially in Victoria, the low-rank coals are mainly used by power generation industries. The use of low-rank coals for power generation in South Australia has not yet been fully explored, but there is the possibility of using South Australian coal reserves in the near future (Linder, 1988; Manzoori, 1990; Brockway, 2000). Based on the impressive amount of coal and the low recovery costs of low-rank coal deposits, Victoria and South Australia have a great potential to provide low cost energy for the needs of the states in the future.

Currently, the technology used for utilising low-rank coals in power generation industries is the pulverised coal fired boiler (p.f.) technology. This technology involves injecting brown coal particles through a high velocity air steam into a preheated chamber where it ignites. The igniting coal particles release heat energy, which is captured by a series of tubes located at the top section of the p.f. unit. Water inside the tubes is converted to steam, which is then used to drive a steam turbine for generating electricity (Patterson, 1990).

It has been reported that the existing technology suffers adversely from coal ash deposition problems at temperatures above 1000°C (Linder, 1984; Rassk, 1985; Durie, 1991; Brockway, 1991; Wall, 1992; Couch, 1994; Benson, 1998). These problems are

known as fouling and slagging. Fouling is the deposition of coal ash particles on the water tubes, while slagging is deposition on the wall of the boiler (Couch, 1994). It is known that fouling and slagging reduce total efficiency of the heat transfer surface, and in some cases fouling and slagging may cause unscheduled process shut down (Banks, 1984; Linder, 1988; Manzoori, 1990; Brockway, 2000).

It has been reported that a brown coal boiler generates higher levels of greenhouse gas species (CO/CO_2), as well as other toxic gas species (NO_x and SO_x), than that from a typical black coal boiler for the same electricity unit generated. This indicates that currently the brown coal industry is more harmful to the environment (Linder, 1988; Zang, 1990; Benson, 1998; Brockway; 2001). Thus, problems associated with coal ash deposition and the global climate concern have created pressure on the brown coal industries to develop alternative technologies that are more efficient and lower in green house gas emissions for utilising Australian brown coals for power generation.

Fluidised bed technologies have long been considered as a possible substitute technology for utilising brown coals in power generation. This is because they usually operate at relatively low temperatures, ca 800-1200°C, compared to that in the existing technology. This means fluidised bed technologies have the potential to reduce the level of NO_x emissions. Moreover, fluidised bed technologies can be designed using additives to capture sulphur (SO_x) from the flue gas before it escapes into the atmosphere (Siegell, 1976; Manzoori, 1990; Patterson, 1991). As the operating temperature of the fluidised bed technologies is relatively lower, the fouling and slagging problems that are found in the pulverised coal fired boiler may also be minimised.

Generally, fluidised bed technology involves floating coal particles in a high velocity gas in a heated chamber. In this chamber, the coal particles are ignited and heat energy is released which is captured by a series of tubes located on the top section of the heated chamber (Manzoori, 1990; Patterson, 1991; Benson, 1998). Water inside the tubes is converted to steam that is then used to drive a steam turbine and generate electricity. The fluidised bed technology is classified into two categories based on the operating atmosphere of the unit (Siegell, 1976; Manzoori, 1990; Patterson, 1991). They are fluidised bed combustion (FBC) and fluidised bed gasification (FBG). The operating atmosphere in the FBC unit is an oxidising atmosphere, while the operating atmosphere in the FBG unit is a reducing atmosphere.

Although the fluidised bed technologies have the potential to minimise the problems of fouling and slagging, the technologies are not fully immune from problems of coal ash deposition. It has been found that coal ash deposition still occurs at temperatures below 1000°C (Goldberger; 1967; William, 1984; Linder, 1988; Skrifvas, 1992; Manzoori, 1992). Recent studies on deposition of low-rank coal ash in fluidised bed combustion units (Goldberger, 1967; William et al, 1984; Linder, 1988; Skrifvas et al, 1992; Manzoori, 1992; Skrifvas et al, 1994; Benson; 1998) have revealed that the deposition of molten ash is the result of the transfer of the molten ash from the burning char particles onto the surface of bed material upon collision between char and bed particles. Furthermore, it is suggested that collisions among the bed particles, coated with a sticky layer of molten ash, also can lead to agglomeration of the fluid bed particles. Consequently, large agglomerates of the fluid bed particles may lead to defluidisation of the fluidised bed unit and in some cases may cause an unscheduled plant shut down (Goldberger, 1967; William et al, 1984; Linder, 1988; Skrifvas et al, 1992; Manzoori, 1992; Skrifvas et al, 1994; Benson; 1998).

Deposition of coal ash in fluidised bed gasification has been found to be different from the deposition of coal ash in a combustion system. Recent studies (Langston et al, 1960; Mason et al, 1980; Falcone et al, 1989; Jung et al, 1992; Benson, 1998) have found that deposition of molten ash occurs on the surface of char particles instead of on the surface of the fluid bed particles. This suggests that in the fluidised bed gasification system, agglomeration of the char particles, rather than the agglomeration of fluid bed particles occurs. However, no definite answer has yet been given in literature as to why deposition of molten ash occurs on the surface of char particles instead of on the fluid bed particles. A good understanding of ash deposition and particle agglomeration under furnace conditions is thus essential to enable stable long-term operation of fluidised bed technologies to be implemented for low-rank coals.

Successful operation of fluidised bed systems for utilising low-rank coals will depend on the ability to control ash deposition on fluid bed materials, which may cause agglomeration and defluidisation of the bed. An understanding of the specific mechanisms involved in agglomeration and defluidisation requires a good knowledge of the intrinsic physical properties of the molten coal ash as a function of the operating conditions, coal type, and chemical and mineral composition of the ash deposit. The rheological properties of coal ash formed under furnace conditions are important in controlling the stickiness and mobility of the molten ash depositing onto bed and char particles. A greater knowledge of rheological properties will lead to improve the

understanding about mechanisms involved in coal ash depositions and agglomeration in FBC and FBG, and will greatly assist in the commercialisation of these technologies.

1.2 AIMS OF THE RESEARCH

The main objective of the present project is to study the rheological characteristics of low-rank coal ashes under conditions relevant to the fluidised bed combustion process. The development of experimental equipment and experimental methods for measuring the rheological properties of low-rank Australian coal ashes is also required. Another objective is to establish a relationship between ash rheology and agglomeration. An outline of the research objectives is listed below:

1. To develop a rheometer for measuring the rheological properties of low-rank coal ashes under the furnace conditions of fluidised bed combustion and gasification.
2. To study the rheological characteristics and measure the rheological properties of low-rank coal ashes under operating conditions relevant to fluidised bed combustion systems.
3. To develop a rheological model as a function of key chemical compositions and process variables for predicting the rheological properties of coal ash.
4. To explain specific mechanisms involved in coal ash deposition and agglomeration using ash rheology.

1.3 OUTLINE OF THE THESIS

According to research activities conducted, this thesis contains eight chapters as listed below: **Chapter Two** will present a literature review on the current understanding of coal ash deposition and agglomeration in FBC and FBG, instruments and techniques recently developed for rheological measurements of coal ash at high temperatures and current knowledge of the rheology of coal ash at high temperatures. Details of the high temperature rheometer developed in this work are given in **Chapter Three**.

Chapter Four presents the experimental results of coal ash samples tested at temperatures ranging from 850°C to 1200°C. In this chapter, the rheological characteristics and properties of the coal ashes are presented. Effects of operating temperature, chemical composition and operating atmosphere on the rheological properties of coal ashes are investigated. **Chapter Five** presents a rheological study of synthetic mixtures, which are used as a model for coal ash samples. In this chapter, effects of chemical compositions on rheological characteristics and properties of the synthetic

mixtures are also investigated. **Chapter Six** presents details of the development of a statistical model to express the relationship between rheological properties, chemical composition and temperature. Predictions of the flow properties of actual coal ash samples using the statistical model developed are also included.

The relevance of ash rheology and synthetic mixture rheology to coal ash agglomeration are developed and presented in **Chapter Seven**. **Chapter Eight** presents conclusions of the key findings in this study and recommendations for further work.

CHAPTER TWO

Literature Review

2.1 INTRODUCTION

The body of this chapter has been divided into four sections, they are:

1. Ash deposition and agglomeration in fluidised bed combustion and gasification.
2. Concepts of rheology.
3. Review of equipment previously used for rheological measurements of coal ash at high temperatures.
4. Factors affecting ash rheology.

2.2 COAL ASH DEPOSITION

Coal is a complex mixture of organic and inorganic species. Inorganic species in coal exist in two-forms; one as organically bound inorganic elements (eg, Na, Ca, Mg) and the other as discrete mineral elements (eg, clay, quartz). During high temperature processes, decomposition of the carboxylic groups occurs producing a porous residual solid particle containing several inorganic species. This residual solid particle is known as "char" (Durie, 1971; Falcone and Schobert, 1986). Simultaneously, the inorganic constituents in the char particle also undergo a series of transformations to form new inorganic compounds, distributed throughout the char structure. As high temperature proceeds, the char surface is reduced, causing the new inorganic compounds to become exposed on the surface of the char particles (Manzoori, 1990; Skrifvas et al, 1994).

Ash deposition in fluidised bed combustion

In fluidised bed combustion the burning char particles covered with a molten ash layer come in contact with inert bed particles. At this time, the molten ash is transferred and deposited onto the surface of the bed particles (Manzoori, 1990; Skrifvas et al, 1994). It has been found that the deposition layer consists (molten ash) of a mixture of sodium-calcium sulphate and a complex mixture of sodium-calcium-magnesium sulphate.

Manzoori (1990) has developed a schematic diagram showing mechanisms of coal ash deposition in fluidised bed combustion. The schematic diagram is shown in Fig 2.1.

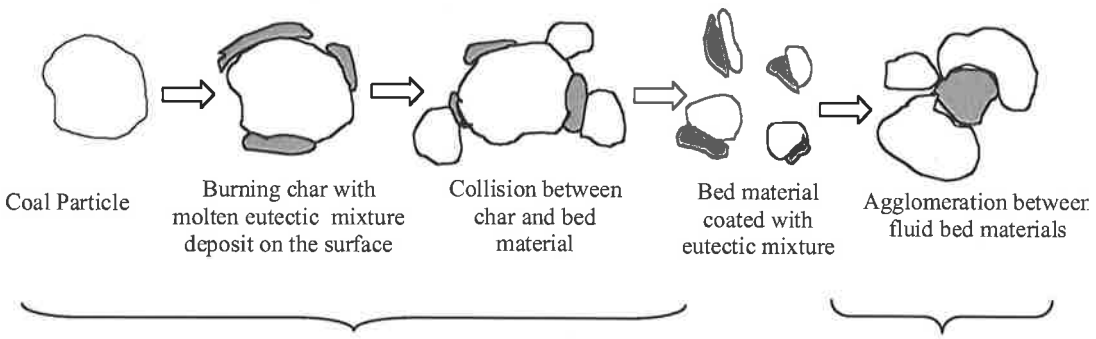

Fig 2.1: Mechanisms of ash deposition during fluidised bed combustion and agglomeration (Manzoori, 1990)

Fig 2.1 shows that when the low-rank coal particles are burnt the surface of the burning char particle is covered by the molten ash. During the fluidised bed combustion process, collisions between char particles that are covered with the molten ash and fluid bed particles occur. The molten ash is then transferred from the surface of the char particles to the fluid bed particles. Manzoori (1990) and Skrifvas et al (1994) have suggested further that collisions among the bed particles, coated with a layer of molten ash, would result in *agglomeration of the bed particles*.

Mechanisms of agglomeration in fluidised bed combustion

Manzoori (1990) and Skrifvas and Hupa (1994) purposed two possible mechanisms that may be relevant to the agglomeration of fluid bed particles of low-rank coals. The mechanisms are *partial melting*, also known as *reactive liquid sintering* and *viscous flow sintering*.

Partial melting or reactive liquid sintering

Ash high sodium, calcium, magnesium and sulphur contents form a low-melting point eutectic mixture of alkali sulphates, which has melting point between 500°C and 700°C. The presence of this liquid phase makes the ash *sticky* and facilitates the transfer and adhesion of ash on the surface of the bed particles. The amount of the molten phase presented may control the stickiness of the ash-coated particles and determines the tendency of the molten layer to adhere inert bed particles together after their collisions.

Viscous flow sintering

This mechanism involves the melting of ash at temperatures above 1000°C, producing a highly viscous liquid phase. The high viscosity of the molten ash may keep the liquid in the glassy phase when the ash is deposited onto the bed particle surface whose temperature is normally lower than that of the char particles. Skrifvars and Hupa (1994) stated that the viscous flow sintering mechanism is normally associated with ash high in silica content. Frenkel (1945) suggested that the viscous flow sintering mechanism is a time-dependent process and the molten ash viscosity has been demonstrated to control neck formation in sintered particles.

Moilanen et al (1989, 1991) developed a micrograph to show the agglomeration of fly ash particles. The photograph showed that there is a neck combining the ash particles together. They argued that sintering began with neck growth between ash particles, resulting in a porous network of particles. The pores were ultimately closed as the necks grew, and eventually series agglomeration took place. Moilanen (1991) suggested that deposit neck formation by this process occurs at much lower temperatures than the ash-melting temperature.

Hupa and Skrifvas (1989) found that ash particles stick together after 30 minutes of heat treatment at 800°C. As temperature is increased, both the viscosity and surface tension of the molten layer decrease while the sintering rate increases. The change in viscosity and surface tension determines the potential for sintering or agglomeration of a particular ash. Raask (1985) found that the viscosity of the molten ash is a significant property controlling the growth of the collided particles.

Tardos et al (1985) studied the limiting gas velocity required to break the largest agglomerates in a fluidised bed combustion unit. They also investigated the minimum gas velocity required to break the agglomerated particles at temperatures above the minimum sintering temperature of the coal sample. Furthermore, Tardos and co workers studied the relationship between the bonding forces holding the agglomerates together and the forces leading to the break-up of agglomerated particles (due to the motion of gas bubbles in the bed). They found that the maximum force acting on the agglomerates can be related to the excess velocity and associated pressure. The maximum pressure that causes failure of the structure can be associated with the yield strength of the agglomerates. Such an evaluation requires knowledge of both the coated ash layer's viscosity and the yield strength of a sinter neck as functions of temperature.

Ash deposition in fluidised bed gasification

Ash deposits in fluidised bed gasification are somewhat different from those found from fluidised bed combustion, and the mechanism of ash deposition is still not fully understood. Davidson (1992) suggested that operating conditions of fluidised bed gasification play a significant role in mechanisms of ash deposition. This is due to the fact that the gasification process has a lower operating temperature and a longer residence time than the combustion process, causing the difference in transformations of inorganic matter of coal samples and hence mechanisms of coal ash deposition. Benson et al (1995) studied physical characteristics of coal ash samples generated by commercial gasifier units. These included the US Kellogg Rust Westinghouse (KRW), Institute of Gas Technology (IGT), Dow gasifier, Texaco, and Shell. They found that most of the commercial systems produce a dry char particle, indicating that there was no deposition layer of the molten ash on the surface of the char particle.

Mechanisms of agglomeration in fluidised bed gasification

Recent studies on agglomeration in fluidised bed gasification (Mason, 1980; Benson, 1998) have found that agglomeration in fluidised bed gasification is *agglomeration of coal ash particles and not fluid bed particles.* They are two reasons; first there are nearly none inert bed particles used in the fluidised bed gasification process, and second there is no deposition of molten ash layer on the surface of the char particle. Thus, there is no transfer of molten ash from the char to the fluid bed particles. However, at this stage the mechanisms causing agglomeration in fluidised bed gasification are largely unknown.

It can be summarised here that successful operation of fluid bed processes for coals with high ash and alkali contents will depend on the ability to control ash deposition. An understanding of the specific mechanisms involved in agglomeration of fluid bed material requires a good knowledge of the intrinsic physical properties of the molten ash as a function of the coal type, the operating temperature and the chemical and mineral composition of the ash deposit. The rheological properties of coal ash under furnace conditions are important in controlling the stickiness and mobility of the molten ash deposition. A greater knowledge about rheological properties of coal ash will improve the understanding of ash deposition mechanisms and may assist in controlling deposition and agglomeration.

2.3 CONCEPTS OF RHEOLOGY

Rheology deals with the deformation and flow of material under the influence of an applied stress. In reality rheology is concerned with the flow, transport and handling of complex fluids such as ash suspensions, polymer melts, emulsions and polymer solutions. Rheology has assumed a very important role in mineral processing and disposal, coal processing and transportation, food processing, pharmaceutical production and metal processing. At the temperature range found in fluidised bed processes, the coal ash sample appears partially molten. Thus, rheology of suspensions appears to be the subject most relevant to this work.

Rheology of suspensions is very complex due to interplay of various physical and chemical factors arising from solid and liquid phases. It has been found that rheological characteristics of suspensions may exhibit either Newtonian or non-Newtonian behaviours depending on concentration of solid particles. At low solid concentrations, a suspension may behave like a Newtonian fluid with viscosity is dependent only on the temperature and concentration of particles. When concentration is increased, non-Newtonian characteristics with a variable of viscosity and the presence of a yield stress are expected. Depending on concentration, particle size, particle distribution and shape, a suspension may behave like either a pseudoplastic or dilatant, or plastic.

In addition, time dependent behaviour is also expected for a concentrated suspension. This means the relationship between shear stress and shear rate depends on time of shearing. Typical time-dependent characteristics are thixotropy (viscosity decreases with time and shear) and anti-thixotropy or rheopexy (viscosity increases with time of shear).

2.3.1 Time independent suspensions

Time independent suspensions can be further divided into two types depending on flow behaviours of the sample; they are viscous behaviour and plastic behaviour. A suspension has viscous behaviour when it readily flows like a liquid under application of shear stress. A suspension is classified as having plastic behaviour when it behaves like a solid at low stress but readily flows like a viscous liquid when a critical shear stress is exceeded. Viscous behaviour and plastic behaviour of a suspension can be determined from relationships of shear stress to shear rate (flow curve). Fig 2.2 shows various types of viscous behaviour, and diagrams of various types of plastic behaviour are shown in Fig 2.3.

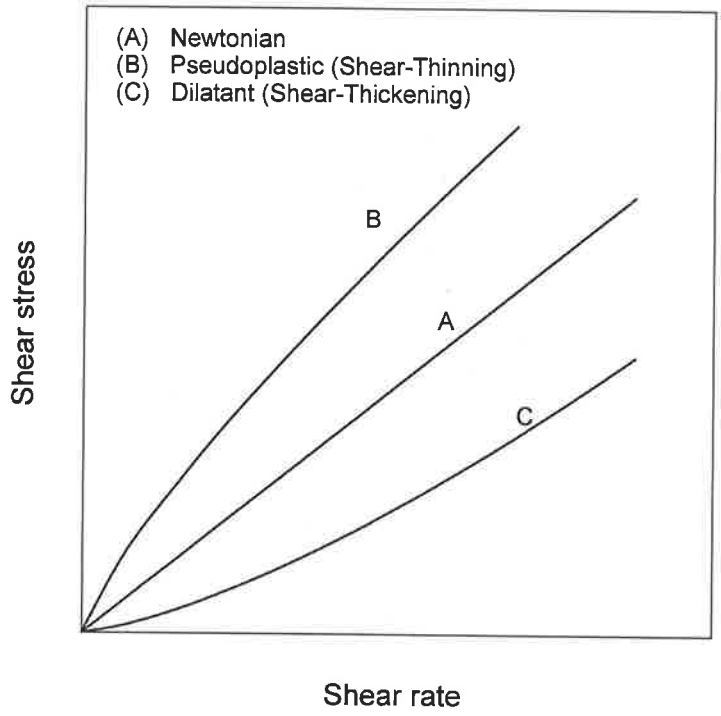

Fig 2.2: Flow curves for time-independent viscous fluids

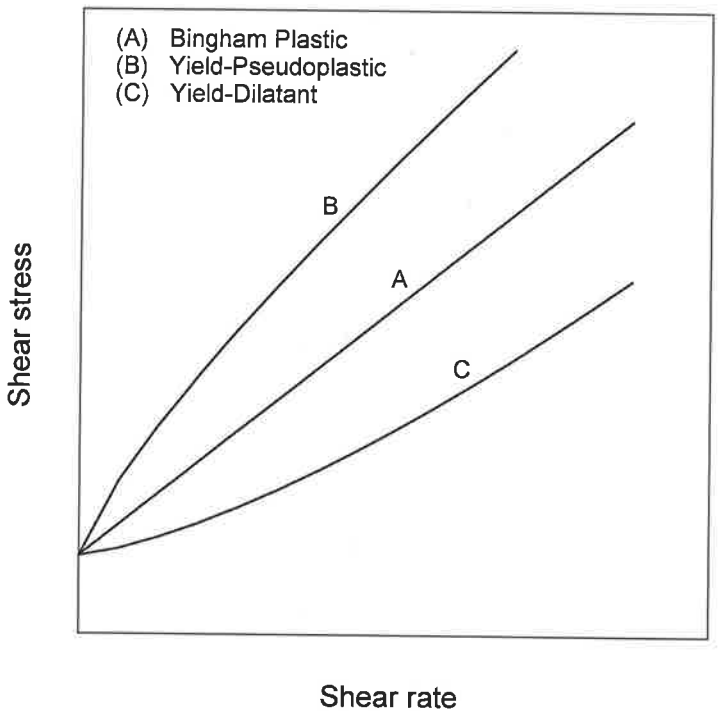

Fig 2.3: Flow curves for time-independent plastic fluids

Viscous behaviour

It can be seen from Fig 2.2 that there are three types of flow behaviours for viscous fluids. They are Newtonian, pseudoplastic (shear-thinning) and dilatant (shear-thickening) fluids. The linear line (curve A) passing through the origin is defined as a Newtonian fluid, whose viscosity is constant over the entire range of the shear rate. Thus

$$\tau = \mu\dot{\gamma} \qquad 2.1$$

where μ is called the Newtonian viscosity.

For curve B, where shear stress concaves downward with increasing shear rate, this fluid type is defined as pseudo-plastic or shear thinning fluid. This fluid is characterised by a viscosity (η) that decreases as the shear rate increases. Pseudoplastic fluids are commonly described by the power law equation, also known as Ostwald-de Waele model (Wilkinson, 1960, Kissa, 2000). The power law equation is:

$$\tau = K\dot{\gamma}^{n} \qquad n < 1 \qquad 2.2$$

where the parameters K and n are defined as consistency index and flow behaviour index, respectively (Metzner, 1956 and Wilkinson, 1960).

Furthermore, the n parameter is either used to determine the degree of pseudo-plastic or the degree of dilatancy of the material depending on its value. In the case where $n<1$, the liquid is a pseudo plastic fluid, and for $n>1$, a dilatant behaviour prevails. For $n=1$ the equation 2.2 is reduced to equation 2.1, for Newtonian systems. Since η is not constant and its value is dependent on shear rate. This applies to all non-Newtonian fluids. Metzner (1965) distinguished η from the Newtonian viscosity (μ) by termed η as '*apparent viscosity*'.

For curve C, the shear stress varies concavely upwards with shear rate. This characteristic is defined as dilatant or shears-thickening fluid and its rheological behaviour is totally opposite to that of pseudo-plastic fluids. Dilatant fluids have apparent viscosity increases with increasing shear rates. Based on the equation 2.2, the power law index or flow behaviour index (n) is greater than unity ($n>1$) (Green et al, 1968, Barnes et al, 1985, Kissa, 2000). Some materials such as concentrated starch paste and mineral slurries are shear-thinning at low shear rates but show shear-thickening behaviour at high shear rates. The shear-thickening effect is caused by some order-disorder transition taking-

place at a critical point under the application of shear. Barnes (1989) compiled the literature data and concluded that concentrated dispersions of non-aggregated solid particles will exhibit shear thickening under certain shearing conditions. Several parameters, such as volume fraction, particle size, shape and size distribution and the medium viscosity affect the degree and onset of shear-thickening.

Plastic behaviour

It can be seen from Fig 2.3 that flow curves of plastic fluids do not pass through the origin. This type of fluid does not readily flow under application of shear stress until critical shear stress is exceeded. The critical stress is called *'yield stress'*. A suspension that has shear stress varies linearly (curve A) with shear rate after the yield stress is exceeded is also known as Bingham plastic fluid (Bingham, 1920) and a suspension that has shear stress varies concavely downwards (curve B) is known as yield pseudo plastic and yield dilatant plastic fluid if shear stress varies concavely upwards with shear rate (curve C).

Bingham model

The Bingham model is given by equation 2.3 and 2.4.

$$\tau = \tau_y^B + \mu_B \dot{\gamma} \qquad (\tau > \tau_y^B) \qquad 2.3$$

$$\dot{\gamma} = 0 \qquad (\tau < \tau_y^B) \qquad 2.4$$

where τ_y^B is the Bingham yield stress and μ_B is Bingham viscosity. The materials described by equation 2.3 are called Bingham plastic fluid. The Bingham model predicts a linear relationship between shear stress and shear rate above the Bingham yield stress (τ_y^B).

Herschel & Bulkley model

This model was developed originally for predicting rheological behaviours of rubber-benzene solution system (Herschel and Bulkley, 1926). The Herschel & Bulkley model is given by equations 2.5 and 2.6:

$$\tau = \tau_y^{H-B} + K\dot{\gamma}^n \qquad (\tau_y > \tau_y^{H-B}) \qquad 2.5$$

$$\dot{\gamma} = 0 \qquad (\tau_y < \tau_y^{H-B}) \qquad 2.6$$

where τ_y^{H-B} is the Herschel & Bulkley yield stress, K and n are constants and equivalent to consistence index and flow behaviour index, respectively. In the case where n<1, the

liquid is a yield pseudo plastic fluid and for n>1, a yield dilatant behaviour prevails. For n=1 the Herschel & Bulkley model becomes the Bingham model (equation 2.21). The Herschel & Bulkley model is applicable to a variety of yield pseudo plastic system (Barnes, 2000 and Kissa, 2001).

Casson model

Casson model was originally developed to describe the rheological behaviour of pigment-oil suspension and later the model has been successfully applied to a variety of fluids such as blood, food products, mineral suspensions and polymer suspensions (Barnes et al, 1985; Kissa, 2000). The Casson model is shown in the equation below:

$$\tau^{1/2} = \tau_C^{1/2} + \eta_c^{1/2}(\dot{\gamma})^{1/2} \quad (\tau \geq \tau_c) \qquad 2.7$$

$$\dot{\gamma} = 0 \quad (\tau < \tau_c) \qquad 2.8$$

where τ_c and η_c is the Casson yield stress and the Casson viscosity, respectively. In some case η_c is also known as infinite shear viscosity (η_α).

Note that there are other empirical models containing yield stress that have also been proposed for particular systems and they are more complicated than the three previously mentioned models. These include the modified Casson model, the generalised Casson model, the Ceowley-Kitzes model and the Gay-Nelson-Armstrong model. Selection of a particular model to describe the rheological properties of a given system depends on a number of factors such as simplicity of constitutive equations, the decency of model fit, and most importantly, the intended application. It has been shown by many researchers that over a restricted shear rate range, sometimes more than one model can be used to describe the experimental data. No single model is adequate in describing the observed flow behaviour over a wide range of shear rates. Nguyen and Boger (1992) have recommended that no matter which models are selected, great care must be taken if the resulting empirical equation is to be used beyond the range of the experimental data obtained.

2.3.2 Time dependent suspensions

There are many real fluids for which shear stress or viscosity varies with time even though the shear rate is maintained constant. In such a case the fluid is called time dependent fluid. If the viscosity of a fluid is observed to gradually decrease with time when subjected to a constant shear stress or shear rate, and if the fluid recovers its original viscosity gradually over a period of time, the phenomenon is called thixotropy and the fluid is

termed a thixotropic fluid. If a fluid shows the opposite behaviour, i.e., the viscosity slowly increases with time at a constant shear stress or shear rate and the recovery of the original viscosity is achieved over a period of time after the absence of the applied shear stress or shear rate, the phenomenon is known as anti-thixotropy or rheopexy.

It has been reported that thixotropic fluid is attributed to breakdown of some structure under shear, followed by gradual structure reformation at rest (Tanner, 1985; Barnes et al, 1989; Kissa, 2000; Morrison, 2001). For example, when a suspension is being sheared, structure of the sample is broken-down into a smaller structure than its original structure. Breakdown in the structure of the suspension can be observed from a decrease in viscosity or shear stress of sample with shearing time. After the applied stress is removed, the original structure is gradually restored. This phenomenon can be observed by a gradually increasing viscosity with resting time. The decrease in viscosity is due to the decrease in the dissipation of energy attributed to the rupture of inter-particle bonds. It can be argued that thixotropy and pseudoplastic and plastic behaviours may be considered as a special case of thixotropy as the change of structures is similar but the time scale of structural change is very different.

The opposite behaviour to thixotropy is anti-thixotropy or rheopexy which is analogous to dilatancy but with measurable time dependent. Rheopectic materials are hardly found in nature, and their effects are not fully understood. Sometimes rheopexy behaviour is confused with thixotropy. For a comprehensive reviews on thixotropy and rheopexy, one can be found from numerous textbooks on rheometry such ash Tanner (1985), Barnes et al (1989), Macosko (1994), Kissa (2000) and Morrison (2001).

2.4 PREVIOUS EQUIPMENT AND TECHNIQUES USED FOR THE RHEOLOGICAL MEASUREMENT OF COAL ASH AT HIGH TEMPERATURES

The principle of rheological measurement is to establish relationships between stress, strain rate and time for a particular test sample. For most commercial rheometers, the primary measurable variables are torque, rotational speeds, and processing time. Torque is converted into a stress value, while the deformation angle observed is converted to a strain rate value in terms of the measuring geometry. Thus, the reliability and accuracy of a rheological characterisation of a material depends strongly on the quality of the measuring technique of the primary variables.

A review of existing literature has revealed that the most widely used measuring system for rheological measurements of coal ash is the rotating concentric cylinder system. This is due to its simplicity in operation and construction. The configuration has been used by many workers (Nicholls and Reid, 1940; Sage and McIlroy, 1960; Boow, 1965; Watt and Fereday, 1969; Schobert, 1985; Jones and Lindsey, 1987; Mills and Rhine, 1989; Oh et al, 1995; Groen et al, 1998; Hurst et al, 1998, 2000, 2001, 2002) for measurement of viscosity of coal ash slags at temperatures ranging from 1300°C to 1600°C. There are two other measuring systems that have also been used in rheological measurements of coal ash slag, they are the rod penetration system (Boow, 1969; Gibb et al, 1986; Moilanen et al, 1991) and the rotating parallel discs system (Fong et al, 1986).

Details of the equipment previously used for rheological measurement of coal ash slag at high temperature are presented in the following sections. The central emphasis is paid to design features of rheometers and the capabilities of rheometers used for the characterisation of coal ash and limitations of the existing measuring techniques.

2.4.1 Concentric cylinder system

The concentric cylinder system consists of two parts, an inner cylinder (bob) and an outer cylinder (cup), with the sample residing in a gap between them. In rheological measurements of coal ash slags, the concentric cylinder system can be further divided into two types depending on their operating techniques. One is the rotating concentric cylinder in a stationary cup and the other is oscillating concentric cylinder in a stationary cup. Methodologists and equations used in the concentric cylinder system are not given here, but one can find from a textbook on rheology.

Rotating concentric cylinder system

Sage and McIlroy (1960) used a rotational-type viscometer to study the effects of viscosity on a slag-tapping boiler during combustion of American coal. A platinum bob and a platinum-rhodium crucible were used. They performed viscosity measurements using a constant rotational speed technique. The bob was connected to a calibrated suspension wire, and the shear stress on the surface of the bob was calculated from the deflection of the suspension. The torsion wire was calibrated with the National Bureau of Standards oils and reference glasses, for which viscosity data was available. Sage and McIlroy (1960) performed viscosity measurements by rotating the bob at a constant speed in a mixture of hydrogen and nitrogen gas. They reported that the viscosity of the American

coal slags were within the range of 1 to 10^3 Pa.s in the temperature range of 1100°C to 1650°C.

Boow (1965) was the first scientist who measured the viscosity of Australian coal ash slags. He used a Brookfield rotating cylinder type viscometer equipped with a molybdenum bob and cup system. He performed viscosity measurements for fifteen Australian coal ash slags in a rich nitrogen gas atmosphere. Moreover, the coal slag samples were assumed to be a Newtonian fluid at temperatures of 1100°C to 1600°C. Boow (1965) stated that the viscosities of Australian coal ash slags were within the range of 2 to 10^3 Pa.s.

Watt and Fereday (1969) used a rotating cylinder type viscometer to study the relationship between viscosity and temperature of British coal slags. They performed viscosity measurements by rotating the molybdenum bob at a constant speed in the molybdenum cup. The torque response value was obtained from an electromagnetic device attached to the crucible. During viscosity measurements, a mixture of nitrogen/helium gas (10% H_2) was used to control the atmosphere of the system. They performed viscosity measurements on 113 British slag samples, and reported slag viscosities over the range of 10^{-2} to 10^3 Pa.s at temperatures between 1000°C and 1800°C.

Schobert et al (1985) measured the viscosity of low-rank coal ash slags using a Haake RV-2 Rotovisco unit equipped with a concentric cylinder system. The bob was made from two different materials, one from a 90/10 percent of platinum/rhodium alloy bob, and the other was made of molybdenum. The platinum bob was used to measure viscosity of coal ash under an oxidising atmosphere (a rich air atmosphere) whereas the molybdenum bob was used for reducing conditions (either a rich N_2 gas or a $20H_2$: $80N_2$ gas mixture atmospheres). Schobert and co workers measured viscosity of low-rank coal slags with temperature range of 1300°C to 1500°C. During viscosity measurement, rotating speed of the bob was increased from 0 rpm to 64 rpm in increment of 4 rpm. They assumed that under the temperature and atmosphere range of interest the coal ash slag exhibited Newtonian behaviour. Nowak et al (1993) also used the similar system to measure viscosity of British coal ashes.

Jones and Lindsey (1987) measured the viscosity of American lignite ashes using a Haake viscometer equipped with a graphite bob and cup system. The viscometer was first tested against the National Bureau of Standards glasses. They stated that the lignite slags were basically having the same compositions as natural glasses. It was found that viscosity of

the lignite slags were similar to the viscosity of natural glasses at temperature ranging from 1200°C to 1650°C, and the viscosity of the lignite slags ranged from 10^0 to 10^3 Pa.s. Jones and Lindsey also developed a relationship of viscosity as a function of temperature and chemical compositions.

Mills and Rhine (1989) carried out viscosity measurements of British coal ash slags obtained from a fluidised bed gasification unit. The viscosity measurements were performed with a Haake 100 Rotovisco viscometer equipped with a molybdenum bob and a graphite cup. The viscosities of four British slags obtained from a gasification unit were reported within the range of 0.5 to 50 Pa.s at temperatures between 1300°C and 1550°C.

Oh et al (1995) used a Haake Rotovisco RV-100 equipped with a concentric cylinder system to investigate the effects of crystalline phases on the viscosity of American coal ash slags. The measuring system consisted of a stationary crucible and a rotating bob with a tapered bottom. The bob and cup were made from a high-density alumina. A gas mixture of CO/CO_2 (60:40) was used to create a reducing atmosphere in the furnace. They reported that the relationship between shear stress and shear rate for the coal ash slags displayed Newtonian characteristics at high temperatures and non-Newtonian characteristics at low temperatures. They also suggested that the non-Newtonian behaviour was a result of the formation of crystalline phases in the slags during the rapid cooling of the slags. However, no flow curves of non-Newtonian slags were shown in their paper. Slag viscosities of up to 300 Pa.s were measured at temperatures in the range of 1150°C to 1500°C.

Groen et al (1998) studied the effect of crystallisation on viscosity characteristics of gasified American coal slag using a Haake Rotovisco RV-100 equipped with a concentric cylinder system. It was found that crystallisation of mineral compounds starts to have an effect on the viscosity behaviour of the slags when the total mass of the crystal structure was more than 30 percent weight of the overall slag sample.

Hurst et al (1998, 2000, 2001, 2002) measured the viscosities of gasified Australian bituminous ash slags and synthetic ash mixtures of the SiO_2:Al_2O_3:CaO and SiO_2:Al_2O_3:CaO-5 percent FeO systems. They performed viscosity measurements using a Haake Rotovisco RV-100 equipped with a molybdenum bob and an alumina cup at temperatures ranging from 1300°C to 1500°C. They found that the viscosity of slags containing < 2.5 percent weight of FeO compound was less than 15 Pa.s. Moreover, Hurst

and co-workers developed empirical models based on an Urbain type equation to predict the flow properties of fluxed Australian coal ashes.

Overall, the rotating concentric cylinder has been used for the measurements of the viscosity of coal ash at temperatures between 1300°C to 1600°C at which most ash materials are completely molten as slag and behave as Newtonian liquid. The measurable viscosity is typically in the range 0.1-1000 Pa.s and is a strong function of temperature and operating atmosphere. Uncertainties such as end effects sometimes do arise due to sample contact between the bottom of the cup and the end of the bob, which give rise to anomalous contribution to observed torque. Nevertheless, a careful design of concentric-cylinder system will satisfy the demands of any practical purpose. However, simple procedure for data reduction is applicable only to homogeneous slags. Shear rate calibration is unavailable when non-homogeneous coal ash, due to the formation of crystalline phases during cooling, are dealt with or wide annulus is adopted.

Oscillating concentric cylinder system

Nicholls and Reid (1940) used the oscillating concentric cylinder system to measure the viscosity of American coal ash slags. The bob used had an extended spindle and was made of platinum with 20 percent rhodium. Nicholls and Reid first calibrated the oscillating viscometer with a known viscosity fluid by oscillating the bob in a simple harmonic motion. The damping and time for the bob to oscillate over a given frequency were measured, and the slag viscosity was measured as a function of the damping of the bob and the inertia of the rotating system. With this instrument, they conducted viscosity measurements of several American coal ash slags, and reported that viscosities were in the range of 1 to 10^7 Pa.s.

Machin and Hanna (1945) constructed an oscillating cylinder-type viscometer using design concepts similar to those of Nicholls and Reid (1940) to measure the viscosity of a CaO-MgO-Al_2O_3-SiO_2 system. They also calibrated the viscometer with a known viscosity material period to measure viscosity of the oxide mixture. For this viscometer, the precision of viscosity measurement was satisfactory in the range of 10^{-1} to 10^5 Pa.s at temperatures up to 1500°C.

It was found that the oscillating technique can measure a large range of slag viscosity of up to 10^7 Pa.s, but relies on empirical correlations obtained by calibrations with Newtonian fluid of known viscosities. This technique may be suitable for coal ash slags,

especially those from bituminous coal or those with high silica content, which usually behave as Newtonian fluids at high temperatures (Vargas et al, 2001).

2.4.2 Rotating parallel discs

Fong et al (1986) developed a fast response plastometer using a concentric parallel disc geometry to measure the viscosity of bituminous coals. Techniques involved measuring the torque required to rotate a thin disc embedded in a thin layer of molten coal sample located between two heated metal plates. The top disc was connected to a torque transducer, which had a measurable range of 10^2 Nm. The bottom disc was attached to a motor. The disc and plate were made of a nickel superalloy for high temperature strength and corrosion resistance. The whole measuring system was enclosed in a high-pressure chamber. Heating was provided by sequentially charging a constant pulse of current through the metal plates for heating up and holding the sample at temperature. During viscosity measurement, torque-time and temperature-time data were recorded. With the viscometer developed, the viscosity of bituminous coal slags were measured up to 7.2×10^4 Pa.s under rapid heating and high temperature conditions.

The major advantage of using the parallel plate system is that the system requires only a small amount for each test, and it is easy to load the sample into the measuring geometry. However, the parallel plate system has non-uniform shear rate and shear stress over the sample volume and problems associated with slipping and ejecting of the tested sample from the measuring geometry during rheological measurements.

2.4.3 Rod penetration or needle penetration system

This measuring system is less conventional than the rotating concentric cylinder system and the parallel plate system. But the rod penetration system has frequently been used in high temperature viscosity measurements of coal ash slags by many workers, including Boow (1969), Gibbs et al (1986), Moilanen et al (1989, 1991). The essential elements of this type of viscometer are a rod (piston or needle), a large crucible (cup), a depth of penetration detector and a penetration controller. During measurement, the rod is axially penetrated into the tested sample by an applied load or the own weight of the rod. The test sample in the gap between the rod and the crucible is under shearing deformation. This measuring system assumes that the applied weight or force is equal to the viscous drag of the adjacent fluid plus the hydrostatic force on the bottom of the rod. Viscosity calculation involved assumed the coal ash to be completely molten and behaved as a Newtonian fluid under the test conditions.

Boow (1969) reported the results of viscosity measurements made for several Australian coal ash slags by a 20 percent platinum-rhodium penetrating rod. The test slag was contained in a molybdenum crucible. A millimetre scale was used to measure the penetrating rate. The slag viscosity was calculated from the slope of the penetration depth and time curve. Boow reported that viscosity of Australian coal ash slags was in the range of 10^4 to 10^8 Pa.s at temperatures ranging from 750 to 1100°C.

Gibb (1986) measured the viscosity of British and South African bituminous coal ash slag using the rod penetration system. The penetrating system consisted of a molybdenum needle and an alumina crucible. A linear displacement transducer was connected to the needle to measure both the depth and rate of penetration. During testing the load imposed on the needle was measured along with the depth and rate of penetration. Gibb performed the viscosity measurements under oxidising (air) and reducing conditions (1:1 CO_2/H_2). The experiments were conducted at temperatures ranging from 900°C to 1550°C. He reported that viscosity of coal ash samples was in the range of 10^2-10^8 Pa.s. Moilanen et al (1991) used the needle penetration system previously designed by Gibb to measure the viscosity of slag from peat ash in the range of 10-10^7 Pa.s at temperature between 816°C to 1300°C.

The advantage of the rod penetration system is that when the rod is raised from the end of the crucible, it refreshes the test sample and provides a good periodic sample renewal. However, Moilanen et al (1991) found that the accuracy of the measured viscosities diminished at a value below 10 Pa.s due to the measuring inaccuracies of the small weight imposed on the needle. In addition, problems associated with corrosion of the needle during viscosity measurements have also affected viscosity measurements of the coal ash slags.

2.4.4 Possible sources of error during viscosity measurements of coal ash

Despite the experimental difficulties, a number of workers made measurements of viscosities of coal ash slags and glass at high temperatures. The researchers had to make many concessions in apparatus design because of the high temperature range, the corrosive characters of the test sample and the high velocity value of coal ash sample. Therefore, the reliability of data should be considered bearing in mind the practical situation. Watt and Fereday (1969) have listed two major possible sources of errors in

determining the viscosity of coal ash slags at high temperature. They are *instrument errors* and *analytical errors*.

Instrument errors

End and wall effects are two major sources of error in a conventional concentric cylinder viscometer. The magnitude of the end effects depends on both the shape of the end of the bob and the extent of non-Newtonian behaviour of the test fluid. Van Wazer et al (1963) have suggested that a large bob with a conical bottom normally results in large end effect errors. With suspensions or two-phase fluids, phase separation at the wall of the cylinders leads to wall slip effects. Nguyen and Boger (1992) suggested that wall slip effects are significant for smooth surface cylinders with small gap spacing and at low rotational rates. However, with the previous coal ash viscometers the problem of the wall slip effect remains unaddressed. Variation of shear rate and shear stress across the gap between the bob and cup are also significant problems when a non-Newtonian fluid is tested (Krieger and Maron, 1954; Van Werzer et al, 1963; Nguyen and Boger, 1983, 1985, 1987; Barnes, 1997; Toorman, 1994). The sample held between the bottom of the cup and the end of the bob also gives rise to the end effect contributing to the torque measurement (Van Werzer et al, 1963) and heat generation within the fluid, especially at high shear rate conditions (Macosko, 1994, Morrison, 2001). Thus, measuring rheological properties of non-Newtonian fluids with the rotating concentric cylinder needs to be used with caution.

Problems of corrosion and reaction between ash and material used for the measuring geometry have also had an effect on the accuracy of the instruments. Materials used to construct the measuring system are critical, as the selected materials must be able to handle high temperature and high reactive conditions, and most importantly must not react with the tested sample. Reviews of previous equipment have found that molybdenum, alumina, platinum-rhodium and graphite were the materials commonly used to fabricate measuring geometries. Out of these materials, molybdenum was the one most commonly used.

However, there were two major problems associated with the use of molybdenum. The first problem was dissolving of molybdenum into the slag sample, which causes change in chemical compositions especially iron content of the test sample (Watt and Fereday, 1969, Gibbs et al, 1986). The second was the reaction between molybdenum and the sulphur dioxide (Boow, 1965). Boow (1965) reported that there was a significant weight loss of the molybdenum bob after high sulphur dioxide ash was measured. Moilanen et al (1991)

also reported that his molybdenum needle was corroded during viscosity measurements of a high concentration of P_2O_5 ash.

Alumina dissolved to some extent in the slags and changed structure of the silicate content, causing rapid changes in viscosity of the sample (Oh et al, 1995; Groen et al, 1998). Under reducing conditions, platinum also reacted with the iron content from slags forming iron-platinum alloy (Nicholls and Reid, 1940; Sage and McIlroy, 1960; Schobert et al, 1985). Graphite was also used to make the measuring parts. This included the work of Machin and Hanna (1945), and Jones and Lindsey (1987). However, graphite was not an ideal material even though it was relatively cheap. This is because graphite does not wet by molten slag, which may cause slipping of the sample during viscosity measurements (Machin and Hanna, 1945). Mills and Rhine (1989) suggested that the successful candidate used for measuring parts would be the one that had least effects on the slag viscosity.

Technical problems at high temperatures especially expansions of the measuring systems and non-uniform temperature distributions in the sample also contribute into the instrument errors. Expansions of the measuring geometries cause changing in size and gap of the measuring geometries (Barnes et al, 1989). The non-uniform temperature distributions may cause a formation of crystal structures, which result in phase separations of the sample (Machin et al, 1952). Thus, in order to minimise the problems associated with high temperature, a correction of the values of the radii of cylinders and the immersion depth as a function of temperature should be established.

Analytical error

The majority of previous work on viscosity measurement of coal ash slags has deduced that coal ash slag exhibits Newtonian fluid behaviour. However, most of the papers published did not show the flow behaviour of samples. Instead the measured value would correspond only to a single point on the flow curve. It has been frequently found that most of the previous works have calculated values of viscosity based on empirical correlations that were obtained by calibrations of the viscometer with standard reference fluids of known properties at both room temperatures (eg silicon oil, mineral oil, polymer solutions etc) and high temperatures (eg polymer melts, molten standard etc). Therefore, the assumption can be satisfactory for high rank coal ash slags (bituminous) and a high silica content ash, which the samples behave as Newtonian fluids at high temperatures (Schobert et al, 1995). Serious error could result at low temperature measurements when

the partially molten ash could be complex in its physical structures and exhibit non-Newtonian behaviours.

Overall, the literature available for coal ash behaviour contributed entirely on American, British or Australian bituminous coal ash slags in the temperature range of 1000°C to 1600°C. This temperature range is well above the liquidus temperature of the slag samples in which the slag may behave as a Newtonian fluid. Very little work has been specifically involved with viscosity measurement at the temperature range of 600°C to 1000°C.

Most of the viscosity measurements of coal ashes were performed using either a rotating-cylinder viscometer or the needle-penetration viscometer. Almost all the existing instruments and viscosity measurements involved with single point measurements and rely on empirical equations based on calibrations with Newtonian standard liquids for determining the viscosity. Such single point measurements may be satisfactory for high rank coal ash slags or high silica content ashes at high temperatures where coal ash sample is completely molten and behaves as a Newtonian liquid. However, the single point measurement may be not suitable and can produce serious error at low temperatures, especially at operating temperatures similar to those found in the fluidised bed process (600°C to 1000°C), where the partially molten ash and non-Newtonian behaviours are expected. These limitations of the existing ash viscometers make them unsuitable for studying rheological behaviours of low-rank coal ash under conditions relevant to the fluidised bed combustion process. Thus, it is necessary to develop a suitable measuring technique and instrument that can be directly measure rheological properties of low-rank coal ashes.

2.5 FACTORS AFFECTING ASH RHEOLOGY

It has been found that rheological properties of coal ash are controlled by three significant factors; they are chemical compositions of coal ash sample, operating temperature and testing environment. In this section, reviews of effects of the key factors on rheological properties of coal ash are presented. In addition, models developed for predicting viscosity of coal ash based on relationships of viscosity-chemical compositions-temperature are presented and discussed.

2.5.1 Effect of chemical composition

The majority of early work on viscosity calculations for coal ash slags had estimated viscosity values of coal ash slags based on a ratio of basic oxide compounds to acid oxide compounds. These included the work by Nicholls and Reid (1932), Lillie (1939) and Nowok et al (1991). This method was also known as the '*bulk composition method*'. A basic oxide is an oxide that donates oxygen chemical compounds, while an acidic oxide is an oxide that receives oxygen chemical compounds. In some cases basic oxides have been referred to as network modifier species and acidic oxides have been referred to as network former species. The equation for the ratio of basic to acidic oxides is given in below:

$$\frac{\text{Base}}{\text{Acid}} = \frac{Na_2O + K_2O + CaO + MgO + FeO}{SiO_2 + Al_2O_3 + Fe_2O_3 + TiO_2} \qquad 2.9$$

where concentration of the chemical compounds in equations 2.9 are all in percent weight (%wt).

Nicholls and Reid (1940) and Reid and Cohen (1944) found that the FeO compound was not a stable species as under furnace conditions it always oxidises and forms Fe_2O_3. Thus, they proposed the '*silica ratio*' and '*ferric percentage*' to evaluate the exact chemical composition of a coal ash slag. Formulas used to calculate values of the silica ratio and the ferric percentage are given in the equations 2.10 and 2.11.

$$\text{Silica ratio} = \frac{SiO_2}{SiO_2 + CaO + MgO + \text{Equivalent } Fe_2O_3} \times 100 \qquad 2.10$$

$$\text{Ferric percentage} = \frac{Fe_2O_3}{Fe_2O_3 + 1.11FeO + 1.43Fe} \times 100 \qquad 2.11$$

where the equivalent Fe_2O_3 is equal to Fe_2O_3+1.11FeO+1.43Fe.

Boow (1969) stated that the ferric percentage was a numerical value that could be used to express the state of oxidation of the iron in the slags. He also suggested that the silica ratio was a useful estimation parameter for predicting the viscosity-temperature characteristics of slags.

Watt and Fereday (1969) found that slags with high silica ratios did not crystallise and flowed easily for both high and low operating temperatures. Slags with low silica ratios were troublesome as they usually crystallised and the crystals formed did not always readily resorb upon heating. Vorres et al (1986) found that the viscosity of synthetic coal ash mixtures increased rapidly with increasing SiO_2 concentration. They also stated that the viscosity of a high SiO_2 synthetic mixture was higher than the viscosity of a high Al_2O_3 content mixture.

Sage and McIlroy (1960) observed that during the combustion of coal, reactions between acidic and basic oxides were likely to occur leading to the formation of low melting point eutectic mixtures. They found that SiO_2, Al_2O_3, CaO and MgO reacted with Na_2O, K_2O and FeO leading to the formation of low melting point compounds. Sage and McIlroy stated that the base to acid ratio can be used as a means of predicting the viscosity of a slag and also as a means of determining what substances must be added to the ash to obtain the desired flow characteristics. They also stated that the viscosity of a slag decreased as the base to acid ratio approached 1.

Watt and Fereday (1969) found that for British coal slags the viscosity value was mainly affected by SiO_2, MgO, Al_2O_3, Fe_2O_3 and CaO, while Na_2O, K_2O and TiO_2 had little effect on the viscosity of the slags and therefore they could be ignored. Jones and Lindsey (1987) found that slags with high concentrations of SiO_2 and Al_2O_3 (refractory components) had higher viscosity values than those that were high in concentration of Fe_2O_3, CaO and Na_2O components (fluxing components). Oh et al (1995) observed that at the sample temperature a slag high in silica content was higher in viscosity than slags with high concentrations of other chemical compounds.

Gibb (1986) suggested that for slagging and fouling it was not just the overall ash composition that was important, but also the distribution of the chemical compounds within the coal ash matrix. He found that calcium was often associated with carbonate groups present in the coal slag matrix. In bituminous coals calcium reacted with carbonate groups and formed calcite ($CaCO_3$) or mixtures of carbonates such as dolomite ($(Ca, Mg)CO_3$) and ankerite ($(Ca, Mg, Fe, Mn)CO_3$) mixtures. It was observed that the

viscosity increased rapidly with increasing calcium content. Based on this observation, they concluded that calcium tended to increase the slagging propensity by promoting coal ash melts with a relatively low viscosity.

It had been suggested that the ferric percentage also has a significant effect on slag viscosity. Nicholls and Reid (1940) observed that the viscosity of British slags in a rich air atmosphere was higher than that in a rich N_2 atmosphere. Based on chemical analysis of the tested slags, Nicholls and Reid found that under the rich air atmosphere the slag was higher in ferric iron content, and under the rich N_2 atmosphere the slag was higher ferrous iron content. Thus, they concluded that the ferric percentage caused a decrease in the liquidus temperature of the slag. However, no definite answer was shown in the literature as to why the ferric percentage affected the viscosity of coal ash slags.

2.5.2 Effect of operating temperature

Temperature history

Nicholls and Reid (1940) observed a hysteresis loop of the viscosity-temperature curve during cooling and heating of coal ash slags. Schobert et al (1985) investigated the viscosity of low-rank coal ash slag and the change of viscosity with temperature for four ashes having various compositions. They found a hysteresis existing during the cooling and heating cycles for most of the slags tested. For a given temperature, the viscosity on the heating cycles was lower than that on the cooling cycles. The results suggested that it is beneficial or perhaps necessary to be at a higher temperature on the heating cycle than on the cooling cycle in order to achieve a desired viscosity. The reason is that if a slag is cooled to a viscosity too high for slag flow, it is necessary to heat the slag to a temperature above that from which it initially cooled to regain satisfactory flow at a sufficiently low viscosity.

Watt and Fereday (Watt et al, 1969) found that after cooling and reheating the viscosity of a slag was often significantly greater, approximately of 12 percent higher, than those of freshly melted ash. This difference signified that the assumption of viscosity being independent of thermal history was not altogether valid. The cause of this viscosity hysteresis was found to be associated with incipient crystallisation. Thus, based on effect of temperature history on crystalline phase formation, most of researchers were performed their experiments by beginning at the highest temperature when complete melting is observed.

Effects of crystalline phase formation

Generally slags are of two types; first is glassy slag and second is crystal slag. The glass slag is a homogeneous slag, while crystal slag is heterogeneous slag. The crystallising behaviours of slags can be studied either from the viscosity-temperature curves or by observing the remelting of crystallised samples of slags in a temperature gradient furnace (Watt and Fereday, 1969). If a coal ash slag is melted at high temperature and then allowed too cool slowly, a temperature will be reached at which the crystals begin to form. This temperature is known as '*liquidus temperature*, T_L'. The liquidus temperature can be defined as the maximum temperature at which the liquid and solid phases coexist in equilibrium. On further cooling of the slag more crystals will be formed and eventually a temperature will reach solidification point in which the sample becomes a solid sample. This temperature is called as '*solidus temperature*, T_s'.

Reid and Cohen (1944) introduced a parameter called *'temperature of critical viscosity*, T_{cv}'. The temperature of critical viscosity is the temperature at which a crystal structure is formed within coal ash matrix. They also suggested that the temperature of critical viscosity could be determined on the basis of a transition occurring from Newtonian to non-Newtonian behaviour in the slag viscosity-temperature curve. Moreover, they suggested that at T_{cv} is the temperature at the point where rapid increases in viscosity occurred on a viscosity-temperature curve.

Watt and Fereday (1969) suggested another temperature, T_J, which is defined as the temperature at which the viscosity of the reheating slag rejoins the curve corresponding to the fully liquid condition. This is the temperature at which, on reheating, the crystals formed on cooling are remelted into the slag thereby eliminating any effects of crystalline phase on viscosity. Clearly, T_{cv} and T_J are the measures of different aspects of crystallising phenomena of slag. T_{cv} was the temperature at which, on cooling, crystallisation of the slag was first to interfere flow behaviours whereas T_J was the temperature at which, on heating, the crystalline phase is being melted. Watt and Fereday (1969) concluded that these two temperatures were strongly dependent on external conditions, in particular on the rate of heating and cooling.

Nicholls and Reid (1940) observed a great distinction to exist between measurements of viscosity at temperatures above and below liquidus temperatures. Above liquidus temperature, the slag is a true liquid and the same value for its viscosity will be obtained will depend upon the method and time-temperature history of the measurement

procedure. Below the liquidus, the viscosity values obtained will depend upon the method and time-temperature history of the measurement procedure. For example, the oscillating method would give higher values for equivalent viscosity than that was obtained from the rotating bob method. This is because numerical values depend upon whether the slag is agitated to break up crystal formations. Thus, any method of measurement when solid phase is present the sample, viscosity of the sample will be arbitrary.

Oh and co-workers (1995) studied the effect of crystalline phase formation on viscosity behaviour under reducing conditions. They found that the shape of the crystal structure was an important factor that had affected the viscosity behaviour of the coal ash slags. Groen et al (1998) and Wright et al (2001) studied the effect of solids content (crystal structure) on the viscosity behaviour of coal ash slags. They stated that solids content had no effect on the viscosity behaviour if the total solid content was less than 30 % of total sample weight.

2.5.3 Effect of testing environment

It was reported that the viscosity values of coal ash tested under reducing (N_2) and oxidising (air) atmospheres were different for a given temperature (Nicholls and Reid, 1940; Schobert, 1985). Nicholls and Reid (1940) measured the viscosity of British coal ash slags under a reducing atmosphere (a rich N_2) and an oxidising atmosphere (a rich air atmosphere). They found that the viscosity values for slags measured under oxidising atmospheres were higher than those measured under a reducing atmosphere. Nicholls and Reid concluded that this was because under a reducing atmosphere, the reactions between chemical compounds in the ash were faster than that in the oxidising atmosphere. Furthermore, they also stated that for the system they studied the formation of metallic iron played a key role in the viscosity behaviour of coal ash slags under a reducing atmosphere. However, there was nothing reported on the effect of the formation of metallic iron on the viscosity behaviour of other coal ash slags elsewhere in the literature.

Schobert et al (1985) studied the viscosity transition from a reducing atmosphere to an oxidising atmosphere of a gasifier American low-rank coal ash slag. They found viscosity of the American slag increased by approximately 11 Pa.s after a transition from reducing to oxidising conditions. They assumed that it was likely the transition to oxidising

atmosphere may cause termination flow ability of the slag; even other factors such as temperature were changed.

2.5.4 Models developed to predict viscosity of coal ash slag

In the past three decades, several models have been developed predicting viscosity of coal ash slag. The early models were developed based on the bulk chemical compositions, and the recent models were developed relating viscosity to temperature and to few key chemical compositions. It has been generally accepted that rheological behaviours of high rank coal slags or silicate melt exhibit Newtonian characteristics. This means the viscosity of the melts is independent of shear rate, but rather dependent on operating temperature and chemical composition. Thus, most of the recent models have been developed relating the viscosity to temperature and to chemical composition. Of the viscosity-temperature relationship, the Arrhenius equation or the Weymann equation are found to be the most popular. Details of the Arrhenius equation (Arrhenius, 1887) and the Weymann equation (Weymann, 1962) are given below:

Arrhenius equation

$$\log\eta = \log A + \frac{Ea}{RT} \qquad 2.12$$

where A is a constant, Ea is the activation energy and R is the gas constant. The parameter A can be used to compare how different in viscosity of samples at the same temperature, while the parameter Ea shows the sensitivity of viscosity to temperature. The model developed to predict viscosity of coal ash slag using the Arrhenius equation is Watt and Fereday model (Watt and Fereday, 1963).

The Watt and Fereday model was originally developed based on viscosity measurements of 113 British coal ash samples. It was found that the model is frequently used for estimating the viscosity of coal ash at temperature between 1000 and 1300°C. However, the model is limited to a specific chemical compositions ranges, which are 30-60 %wt SiO_2; 15-35 %wt Al_2O_3; 3-30 %wt Fe_2O_3; 2-30 %wt CaO. Formula of the Watt and Fereday model is shown below:

$$\log\eta = \frac{m \times 10^7}{(T - 423)^2} + c \qquad 2.13$$

where T is the temperature in Kelvin (K), m = 0.00835 SiO_2 + 0.00601 Al_2O_3 – 0.109 and c = 0.0415 SiO_2 + 0.0192 Al_2O_3 + 0.0276 Fe_2O_3 + 0.016 CaO. Concentration of the chemical compositions in equation 2.13 is in %wt unit.

It can be seen that temperature dependence of viscosity is affected by concentrations of SiO_2 and Al_2O_3 compositions, as viscosity also becomes more dependent on temperature when concentration of SiO_2 and Al_2O_3 compositions are increased. At the same temperature the viscosity of British coal ash samples is strongly affected by concentration of SiO_2, Al_2O_3, Fe_2O_3 and CaO compositions: viscosity of British coal ash is increased with increasing concentration of these chemical compositions.

Weymann equation

$$\log\eta = \log A + \log T + \frac{B}{T} \qquad 2.14$$

where A and B are composition specific constants and T is the absolute temperature.

It can be seen that the Weymann equation is developed base on the Arrhenius equation by including an extra absolute temperature term. In some case the equation is also known as the Frenkel model.

The Weymann equation has been extensively used for describing temperature dependence of viscosity of silicate melts. These included models developed by Urbain (1981), Ribound (1981), Streeter (1984), Kalmanovitch et al (1988), Hurst and Patterson, (1997, 1998, 2000) and Zhang and Jahanshahi (1998). Out of these models, Streeter's model (Streeter, 1981) was found to be relevant to low-rank Australian ashes.

Streeter developed his model based on viscosity measurements of 17 Wester US lignite and sub-bituminous coal slags within the compositional range of 0.25-0.7 SiO_2, 0.08-0.27 Al_2O_3, 0-0.09 Fe_2O_3, 0.08-0.33 CaO, 0.04-0.13 MgO and 0-0.11 Na_2O. Streeter, Diehl and Schobert proposed a correction term to the Weymann equation, which is

$$\ln\eta = \ln A + \ln T + \frac{10^3 B}{T} - \Delta \qquad 2.15$$

where $\Delta = mT + c$ and the lnA and B parameters are gibe by:

$$-\ln A = 0.2693(B) + 13.9751 \qquad 2.16$$

$$B = 16.5 + 23.1SiO_2 - 54.3SiO_2^2 + 79.1SiO_2^3 \qquad 2.17$$

The evaluation of Δ was divided into three groups according to the silica content of the melt.

- High silica slags (B>28):

$$F = SiO_2/(CaO+MgO+Na_2O+K_2O) \quad 2.18$$

$$10^3m = -1.7264\,F + 8.4404 \quad 2.19$$

$$c = -1.7137(10^3m) + 0.0509 \quad 2.20$$

- Intermediate silica slags (24<B<28):

$$F' = B(Al_2O_3 + FeO) \quad 2.21$$

$$10^3m = -1.3101F'+9.9279 \quad 2.22$$

$$c = -2.0356(10^3m) + 1.1094 \quad 2.23$$

- Low silica slags (B<24)

$$F'' = CaO/(CaO+MgO+Na_2O+K_2O) \quad 2.24$$

$$10^3m = -55.365F'' + 37.92 \quad 2.25$$

$$c = -1.83(10^3m) + 0.9416 \quad 2.26$$

Overall, the viscosity of coal ash slags was found to be the function of temperature, chemical composition and atmosphere. Temperature dependence of viscosity was observed as viscosity decrease with increasing temperature. The slag having high concentrations of refractory components show very high viscosities; whereas increasing the fluxing components leads to rapid decrease in the viscosity. The viscosity found to be higher in the oxidising atmosphere than that in the reducing atmosphere. The formation of crystalline phase dure to temperature history has also affects viscosity of coal ash slags; viscosity is dramatically increased when there is a crystalline phase presented in the melt. The models relate viscosity to chemical composition and to temperature were developed base on either the Arrhenius equation or the Weymann equation. However, neither of the models appear to predict rheological properties of coal ash sample. This is due to the models was developed for Newtonian fluids, and the chemical species used to develop the models may not be similar to those found in low-rank Australian ashes.

2.6 CONCLUSIONS

This review of previous work in the study of the rheological behaviour of coal ash leads to the following conclusions being drawn:

- In the fluidised bed combustion process, depositions of molten ash layer on the surface of fluid bed particles causes agglomeration of fluid bed particles. It has also been found that the physical properties of the molten ash deposition are the key parameter controls agglomeration. In the fluidised bed gasification, mechanisms of agglomeration are not fully understood, but they are appear to be different from those found in the fluidised bed combustion process. Evidences to date have revealed that agglomeration of char or ash particles occurs instead the agglomeration of fluid bed particles.

- There are three different types of measuring systems used for the rheological measurement of coal ash at high temperatures. They are concentric cylinder, rotating parallel discs and needle penetration systems. Out of these systems, concentric cylinder is the one most commonly used. However, there are several problems defecting the suitability of the existing system for measuring rheological properties of low-rank coal ash under conditions relevant to fluidised bed processes. This is because at the temperature range of interest, the ash may be partially molten and heterogeneous in nature and may exhibit non-Newtonian flow behaviours. A new rheometer for measuring the rheological properties of low-rank coal is urgently needed.

- Temperature, chemical composition and operating atmosphere are key factors affecting ash rheology. Temperature, especially temperature history causes crystal structures to be formed in the slag sample. SiO_2, Al_2O_3, Na_2O, K_2O and Fe_2O_3 are found to be the significant chemical compositions controlling ash rheology. Operating atmosphere changes the reactions between chemical compounds. It has been found that the viscosity of coal ash under oxidising atmosphere was higher than those measured under a reducing atmosphere.

CHAPTER THREE

Experimental Equipment and Techniques

3.1 INTRODUCTION

It has been summarised in chapter 2 that almost all the existing instruments have been developed for single-point rheological measurements and rely on empirical equations based on calibrations with standard Newtonian liquids for determining the viscosity. This approach may be satisfactory for coal ash slags, especially those generated from bituminous (black) coal or those with high silica content, which usually behave as Newtonian liquids at high temperatures (Schobert et al, 1985; Vaisburd et al, 1997; Vargas et al, 2001), but can produce serious errors at lower temperatures where the coal ash may be partially molten and may exhibit non-Newtonian behaviour. These major disadvantages of the existing ash viscometers make them unsuitable for rheological measurements of coal ash under the conditions of interest in the present work. Thus, development of a more suitable high temperature ash rheometer that can directly measure rheological property of low-rank coal ash is urgently required.

This chapter contains six sections. The first section discusses about the design concepts of a new high-temperature rheometer are presented and described. The second section deals with descriptions of the newly developed high temperature rheometer. Details of the unique features of the rheometer are also described. Experimental technique and procedures are given in section three. Section four deals with coal ash preparations and chemical and mineralogical analyses used in this work. Testing of the rheometer with a standard fluid and a known viscosity material is presented in section five. Finally, conclusions are presented in section six.

3.2 DESIGN CONCEPTS AND FEATURES OF A NEW HIGH TEMPERATURE ASH RHEOMETER

The information obtained in the previous section has addressed the essential design concepts and the significant features that need to be included within the new high temperature ash rheometer. The new rheometer must have the capability of determining the fundamental rheological properties using the basic principle of rheomerty and fundamentals of fluid mechanics. This means the rheological properties of coal ash samples can be obtained without relying on calibrations with fluids of known rheological properties. The newly developed rheometer must provide the basic rheological data, especially shear stress and shear rate, to characterise flow behaviours of a tested fluid. Other significant features of a new ash rheometer are listed below:

- The new rheometer must be capable of directly performing measurements of the rheological properties of materials over a wide range of temperatures and operating conditions.
- The new rheometer must generate a uniform shear rate distribution, and overcome all slipping problems.
- The new rheometer must be capable of measuring torque over a significantly wide range.
- The new rheometer must be capable of withstanding high temperatures and reactive environments while in direct contact with corrosive molten ash.

The principle of rheological measurement is to establish the relationships between stress, strain rate and time for a particular test sample. Primary variables to be measured are, for most of the commercialised rheometers, torque, rotating speed and duration or deformation angles under different torque levels within a certain time. The torque is converted to stress value, while the deformation angle is converted to strain value in terms of measuring geometry being used. Thus, reliable and precise rheological characterisations of materials depend strongly on the quality of the measuring technique of primary variables.

In this work, a new ash rheometer is designed using concepts of the shear flow rheometry. There are four measuring geometries designed using the shear flow concepts; they are capillary flow, concentric cylinders (couette flow), cone and plate, and parallel disks (torsional flow). Of the four measuring geometries available, the cone and plate system is found to be the most suitable system that meets all the essential criteria and features.

There are several advantages of using cone and plate geometry. First the rheological data obtained from the system can be readily determined from the measured quantities without any elaboration and data reduction processes. Second, the cone and plate system requires a small amount of coal ash sample for each test. This implies that a uniform temperature distribution across the sample is easier to achieve. Third, the shear rate over the shearing surface of the sample is uniform provided that a small cone angle (< 4°) is used (Van Wazer et al, 1963). Therefore, the advantages of the cone and plate system make this geometry superior to the other geometries in the shear flow category. A schematic drawing of a cone and plate system is shown in Fig 3.1 where the cone is the rotating part.

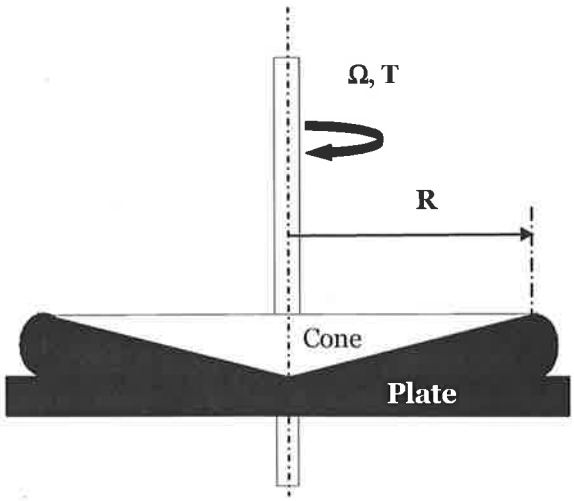

Fig 3.1: Schematic diagram for a cone and plate system

The cone and plate measuring system involves shearing a volume of molten sample contained in a thin gap between a flat plate and small angle cone. The resistance force of the tested sample to the shearing motion is transferred through the shaft and causes deflection of the torsion bar. Thus, shear stress can be calculated, based on the measured torque and the dimensions of the cone as given in the equation below:

$$\tau = \frac{3T}{2\pi R^3} \qquad 3.1$$

where T is torque on the cone and R is the cone radius. The shear rate in the sample can be calculated by:

$$\dot{\gamma} = \frac{\Omega}{\theta} \qquad 3.2$$

where Ω is the angular velocity of the rotating cone (Rad/s) and θ is the cone angle in radian.

However, there are possible sources of error for a cone and plate system, including edge fracture of the sample, sample ejecting of the geometry, slipping of the sample and particle jamming in the cone apex. For an ash sample, the ejecting of the ash sample may be the critical issue. Slipping of the sample and jamming of the coal ash particles may also affect rheological measurements, but these problems can be minimised by roughing surfaces of cone and plate and by truncating the cone tip respectively. The edge fracture of the sample appears to be minimal in this work. Comparing to other shear flow geometries, it is obvious that cone and plate is the most suitable geometry for a new high temperature ash rheometer.

3.3 THE HIGH TEMPERATURE RHEOMETER

3.3.1 General descriptions

The High Temperature Rheometer (HTR) constructed in this work has been designed for direct measurement of the rheological properties of coal ash under a controlled environment at temperatures between 600°C and 1300°C. This range of operating temperatures is similar to that of fluidised bed combustion and gasification of low-rank coals. A schematic diagram and a photograph show the equipment and its essential components, and these are given in Fig 3.2, and Fig 3.3.

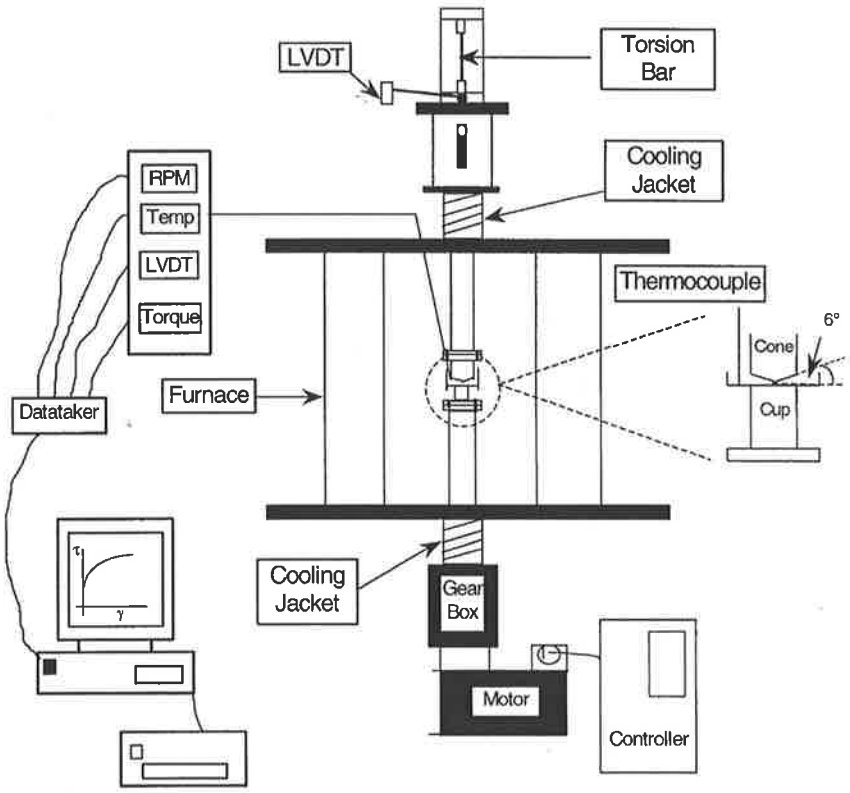

Fig 3.2: Schematic diagram of the ash rheometer rig

Fig 3.3: A photograph of the high temperature ash rheometer

The rheometer employs the cone and plate principle for rheological measurements, which involves shearing a volume of molten ash sample contained in a thin gap between a flat plate and small angle cone. The cone has a 6° angle with variable diameter ranging from 20 to 40 mm. The flat plate, which also acts as a crucible containing the sample, is attached to an AC motor equipped with a programmable controller to deliver constant speeds as required. The cone and plate geometry is constructed of a special alloy (Inconel 601) that can withstand the high temperatures and reactive environment, while in direct contact with the corrosive molten ash.

A vertical tube furnace equipped with a microprocessor temperature controller is used to heat the sample to the required test temperature of 1300°C. The temperature of the ash sample in the hot zone and in the measuring system is monitored using type K thermocouples. Interchangeable torsion bars, coupled with an LVDT (Linear Variable Differential Transducer) located at the top section of the HTR, are used to measure the torque imposed on the torsion bar. The shear stress can then be calculated based on the torque and the dimensions of the measuring unit. A data logger collects and stores data into a PC for on-line processing and analysis.

3.3.2 Detailed descriptions

The rheometer rig can be divided into four major sections as given below:

1. Torque measurement assembly
2. Rheological measuring unit
3. Temperature and ambient environment control unit
4. Ancillary devices and data acquisition unit

Torque measurement assembly unit

This unit was located at the top part of the HTR as observed in Figs 3.2 and 3.3. A clear picture of the torque measurement unit is given in Fig 3.4. It is shown that there are six different components in the torque measurement assembly, namely the torsion bar, the LVDT, the torsion bar anchorages, the stationary mount, the torsion bar arm and the regulator for adjusting position of measuring geometry in the torque measurement section.

The torsion bar unit was used to detect the angle of deflection, which is converted to torque. The torsion bar was calibrated using a standard weight method (Steerer et al, 1990). The LVDT (Lucas Schaevitz Inc) unit was used to measure the linear movement of an arm attached to the torsion bar. The shear stress is calculated based on the measured torque and the dimensions of the measuring unit.

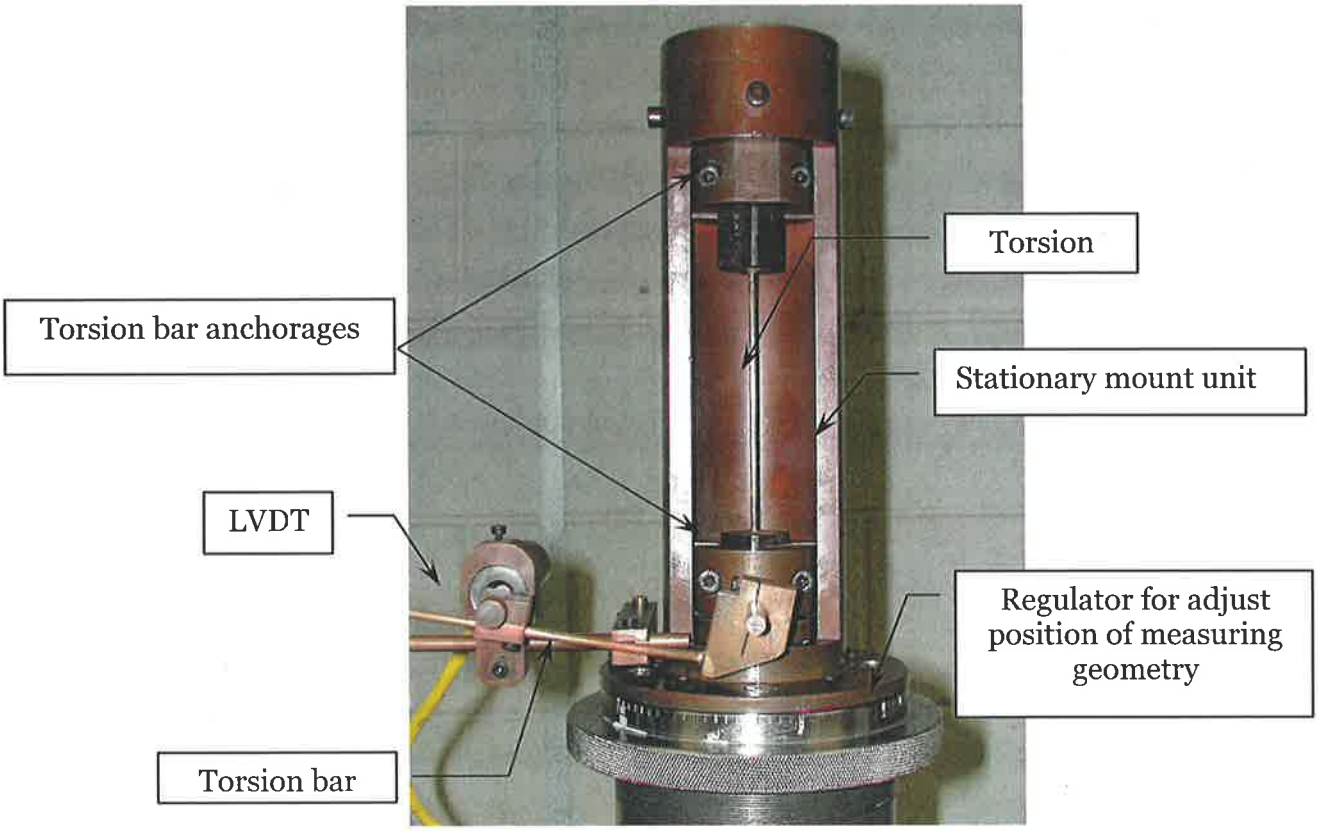

Fig 3.4: View of torque measurement assembly units

Fig 3.4 also shows that the torsion bar was firmly clamped between two torsion bar anchorages, which were located within the stationary mount unit. This means that the torsion bar is firmly placed in the stationary mount unit throughout the rheological measurement process. Moreover, using the torsion bar anchorage technique also allows the torsion bar unit to be changed by simply removing these anchorages. The torsion bar anchorages and the stationary mount unit were made from a stainless steel material.

The regulator unit was used to adjust the position of measuring geometry by turning the regulator either in clockwise or anti-clockwise directions in order to lower or raise the measuring geometry. With each full turn of the regulator, the position of the measuring geometry is changed by 1mm. The speciality of using the regulator technique is that the gap width of the cone and plate geometry can be precisely controlled.

Measuring geometry unit

Fig 3.2 shows that the measuring geometry is located inside a furnace, and it is a cone and plate system. Fig 3.3 also reveals that the cone section was connected to an upper shaft, which was attached to the torque-measuring unit. The plate section was connected to a lower shaft, which was attached to an AC motor.

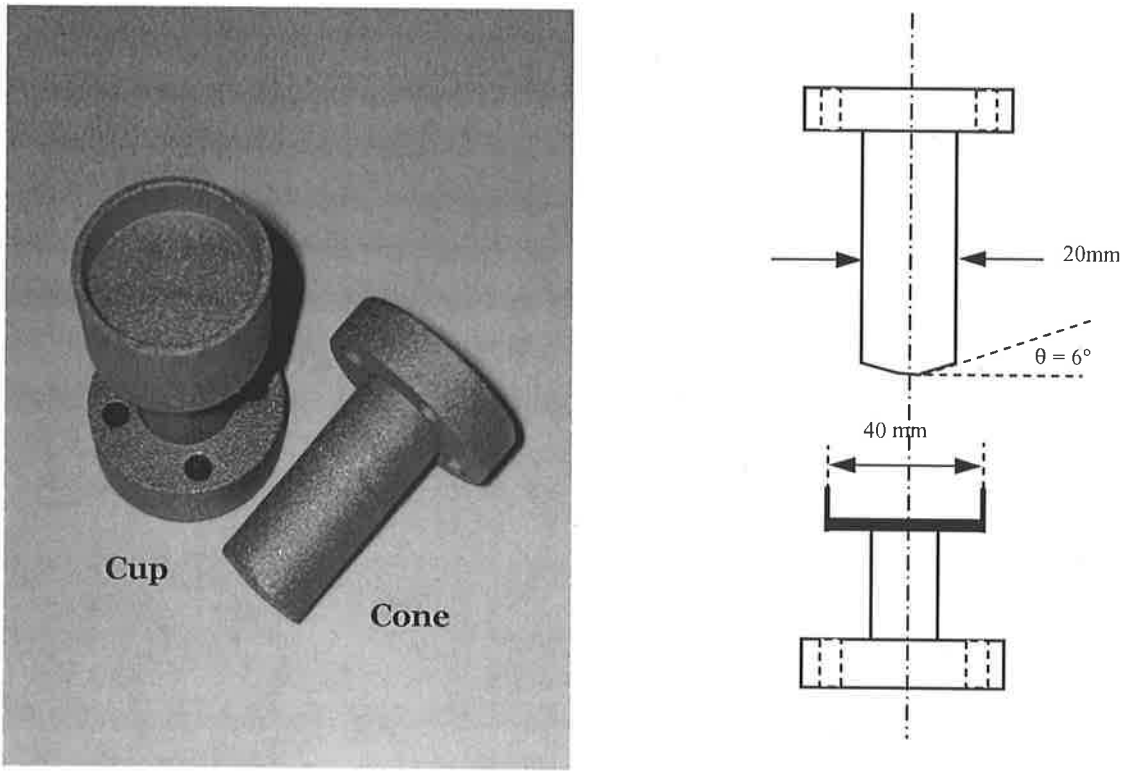

Fig 3.5: (a)- A photograph of the cone and parallel plate geometries used in this study; **(b)**- A schematic diagram of the cone and parallel plate geometries used in this study

With regard to the rotating plate section, this section was comprised of an AC motor (Baldor Electric Co., Ltd), which was used to drive the plate through a lower shaft. With the system developed here, it was designed to allow the motor to connect with the lower shaft either directly or through a gearbox. The AC motor was equipped with a programmable controller (Baldor Electric Co., Ltd) for controlling the rotational direction of the motor, rotating speed and accelerating rate of the motor. With the controller unit used, the cup could be rotated either in a clockwise or anti-clockwise direction.

It was found by trial and error that the minimum steady rotational speed achievable with the AC motor was 5 rpm with fluctuation of ± 1 rpm. This implies that with the use of a 10:1 ratio gearbox the minimum rotational speed of the bottom shaft was 0.5 rpm. After obtaining the rotational speed of the motor, the shear rate value can be calculated in terms of the measuring geometry using the equation 3.2, where Ω is the angular velocity (Rad/s) of the rotating cup and θ is the cone angle (6°).

In this work surfaces of the cone and plate units were roughened by the sand blasting technique in order to minimise the slip problem. For particle jamming in the cone apex, the tip of the cone was truncated with a dimension of 2 mm.

Temperature and ambient environment control chamber

A vertical tube electric furnace (Ceramic Engineering Co., Ltd) equipped with a microprocessor control unit was used. It has the ability to achieve a constant temperature at temperatures ranging from 500°C to 1300°C.

The vertical tube furnace consisted of four-spiral type heating elements (Kanthal AMP Co., Ltd), and a ceramic tube, which were all installed inside a stainless steel case. The dimensions of the ceramic tube were 60 mm ID × 70 mm OD × 600 mm L. During the operation, the ceramic tube was heated by the heating elements up to the desired temperature. Simultaneously, the heat energy was transferred from the ceramic tube to the measuring geometry and test sample by convection.

The reason for using the ceramic tube is to transfer heat to the test sample instead of heating the sample directly was to ensure that clean and uniform heat transfer can be delivered. Moreover, the ceramic tube also acts as an environment control chamber. A desired gas mixture (neutral, reducing or oxidising) can be introduced into the furnace chamber to control the test environment. With a good seal at both ends of the ceramic tube and due to the non-porosity of the ceramic tube surface, this can ensure that the test environments can be fully controlled.

Ancillary devices

The ancillary units in this device included water and gas valves, a cooling water system, thermocouples, a pressure gauge for compressed air, a pneumatic air lift jacket, several boxes for sheltering main switches, a relay device and signal converter, a flow monitor for the cooling water, an alarm bell, a warning light, an electronic display panel, and a data taker.

A copper tube with an inside diameter of 1/4" was used to make the cooling water system. The system is located just above the furnace unit as shown in Fig 3.2. A thermally actuated flow monitor (A.P.C.S Co., Ltd) was used to monitor the flow of the cooling water system. The cooling water system and flow monitor system used in this work was designed as a safety system as well as for preventing the bearings and the HTR from over heating. If no flow is detected, the flow monitor sends a signal to the relay device to

bypass the current from the furnace to the safety switch to turn the warning light and alarm bell on. If this situation occurs then the furnace cannot be heated up.

A type K thermocouple was (Pyrometric Instrument Co., Ltd) used to measure the temperature of the test atmosphere and sample. Two pneumatic air lift jackets (FESTO) with maximum operating pressure of 120 bars or 180 psi were used to move the furnace up and down. A signal converter (A.P.C.S Co., Ltd) was used to convert the signal from digital to analog before it was displayed on electronic display panels (Inspecta Co., Ltd). There were four display panels on the display board. They are motor speed; motor torque, temperature, and LVDT display panels. At the display panels, the input signals were corrected by a data logger (Pico Technology Co., Ltd) and the data was stored into a PC for on-line processing and analysis. The data logger also converted the input signal to a given parameter, and to produce text and graphical reports.

3.4 SELECTION OF MATERIALS FOR CONSTRUCTING CONE AND PLATE GEOMETRY

Chapter 2 (section 2.3.4) revealed that molybdenum was the material most commonly used to make the measuring geometries. However, molybdenum is not stable under the oxidising atmosphere as the material is oxidised and forms a crystalline phase. Moreover, molybdenum is dissolved in sulphur dioxide, causing a significant weight loss of the material (Boow, 1961). Alumina and graphite were not considered in this work. This is due to the fact that these materials are too fragile. Platinum-rhodium was also not an option due to its high cost.

In this work, Inconel (Inconel-601, Aus-Steel Co., Ltd) was used for constructing the cone and plate units. This material is a high nickel content steel, which has a melting temperature at above 1500°C. The material is also not sensitive to chemicals, especially sulphur dioxide. Most importantly, Inconel is relatively cheap.

3.5 RELATIONSHIP BETWEEN FURNACE TEMPERATURE AND SAMPLE TEMPERATURE

A relationship between furnace temperature and sample temperature was established by measuring the temperature of the coal ash sample as a function of furnace temperature. In this work, the cup was heated to the desired temperature, and after one hour of isothermal holding the appropriate amount of dry coal ash sample was loaded onto the plate. Simultaneously, three thermocouples of type K (Pyrometric Instrument Co., Ltd)

A, B and C were inserted into the sample as shown in Fig 3.6. The thermocouples A and C were placed close to the edge of the coal ash sample, while the thermocouple B was placed at centre of the sample, and the heating was continued. The main reason of using three thermocouples was to determine the temperature gradient within the coal ash sample simultaneously.

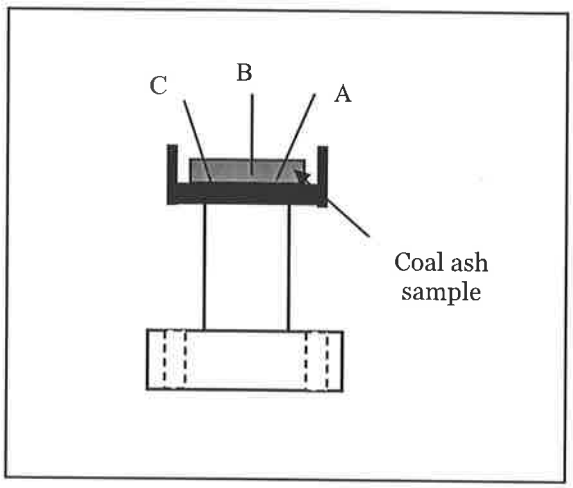

Fig 3.6: A schematic shows testing of temperature gradient of coal ash sample

In this work, the temperature distribution of coal ash sample was determined by the calculation of the temperature difference between the thermocouples A and B, and between the thermocouples B and C. Temperature distribution within coal ash sample is shown in Fig 3.7.

It appears that the distribution of temperature in the coal ash sample from the thermocouple B (temperature at centre of sample to the thermocouples A and C vary within ±1°C, indicating a relatively small temperature distribution within the coal ash sample. Based on the temperature difference, it confirmed that the temperature in the cone and plate geometry was uniform, and that the temperature at the centre of sample may be referred as the sample temperature. In addition, Fig 3.8 shows a relationship between furnace temperature and sample temperature.

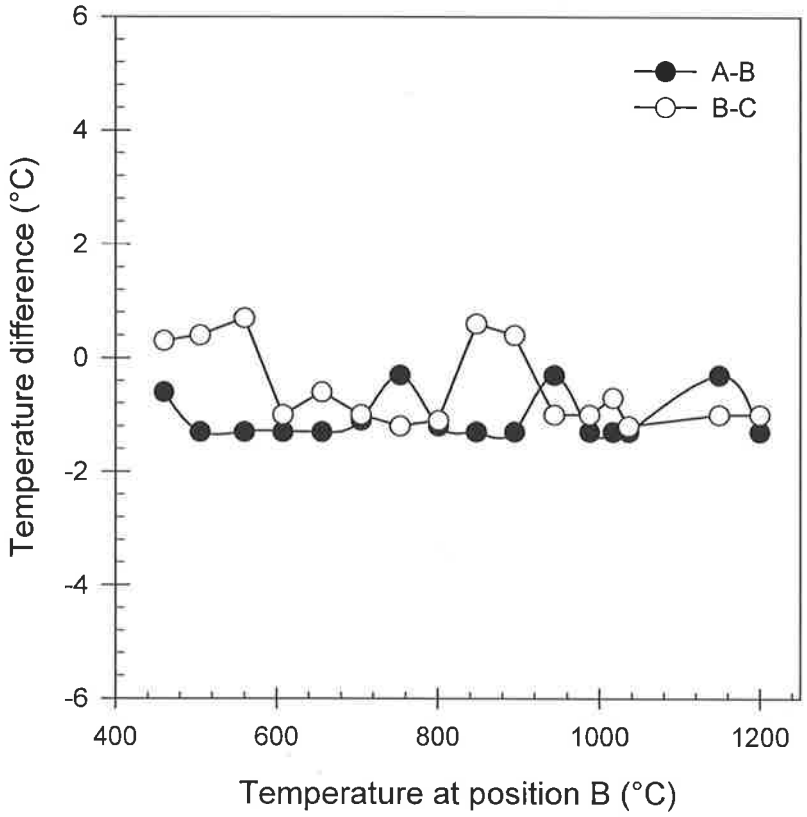

Fig 3.7: Temperature difference in coal ash sample

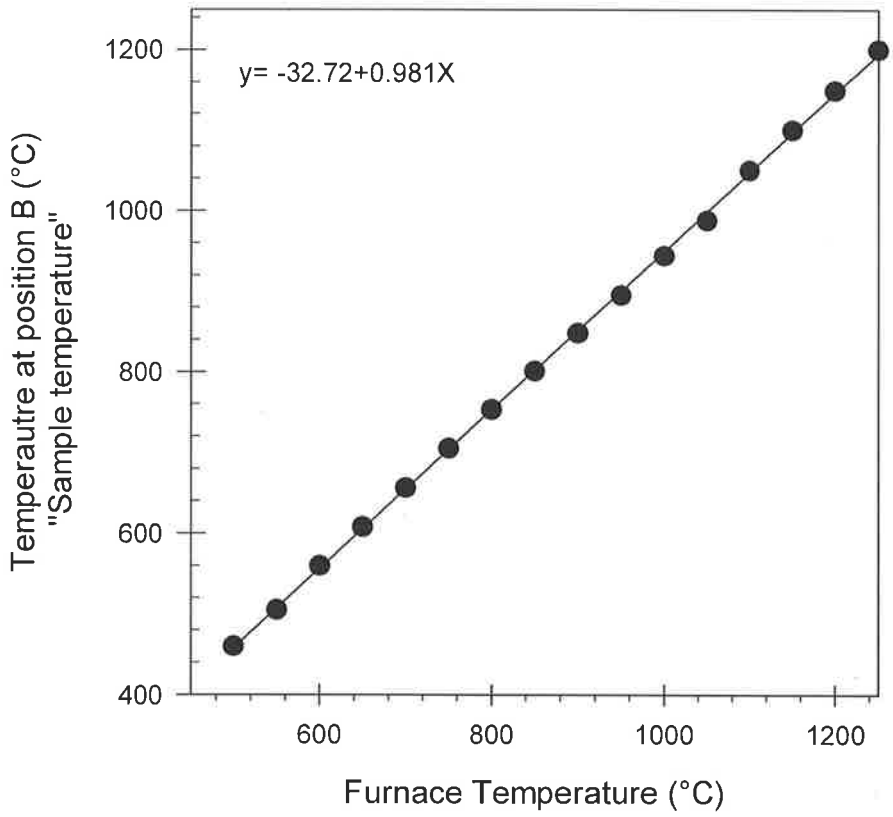

Fig 3.8: Relationship between furnace temperature and temperature at the central of sample (the position B)

Fig 3.8 clearly demonstrates a linear relationship between furnace temperature and sample temperature. Based on the empirical relationship between furnace and sample temperature, it was found that there was an approximately 30°C difference between temperature at the furnace and at the sample. By using the empirical relationship, the temperature of coal ash sample at a desired furnace temperature could be estimated.

3.6 EXPERIMENTAL PROCEDURES AND TECHNIQUES

3.6.1 Experimental procedures

Rheological measurements on the coal-ash at high temperatures were carried out using the following procedure. First, the measuring cone-plate system together with the upper and lower shafts were preheated to a desired temperature in order to correctly set a zero gap setting between the cone and the plate. The zero gap was then determined and marked on a gap regulator after the measuring system had been in a state of thermal equilibrium for at least one hour. This enabled the materials of the measuring system and shafts to be fully expanded at the test temperature. The cone was next raised by means of the gap regulator, and the appropriate amount of dry coal ash sample was loaded onto the plate.

A desired gas mixture (neutral, reducing or oxidising) was introduced into the furnace chamber to control the test environment. The sample was then heated to the test temperature, and heating was continued at this temperature for at least one hour to ensure that the whole sample reached a state of thermal equilibrium. The cone was then lowered to a preset gap and the sample was allowed to stand for half an hour to eliminate any stress in the sample due to loading. Testing commenced by rotating the plate at a low speed and measuring the torque acting on the cone. The rotational speed was then increased in steps and the torque response at each constant speed recorded. After each test run at a fixed temperature, the molten ash sample was removed and discarded.

3.6.2 Experimental techniques

In the studies of rheological characteristics of low-rank Australian coal ash samples (Chapter 4) and synthetic ash mixtures (Chapter 5), two measuring techniques were used. They are the sweep shear and the steady shear techniques.

In the sweep shear method, the shear rate is increased linearly from zero to a maximum shear rate, followed by linear decreases back to zero. Simultaneously, the shear stress is measured as a function of shearing time and shear rate. This type of experiment is often

used to investigate and to demonstrate time and shear dependency of the test sample. If the test sample is a time dependent material, hysteresis loop of the flow curve will be observed. If no hysteresis loop is observed, it can rightfully be assumed that the test sample is a time independent material.

The steady shear experiment involves shearing a sample at a constant shear rate. The apparent viscosity, defined as the ratio of shear stress to shear rate, is measured as a function of shearing time until the equilibrium in viscosity is reached. Ideally, a fresh sample is required for each steady shear test, but in this study this was not practical. This is due to the high operating temperature of the rheometer, which constrains the ability to remove and reload the sample after each test. From experimental trial and error, it was found that after each equilibrium state at a given shear rate had been achieved, the sample needed to be rested for a minimum period of 2 hours before a new measurement at a new shear rate value is commenced.

3.7 COAL ASH PREPARATIONS AND ANALYSES

3.7.1 Ash preparation

In this work, three low-rank Australian coal ash samples were prepared in a laboratory muffle furnace. The three laboratory ashes prepared were from two South Australian coals, Bowmans and Lochiel, and one Victorian coal; Loy Yang. The laboratory ashes were prepared using the Standard Ash Procedure (Standard Australian-AS 4264.3, 1996). The technique used is described below:

1. A raw coal sample was crushed, and then sieved to a maximum particle size of 212 μm.
2. The sieved sample was heated at temperatures of 500°C in a rich air atmosphere for 60 minutes.
3. The preheated sample was further heated at a fixed temperature of 800°C for 2 hours before the furnace was cooled down and the coal ash samples collected. During this process the sample was randomly stirred in order to cook the coal sample completely.
4. It should be noted that the furnace door was left slightly open to provide sufficient airflow and maximise sulphur retention. This is an essential requirement of the procedure.

In addition, three other low-rank coal ash samples obtained from Circulating Fluidised Bed Combustion (CFBC) plant were also used. Theses three CFBC's ashes were the ashes retained from the fluidised bed chamber by the fluidising gas. These fly ash samples were collected with a fabric filter unit (Bhattacharya et al, 1999). For the CFBC's ashes, two were from Victoria (Loy Yang ash and Morwell ash), and one from South Australia (Lochiel ash). All of the CFBC's samples were generated by combusting the Loy Yang coal, the Morwell coal or the Lochiel coal at a temperature of 850°C under a rich air atmosphere.

To distinguish clearly between the laboratory ash and the CFBC ash, the laboratory ashes have been labelled with capital **A** and the CFBC ashes are labelled with capital **B**. Thus the laboratory ashes are referred to as Loy Yang-**A** ash, Lochiel-**A** ash and Bowmans-**A** ash, while the CFBC ashes are referred to as Loy Yang-**B** ash, Lochiel-**B** ash and Morwell-**B** ash.

3.7.2 Ash analyses

Chemical analysis

Composition of coal ash is a key factor that affects its rheological characteristics and properties. Therefore, a proper analysis for ash composition is vital to precisely estimate the ash viscosity and tailor its value to meet the requirement of long-term processing operation of fluidised-bed combustion and gasification. Coal ash usually consists of organic (eg organic sulphur) and inorganic components. The inorganic components normally contain minerals (eg. Pyrite and marcasite) and non-mineral matters migrated by diffusion through coal (eg. iron, calcium, magnesium, sodium, aluminium and sulphur).

Calculation of coal ash composition from direct analysis of minerals and non-mineral inorganic elements in coal can be performed, but it requires ash formation chemistry and the assumption in which coal ash retains all inorganic elements presented in the coal except sodium and chlorine. The chemical analysis of coal ash samples was carried out using the Australian Standard for Coal Ash Chemical Analysis (Standard Australian 1038.6.3.1, 1986). In this work an external party, AMDEL Co Ltd in Adelaide, South Australia, performed analysis of coal ash chemical composition. The analysis procedure is given below:

1. A coal ash sample was preheated in a rich air atmosphere at 600°C for three hours and the sample weight loss was monitored.
2. The sample was fused with sodium metaborate at 900°C to separate cations species from the oxides species.
3. The fused sample was added in nitric acid to extract the cations from the ash samples.
4. Chemical compositions were determined by an Induction Coupled Plasma (ICP) - Mass Spectrometer (MS) for minerals.

Thermal Mechanical Analyser (TMA)[1]

The TMA is an instrument used to record the change in height or of the tested sample as a function of temperature under a constant heating rate (TA-Inst Co., Ltd, Newcastle, DE, USA). The information obtained was used to determine the phase change temperature of a coal ash sample. This temperature is important as it indicates the temperature at which a liquid phase is formed inside the ash sample. The phase change temperature also determines a starting temperature at which a rheological measurement can be performed. In this work, the phase changing temperature was measured within a temperature range of 800 to 1200°C, which is similar to the operating temperature in a fluidised bed combustion unit (Manzoori, 1990; Skrifvas et al, 1995; Bhattacharya, 1999; Vuthaluru et al, 2001). The procedure used is given below:

1. A coal ash sample was placed inside an aluminium crucible where it was compacted to a diameter of 3 mm and a height of 5 mm.
2. The compacted sample was placed inside a furnace where there was a probe positioned firmly on the top section of the sample. The other end of this probe was connected to a scale that detected movement of the probe.
3. The furnace was heated from room temperature to a maximum temperature of 1200°C at a constant heating rate of 20°C/min. Simultaneously, the height of the sample (position of the probe) was recorded.
4. This process continued until the maximum temperature of 1200°C was reached.

Scanning Electron Microscope (SEM-EDX)[2]

Generally, the SEM technique measures the reflection of electron beams on a tested sample and creates the magnified images by using these reflections. A high density composition (a solid phase) causes more reflection of the electron beam than a low

[1] The TMA experiments were conducted by an external body (HRL Co Ltd, Melbourne, Victoria).
[2] In this work, the SEM was performed by a researcher at Adelaide Microscopy (CEMSA, University of Adelaide, Adelaide, Australia).

density composition (a molten or liquid phase). Also values of the electron beam reflection are counted and then used to calculate the proportion of chemical components in the tested sample. The energy-dispersive X-ray system (EDX) was used for elemental analysis of individual ash particles.

In order to perform the SEM test, a tested sample was first mounted in an epoxy resin with dimensions of 1"x1"x0.5"[3]. Secondly, surface of the mounted sample was polished and coated with a carbon composite material in order to gain a good electron conductivity of the sample[4].

X-Ray Diffraction (XRD)[5]

The XRD technique involves measuring the diffraction of an x-ray beam on a tested sample. The pattern of the x-ray diffraction is converted into possible chemical species and formations. Simultaneously, values of the diffraction are counted and converted to concentrations of chemical species/formations. The XRD technique was used to determine phase formation of chemical compounds in coal ash samples.

3.8 TESTING OF THE RHEOMETER

It is necessary to test the newly developed high temperature rheometer for its accuracy and reliability using Newtonian fluids of known viscosities. In this work, the newly develop ash rheometer was tested with a certified material (borosilicate glass) and a known viscosity material (a ternary oxide mixture).

3.8.1 Testing with viscous standard fluid (Borosilicate glass)

Fig 3.9(**a**) shows the results obtained for a certified standard borosilicate glass (Corning Inc.) using the cone and plate system. The borosilicate glass is commonly used as a reference material for high-temperature viscosity measurements, in the form of shear stress versus shear rate plots. Over the test temperature range of 840°C to 920°C, where the material is completely molten, the observed rheological flow curves are linear and pass through the origin. This behaviour is typical of Newtonian fluids whose viscosity is dependent on temperature only. In Fig 3.9(**b**), the viscosity determined from the slopes of the linear shear stress-shear rate flow curves is plotted as a function of temperature and compared with the certified standard viscosity data. It can be seen that the

[3] Mounting of the low-rank coal ash samples were performed at Ian Pontifex Co., Ltd, Adelaide, SA.
[4] Coating of the mounted sample was carried out by CEMSA.
[5] In this work the XRD measurements were conducted by CSIRO (Land and Water Division-Adelaide, SA).

agreement between the viscosity data obtained using the ash rheometer and the reference viscosity is excellent, with a level of error at ± 7 percent.

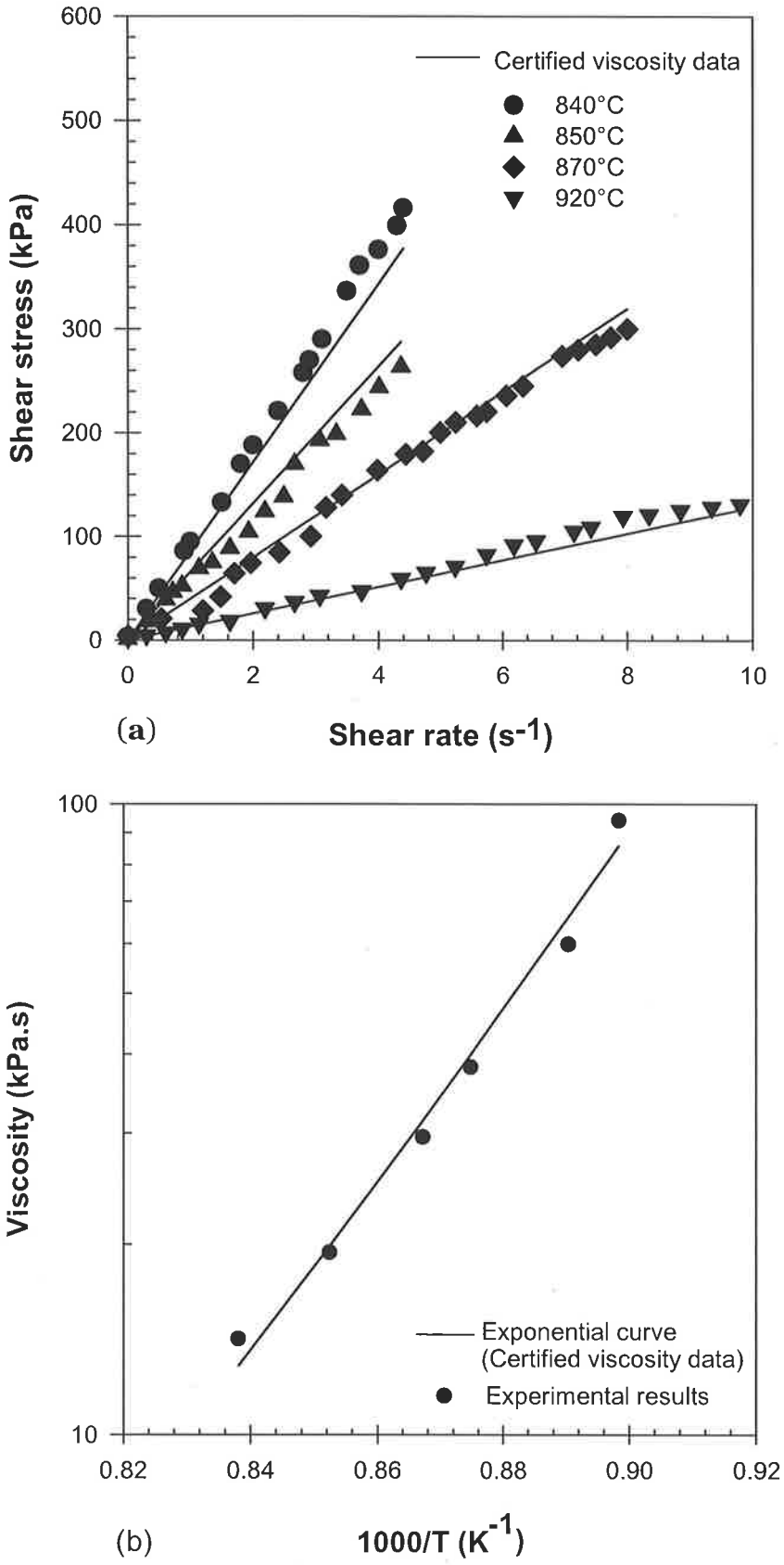

Fig 3.9: (a)-Experimental flow curves for borosilicate glass standard as function of temperature; **(b)**-Comparison with certified viscosity data

3.8.2 Test with ternary oxide eutectic mixture

A ternary oxide mixture composed of 38% CaO, 20% Al_2O_3 and 42%SiO_2, for which viscosity data is available in the literature, has also been prepared and tested using the ash rheometer. Fig 3.10 (**a**) shows the experimental shear stress-shear rate data for the melt as a function of temperature ranging from 1150°C to 1300°C. The results indicate that this oxide melt is Newtonian over the range of temperatures used for the tests. In Fig 3.10 (**b**), the measured viscosity data is compared with the published data for the melt from other studies over a higher temperature range of 1300°C to 1600°C (Belyankin et al, 1954; Elliot et al, 1963; Slag Atlas, 1995). The agreement between the data obtained using the high-temperature rheometer and the literature data is excellent, as demonstrated by the fact that all of the viscosity - temperature data can be fitted by a single Arrhenius model over the whole temperature range of 1100°C to 1600°C.

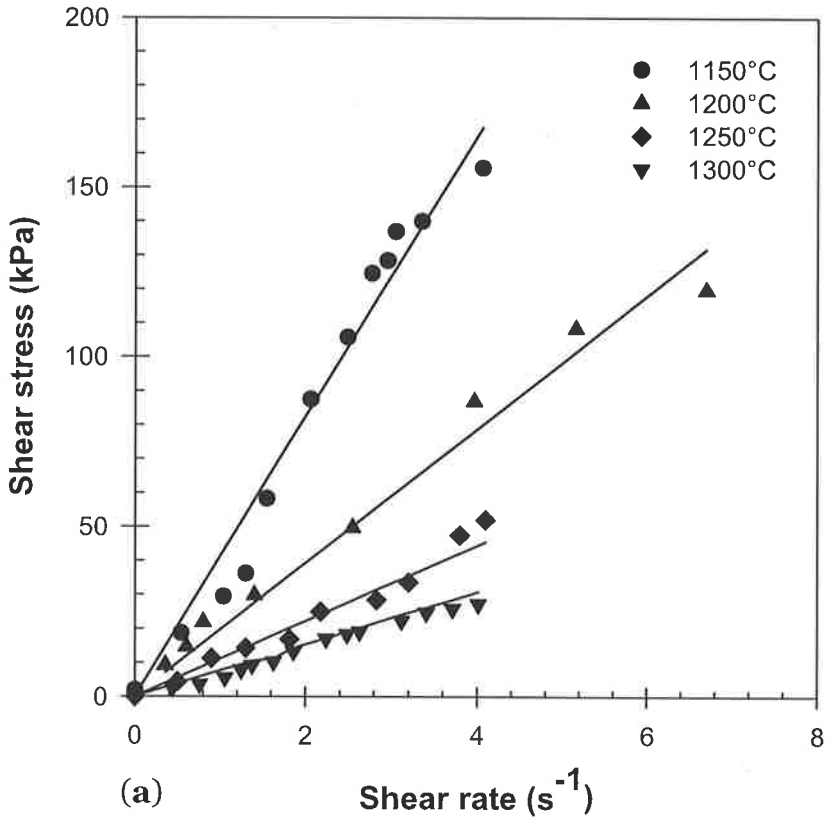

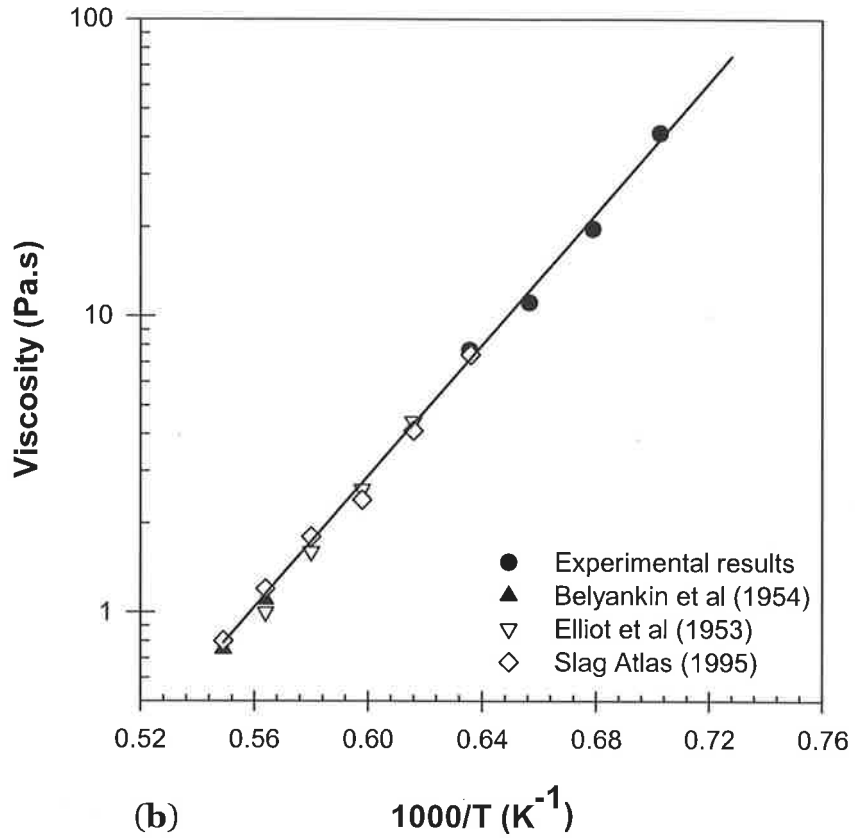

Fig 3.10: (a)-Experimental flow curves for the ternary oxide melt;
(b)-Comparison between measured viscosity and reference data

3.9 CONCLUSIONS

- The ash rheometer developed in this work is unique in that it is designed based on the principles of viscometric flow for measuring rheological behaviour of material under operating conditions relevant to fluidised bed processing of low-rank coals.

- The newly developed high temperature rheometer is equipped with a cone-plate measuring system. The cone-plate geometry is constructed from a special alloy that can withstand high temperature and reactive environments while contacted with corrosive molten ash. There are several advantages to the use of the cone-plate system. They are: uniform shear rate distribution across the shearing surface, a small amount of sample is required for each test, and the rheological data that is obtained can be readily determined without any elaboration.

- The rheometer was tested with two different materials to establish its suitability and accuracy for rheological measurements at high temperatures, without using any calibrations. The materials used were a borosilicate glass (standard glass material) and a ternary oxide eutectic mixture (reference material). All rheological measurements were performed using a cone and plate measuring system. Excellent agreement was found between the HTR results and the certified viscosity value (borosilicate glass) as well as the viscosity data of the ternary oxide mixture.

- In this work, six Australian low-rank coal ashes are used. Three were prepared in a laboratory muffle furnace, and the other three were collected from a CFBC plant. The laboratory's ashes were prepared from two South Australian coals, Bowmans and Lochiel coal and one Victorian coal, Loy Yang coal. The CFBC's ash was the fly ash obtained from the fluidised bed chamber. For the CFBC's samples, two were Victorian ashes (Loy Yang and Morwell ashes), and one was from South Australia (Lochiel ash).

CHAPTER FOUR

Rheological Properties of Australian Low-Rank Coal Ash

4.1 INTRODUCTION

In this chapter the flow characteristics and properties of low-rank Australian coal ashes at temperatures ranging from 850°C to 1200°C are presented. Flow characteristics and properties of six low-rank Australian coal ashes were measured. Three were generated in a laboratory furnace and the other three were produced in a Circulating Fluidised Bed Combustion (CFBC) plant located in Osborne, South Australia. The particular aims of this work are to answer the following questions:

1. What are the flow characteristics of low-rank Australian coal ash at temperatures between 850°C and 1200°C?
2. How does the chemical composition of low-rank Australian coal ash affect its flow properties and characteristics?
3. How does operating temperature affect the flow characteristics of low-rank Australian coal ash?
4. How does atmospheric condition affect the flow characteristics of low-rank Australian coal ash?

This chapter is divided into four sections. The first section gives details about the coal ash samples and chemical composition of the ash samples. The second section covers details of experimental methods used for rheological measurements of coal ash samples. The time and the shear dependency of the coal ash samples are investigated. Development of time dependent models and equilibrium flow curves are also presented. The third section presents effects of operating temperature, chemical composition and operating atmosphere on flow properties of the coal ashes. Finally, conclusion and answers to the questions outlined earlier are given in the fourth section.

4.2 COAL ASH SAMPLES

4.2.1 Chemical composition of coal ash

In this work, an external party, AMDEL Co Ltd in Adelaide, South Australia, performed the analysis of coal ash chemical composition. The analysis was carried out using the Australian Standard for Coal Ash Chemical Analysis (Standard Australian 1038.6.3.1, 1986), and details of the analysis procedure were described in chapter 3, section 3.7.2. Table IV.1 shows the chemical analysis of the low-rank coal ash samples studied in this work.

Table IV.1: Chemical analysis of the low-rank Australian coal ash samples studied[1]

Source of coal ash	LOI (%)	SiO_2 (%)	Al_2O_3 (%)	Fe_2O_3 (%)	CaO (%)	MgO (%)	K_2O (%)	Na_2O (%)	TiO_2 (%)	SO_3 (%)
Loy Yang-**A**	10.9	40.3	15.3	9.7	4.6	6.6	0.5	4.8	0.5	6.6
Lochiel-**A**	6.7	23.3	5.7	5.3	10.9	8.9	0.3	12.8	0.5	30.6
Bowmans-**A**	2.7	20.9	7.7	1.7	7.0	10.0	0.1	16.2	0.1	33.6
Loy Yang-**B**	4.3	34.7	16.9	4.2	4.5	9.5	0.4	7.9	1.1	11.5
Lochiel-**B**	3.3	21.7	4.1	7.7	14.8	7.1	0.4	11.0	0.2	29.5
Morwell-**B**	5.9	16.4	7.7	11.1	25.0	13.0	0.4	4.2	0.3	16.0

The chemical analysis data in Table IV.1 shows that the concentration of SiO_2 was above 20 % weight in most of the coal ash samples, the exception being the Morwell-**B** ash where the concentration of SiO_2 was found to be 16.4 %wt. The concentrations of the other chemical components such as Na_2O, Fe_2O_3, MgO and CaO were found to vary from sample to sample. However, the concentrations of TiO_2 and K_2O components were similar in all six coal ash samples used, as the concentration of these two chemical species was below 0.5 %wt in each of the coal ash samples.

It was also found that there is a difference between the concentration levels of chemical compositions in ash from the same coal that were obtained differently, indicating effects of the ash preparation on the concentration levels of chemical components in coal ash. Comparing the chemical concentration between the Loy Yang-**A** (laboratory ash) and the Loy Yang-**B** (CFBC ash), it was found that the Loy Yang-**A** is lower in concentration of MgO, Na_2O and SO_3 than the Loy Yang-**B** ash, but the Loy Yang-**A** is higher in Fe_2O_3

[1]Concentration of all chemical compounds listed in Table IV.1 is in %weight unit (% wt)

concentration than the Loy Yang-**B** ash. This may be because of in the CFBC unit, there is a possibility of the evaporated compounds of MgO, Na_2O and SO_3 coming into contact with fly ash particles and deposited on the surface of fly ash particles. Unlike the laboratory ash, the evaporated compounds of MgO, Na_2O and SO_3 are permanently released from the ash particles during preparation. The Fe_2O_3 component is not evaporated and it remains on the ash particles. This may be the reason why the concentration of the Fe_2O_3 component in the laboratory ash is higher than it is in the CFBC ash. The CaO compound is also evaporated during fluidised bed combustion process and deposited on the surface of the fly ash particles, resulting in a higher concentration of the CaO component in the Lochiel-**B** (14.8%wt) than in the Lochiel-**A** ash (10.9 %wt).

Comparisons between the laboratory ash samples found that the Bowmans-**A** and Lochiel-**A** are high in concentration levels of SO_3, CaO and, MgO and Na_2O components. The Loy Yang-**A** was high in the concentration level of Al_2O_3 component. For the CFBC ashes, the Lochiel-**B** was high in SO_3 component, while the Loy Yang-**B** was high in Al_2O_3 component, and the Morwell-**B** was high in concentration levels of CaO and MgO components.

4.2.2 Measurement of the coal ashes phase changing temperature

The phase changing temperature of a coal ash sample is important as it indicates the temperature at which a liquid phase is formed inside the ash sample. The temperature also determines a starting temperature at which a rheological measurement can be performed. In this work, the phase change temperature was measured within a temperature range of 800 to 1200°C, which is similar to the operating temperature in a fluidised bed combustion unit (Manzoori, 1990; Skrifvas et al, 1995; Bhattacharya, 1999; Vuthaluru et al, 2001). The procedures used to measure phase changing temperature were described in section 3.7.2 in the previous chapter.

Table IV.2: Temperatures where phase changes occurred for the coal ash samples

Source of coal ash	Solidus temperature (°C)	Liquidus temperature (°C)
Loy Yang-**A**	793	1097
Lochiel-**A**	710	1019
Bowmans-**A**	680	1003
Loy Yang-**B**	806	1127
Lochiel-**B**	725	1012
Morwell-**B**	826	1143

Data of the TMA in Table IV.2 shows that there are two temperature points, one lower than the other, where phase changing in the coal ash samples occurred. The first temperature corresponds to the solidus temperature, the lowest temperature at which a liquid phase is formed in the ash matrix (Watt, 1969). The second temperature, the liquidus temperature, is the highest temperature at which that phase changing occurs within the temperature range of interest in this work. Based on the TMA results, the minimum temperature at which a liquid phase is formed, and hence the minimum temperature for rheological measurements is 850°C.

Comparing the solidus and liquidus temperatures in Table IV.2, it can be seen that the solidus temperatures of the Lochiel-**A**, **B** and Bowmans-**A** ashes are lower than the Loy Yang-**A**, **B** and Morwell-**B** ashes. A liquid phase is starting to form in the Lochiel-**A**, **B** and Bowmans-**A** ashes at a temperature below 700°C, while a liquid phase appears in the Loy Yang-**A**, **B** and Morwell-**B** ashes at a temperature above 810°C. The liquidus temperature of the Lochiel-**A**, **B** and Bowmans-**A** ashes was at 1000°C and at 1150°C for the Loy Yang-**A**, **B** and Morwell-**B** ashes. The differences seen in the solidus and liquidus temperatures of the coal ashes prepared from different sources may result from the variations in the samples' chemical compositions. It appears that ash with high concentrations of Na_2O and SO_3 has lower contraction temperatures than those with high concentrations of Fe_2O_3, Al_2O_3 and CaO.

4.3 MEASUREMENTS OF RHEOLOGICAL PROPERTIES OF COAL ASH

Two measuring techniques were used to measure flow characteristics and properties of the six low-rank Australian coal ashes in this study. They are the sweep shear and the steady shear techniques. Details for these two measuring techniques have been already given in section 3.6.2. In this work the sweep shear test was performed by loading a fresh coal ash sample into the cup of the high temperature rheometer. After a period of 30 minutes, to allow the material to recover from any stress incurred in the loading process, the sweep process is started. In addition, it must be noted here that the sweep shear and steady shear experiments were performed with the laboratory samples only. There were no sweeping shear and steady shear experiments performed with the CFBC's ashes. This is due to the amount of the CFBC's ash samples obtained, which constrained the investigations.

4.4 RESULTS FROM RHEOLOGICAL TESTING

4.4.1 Sweep shear results

Figs 4.1 shows the sweep shear results of the three laboratory ash samples tested at a temperature of 850°C. In this work, the maximum shear rate value was restricted to 10 s^{-1}. This is because at a higher shear rate, the tested sample was pushed off the cone and plate system, resulting in errors in the shear stress value. Moreover, the fastest sweep cycle time possible was found to be 10 minutes. At a quicker sweeping cycle, the tested sample was also ejected out off the measuring geometry. Thus, the maximum operating conditions of sweep shear experiments in this work were a sweeping cycle time of 10 minutes at a maximum shear rate of 10 s^{-1}.

Fig 4.1 shows that the apparent viscosity decreases with time as the shear rate is increased from zero to the maximum value and subsequently increases with time as the shear rate is decreased from the maximum back to zero. The experimental results clearly demonstrate a viscosity hysteresis, which is typical of a thixotropic fluid, as the up-curve (corresponding to the ascending shear rate) always lies above the down-curve (descending shear rate). In addition, the area enclosed by the hysteresis loop is often quantitatively indicated as the material's degree of thixotropy. It was found in this study that the area of hysteresis loops for the Loy Yang-**A** ash is larger than that in the Lochiel-**A** and Bowmans-**A** ashes. It must be firstly note here that the area enclosed by the hysteresis loop depends on the cycle time as well as the maximum shear rate tested. Thus, based on the sweep shear conditions of sweep cycle of 10 minutes and a maximum

shear rate of 10 s^{-1}, the degree of thixotropy of the Loy Yang-**A** ash is higher than the Lochiel-**A** and Bowmans-**A** ashes.

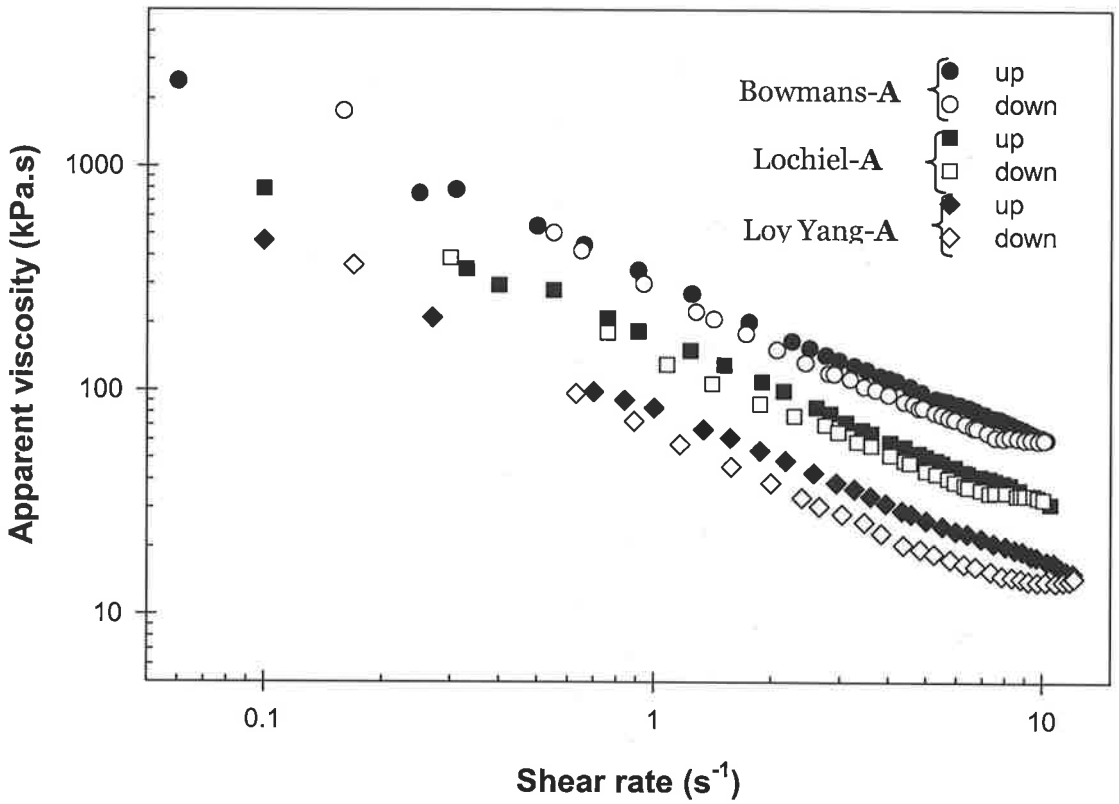

Fig 4.1: Transient viscosity behaviour of the laboratory's ash samples (the Bowmans-**A**, the Lochiel-**A** and the Loy Yang-**A**) at 850°C: Total sweep time =10 minutes

4.4.2 Steady shear results

Fig 4.2 shows plots of apparent viscosity, defined as the rate of shear stress to shear rate, versus shear time for the three laboratory ash samples. The experimental results were obtained by shearing the coal ash samples at a fixed shear rate of 3 s^{-1} and at a fixed temperature of 850°C. The experimental results show that viscosity values of the coal ash samples decreased rapidly with time within the first few minutes of shear before approaching their equilibrium states after five minutes.

Focussing on the initial viscosity value (η_o), defined as the viscosity at t=0 or the 'structure state', it can be seen that the initial viscosity of the South Australian ashes is higher than that of the Victorian ashes. This indicates that the structure of Lochiel-**A** and Bowmans-**A** ashes is stronger than the structure of the Loy Yang-**A** ash. Also, at the equilibrium viscosity state (η_α), defined as the viscosity as $t \rightarrow \alpha$ or the 'equilibrium

structure state', the viscosity values of the Lochiel-**A** and Bowmans-**A** ashes are higher than the Loy Yang-**A** ash. This suggests that at the same shear rate the Lochiel-**A** and Bowmans-**A** ashes are more viscous than the Loy Yang-**A**. Further inspections on the slope of the viscosity versus time curves found that the rate of viscosity decreased with shear time for the Loy Yang-**A** ash is faster than those found from the Lochiel-**A** and Bowmans-**A** ashes. This indicated that the viscosity of the Loy Yang-**A** ash changes more rapidly with time than the viscosity of the Lochiel-**A** and Bowmans-**A** ashes.

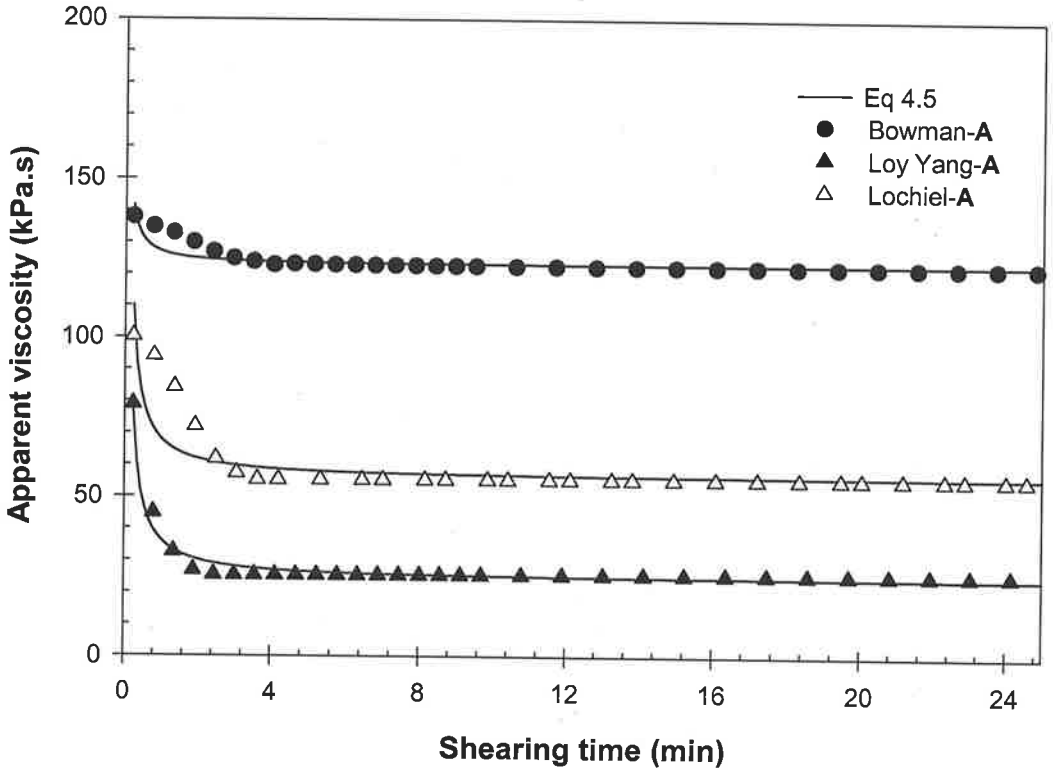

Fig 4.2: Transient viscosity data at constant shear rate ($\dot{\gamma}$ =3s^{-1}) for the laboratory's ash samples at temperature of 850°C

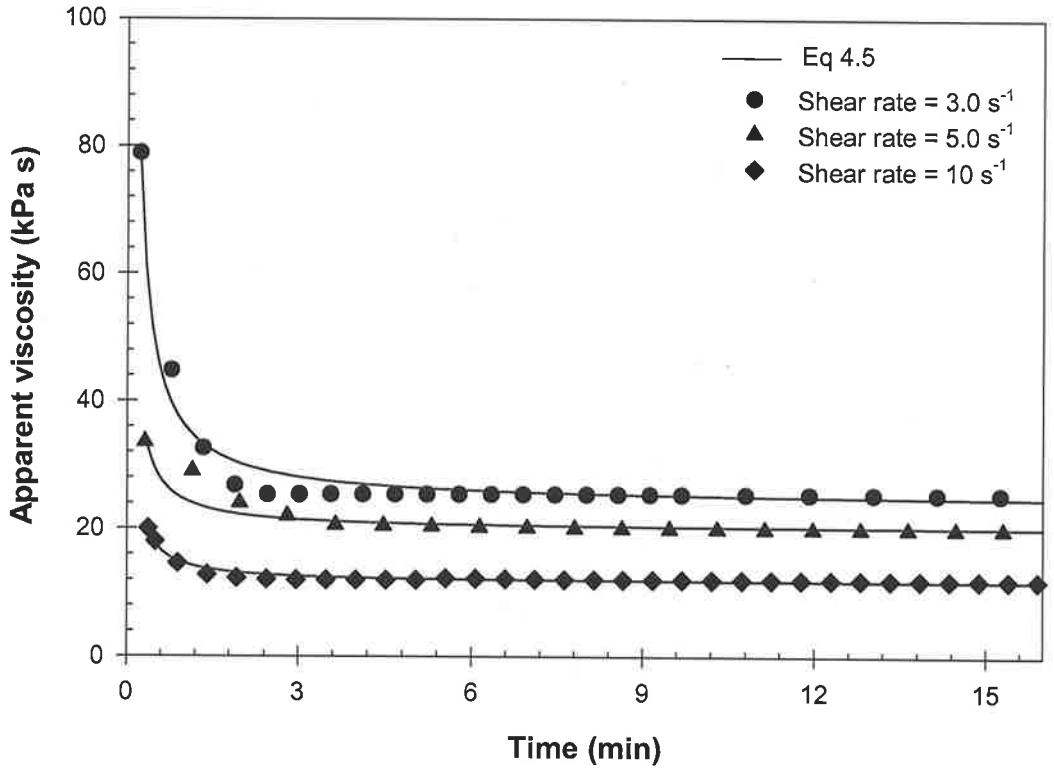

Fig 4.3: Transient viscosity data at constant shear rates for the Loy Yang-**A** ash at 850°C- Effect of shear rate

Fig 4.3 shows the effect of shear rate on the viscosity of the Loy Yang-**A** ash. The coal ash sample was sheared at three shear rate values of 3, 5 and 10s^{-1}, all at the fixed temperature of 850°C. Fig 4.3 demonstrates clearly that the initial and equilibrium viscosities were strongly affected by the shear rate as they decrease with increasing shear rate. This behaviour is typical of a shear thinning material. Moreover, Fig 4.3 shows that the slope of viscosity versus time rate is also affected by shear rate, as the viscosity decreases more rapidly as shear rate increases.

Fig 4.4 shows the effect of temperature on the viscosity of the coal ash sample. The experimental program was conducted by shearing the Loy Yang-**A** sample at a fixed shear rate of 3 s^{-1} but under three different temperatures of 850°C, 1000°C and 1200°C. Experimental results reveal that temperature has a significant effect on the initial viscosity and the equilibrium viscosity of the coal ash sample. It was found that the initial viscosity value and the equilibrium viscosity values decrease as temperature increases. Furthermore, it was also found that the temperature also influences the rate of breakdown in coal ash structure, with the structure breaking down more rapidly as temperature increases. This behaviour indicates that temperature has a dominant effect on the viscosity and the thixotropic behaviour of the coal ash samples.

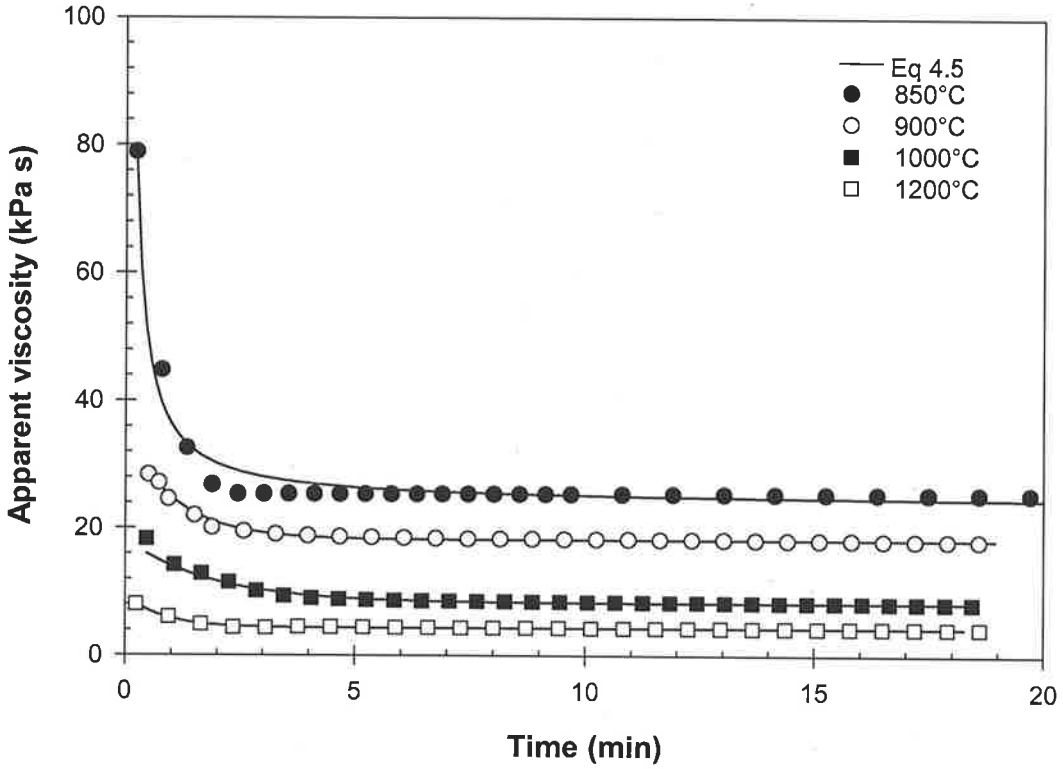

Fig 4.4: Transient viscosity data at a constant shear rate ($\dot{\gamma}$ =3s^{-1}) for the Loy Yang-**A** ash-Effect of operating temperature

4.4.3 Interpretation of thixotropic results

The objective of studying time dependent behaviours of the coal ash samples is to formulate a model capable of describing the observed dependence of coal ash viscosity on time of shear. In this work, time dependent flow behaviours of the coal ash samples can be analysed using a structural kinetic approach. This approach has been successfully employed for mineral, food and other industrial suspensions (Cheng et al, 1965; Nguyen et al, 1985). These works postulated that the change in the rheological properties is associated with shear-induced breakdown of the internal fluid structure in the coal ash sample. The structural kinetic approach can be applied to the coal ash system as expressed in the equation below:

$$\text{(Structured)} \leftrightarrow \text{(Non-structured)} \qquad 4.1$$

In this study, it was initially assumed that the thixotropic structure of the coal ash sample breaks down with a very slow rate of structure recovery. If this assumption is correct then the structural breakdown process of the coal ash samples can be described as Structured

→ Non-structured. According to the analogy of irreversible chemical reactions, the rate of structural breakdown can be postulated as:

$$-d\psi/dt = k\,(\psi-\psi_\alpha)^m \qquad 4.2$$

where ψ is a dimensionless unit representing the structured state of thixotropic material at any time t, k is the rate of structure breakdown and m is an arbitrary order of the irreversible reaction. In addition, equation 4.2 is also called as irreversible structure kinetic approach, which was first proposed by Tiu and Boger (1974).

At the initial state, t=0; $\psi=\psi_0$ and at the equilibrium state, $t\rightarrow\alpha$; $\psi=\psi_\alpha$. Under a constant applied shear rate, with integration of equation 4.2 from t=0 to α, the equation becomes;

$$(\psi-\psi_\alpha)^{1-m} = (m-1)\,k\,t + (\psi_0-\psi_\alpha)^{1-m} \qquad 4.3$$

In order to apply equation 4.3 to the experimental transient viscosity data a relationship between ψ and measurable rheological parameters needs to be determined. In this study ψ has been defined in terms of apparent viscosity ($\eta=\tau/\dot{\gamma}$). Thus;

$$\psi(\dot{\gamma},t) = (\eta-\eta_\alpha)/(\eta_0-\eta_\alpha) \qquad 4.4$$

where η_0 is the initial viscosity (or structured state) and η_α is the equilibrium viscosity (or equilibrium structured state). In this study both η_0 and η_α are a function of shear rate only. Thus, the equation used to describe the structural breakdown of a coal ash sample is

$$(\eta-\eta_\alpha)^{1-m} = [(m-1)\,k\,t + 1]\,(\eta_0-\eta_\alpha)^{1-m} \qquad 4.5$$

where k is the rate of structural breakdown, m is an arbitrary order of the irreversible reaction and t is shearing time. Note here that equation 4.5 is valid only under the constant shear rate condition. Under the constant shear rate condition, $\eta_0=\eta$ at t=0 and $\eta_\alpha=\eta$ at $t=t_\alpha$. By fitting equation 4.5 at given values of the kinetic order (m=1, 2, 3..) back into steady shear experimental data, the rate of structure breakdown (k) can be determined.

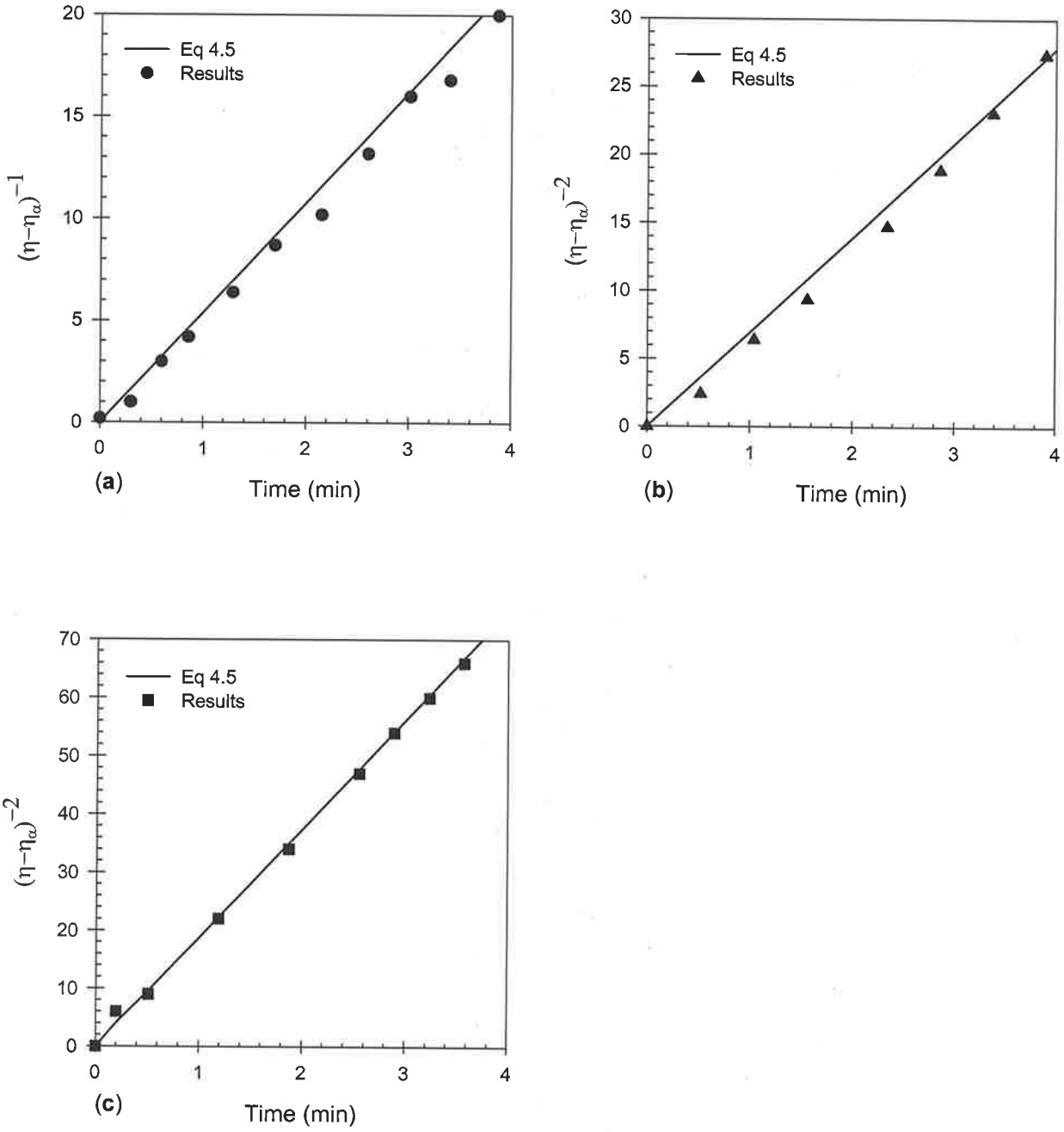

Fig 4.5: Testing of the structured kinetic model (eq 4.5) with the three laboratory ash samples sheared at $\dot{\gamma} = 3s^{-1}$, 850°C-Effect of coal type. (**a**) the Bowman-**A**; (**b**) the Lochiel-**A**; (**c**) the Loy Yang-**A**

Fig 4.5 shows plots of $(\eta-\eta_\alpha)^{1-m}$ versus time for the three laboratory ash samples tested at 850°C with a fixed shear rate of 3 s^{-1}. The Fig shows that a linear relationship occurs between the $(\eta-\eta_\alpha)^{1-m}$ and t for all coal ash samples and the data agrees well with the model according to equation 4.5. Similar results were also observed for the Loy Yang-**A** ash tested at different shear rates and operating temperatures, and these results are presented in Figs 4.6 and 4.7 respectively. Figs 4.5 to 4.6 show comparisons between the model fit (solid line) with the experimental viscosity-time data. A good agreement

between the model and the experimental data has been observed, confirming that structural breakdown of the coal ash samples is an irreversible process and the assumption given at the beginning of this section is correct.

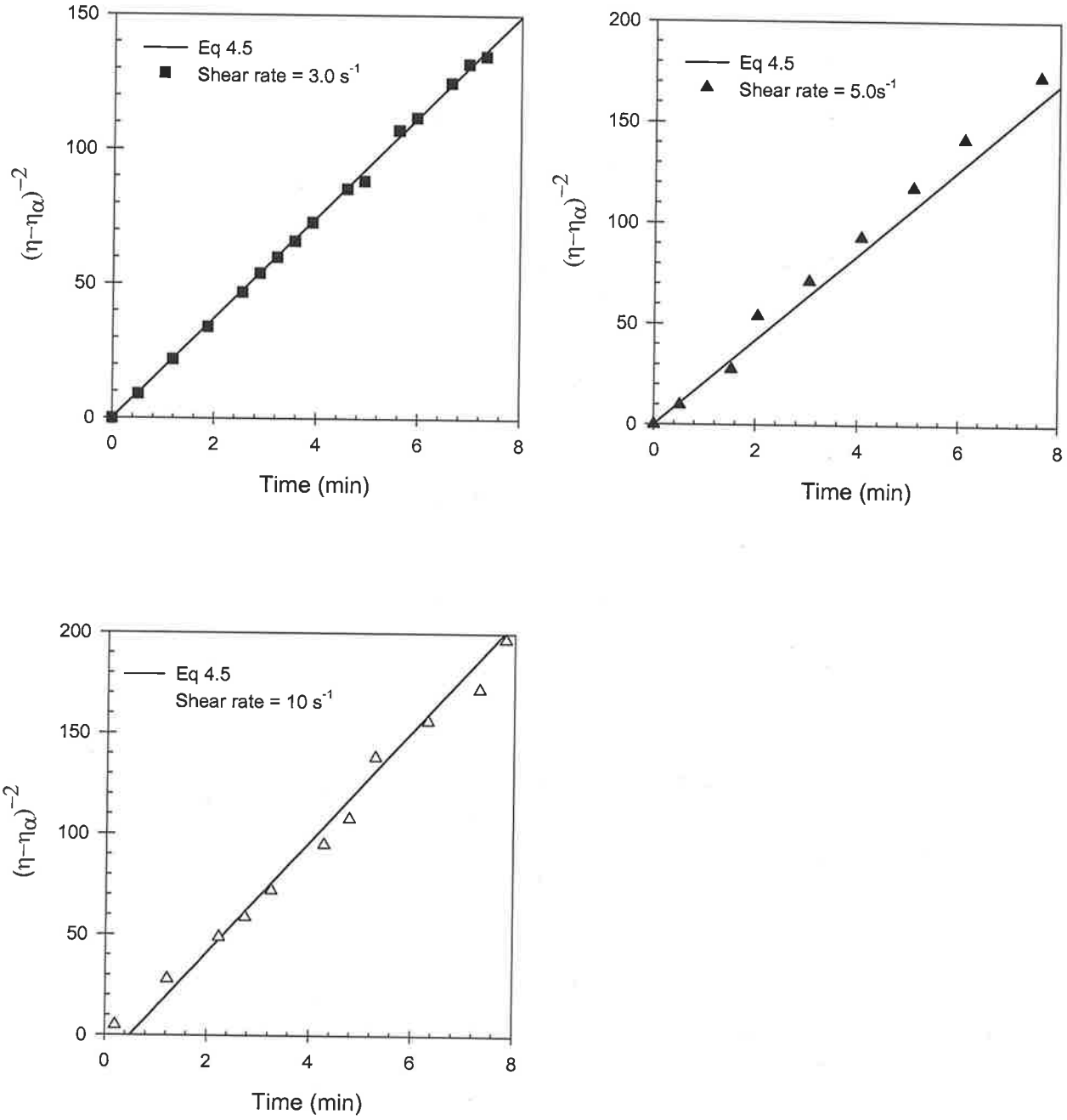

Fig 4.6: Testing of the structured kinetic model (equation 4.5) with the Loy Yang-A sample sheared at a fixed temperature of 850°C- Effect of shear rate.

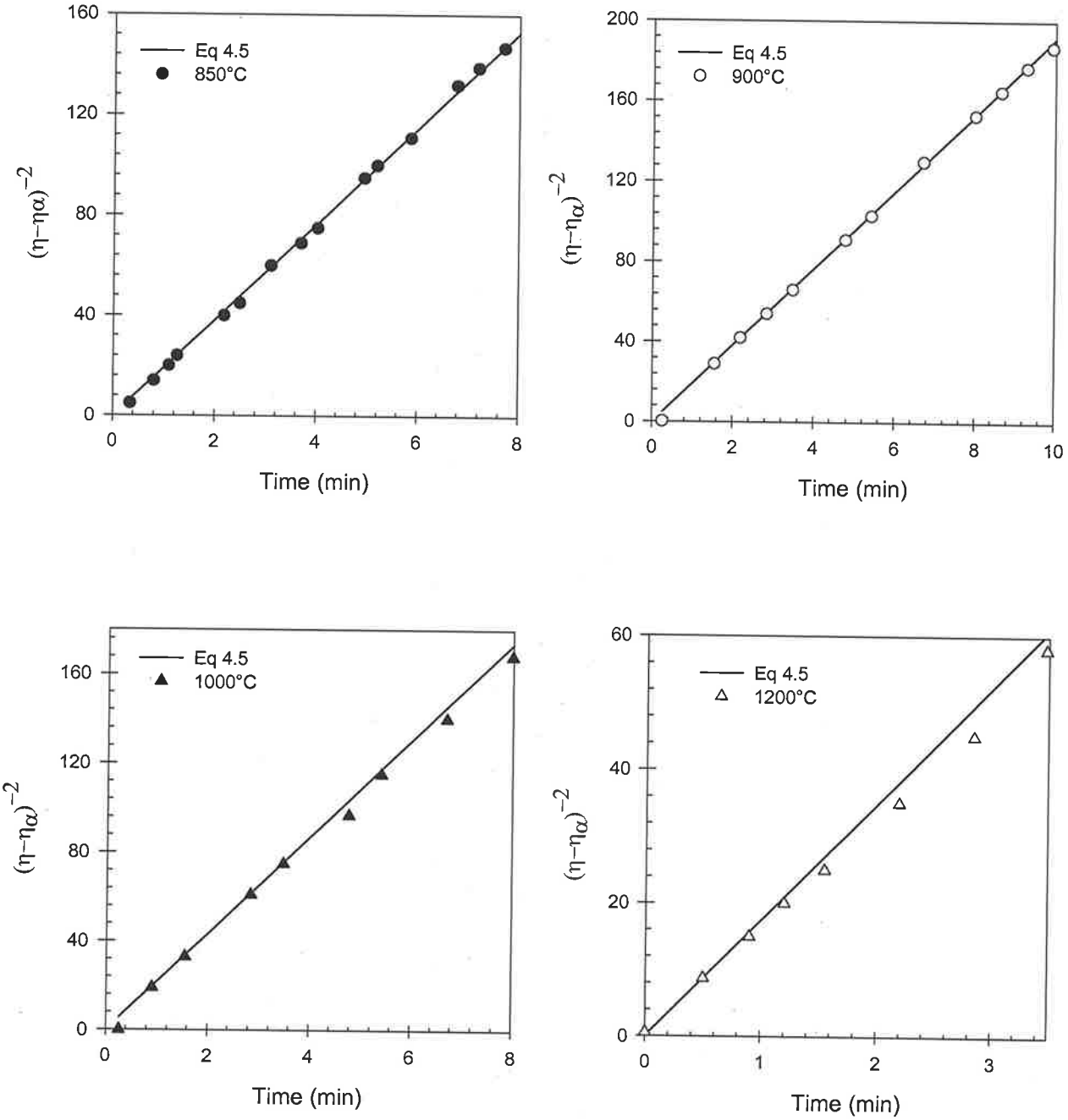

Fig 4.7: Testing of the structured kinetic model (equation 4.5) with the Loy Yang-**A** sample sheared at a fixed shear rate of 3 s^{-1}- Effect of temperature

Table IV.3 summarises values of the rate constant (k), the order of breakdown in structure (m), and the ratio of the initial viscosity to the equilibrium viscosity (η_0:η_α). The k parameter is an indication of the rate of thixotropic breakdown. The η_0:η_α indicates the extent of thixotropy.

Table IV.3: Structural breakdown parameters; order of breakdown in thixotropic structure (m); breakdown rate constant (k) and viscosity ratio (η_0:η_α)

Coal Type	Temperature (°C)	Shear rate (s^{-1})	m	k (s^{-1})	η_0:η_α
Loy Yang-**A**	850	3	3	0.30	1.75
Lochiel-**A**			3	0.116	1.5
Bowmans-**A**			2	0.099	1.30
Loy Yang-**A**	850	3.0	3	0.30	1.5
		5.0	3	0.35	1.80
		10.0	3	0.40	1.95
Loy Yang-**A**	850	3.0	3	0.312	1.58
	900		3	0.32	1.6
	1000		3	0.36	2.01
	1200		3	0.38	2.17

Table IV.3 shows that the m parameter of the Loy Yang-**A** and Lochiel-**A** is similar, as its value equals to three (m=3) for these two ash samples. This suggests that during high temperature rheological measurements both the Loy Yang-**A** and Lochiel-**A** samples may breakdown under a similar order. On the other hand, it has been found that the value of the m parameter for the Bowmans-**A** ash is equal to 2 (m=2), indicating a difference in the order of the breakdown kinetic.

The rate of breakdown in thixotropic structure (k) and the extent of thixotropy (η_0:η_α) are found to be dependent on coal type. Comparing the rate of structure breakdown (k), it was found that the rate of structure breakdown (k) for the Bowmans-**A** sample was 10 and 30 times slower than the Lochiel-**A** and Loy Yang-**A** respectively. The rate of structure breakdown can be listed in descending order as Loy Yang-**A**>Lochiel-**A**>Bowmans-**A**. The rate of structure breakdown suggested that under the same shear rate condition; thixotropic structure of the Loy Yang-**A** ash breaks down more rapidly than the Lochiel-**A** and Bowmans-**A** ashes. In addition, comparing the viscosity ratio, (η_0:η_α), it was found that the extent of thixotropy for the Loy Yang-**A** is higher than the Lochiel-**A** and Bowmans-**A**, indicating the more shear sensitive thixotropic nature of the Loy Yang-**A** ash compared to the Lochiel-**A** and Bowmans-**A** ashes.

Regarding to the effect of shear rate on the structural kinetic parameters (m and k), it was found that the value of the irreversible kinetic parameter (m) for the Loy Yang-**A** ash is

constant at three for the whole shear rate range. This suggests that the coal ash follows a third order irreversible kinetic model and it is independent of shear rate. Furthermore, it can be seen that the k and the η_0:η_α parameters are dependent on shear rate as these two values both increase with increasing shear rate. Similar behaviour was also observed for the effect of temperature on the structural kinetic parameters.

4.4.4 Flow characteristics of coal ashes

In this section equilibrium flow curves of the six coal ash samples tested at temperatures ranging from 850°C to 1200°C under a rich air atmosphere are presented. Fig 4.8 reveals that the flow curves of the coal ash samples are non-linear and intercept the shear stress axis. These characteristics suggest that the coal ash samples are non-Newtonian materials with yield stress characteristics. Fig 4.9 shows plots of viscosity versus shear rate for the six coal ash samples. It shows that the apparent viscosity of the six coal ash samples decreases rapidly as shear rate increases, indicating shear thinning behaviour.

Comparing the flow data between the laboratory ash samples found that the Bowmans-**A** and Lochiel-**A** ashes are more viscous and have higher yield stress than the Loy Yang-**A** sample. For the CFBC ashes, the Lochiel-**B** is more viscous and has a higher yield stress than the Loy Yang-**B** and Morwell-**B** ashes. All in all, the quantitative comparisons show that the South Australian ashes are more viscous and higher in yield stress than the Victorian ashes over the range of temperature and shear rate tested.

In addition, comparisons between the Lochiel-**A** ash (the lab ash) and the Lochiel-**B** ash (the CFBC ash) demonstrated that the Lochiel-**A** is more viscous and higher in yield stress than the Lochiel-**B** ash. Higher viscosity and higher yield stress characteristics were also found when comparing the Loy Yang-**A** and Loy Yang-**B** ashes. The chemical analysis of coal ash samples (Table IV.1) shows that the difference in flow properties of coal ash samples may be the result of the concentration levels of chemical compositions inherent within the coal ash sample. Based on the flow data and chemical compositions, it appeared that samples with a higher in concentration of SO_3, Na_2O, CaO and MgO have higher viscosity and yield stress. Samples with a higher concentration of SiO_2, Al_2O_3 and Fe_2O_3, have lower viscosity and yield stress.

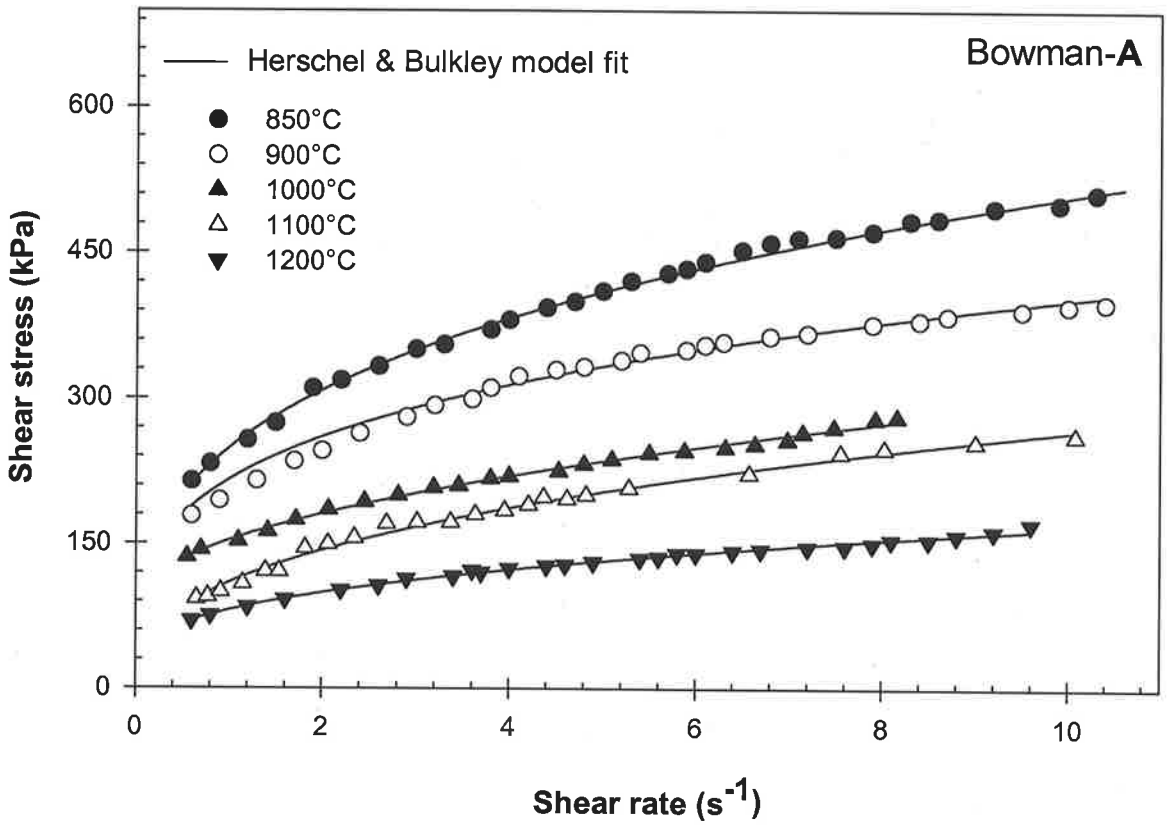
Herschel & Bulkley model fit
Bowman-A
850°C
900°C
1000°C
1100°C
1200°C
Shear stress (kPa)
600
450
300
150
0
0
2
4
6
8
10
Shear rate (s-1)

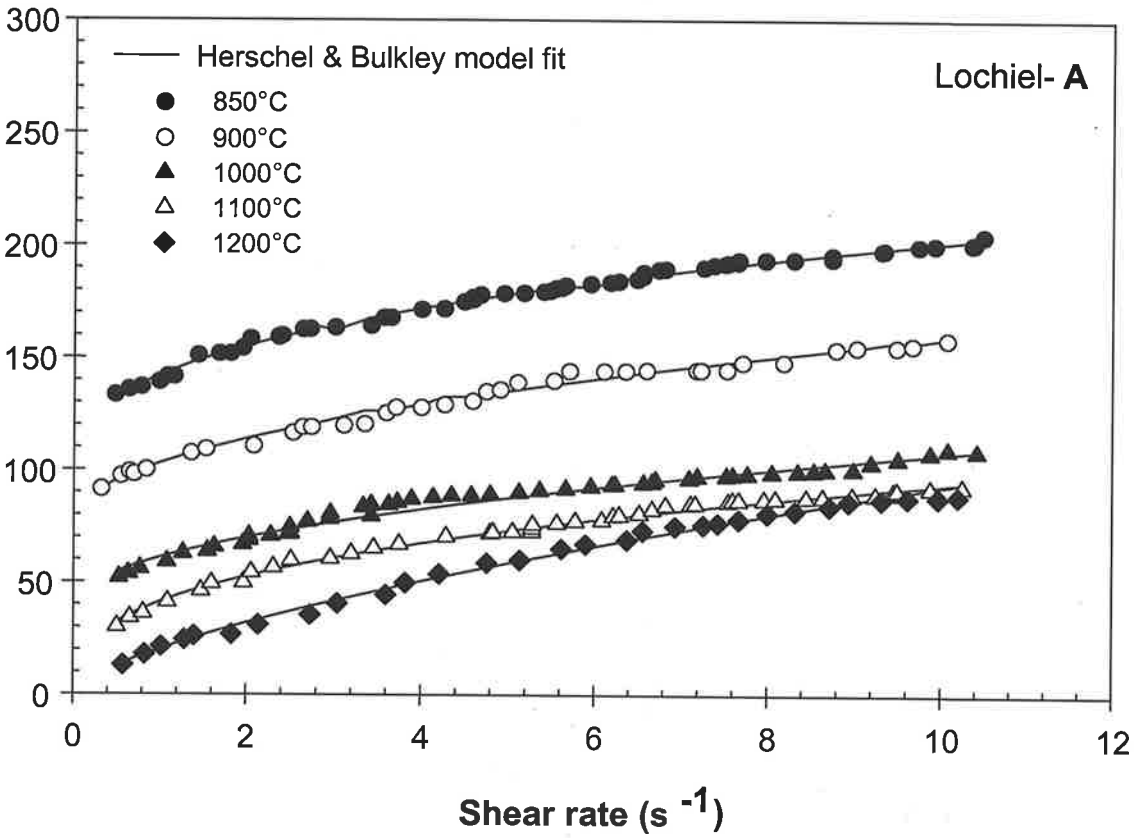
Herschel & Bulkley model fit
Lochiel- A
850°C
900°C
1000°C
1100°C
1200°C
300
250
200
150
100
50
0
0
2
4
6
8
10
12
Shear rate (s -1)

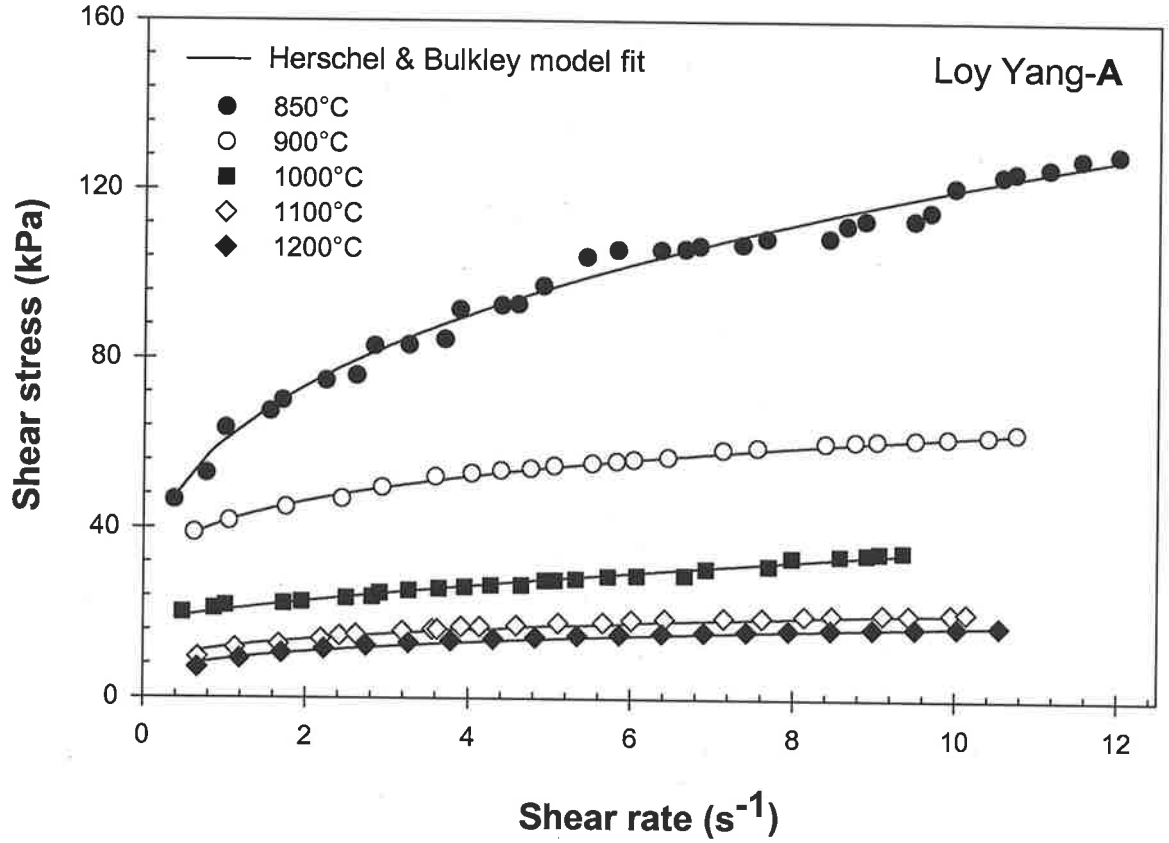
Herschel & Bulkley model fit
850°C
900°C
1000°C
1100°C
1200°C
Loy Yang-A
Shear stress (kPa)
Shear rate (s-1)
0
40
80
120
160
0
2
4
6
8
10
12

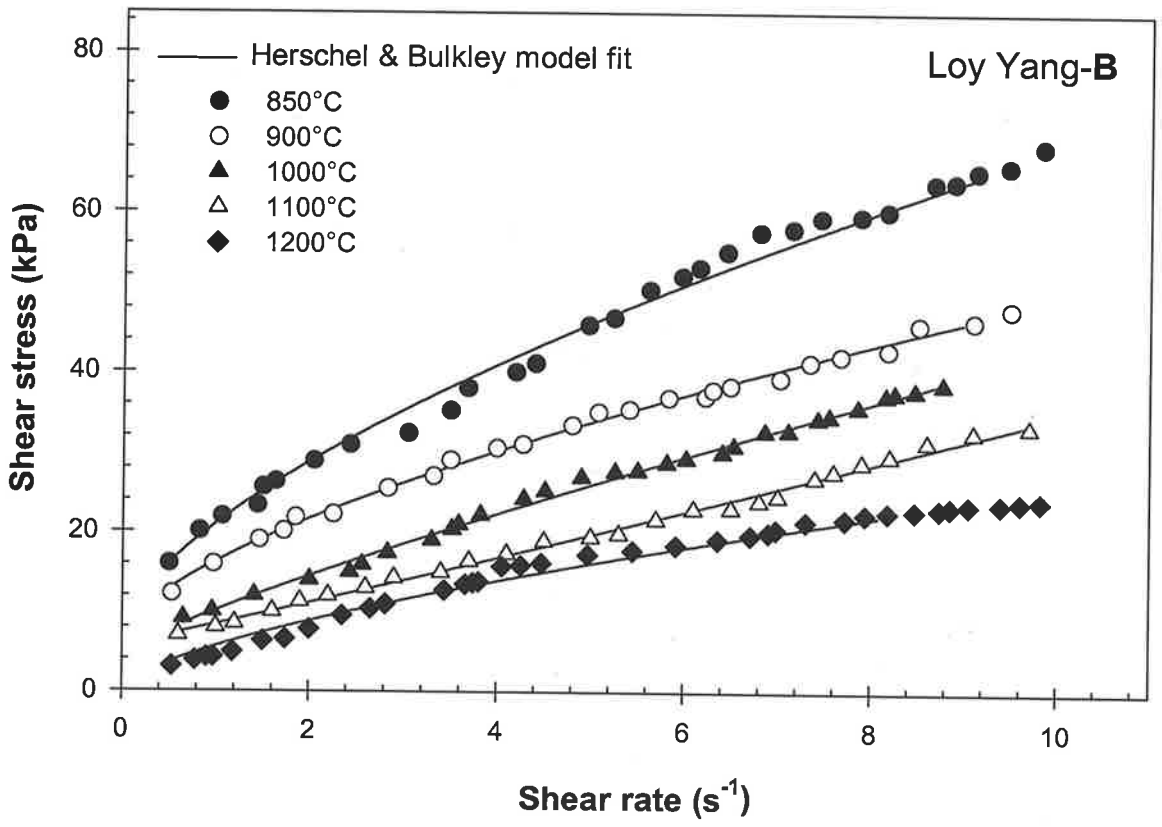
Herschel & Bulkley model fit
850°C
900°C
1000°C
1100°C
1200°C
Loy Yang-B
Shear stress (kPa)
Shear rate (s-1)
0
20
40
60
80
0
2
4
6
8
10

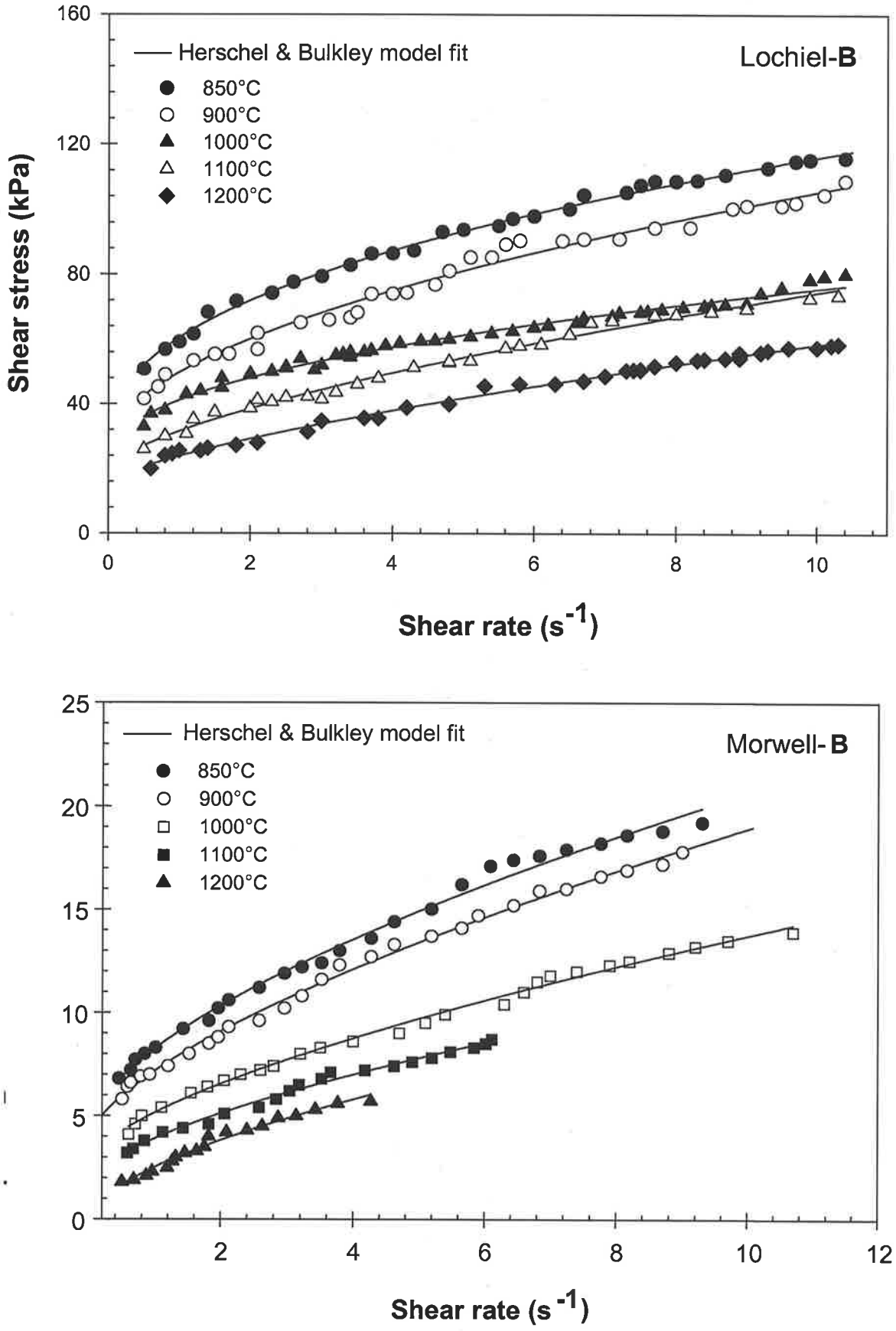

Fig 4.8: Flow curves of the six coal ashes tested at five temperatures ranging from 850°C to 1200°C under the rich air atmosphere

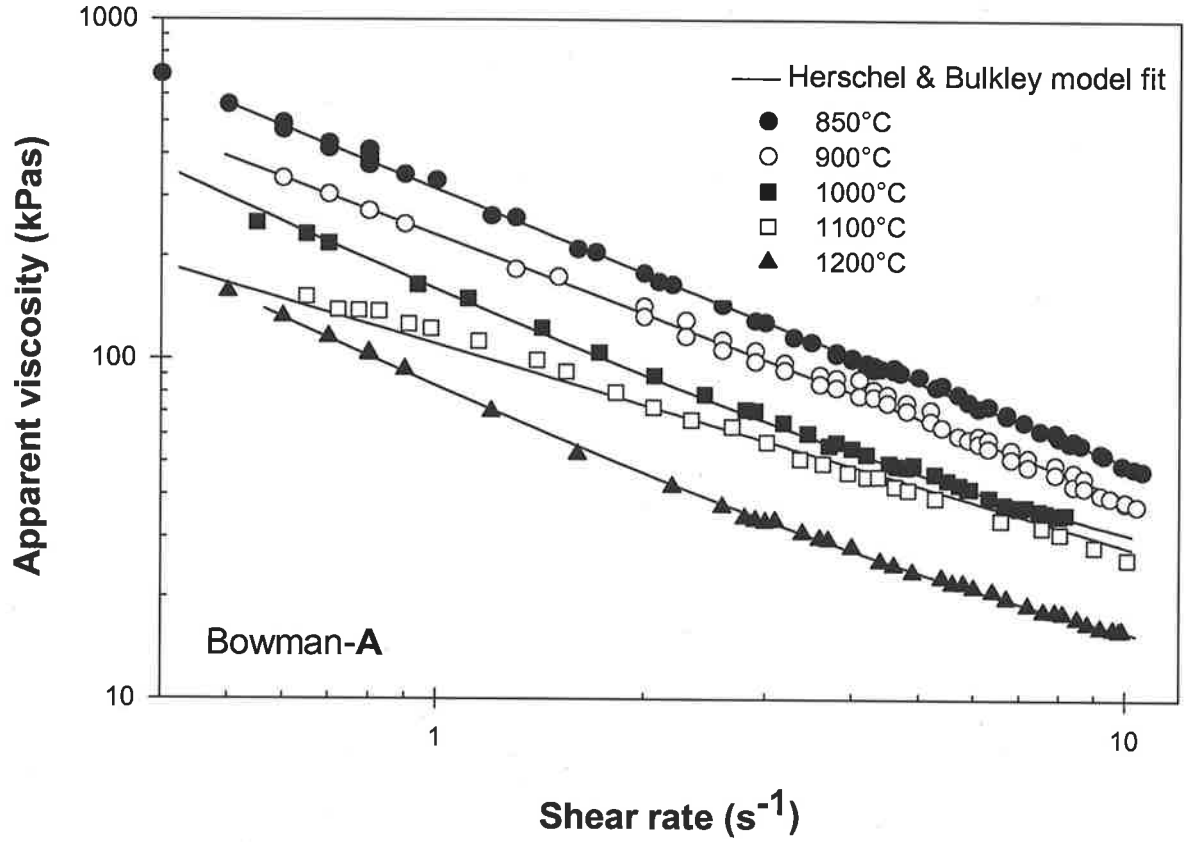
1000
100
10
1
10
Apparent viscosity (kPas)
Shear rate (s-1)
Herschel & Bulkley model fit
850°C
900°C
1000°C
1100°C
1200°C
Bowman-A

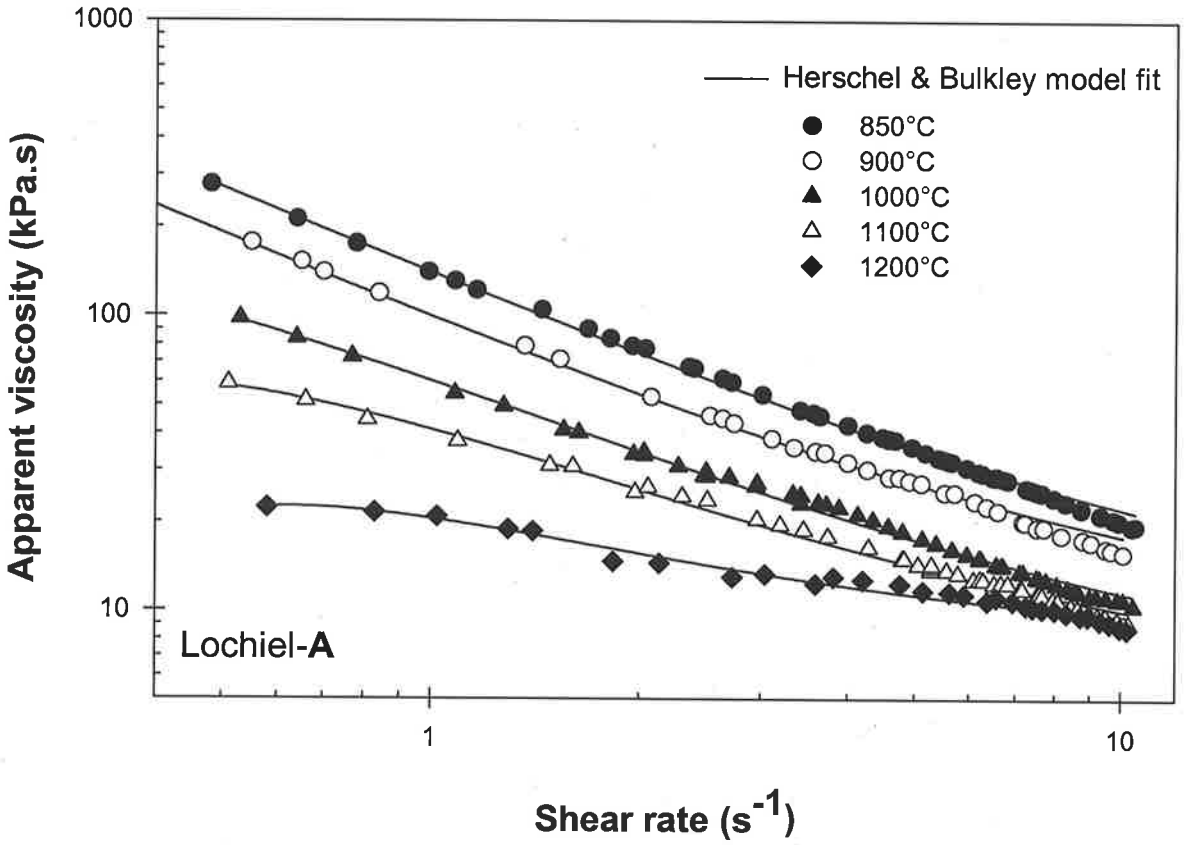
1000
100
10
1
10
Apparent viscosity (kPa.s)
Shear rate (s-1)
Herschel & Bulkley model fit
850°C
900°C
1000°C
1100°C
1200°C
Lochiel-A

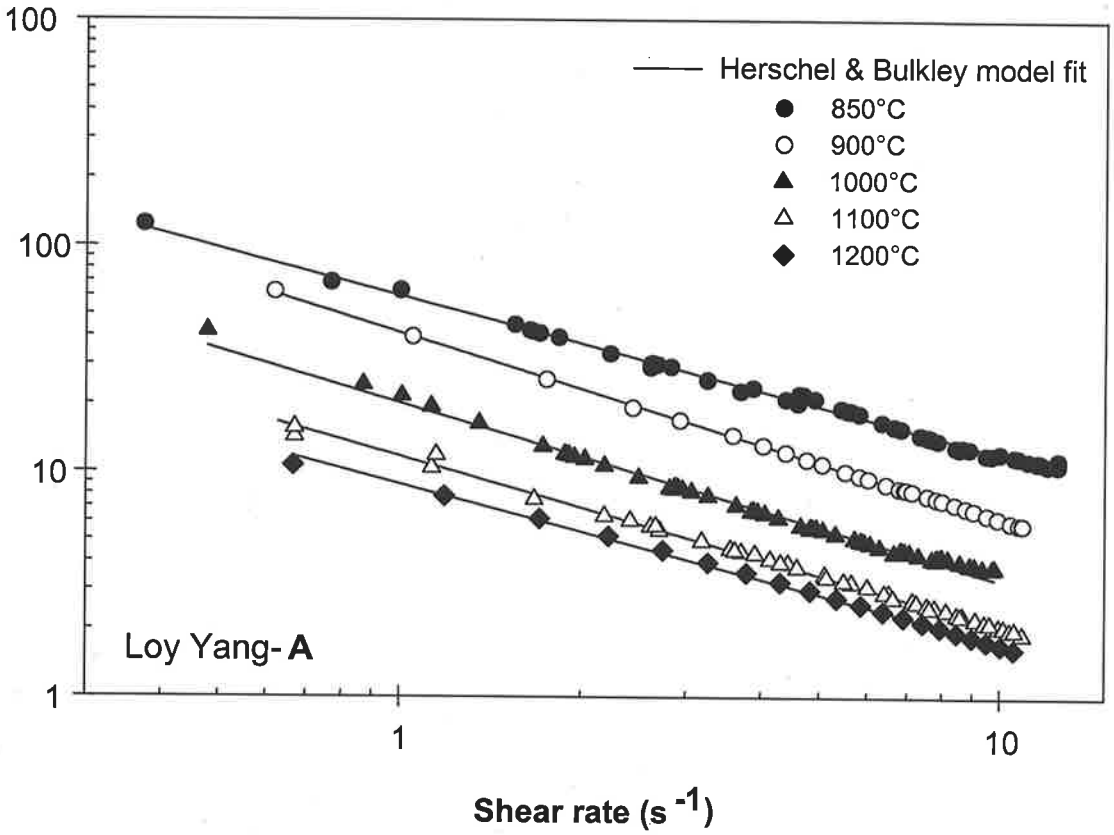
100
100
10
1
1
10
Herschel & Bulkley model fit
850°C
900°C
1000°C
1100°C
1200°C
Loy Yang- A
Shear rate (s -1)

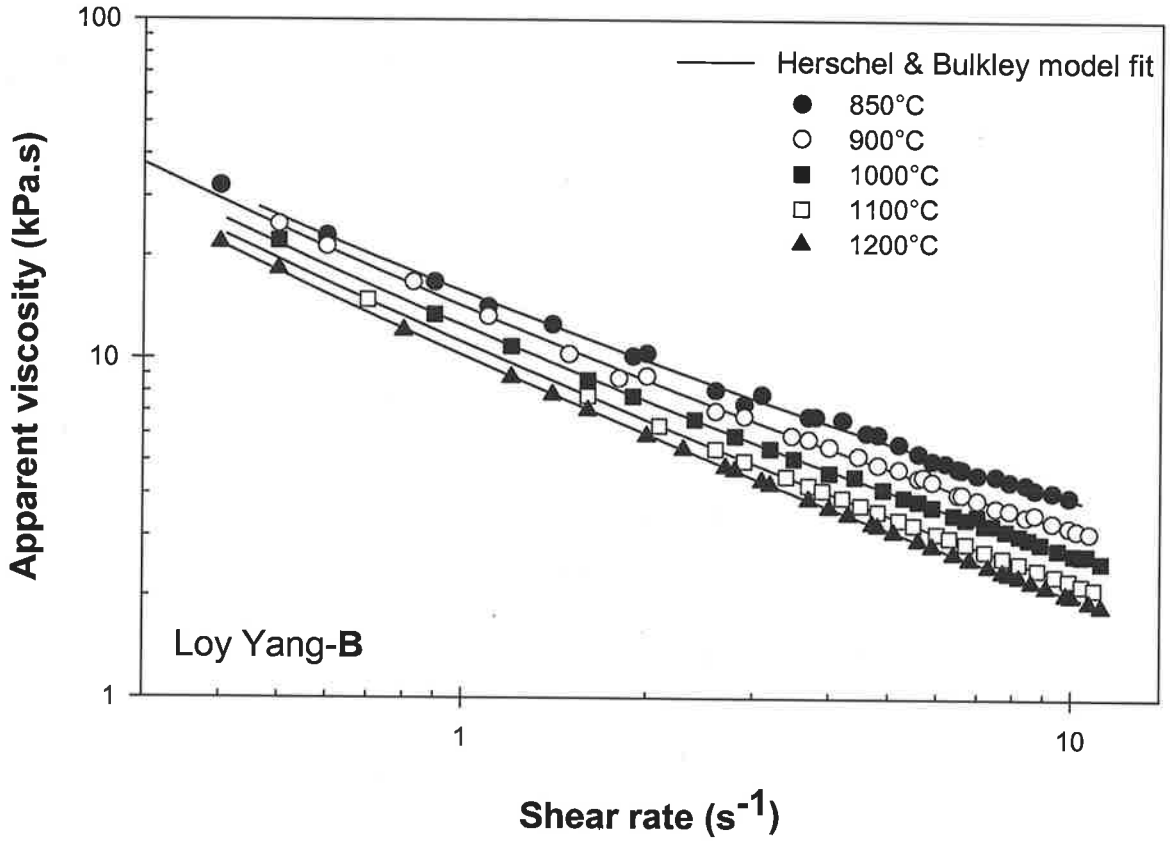
100
10
1
1
10
Herschel & Bulkley model fit
850°C
900°C
1000°C
1100°C
1200°C
Loy Yang-B
Apparent viscosity (kPa.s)
Shear rate (s-1)

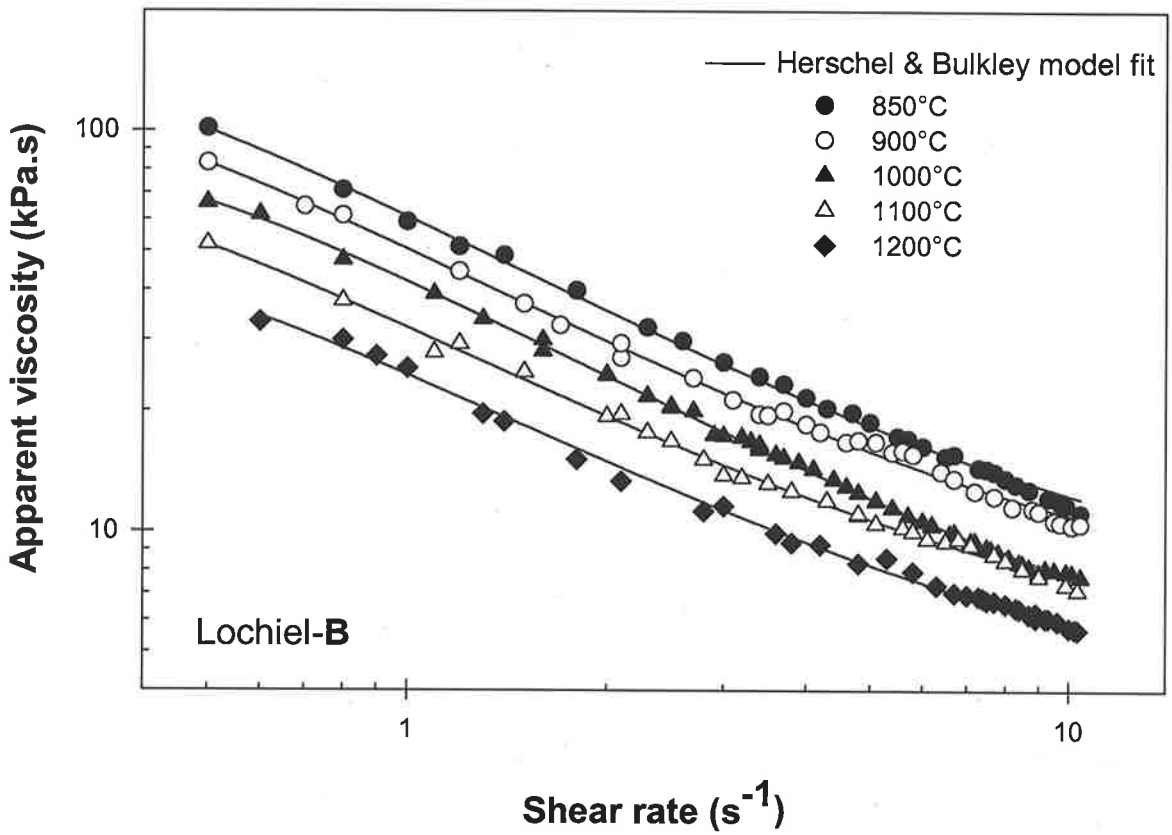

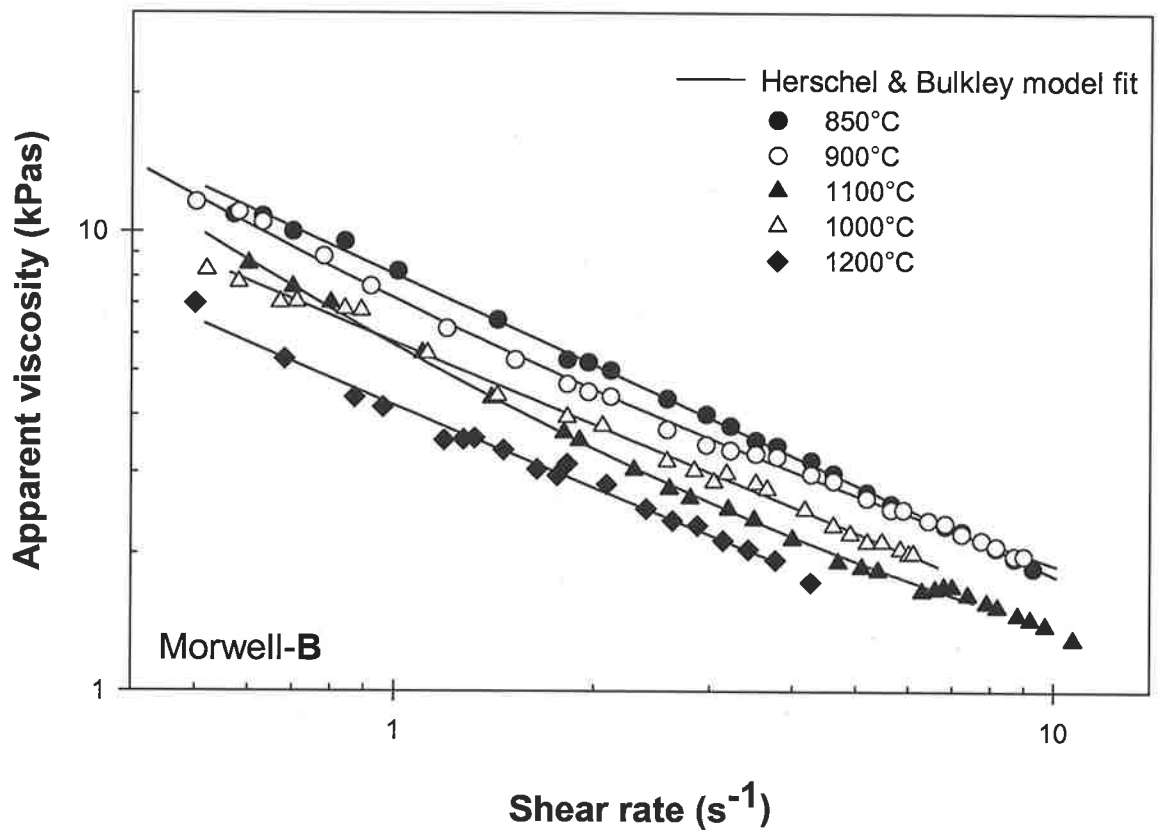

Fig 4.9: Apparent viscosity of the of the six coal ashes tested at five temperatures ranging from 850°C to 1200°C under the rich air atmosphere

4.4.5 Treatment of rheological data

Although direct comparison can be made using the flow data shown in Figs 4.8 and 4.9, it is fundamentally desirable that the data be analysed in terms of rheological models. From a large number of (inelastic fluids) yield stress models, the Herschel & Bulkley model was found to be the most suitable to describe flow data of the low-rank Australian coal ashes in this work. The formula of the Herschel & Bulkley model has already been given in chapter 2, section 2.3.1. To obtain values of the Herschel & Bulkley model parameters, a plot of $(\tau - \tau_y^{H-B})$ versus $\dot{\gamma}$ on a logarithmic scale diagram was made, with different trials for the values of τ_y^{H-B} until the plot become linear. A statistical least square method involving iteration was used for this purpose. Then a linear line was drawn through the data points. The slope and interception of this straight line were referred to the flow behaviour index (n) and consistency index respectively. The final results obtained for the Bowmans-**A** ash sample are shown in Fig 4.10. As seen, the plots are linear over the entire range of the shear rate tested at all temperatures. These results thus validate the suitability of the Herschel & Bulkley model for the low-rank Australian coal ash samples. Values of the constants in Herschel & Bulkley model for the six low-rank Australian coal ashes are given in Table IV.4.

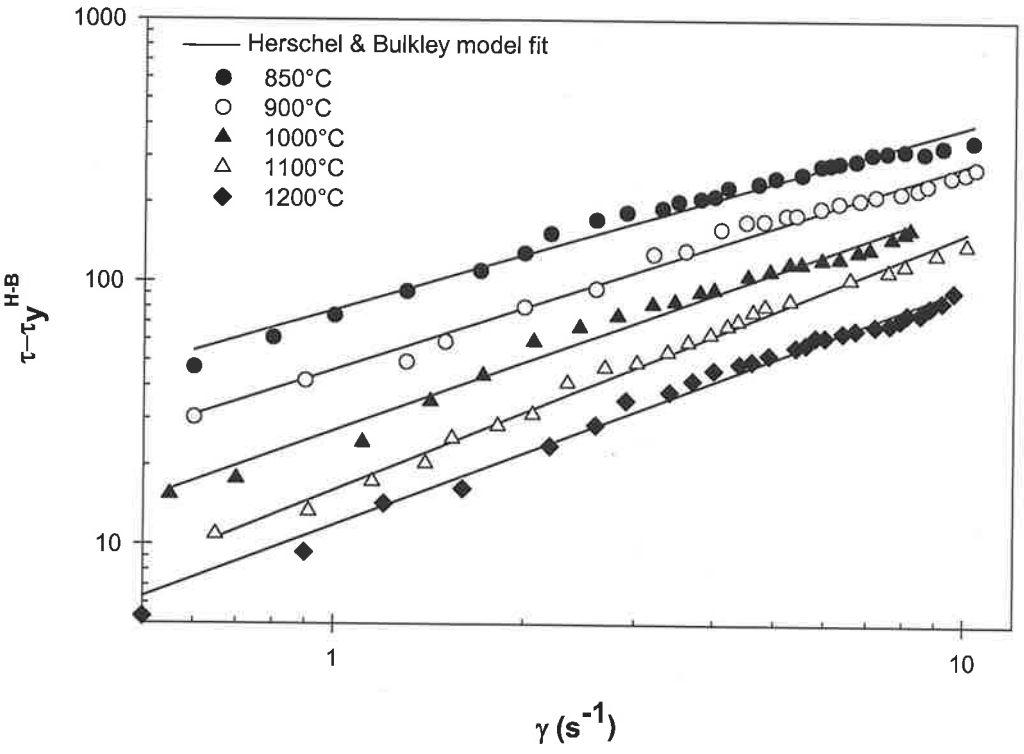

Fig 4.10: Testing of the Herschel & Bulkley model (the Bowmans-**A** ash)

Table IV.4: Values of the constants (τ_y^{H-B}, K and n) in the Herschel & Bulkley model for the six coal ash samples

	Coal ash sample	850°C	900°C	1000°C	1100°C	1200°C
τ_y^{H-B} (kPa)	Bowmans-**A**	163.5	148.4	104.0	70.0	54.0
	Lochiel-**A**	113.6	81.4	50.3	28.1	13.0
	Loy Yang-**A**	38.1	32.5	19.2	10.8	8.1
	Morwell-**B**	6.2	4.8	3.4	2.2	1.2
	Lochiel-**B**	42.3	36.7	27.0	18.4	14.1
	Loy Yang-**B**	12.1	9.4	7.8	6.4	3.5
K (kPa s^n)	Bowmans-**A**	114.4	109.6	67.0	50.0	38.8
	Lochiel-**A**	106.3	79.5	62.1	53.0	33.2
	Loy Yang-**A**	44.5	25.0	17.2	11.1	9.6
	Morwell-**B**	0.72	0.58	0.36	0.24	0.19
	Lochiel-**B**	28.1	24.5	18.1	12.4	10.4
	Loy Yang-**B**	7.2	4.6	4.1	3.2	1.8
n	Bowmans-**A**	0.40	0.41	0.42	0.43	0.45
	Lochiel-**A**	0.38	0.55	0.42	0.44	0.46
	Loy Yang-**A**	0.37	0.36	0.38	0.38	0.33
	Morwell-**B**	0.63	0.61	0.57	0.64	0.56
	Lochiel-**B**	0.59	0.53	0.56	0.61	0.54
	Loy Yang-**B**	0.65	0.74	0.73	0.65	0.6

Table IV.4 shows that values of the constants in the Herschel & Bulkley model, especially the yield stress and the consistency index, are higher for the Bowmans-**A** and Lochiel-**A** ashes than the Loy Yang-**A** ash. The yield stress of the Bowmans-**A** ash is 1.5 times higher than the Lochiel-**A** ash and 3 times higher than the Loy Yang-**A** ash. For the value of the consistency index (K), the Bowmans-**A** ash is 2 and 3.2 times higher than the Lochiel-**A** ash and the Loy Yang-**A** ash respectively. In addition, Table IV.4 shows that the flow behaviour index (n) of the Loy Yang-**A** ash is smaller than the Bowmans-**A** and Lochiel-**A** ashes over the tested temperature range. This indicates that the viscosity of the Loy Yang-**A** is more sensitive to shear rate than that of the Bowmans-**A** and Lochiel-**A** ashes.

The chemical analysis in Table IV.1 shows that the Lochiel-**A** and Bowmans-**A** ashes are high in the concentration levels of SO_3, CaO, Na_2O and MgO components, while the Loy Yang-**A** is high in SiO_2, Al_2O_3 and Fe_2O_3 components. Concentration levels of the other

chemical components were found to be similar for these three coal ash samples. Based on the flow data and the chemical compositions of the laboratory ash samples, it appears that SO_3, CaO, Na_2O and MgO are the key chemical components that cause high viscosity and high yield stress behaviours, while the SiO_2, Al_2O_3 and Fe_2O_3 are the key chemical components that cause low viscosity and yield stress behaviours of the laboratory ashes. Moreover, the SiO_2, Al_2O_3 and Fe_2O_3 are the key chemical components causing the more shear-sensitive viscosity behaviour of the coal ash samples.

Comparisons between the three CFBC samples found that the Lochiel-**B** sample is the more viscous and has a higher yield stress than the Loy Yang-**B** and Morwell-**B** ashes. The yield stress of Lochiel-**B** is 4 and 7 times higher than the Loy Yang-**B** and Morwell-**B** ashes respectively. The Lochiel-**B** has the consistency index value 4 times higher than the Loy Yang-**B**, and 20 times higher than the Morwell-**B**. In regard to the flow behaviour index (n), it was found that value of the index of the Lochiel-**B** was smaller than the Loy Yang-**B** and Morwell-**B** ashes, indicating more shear sensitivity of viscosity of the Lochiel-**B** than the Loy Yang-**B** and Morwell-**B** ashes. The chemical analysis shows that the Lochiel-**B** is high in concentration of SO_3 and Na_2O compositions, the Loy Yang-**B** is high in Al_2O_3 and the Morwell-**B** is high in concentration of Fe_2O_3 and CaO compositions. From the comparisons of flow properties, it appeared that SO_3 and Na_2O are the key chemical components causing high viscosity and yield stress behaviours of the CFBC ash, while Fe_2O_3 and Al_2O_3 cause low in viscosity and yield stress behaviours. The effects of SO_3, Na_2O and Fe_2O_3 on flow properties appear to be similar to those found with laboratory ash samples. However, the effect of CaO component on flow properties of the CFBC ashes was opposite to that found in the laboratory ashes. This may suggest that if CaO is the dominant component in coal ash, low viscosity and yield stress can be expected. However, if other chemical compounds, especially Na_2O, SO_3 and MgO, are also the dominant compounds, then CaO can cause a high yield stress and viscosity.

Moreover, comparing the flow data of ash samples from the same coal that were obtained differently (the laboratory ash and the CFBC ash), it was found that the laboratory ashes were more viscous and higher in yield stress than the CFBC ashes. Table IV.4 showed that the yield stress and viscosity of the Lochiel-**A** ash were 3 and 5 times higher than those found in the Lochiel-**B** sample. The major difference in the concentration levels of chemical components between these two coal ashes was CaO. This means that CaO caused the low viscosity and yield stress of the Lochiel ash. Comparisons between the value of the flow behaviour indexes of Lochiel-**A** and Lochiel-**B** found that the Lochiel-**A**

sample has a smaller n value than the Lochiel-**B** sample, indicating that the viscosity of the Lochiel-**A** sample is more shear sensitive.

Table IV.1 revealed that the Loy Yang-**A** was high in the concentration level of Fe_2O_3 component and the Loy Yang-**B** was high in SO_3, Na_2O and MgO components. The comparison between the Loy Yang-**A** and Loy Yang-**B** revealed that Fe_2O_3 is another chemical component that causes the high viscosity and yield stress of a coal ash sample. It was found that between the Lochiel-**A** and Lochiel-**B**, Lochiel-**A** was higher in viscosity and yield stress. Chemical analyses of these two coal ash samples show that concentration levels of Na_2O, MgO, SO_3, SiO_2 and Al_2O_3, compositions are similar, but the Lochiel-**B** is higher in CaO than the Lochiel-**A**. The observations on the effects of CaO on flow properties were similar to those found with the CFBC ashes.

Overall, the quantitative comparisons of different coal ash samples indicated that the Bowmans and Lochiel ashes are more viscous and high in yield stress than the Loy-Yang and Morwell ashes. The viscosity and yield stress can be ranked in the descending order of Bowmans-**A**>Lochiel-**A**>Lochiel-**B**>Loy Yang-**A**>Loy Yang-**B**>Morwell-**B**. The differences in values of the flow properties may be due to the concentration level of chemical compositions and methods used for preparing coal ash samples. The comparisons have demonstrated explicitly that MgO Na_2O and SO_3 are key chemical compositions causing an increase in the viscosity and yield stress of coal ash. The effects of CaO and Fe_2O_3 on flow properties of coal ash are not clear and a further investigation is required. For the effects of chemical compositions on the flow behaviour index, it was found that SiO_2, Al_2O_3, Fe_2O_3 and CaO are key chemical compositions that cause greater shear-sensitivity in the viscosity behaviour of the coal ash samples.

4.5 FACTORS WHICH INFLUENCE THE RHEOLOGICAL PROPERTIES OF COAL ASHES

4.5.1 Effect of temperature on the rheological properties of coal ashes

The values of the constants in the Herschel & Bulkley model given in Table IV.4 show that the yield stress and the consistency parameter of the coal ash samples change drastically with temperature, while the flow behaviour index appeared to be relatively insensitive to temperature. Figs 4.11 to 4.13 show the effects of temperature on the yield stress, the consistency parameter and the flow behaviour index.

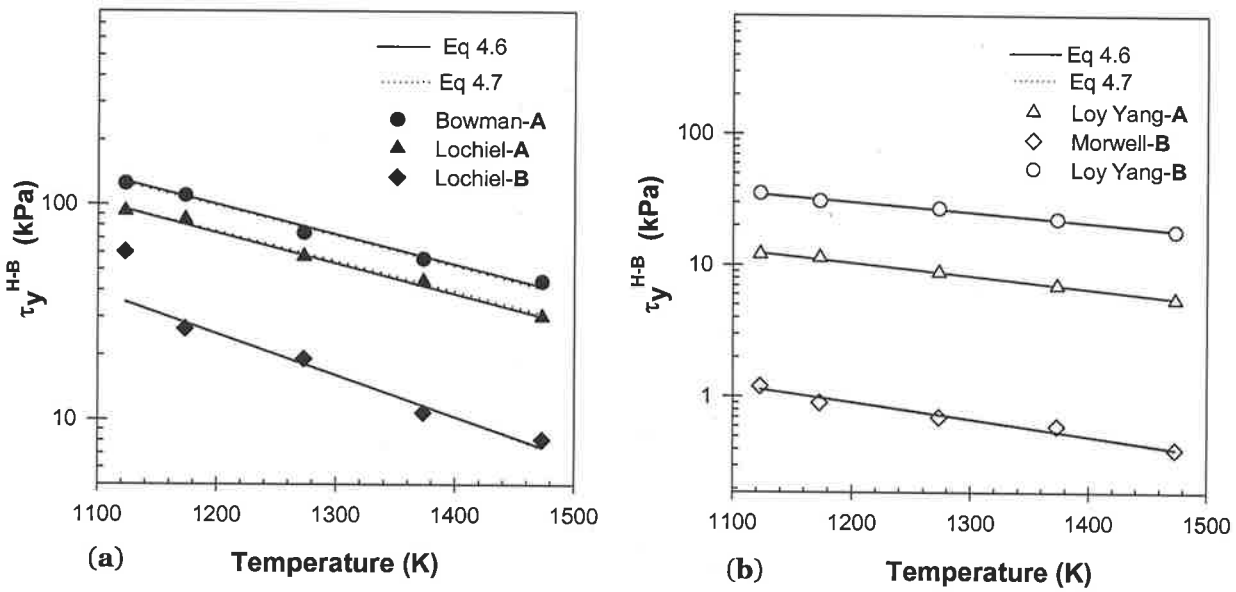

Fig 4.11: Effect of temperature on the yield stress parameter (τ_y^{H-B}). (**a**) the SA ashes; (**b**) the VIC ashes

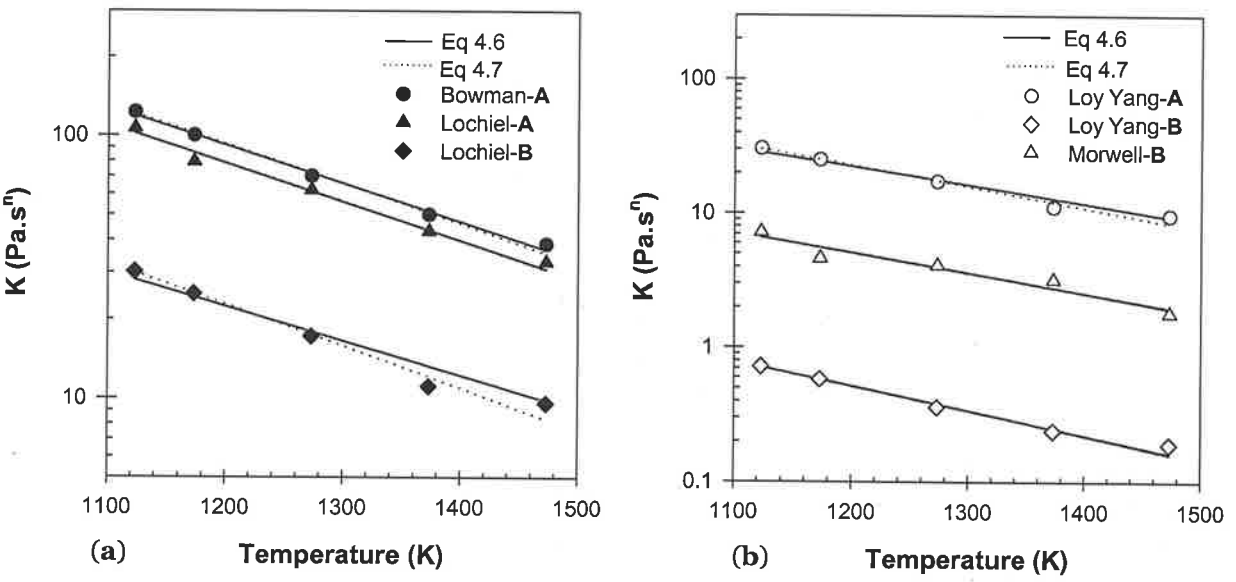

Fig 4.12: Effect of temperature on the consistency parameter (K). (**a**) the SA ashes; (**b**) the VIC ashes

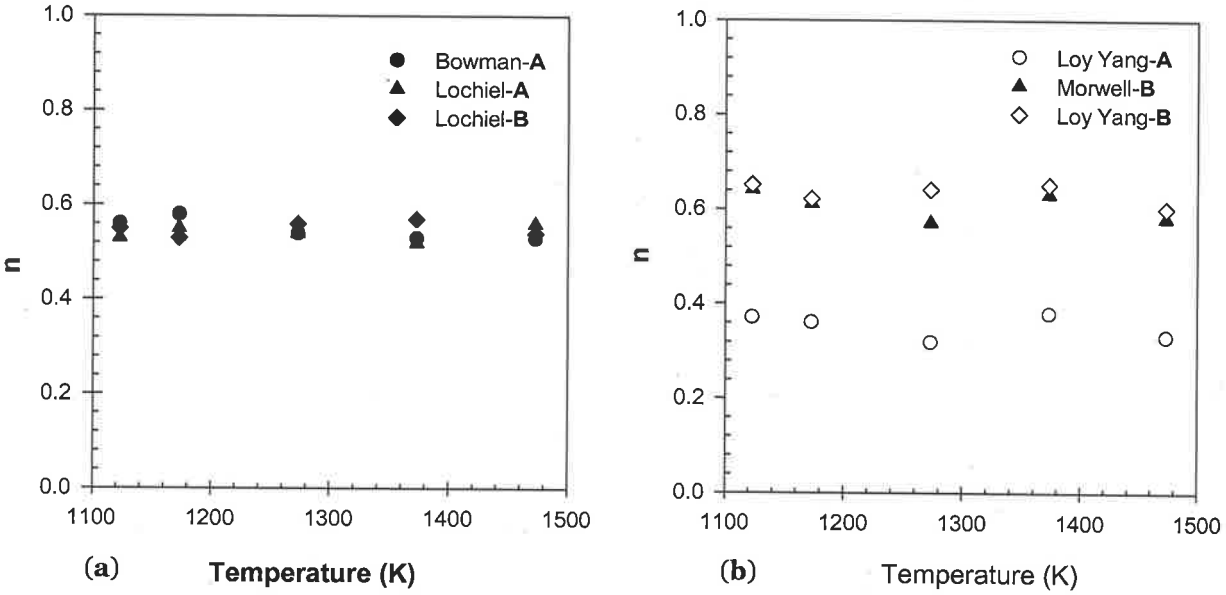

Fig 4.13: Effect of temperature on the flow behaviour index parameter (n). (**a**) the SA ashes; (**b**) the VIC ashes

Figs 4.11 to 4.13 reveal explicitly that the yield stress and the consistency parameter decrease dramatically as temperature increases, while the flow behaviour index is relatively constant over the whole temperature range. There are two equations often used to describe temperature dependent viscosity of coal ash slags (see section 2.3.2 for more detail). They are the Arrhenius type, and Weymann type equations. Formulas for these two equations are given in equations 4.6 and 4.7.

$$\log \mathbf{Y} = \log \mathbf{A} + \left(\frac{Ea}{RT}\right) \qquad 4.6$$

where **Y** represents one of the Herschel and Bulkley constants, **A** is a pre-exponential parameter, Ea is the activation energy, R is the universal gas constant and T is the temperature in absolute units.

$$\ln \mathbf{Y} = \ln \mathbf{A} + \ln \boldsymbol{T} + \frac{\boldsymbol{B}}{\boldsymbol{T}} \qquad 4.7$$

where $\boldsymbol{A}$ and $\boldsymbol{B}$ are composition specific constants and $\boldsymbol{T}$ is the temperature in absolute units.

The Arrhenius equation (equation 4.6) and Weymann equation (equation 4.7) were both found to be suitable for describing the temperature dependence of yield stress and consistency parameters of the coal ash samples. The applicability of these two equations is shown in Figs 4.11 to 4.12, where the equations were plotted together with the

rheological data. The equal applicability of the Arrhenius equation and the Weymann equation to the yield stress and consistency of low-rank Australian coal ashes is interesting. In fact, the Weymann equation was originally developed the Arrhenius equation by adding the extra term, which is ln ***T***, into the Arrhenius, and the parameter ***B*** is actually equal to the ***Ea/R*** term in the Arrhenius equation. In this work, equation 4.6 was selected to describe the temperature dependency of rheology. This is due to the simpler structure of the Arrhenius equation, which has fewer parameters than the Weymann equation.

Table IV.5: Values of the constant parameters in the equation 4.6

Coal ash samples	$\tau_y^{H\text{-}B}$ (kPa)		K (kPa s^n)	
	A (kPa)	***Ea*** (kJ/mol)	**A** (kPa)	***Ea*** (kJ/mol)
Bowmans-**A**	4315.34	25	4744	27
Lochiel-**A**	3908.81	27	2661.4	25
Loy Yang-**A**	1542.44	15	764.85	24
Morwell-**B**	19.11	21	56.28	32
Lochiel-**B**	3433.92	34	1166.02	27
Loy Yang-**B**	192.55	22	185.65	25

Table IV.5 shows that the values of the parameter **A** in the yield stress parameter for the South Australian ashes are higher than the Victorian ashes. This indicates that at the same temperature the value of the yield stress of the South Australian ash is higher than that of the Victorian ash. Among the coal ash samples tested, the Lochiel-**B** has the highest value of the ***Ea*** parameter at 34 kJ/mol, while the Loy Yang-**A** sample has the lowest value at 15 kJ/mol. The different in values of the ***Ea*** parameter mean that the yield stress of the Lochiel-**B** was the most sensitive to temperature. Values of the ***Ea*** parameter in the Bowmans-**A**, Lochiel-**A**, Morwell-**B** and Loy Yang-**B** ash samples were found to be similar, indicating that the sensitivity of the yield stress of these coal ash samples to temperature was similar. For the consistency parameter, it was found that the sensitivity and dependency of this parameter on temperature was similar to the Morwell-**B** sample. It appeared that the consistency (a measure of the viscous property) of the Morwell-**B** ash was more temperature sensitive than the other coal ashes.

4.5.2 Effect of chemical composition

Numerous articles have been published about techniques that can be used to investigate the effect of chemical composition on the physical properties of coal ash samples (Manzoori, 1990; Oh et al, 1995; Benson et l, 1998), however only two techniques were selected in this work. They are: a Scanning Electron Microscope (SEM) technique and an X-Ray Diffraction (XRD) technique. Details about the measuring techniques of the SEM and XRD were given in Chapter 3 Section 3.7.2. In this work, the SEM analysis was only performed with the laboratory ashes - the Bowmans-**A** ash, the Lochiel-**A** ash and the Loy Yang-**A** ash. For the XRD analysis all six ash samples were analysed for their chemical formations.

SEM results

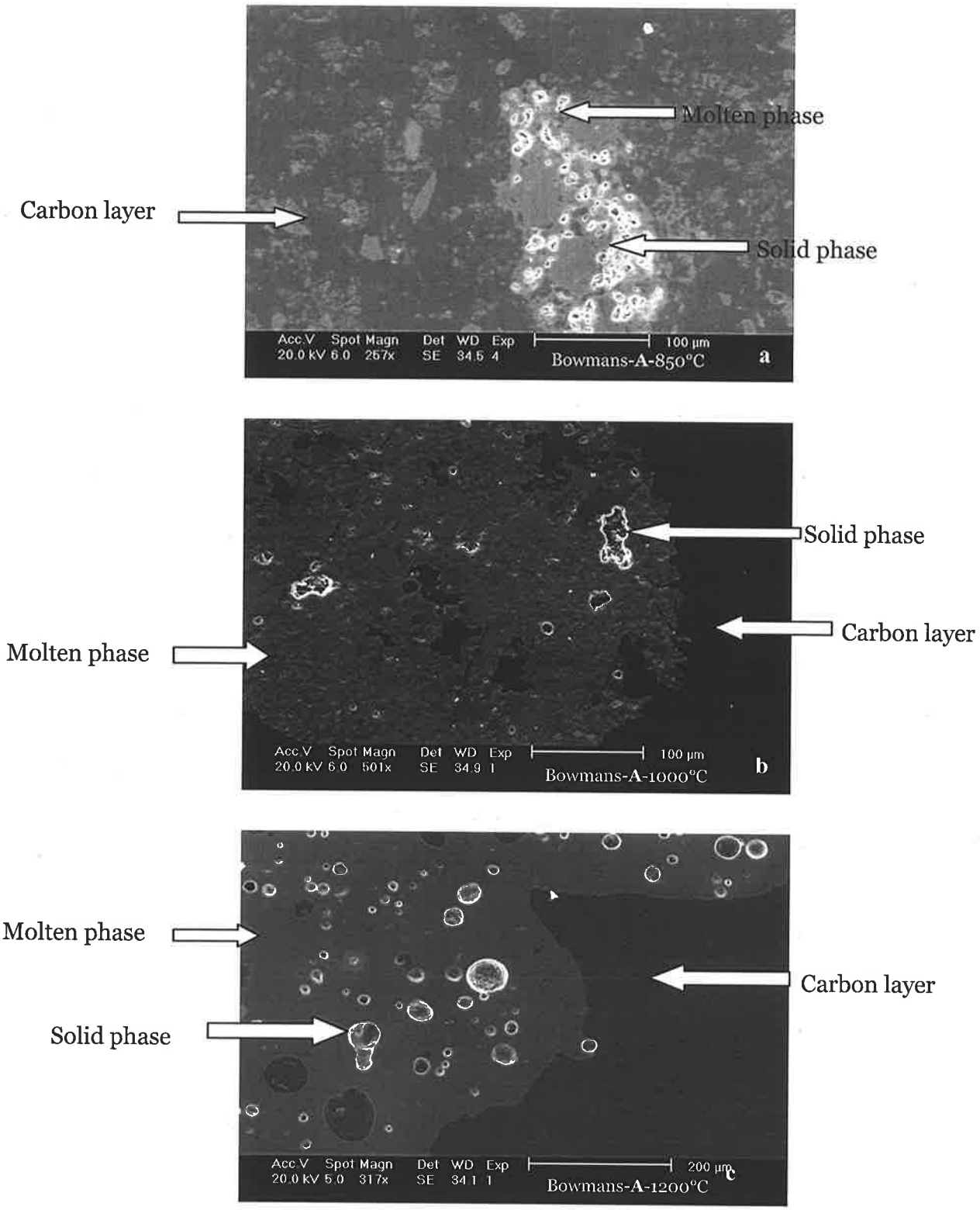

Fig 4.14: SEM's results for the Bowmans-**A** ash **(a)** 850°C; **(b)** 1000°C; **(c)** 1200°C

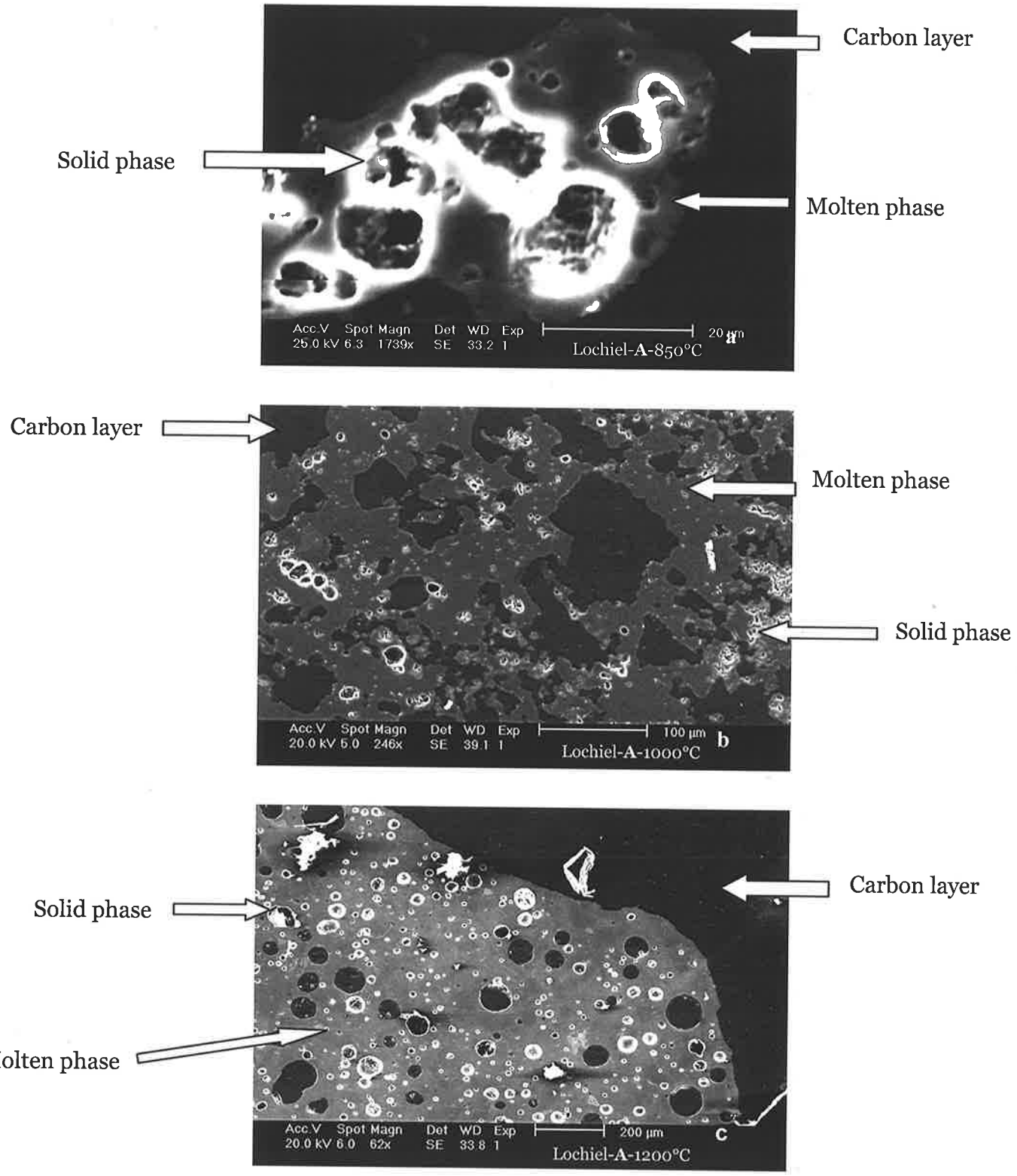

Fig 4.15: SEM results of the Lochiel-**A** ash **(a)** 850°C; **(b)** 1000°C; **(c)** 1200°C

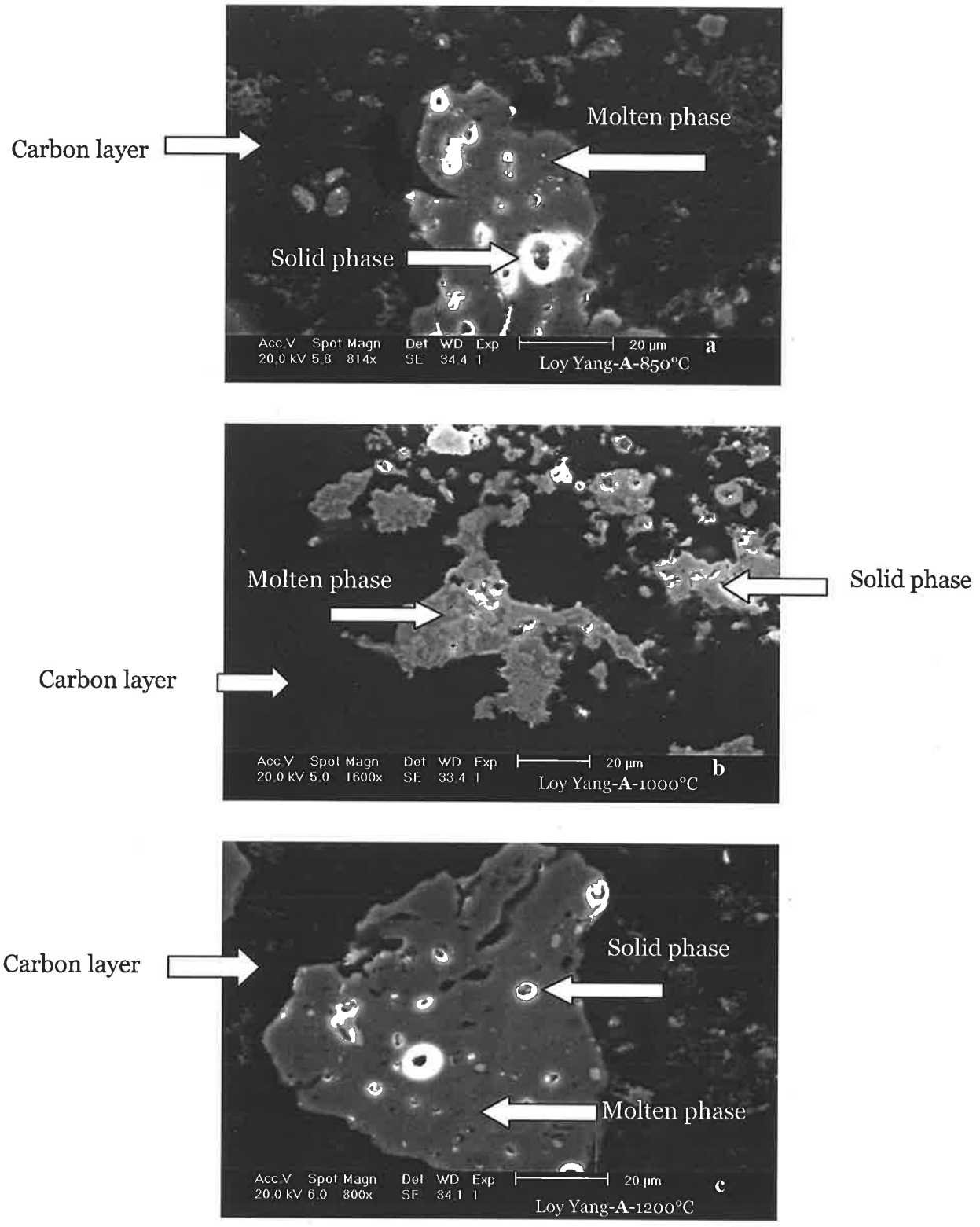

Fig 4.16: SEM results of the Loy Yang-**A** ash **(a)** 850°C; **(b)** 1000°C; **(c)** 1200°C

Figs 4.14-4.16 show the SEM results of the Bowmans-**A**, the Lochiel-**A** and the Loy Yang-**A** ashes that were corrected after finished rheological measurements at temperature of 850°C, 1000°C and 1200°C. The ash samples were examined using different intensities of the electron beam in order to obtain the best response of the electron beam, which was reflexed from the surface of each sample. In this work, the intensity of the electron beam used ranged from 20 kV to 25 kV.

Inspection of the SEM results found that there were three colours appearing in the SEM Figs - a dark colour, a light grey colour (molten phase) and a bright/white colour (solid phase). From the chemical analysis mode of the SEM, it was found that the dark colour is the carbon composition that coated the surface of the SEM samples. The light grey colour contains CaO, MgO, Na_2O and SO_3 and the bright colour contains of SiO_2, Al_2O_3, Fe_2O_3, CaO, MgO, Na_2O and SO_3 compositions. This means that during high temperature rheological measurements, the Bowmans-**A**, the Lochiel-**A** and the Loy Yang-**A** ashes behave as a suspension in which the solid phase of SiO_2, Al_2O_3, Fe_2O_3, CaO, MgO, Na_2O and SO_3 components were suspended in the molten phase of CaO, MgO, Na_2O and SO_3 compositions. Furthermore, the SEM results show that the amount of the molten phase was increased as temperature increased. Fig 4.17 shows the concentration in % volume of solid and liquid phases found in the coal ash samples, and the data of the solid and liquid phases is given in Table IV.6.

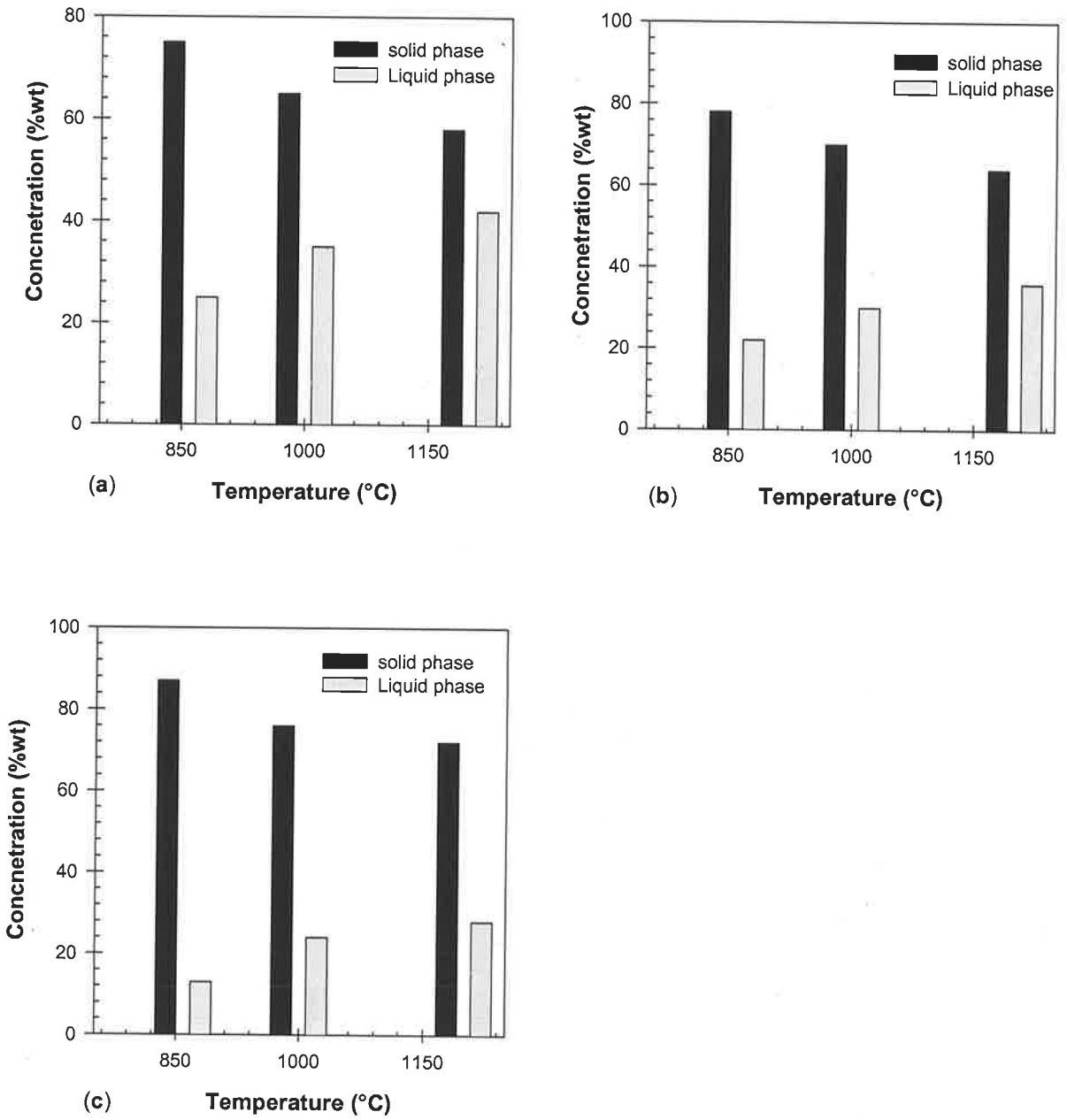

Fig 4.17: Amount of the solid and liquid phase (% volume) found in the laboratory ashes at temperature ranging from 850°C to 1200°C. (**a**) the Bowman-**A**; (**b**) the Lochiel-**A**; (**c**) the Loy Yang-**A**

Table IV.6: The concentration in % volume of solid and liquid phases found in the laboratory ashes

Temperature (°C)	Bowmans-**A**		Lochiel-**A**		Loy Yang-**A**	
	Solid phase	Liquid phase	Solid phase	Liquid phase	Solid phase	Liquid phase
850	72	26	85	15	80	20
1000	64	36	79	21	74	26
1200	54	46	70	30	66	34

The data in Table IV.6 shows that over the tested temperature range, the amount of molten phase in the Bowmans-**A** ash and the Lochiel-**A** ash was higher than that in the Loy Yang-**A** ash. The amount of the molten phase can be ranked in the following order; Bowmans-**A**>Lochiel-**A**>Loy Yang-**A**. In contrast, the amount of the solid phase decreased as temperature increased. It was found that at temperatures ranging from 850°C to 1200°C, the amount of the liquid phase in these coal ash samples was increased by approximately 2 times. The amount of the solid phase was decreased by 1.5 times in all the ash samples. The chemical analysis mode of the SEM analysis has shown that the concentration of CaO, MgO, Na_2O and SO_3 components previously contained in the solid phase has decreased, while the concentration of SiO_2, Al_2O_3 and Fe_2O_3 compositions remained unchanged. This suggests that more CaO, MgO and Na_2O components are molten as temperature increases, while the SiO_2, Al_2O_3 and Fe_2O_3 do not participate in the formation of the molten phase and remain as solid components throughout the whole range of temperatures tested. Although only the laboratory's samples were studied for their physical and chemical formations, the same conclusions may also be applied to the CFBC's ashes.

XRD results

Table IV.7: XRD results[2] (**a**) Coal ashes tested at 850°C; (**b**) Coal ashes tested at 1000°C; (**c**) Coal ashes tested at 1200°C

Coal ash sample	Anhydrite $CaSO_4$	Forsterite $MgSO_4$	Quartz SiO_2	Hematite Fe_2O_3	Aluminosilicate $Na_2AlSi_3O_8$	Thenardite Na_2SO_4
Loy Yang-**A**	T	T	D	M	T	T
Loy Yang-**B**	T	T	D	M	M	T
Morwell-**B**	T	T	D	M	M	T
Lochiel-**A**	M	M	D	T	T	SD
Lochiel-**B**	M	M	SD	T	T	SD
Bowmans-**A**	M	M	SD	T	T	D

(**a**)

Coal ash sample	Anhydrite $CaSO_4$	Forsterite $MgSO_4$	Quartz SiO_2	Hematite Fe_2O_3	Aluminosilicate $Na_2AlSi_3O_8$	Thenardite Na_2SO_4
Loy Yang-**A**	M	M	D	M	T	M
Loy Yang-**B**	M	M	D	M	M	T
Morwell-**B**	M	M	D	M	M	T
Lochiel-**A**	M	M	D	T	T	D
Lochiel-**B**	M	SD	SD	T	T	D
Bowmans-**A**	M	M	SD	T	T	D

(**b**)

Coal ash sample	Anhydrite $CaSO_4$	Forsterite $MgSO_4$	Quartz SiO_2	Hematite Fe_2O_3	Aluminosilicate $Na_2AlSi_3O_8$	Thenardite Na_2SO_4
Loy Yang-**A**	M	M	D	M	T	M
Loy Yang-**B**	M	M	D	M	M	T
Morwell-**B**	M	M	D	M	M	T
Lochiel-**A**	M	SD	D	T	T	D
Lochiel-**B**	M	SD	SD	T	T	D
Bowmans-**A**	M	M	SD	T	T	D

(**c**)

[2]D-dominant (>60 % volume), SD-sub-dominant (20-60 % volume), M-minor (5-20 % volume), T-trace (<5 % volume)

Table IV.7 shows the XRD results for the six coal ash samples collected at temperatures 850°C, 1000°C and 1200°C. The XRD results reveal that there are chemical reactions, especially between alkali metals (Na_2O, CaO and MgO) and sulphite (SO_3), during ash formation. Reactions between these chemical components lead to the formation of the alkali sulphate compounds $CaSO_4$, $MgSO_4$ and Na_2SO_4. According to a phase diagram book by Hall (1947) $CaSO_4$, $MgSO_4$ and Na_2SO_4 can further react and form a low melting-point eutectic mixture. The phase diagram book also indicates that the melting temperature of alkali sulphate mixtures can vary from 600°C to 850°C depending on the concentrations of chemical components in the mixture. Moreover, the XRD also shows that Na_2O, Al_2O_3 and SiO_2 react together and form aluminosilicate ($NaAlSi_3O_8$). However, only small concentrations of this compound were found, as the concentration of the aluminosilicate appeared to be at the trace level (T; < 5 % volume).

The XRD results demonstrate that at a given temperature, concentration levels of $CaSO_4$, $MgSO_4$ and Na_2SO_4 compounds in the Victorian ashes are lower than those in the South Australian ashes. At an operating temperature of 850°C concentration levels of $CaSO_4$ and $MgSO_4$ are at the minor level (M; 5-20 % volume) and Na_2SO_4 is at the trace level (T; < 5 % volume) for the Victorian ashes, while these three alkali sulphate components are at the sub-dominant level (SD; 20-60 % volume) for the SA ashes. The XRD also indicates that the concentration levels of $CaSO_4$, $MgSO_4$ and Na_2SO_4 in the Victorian ashes increases with temperature, as concentration of these three alkali sulphate components shift from the trace level (T; <5 % volume) to the minor level (M; 5-20 % volume). For the South Australian ashes only the concentration levels of Na_2SO_4 change from the sub-dominant level (SD; 20-60 % volume) to the dominant level (D; >60 % volume), while the concentration of $CaSO_4$ and $MgSO_4$ remain at the minor level (M; 5-20 % volume). It was also found that the concentration of SiO_2, Fe_2O_3 and NaCl did not change over the whole range of temperature tested as the concentration of these three components remained at the dominant level (D; >60 % volume), the sub-dominant level (SD; 20-60 % volume) and the trace level (T; <5 % volume) for SiO_2, Fe_2O_3 and NaCl respectively.

From the information obtained from the SEM and the XRD, it can now be categorically concluded that the role of chemical compositions, especially the alkali sulphates ($CaSO_4$, $MgSO_4$ and Na_2SO_4), on the rheological properties of the coal ash samples is significant. These three-alkali sulphate components react together and form a low melting-point eutectic mixture of alkali sulphate compounds. In contrast, at temperatures ranging from 850°C to 1200°C, the SiO_2, Fe_2O_3 and Al_2O_3 components are in the solid phase and they do not react with any other chemical components. The SEM and XRD analyses have

clearly demonstrated that during rheological measurements, the low-rank Australian coal ash samples were a solid and liquid mixture in which the solid phase was the SiO_2, Fe_2O_3 and Al_2O_3 and the liquid phase was a low melting-point eutectic mixture of $CaSO_4$, $MgSO_4$ and Na_2SO_4.

The information obtained from the bulk chemical composition analysis, flow properties, SEM and XRD have yielded the understanding on how chemical compositions control the rheological properties of low-rank Australian coal ashes. It become clear that the South Australian ashes are more viscous and have a higher yield stress than Victorian ashes because the South Australian ashes are higher in concentration levels of CaO, MgO, SO_3 and Na_2O components, which is a consequence of high concentrations of the alkali sulphate mixture, than the Victorian ashes.

Comparing between the South Australian ashes, it was found that viscosity and yield stress were increased as concentration levels of CaO, MgO, SO_3 and Na_2O increased. The evidence was clearly observed when comparing the flow data between the Bowmans-**A** and the Lochiel-**A** and Lochiel-**B** samples. Effects of chemical compositions are also similar for the Victorian ashes as the Loy Yang-**A** was more viscous and high in yield stress than the Loy yang-**B** and the Morwell-**B** ashes.

In addition, comparing ashes that are from the same coal but were obtained differently (the laboratory ash and the CFBC ash) has revealed the effects of $MgSO_4$ on the rheological properties of coal ashes. The $MgSO_4$ in the Lochiel-**A** was at trace level (<5%volume), but was at minor (5-20%volume) for the Lochiel-**B** sample. This evidence indicates that when the level of $MgSO_4$ increased, the viscosity and yield stress were decreased. Comparing the Loy Yang-**A** and the Loy Yang-**B** samples, it appears that aluminosilicate composition ($Na_2AlSi_3O_8$) plays the key role on the rheological properties of this ash. The $Na_2AlSi_3O_8$ was at a minor level for the Loy Yang-**B**, but at the trace level for the Loy Yang-**A** ash. However, in this work the effect of aluminosilicate on rheological properties was found only with the Loy Yang ash and further investigation is necessary.

Regarding the effects of SiO_2, Fe_2O_3 and Al_2O_3 components, it was found that ashes high in concentration of these compositions are low in viscosity and yield stress. The observations appear to contradict the findings previously established by other works (Nicholls et al, 1940; Vorres et al, 1986; Oh et al, 1995). Nicholls et al (1940), Vorres et al (1986) and Oh et al (1995) studied viscosity of British and American bituminous coal ash slags, which are high in SiO_2, Al_2O_3 and Fe_2O_3 components. Moreover, the rheological

measurements were performed at a temperature above 1300°C, which is well above the liquidus temperature, and SiO_2, Fe_2O_3 and Al_2O_3 components are completely molten at this temperature. In this work, the rheological measurements were performed at temperatures ranging from 850°C to 1200°C, which is the typical operating temperature found in the fluidised bed combustion process. At this temperature range SiO_2, Fe_2O_3 and Al_2O_3 compositions do not melt and remain as a solid phase throughout the tests. There is evidence of the formation of an aluminosilicate mixture ($Na_2AlSi_3O_8$), which is the molten phase of SiO_2 and Al_2O_3 when they react with Na_2O component. However, the concentration level of aluminosilicate is relatively small in comparison to the $CaSO_4$, $MgSO_4$ and Na_2SO_4 components. Thus, the effects of aluminosilicate mixture ($Na_2AlSi_3O_8$) may be neglected.

All in all, the chemical analyses performed in this work have shown that during rheological measurements of low-rank Australian ashes under temperatures relevant to those found from fluidised bed combustion, the coal ash samples are solid and liquid mixtures. The solid phase is mainly SiO_2, Fe_2O_3 and Al_2O_3, and the liquid phase is mainly a low melting point eutectic mixture of $CaSO_4$, $MgSO_4$ and Na_2SO_4. Concentration levels of $CaSO_4$, $MgSO_4$ and Na_2SO_4 are found to be the key factor affecting the rheological property of low-rank Australian coal ashes. However, in this chapter only the quantitative analysis has been investigated. This is due to the inconsistency of $CaSO_4$, $MgSO_4$ and Na_2SO_4 in the coal ash samples that constrains a systematic investigation. Thus, further systematic investigation into the effects of $CaSO_4$, $MgSO_4$ and Na_2SO_4 on rheological behaviours and properties of low-rank Australian coal ashes is required.

4.5.3 Effect of atmosphere on the rheological properties of coal ashes

Figs 4.18 shows the equilibrium flow curves of the Lochiel-**A** ash tested under three different atmospheres- the rich O_2 (representing the oxidising condition), the rich N_2 (representing the neutral environment) and the rich air (representing the actual condition in FBC). The experimental results show that the coal ash samples tested under the different atmospheres are similar in their flow characteristics, as they exhibit viscoplastic behaviour and a yield stress. However, the comparison of the flow curves found that the flow curves obtained from the neutral atmosphere appear to be more viscous and higher in yield stress than those obtained from the oxidising and air atmospheres. To facilitate the comparison, flow data is described using the Herschel & Bulkley model and values of the model parameters are given in Table IV.8.

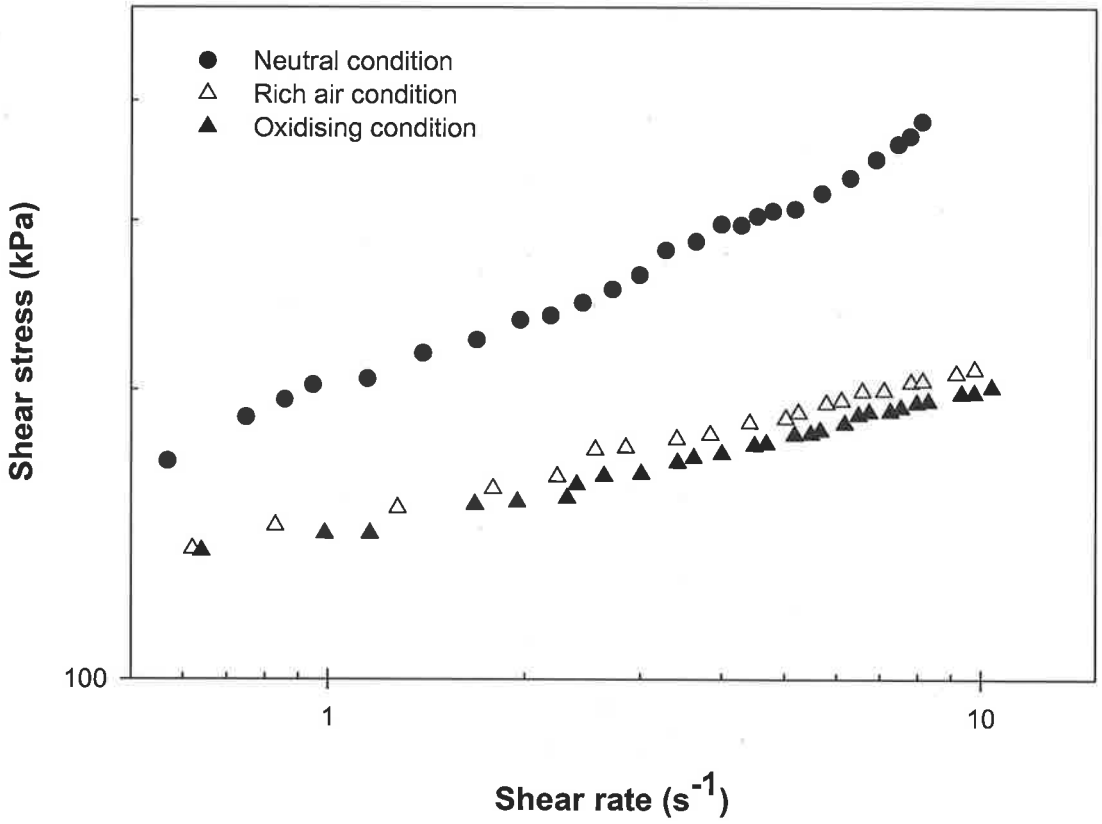

Fig 4.18: Comparison of flow data for the Lochiel-**A** ash tested at 850°C- Effect of operating atmosphere

Table IV.8: Values of the constants in the Herschel & Bulkley model

Operating condition	τ_y^{H-B} (kPa)	K (kPa s^n)	n (-)
Neutral	117.6	80.7	0.54
Oxidising	72.24	53.3	0.36
Rich air	87.9	58.4	0.32

Close inspection of the model parameter values for the Lochiel-**A** ash found that yield stress values of the coal ash tested under the neutral atmosphere are 1.3 times higher than yield stress values under the oxidising and the air atmospheres. For the apparent viscosity parameter, it was also found that values of the neutral atmosphere's ashes are 1.5 times higher than the values of coal ashes tested under the oxidising and air atmospheres. Regarding the flow behaviour index parameter, it was found that value of this parameter varies from 0.32 to 0.54 from the oxidising to neutral atmosphere. This suggests that the

degree of shear thinning behaviour decreases as the operating atmosphere is changed from the oxidising atmosphere to the neutral atmosphere.

The distinct change in the flow properties, especially the yield stress and viscosity, may be due to the difference in chemical formations that form from reactions of inorganic constituents during high temperature flow measurement. It has been reported that under a neutral atmosphere, the Na_2O can react with Cl causing formation of an NaCl mixture (Benson et al, 1998; Kosminski, 2001). With the presence of sodium chloride, a reaction of NaCl with SiO_2 and Al_2O_3 can occur, which leads to the formation of sodium silicates and aluminosilicate respectively. Sodium silicates under neutral conditions have significantly low melting points and are expected to contribute to the flow properties of the coal ash sample (Benson et al, 1998; Telfer, 1999; Kosminski, 2001).

4.6 CONCLUSIONS

The rheological characteristics of low-rank Australian coal ashes have been studied. Time dependency and shear dependency characteristics of coal ash samples have also been studied extensively. The effect of various parameters on the rheological characteristics and properties of coal ashes including chemical composition, operating temperatures and operating atmospheres have been investigated and discussed. The experimental findings allow the following conclusions to be drawn;

- In this chapter rheological characteristics and properties of the six low-rank Australian coal ashes were investigated. The measured flow property data have indicated that coal ash samples, at the equilibrium state, are highly non-Newtonian and characterised by shear thinning behaviour and a yield stress.

- Investigation into the time dependency of coal ash samples found that coal ashes are thixotropic materials. Studying the structural kinetics of the coal ash samples has shown that coal ash structures break down during the shearing process and this is an irreversible process. Also, coal ash structures are strongly dependent on coal type, shear rate and operating temperature.

- It has been found that the chemical components in coal ash react together, especially the alkali (CaO, MgO and Na_2O) and sulphite (SO_3) components, forming alkali sulphate compounds of $CaSO_4$, $MgSO_4$ and Na_2SO_4. These three alkali sulphates can react together and form a low melting point eutectic mixture.

It has been found that the values of the yield stress, the apparent viscosity and the flow behaviour index are strongly dependent on concentration levels of these three alkali sulphate compounds.

- It has been found that the yield stress and viscosity of coal ash samples are strongly dependent on temperature as they decrease with increasing temperature, while the flow behaviour index is independent of temperature. In this work, the temperature dependence characteristics have been characterised by the Arrhenius equation. It has been found that the sensitivity of yield stress and viscosity of coal ash samples to temperature is similar over the whole range of temperatures tested. However, the SA ashes are more viscous and higher in yield stress than the Victorian ashes at the same temperature.

- The effect of atmosphere has also been investigated and it was found that under a neutral condition the coal ash samples seem to be higher in yield stress, viscosity and lower in flow behaviour index than under oxidising and rich air atmospheres. Only a qualitative statement can be made here, that the operating atmosphere may have an effect on transformation of the chemical components in coal ash samples, which can lead to the formation of different types of chemical compounds.

Chapter Five

Rheological study of synthetic ash mixtures

5.1 INTRODUCTION

It is important to have a good knowledge about rheology of low-rank Australian coal ashes under conditions similar to fluidised bed combustion. This leads to an improvement in the understanding of the mechanisms involved in coal ash depositions and agglomeration in fluidised bed combustion. In addition, the development of a rheological model for low-rank Australian coal ashes is also significant as the model can be used as an input for simulating flow characteristics and behaviours of coal ash during fluidised bed combustion process.

The study in the previous chapter has shown that three alkali sulphates of $CaSO_4$, $MgSO_4$ and Na_2SO_4 are key chemical compounds that control the rheology of various low-rank Australian coal ashes. These three alkali sulphate compounds react together and form a low melting point eutectic mixture in the ash matrix. Effects of other chemical compounds appear to be minimal and can be neglected. SiO_2, Al_2O_3 compounds can be considered as unmelted solid particles suspended in a molten eutectic of $CaSO_4$-$MgSO_4$-Na_2SO_4 mixtures. However, effects of $CaSO_4$, $MgSO_4$ and Na_2SO_4 compounds on rheological properties of coal ash sample are not fully understood and it is urgently required. This is because of chemical compounds in the actual ash sample is complex and inconsistencies in the concentration level of chemical compound, which are constraining a systematic investigation of how chemical compounds affect the rheological properties of coal ash. Thus, it is necessary to replace coal ash samples with synthetic mixtures containing few chemical components. The previous chapter has also identified that the unmelted solid particles is mainly SiO_2 compound.

This chapter presents investigations into the effects of $CaSO_4$, $MgSO_4$ and Na_2SO_4 on the rheological characteristics and properties of synthetic ash mixtures at temperatures ranging from 850°C to 1200°C. The synthetic ash contains only a few of the chemical compounds found in coal ash samples. With the use of a synthetic ash mixture, the

concentration levels of chemical compounds can be controlled. This chapter aims to answer the following questions:

1. What are the flow characteristics of synthetic mixtures at temperatures between 850°C and 1250°C, and are they similar to the flow characteristics of coal ash samples?
2. What is the effect of $CaSO_4$, $MgSO_4$ and Na_2SO_4 compounds on flow characteristics and properties of synthetic ash mixtures?
3. Can results obtained from synthetic ash mixtures be compared with, and used to describe the time dependent characteristics of coal ashes?
4. Can results obtained from synthetic ash mixtures be compared with, and used to describe the equilibrium rheological characteristics and properties of coal ashes?

The structure of this chapter is as follows. Details of a factorial design experiment, materials used, and preparation methods of synthetic ash mixtures are given in the first section. In the second section, transient flow characteristics of synthetic mixtures are discussed. Effects of chemical compositions on time dependent characteristics and properties of synthetic mixtures are investigated in section three. The experimental results are also statistically analysed, which leads to the identification of key chemical compounds. Section three also presents the effects of shear rate and temperature. The forth section involves investigating the effect of alkali sulphates on equilibrium flow properties. Statistical analysis of the equilibrium flow properties is also performed and discussed. Finally, conclusions and answers to the questions outlined earlier are given.

5.2 MATERIALS AND PREPARATIONS

The previous chapter reported that during a rheological measurement, an ash sample is a mixture of solid and liquid compounds. The liquid phase is a combination of $CaSO_4$, $MgSO_4$ and Na_2SO_4 compounds, while the solid phase is mainly SiO_2. This means a synthetic mixture must contain the key chemical compounds that represent the liquid phase and the solid phase of the coal ash sample.

In this work, anhydrous $CaSO_4$, $MgSO_4$ and Na_2SO_4 compounds, and a unilab grade of SiO_2 were used. The preparation of a synthetic ash mixture consisted of two initial steps. First, the SiO_2 compound was crushed and sieved down to a particle size of 212 μm. Second, the crushed SiO_2, $CaSO_4$, $MgSO_4$ and Na_2SO_4 compounds were dried in a laboratory oven at temperature of 105°C for two hours to eliminate excess moisture.

Lastly the dried chemical compounds were stored in a silica dish before being used for making a synthetic ash sample.

5.3 EXPERIMENTAL DESIGNS

In this work, a factorial design technique was used to design the experimental program of the synthetic ash mixtures. Factorial design offers a more effective way of investigating the effects of various factors, when the levels of those factors are varied, on responses of a system than if each one was studied separately (Montgomery, 1991). Moreover, the factorial design requires a minimum number of experiments to be performed and still obtains all the significant information (Montgomery, 1991).

In this study, the factorial design technique was used to investigate effects of $CaSO_4$, $MgSO_4$ and Na_2SO_4 compositions at two significant levels, upper level (high concentration) and lower level (low concentration). Concentrations at the low level and the high level were calculated from known compositions of six low rank Australia coal ash samples and values of concentration at low and high levels are given in Table V.1.

Table V.1: Minimum and Maximum concentration levels of $CaSO_4$, $MgSO_4$ and Na_2SO_4 compounds (in molar percent)

Chemical composition	Maximum (high) concentration level (+)	Minimum (low) concentration level (-)
$CaSO_4$	26.0	11.0
$MgSO_4$	21.0	5.0
Na_2SO_4	19.0	10

The number of experimental sets of a full factorial design at two levels of concentration with three compositions (factors) can be calculated using a 2^n formula (Montgomery, 1991). This means a total of 2^3 or eight experimental sets were needed for this study. The orders in which sets of data were collected was designed in a random fashion in order to gain unbiased information. The compositions of the eight alkali sulphate samples tested are shown in Table V.2, with the samples labelled in alphabetical order from A to H. The experimental program was duplicated with the aim of checking the reproducibility of the results.

Table V.2: Full factorial design experiment of three alkali sulphates at two levels and their melting point temperatures

Sample	$CaSO_4$ (%mol)	$MgSO_4$ (%mol)	Na_2SO_4 (%mol)	SiO_2 (%mol)	Total (mol)	Melting Temp (°C)
A	26.0 (+)	21.0 (+)	19.0 (+)	34.0	100	810
B	26.0 (+)	5.0 (-)	10.0 (-)	59.0	100	845
C	11.0 (-)	21.0 (+)	10.0 (-)	58.0	100	825
D	26.0 (+)	21.0 (+)	10.0 (-)	43.0	100	810
E	11.0 (-)	5.0 (-)	19.0 (+)	65.0	100	636
F	26.0 (+)	5.0 (-)	19.0 (+)	50.0	100	820
G	11.0 (-)	21.0 (+)	19.0 (+)	50.0	100	723
H	11.0 (-)	5.0 (-)	10.0 (-)	74.0	100	780

The data in Table V.2 indicate that the total number of moles of each sample tested was equivalent to 100. The amount of SiO_2 in each mixture was determined by subtracting the sum of the number of moles of $CaSO_4$, $MgSO_4$ and Na_2SO_4 in the mixture from the total number of moles of the sample. For example, sample A has a composition of 26 % $CaSO_4$, 21 % $MgSO_4$ and 19% Na_2SO_4, which means the amount of SiO_2 will be 34%.

The positive symbol (+) has been used to indicate a compound is at its high concentration level and the negative symbol (-) shows a compound at its low concentration level. For example, sample F was designed to study the interaction between $CaSO_4$ and Na_2SO_4, and their effect on the rheological properties; thus $CaSO_4$ (+) and Na_2SO_4 (+) are both at a high level. Sample B was designed to study the effect of $CaSO_4$ therefore $CaSO_4$ (+) is at a high level, while the other two compounds are at a low level (-).

Melting temperatures of the synthetic mixtures used in this study were obtained using a Thermal Mechanical Analyser (TMA), and are given in Table V.2. Details about the procedures used in TMA can be found in section 4.2.3. Table V.2 shows that the melting temperatures of the factorial mixtures varied from 650°C to 850°C, depending on the composition. It appears that mixtures predominantly high in Na_2SO_4 are lower in melting temperature than those predominantly high in either $MgSO_4$ or $CaSO_4$, or a combination of both compounds. TMA results also suggest that rheological measurements of the synthetic ash mixtures can start at temperature of 850°C, where all alkali sulphate compounds are completely melted.

5.4 EXPERIMENTAL CHARACTERISATIONS

There were two experimental methods used for measuring the flow characteristics and properties of the eight synthetic ash mixtures. These are the sweep shear and the steady shear techniques. Details about the experimental procedures used in the sweep shear and the steady shear techniques were given in chapter four, section 4.3.

5.5 EXPERIMENTAL RESULTS

5.5.1 Sweep shear results

Fig 5.1 shows transient viscosity data obtained from the sweep shear experiment for the synthetic ash mixtures B, C and E tested at 850°C. The sweep shear experiment was performed under conditions of a maximum shear rate ($\dot{\gamma}_{max}$) of 10 s^{-1} and 10 minutes/cycle (similar operating conditions to that used with the coal ash samples). Experimental results show a viscosity hysteresis in the synthetic mixtures with the pattern of viscosity of the up-curve (ascending shear rate) being situated above the down-curve (descending shear rate).

Comparison of the area enclosed by the hysteresis loop (a measure of degree of thixotropy) found that the degree of thixotropy of sample B, predominantly high in $CaSO_4$, and sample C, predominantly high in $MgSO_4$, were similar. The degree of thixotropy of sample E was found to be the lowest of all the three samples tested.

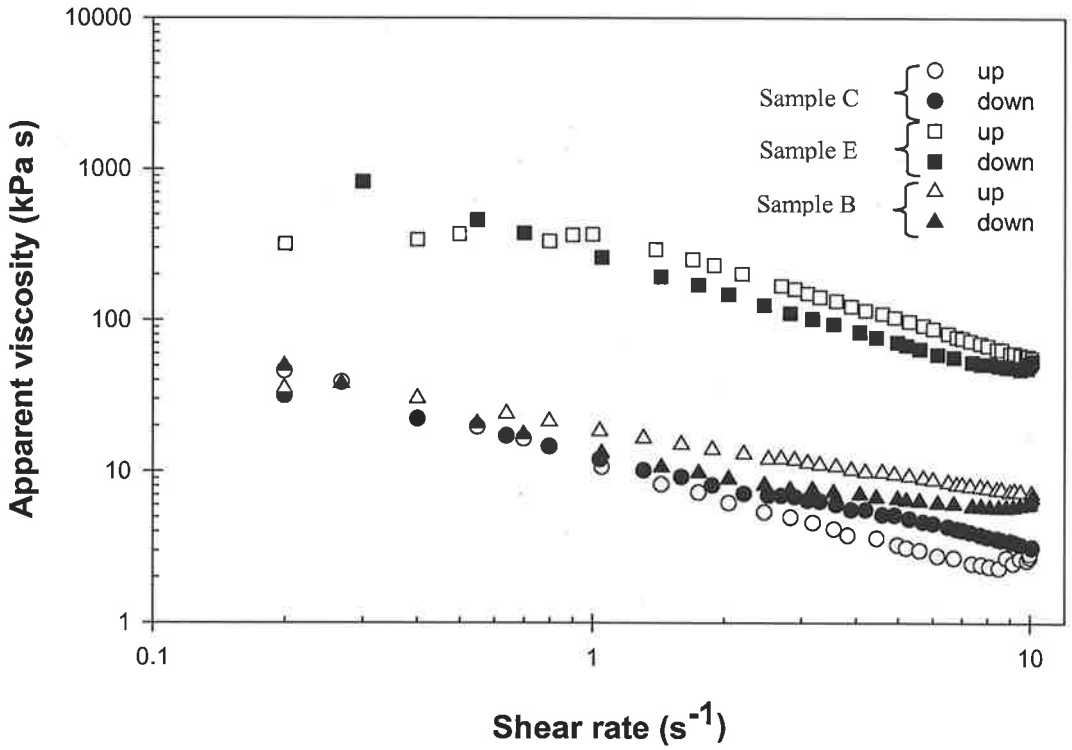

Fig 5.1: Transient viscosity behaviours of synthetic mixtures B, C and E at 850°C: Total sweep time = 10 minutes

5.5.2 Time dependent flow properties

Effect of chemical compositions

Fig 5.2 shows plots of viscosity versus shear time for the eight synthetic mixtures tested at a fixed shear rate of 3 s^{-1}, and at a constant temperature of 850°C. The experimental results show that at a fixed shear rate the viscosity decreases dramatically within a few minutes of shearing and approaches an equilibrium state. This behaviour indicates that the synthetic ash mixtures have time dependent characteristics.

The experimental results reveal that sample E has both the highest initial viscosity (η_o or the 'structured state') and the highest equilibrium viscosity (η_α, or the 'equilibrium structure state'). Sample B has both the lowest initial viscosity and the lowest equilibrium viscosity of all samples tested. Comparisons between samples E and B found that the sample E had initial and equilibrium viscosities 15 and 40 times higher than those found in the sample B respectively. The initial and equilibrium viscosity of the sample E were 20 and 24 times higher than the sample C. Moreover, it was found that the initial and

equilibrium viscosities of the samples high in Na_2SO_4 (samples E, F and G) are also higher in than the samples high in either $CaSO_4$ or $MgSO_4$ (samples B, C and D), or combination of both. The observation suggests that Na_2SO_4 is a significant compound causing high initial and equilibrium viscosities, while $CaSO_4$ and $MgSO_4$ can cause a reduction in initial and equilibrium viscosities.

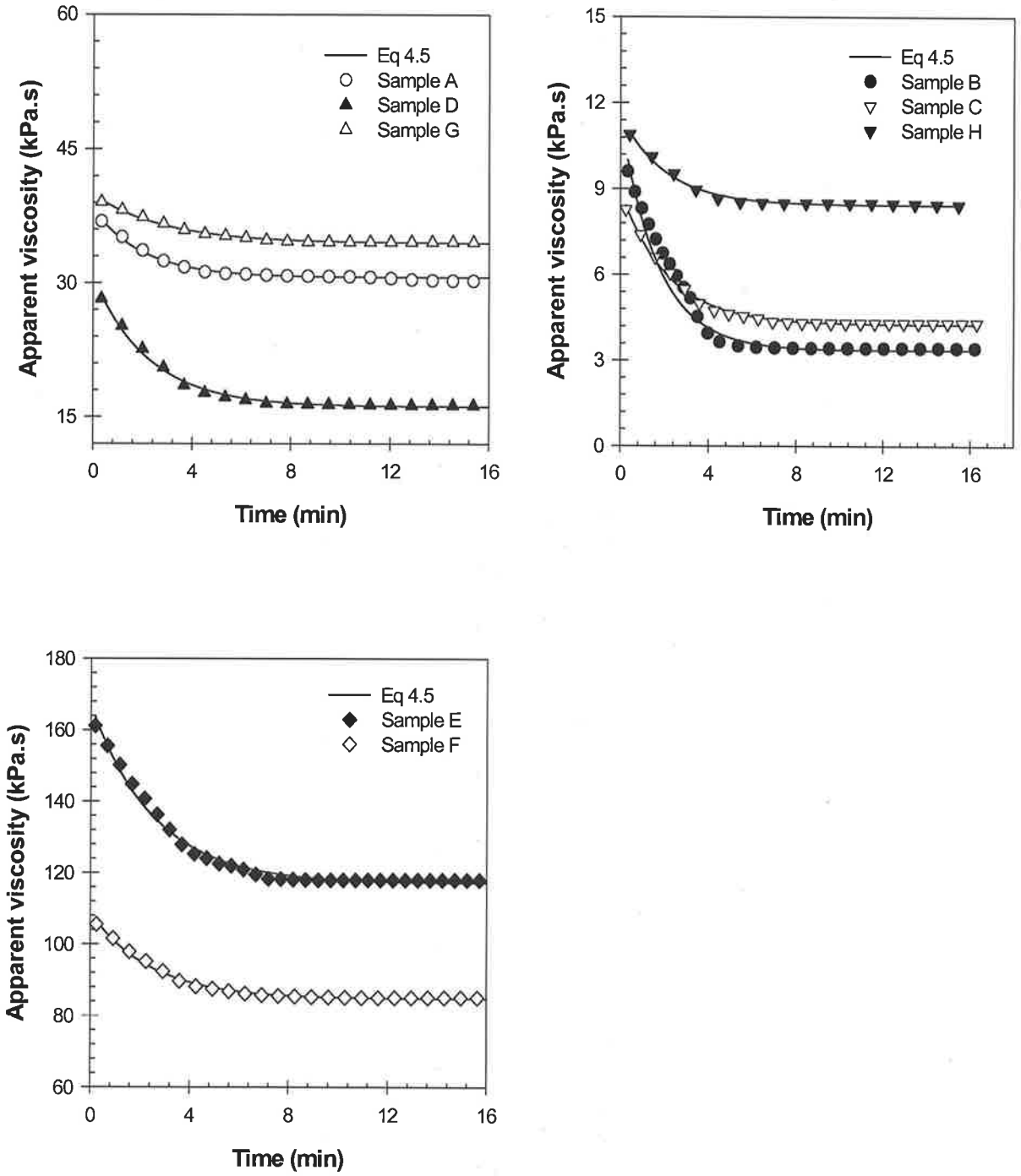

Fig 5.2: Transient viscosity data at constant shear rate ($\dot{\gamma}$ =3s^{-1}) for the mixtures A, B, C, D, E and F tested at a temperature of 850°C - Effect of chemical composition

Based on the structural kinetic approach, given in section 4.4.3, the time-dependent viscosity data were presented in Figs 5.3 and 5.4. It was found that the relationship between $(\eta - \eta_\alpha)^{1-m}$ and shear time for all synthetic mixtures is linear and this relationship can be well described using equation 4.5. This confirms that the structural breakdown of the synthetic mixtures is an irreversible process and the assumption given at the beginning of this section is correct.

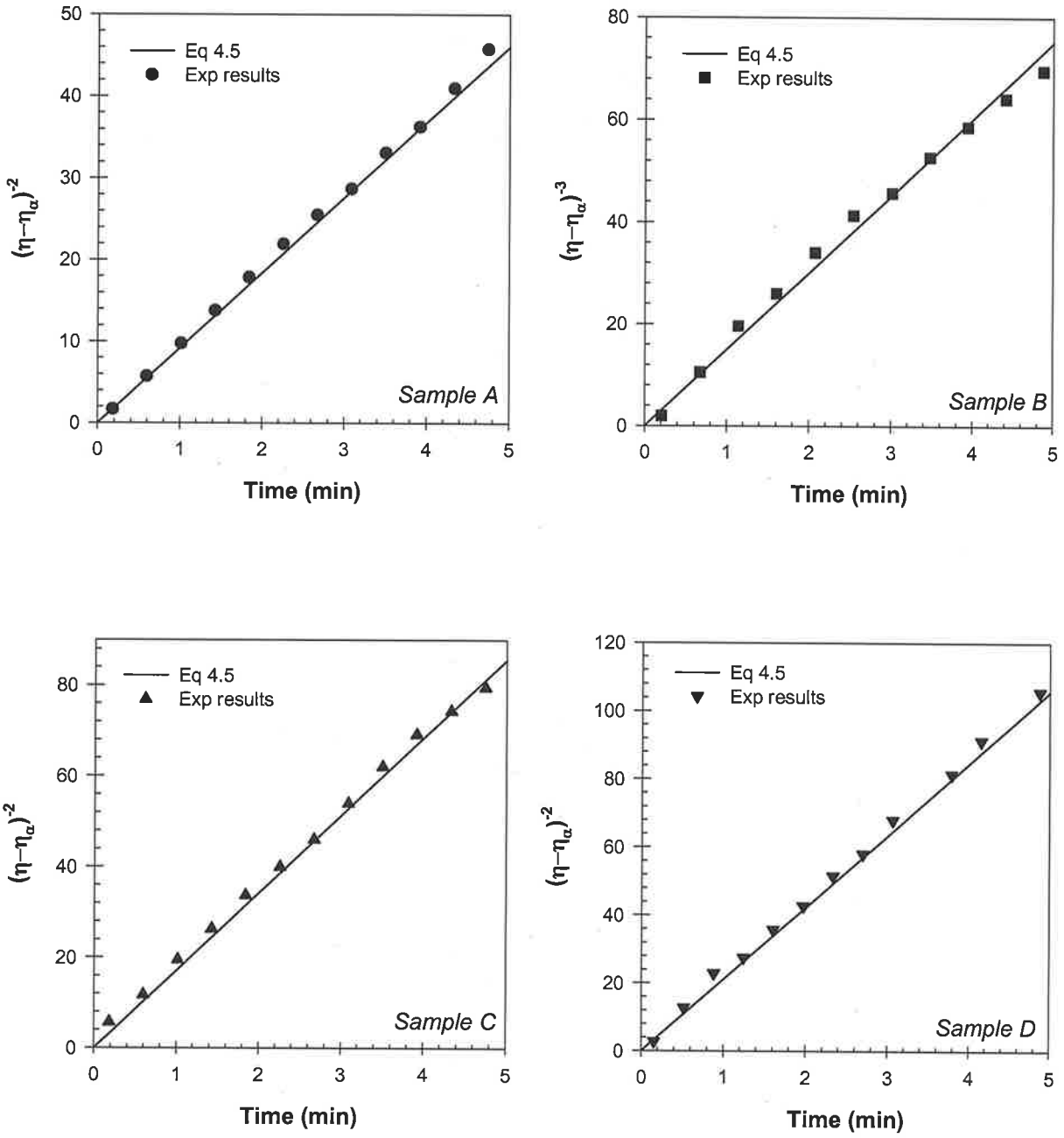

Fig 5.3: Testing of the structural kinetic model (eq4.5) with synthetic ash A, B, C and D sheared at $\dot{\gamma}$ =3s^{-1}, 850°C - Effect of chemical compositions

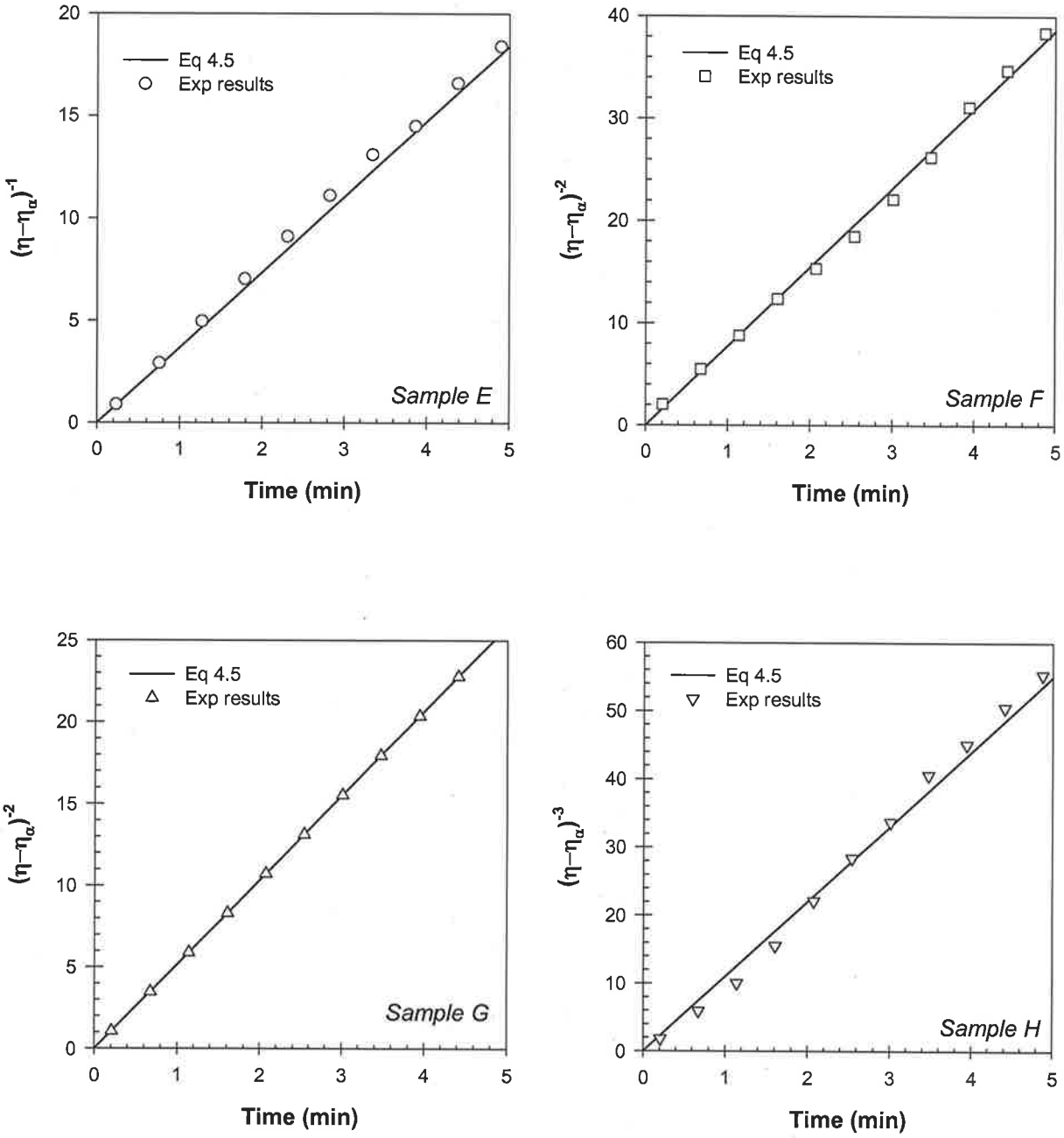

Fig 5.4: Testing of the structural kinetic model (eq4.5) with synthetic ash E, F, G and H sheared at $\dot{\gamma}$ =3s^{-1}, 850°C - Effect of chemical compositions

Table V.3 provides a summary of the values of the order of thixotropic structure breakdown (m), the rate of thixotropic structure breakdown (k) and the viscosity ratio (η_0:η_α) for the synthetic mixtures tested in this study.

Table V.3: Values of parameters in equation 4.5-Effect of chemical compositions

Sample	Temperature (°C)	Shear rate (s^{-1})	m	k (s^{-1})	$\eta_0:\eta_\alpha$
A	850°	3	3	0.165	1.24
B			4	0.25	1.35
C			3	0.275	2.1
D			3	0.34	1.72
E			2	0.06	1.34
F			3	0.125	1.24
G			3	0.08	1.2
H			3	0.165	1.24

Table V.3 shows that synthetic mixtures B (predominantly high in $CaSO_4$) and E (predominantly high in Na_2SO_4) have the order of thixotropic structure breakdown (m) of 4 and 2 respectively. This suggests that under the same temperature and shear rate conditions, the thixotropic structure of sample B goes through breakdown with a higher order than the thixotropic structure of sample E. Moreover, the degree of thixotropy obtained from the structure kinetic approach appears to agree well with the hysteresis results, in terms of the relative degree of thixotropy. From the hysteresis loop test, sample C was the highest degree of thixotropy, while sample E was the lowest. Similar characteristics were also obtained from the structure kinetic approach in which the order of thixotropic (m) of sample C is higher than sample E. Samples A, C, D, F, G and H were found to have the same value of the order of thixotropic structure breakdown (m=3 for these synthetic mixtures), indicating that under the sample shear rate and temperature tested, the thixotropic structures of these samples undergo breakdown under the sample rate.

Table V.3 reveals also that sample E has the lowest rate of thixotropic structure breakdown (k=0.06 s^{-1}) of all samples tested. Comparing values of the k parameter for samples B, C and D, it was found that the rate of thixotropic breakdown in the samples B and C was higher than that in sample E. Moreover, comparing values of the k parameter for sample E (predominantly high in Na_2SO_4) and F (predominantly high in $CaSO_4$ and Na_2SO_4), it was also found that the rate of thixotropic structure breakdown is also increased, as it increased from 0.06 s^{-1} to 0.13 s^{-1}. The observation reveals that $CaSO_4$ and $MgSO_4$ have a significant effect on increasing the rate of thixotropic breakdown, while

Na_2SO_4 has the opposite effect. Table V.3 also shows that the predominantly high in $CaSO_4$ sample (sample B) has the highest viscosity ratio value (η_0/η_α). This suggests that the values of the viscosity of sample B changes more rapidly from the initial to the equilibrium than the other synthetic mixture samples.

Effect of shear rate

The effect of shear rate on the transient viscosity of synthetic mixtures was also investigated. This was determined by shearing the synthetic mixture E at three shear rate values of 0.7, 3 and 10 s^{-1} all at a fixed temperature of 850°C. The effect of shear rate on the viscosity of sample E is shown in Fig 5.5. The experimental results show that the initial viscosity and the equilibrium viscosity are smaller at higher shear rates. These characteristics indicate that the sample is a shear thinning material.

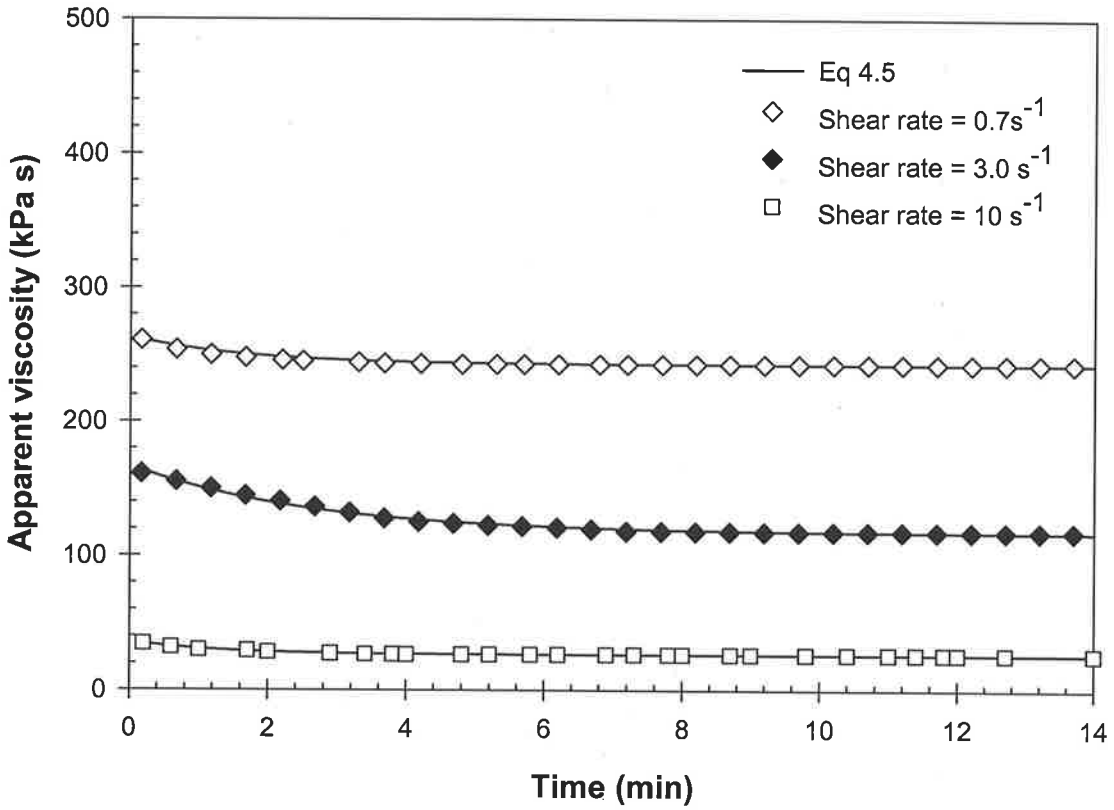

Fig 5.5: Transient viscosity data for mixture E- Effect of shear rate

Effect of temperature

The effect of temperature on the transient viscosity of synthetic mixtures was investigated by shearing sample E at a fixed shear rate of 3 s^{-1}, and under three different temperatures, namely 850, 1000 and 1200°C. The results are shown in Fig 5.6. Experimental results show that the initial viscosity and the equilibrium viscosity were decreased as temperature increased.

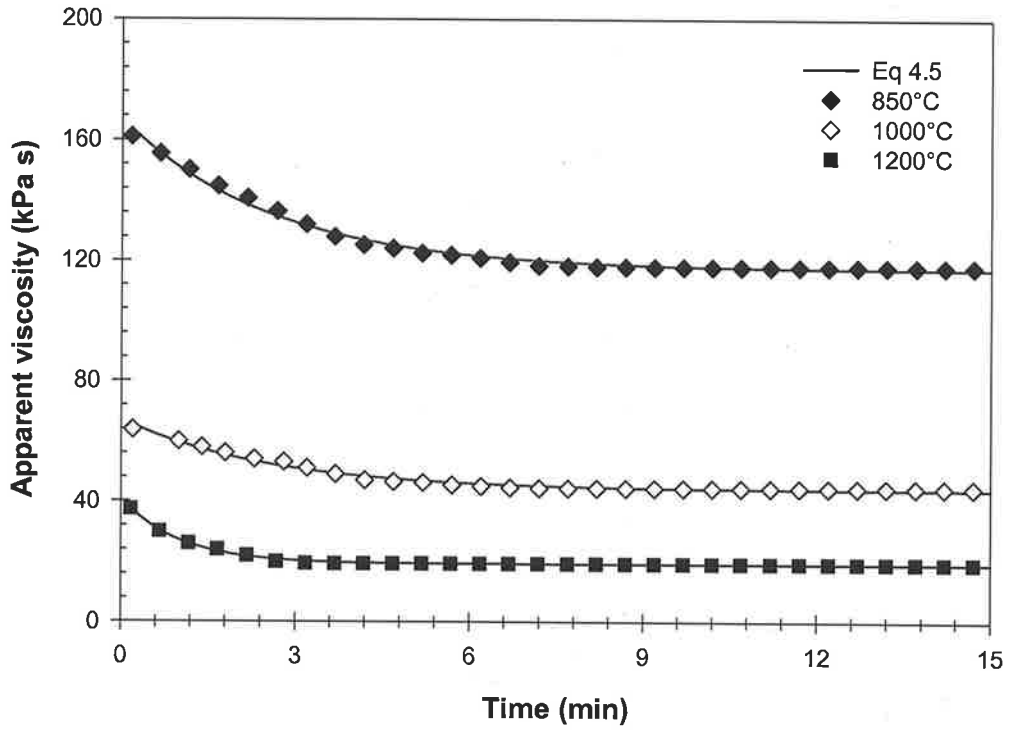

Fig 5.6: Effect of temperature on transient viscosity data of the synthetic mixture E tested at a fixed shear rate of 3 s^{-1}

Table V.4: Values of parameters in equation 5.1-Effect of shear rate and temperature

Sample	Temperature (°C)	Shear rate (s^{-1})	m	k (s^{-1})	$\eta_0:\eta_\alpha$
E	850°	0.7	2	0.06	1.04
		3.0	2	0.12	1.25
		10	2	0.18	1.32
E	850	3	2	0.06	1.34
	1000		2	0.08	1.42
	1200		2	0.12	1.6

Table V.4 shows the rate of thixotropic breakdown (k) and extent of thixotropy (η_0:η_α) of sample E are strongly affected by shear rate and temperature. The rate of thixotropic structure breakdown increased by a factor of 3, and the extent of thixotropy was also increased 1.2 times when the shear rate was increased from 0.7 s^{-1} to 10 s^{-1}. The rate of thixotropic structure breakdown was increased 2 times when increasing the operating temperature from 850°C to 1200°C. The viscosity ratio value was also increased with increasing temperature, indicating that viscosity of the synthetic mixture change more rapidly as temperature increased.

5.5.3 Equilibrium flow properties

In this section the equilibrium flow curves of all synthetic mixtures are presented. Fig 5.7 shows the equilibrium flow curves of all eight synthetic mixtures tested at a fixed temperature of 850°C and under a rich air atmosphere. A non-linear relationship between shear stress and shear rate is found in all synthetic mixture samples. This relationship indicates that the synthetic mixtures are non-Newtonian materials. It was also found that all flow curves intercept the shear stress axis at a shear rate of zero, indicating the apparent yield stress behaviour of the synthetic ash samples.

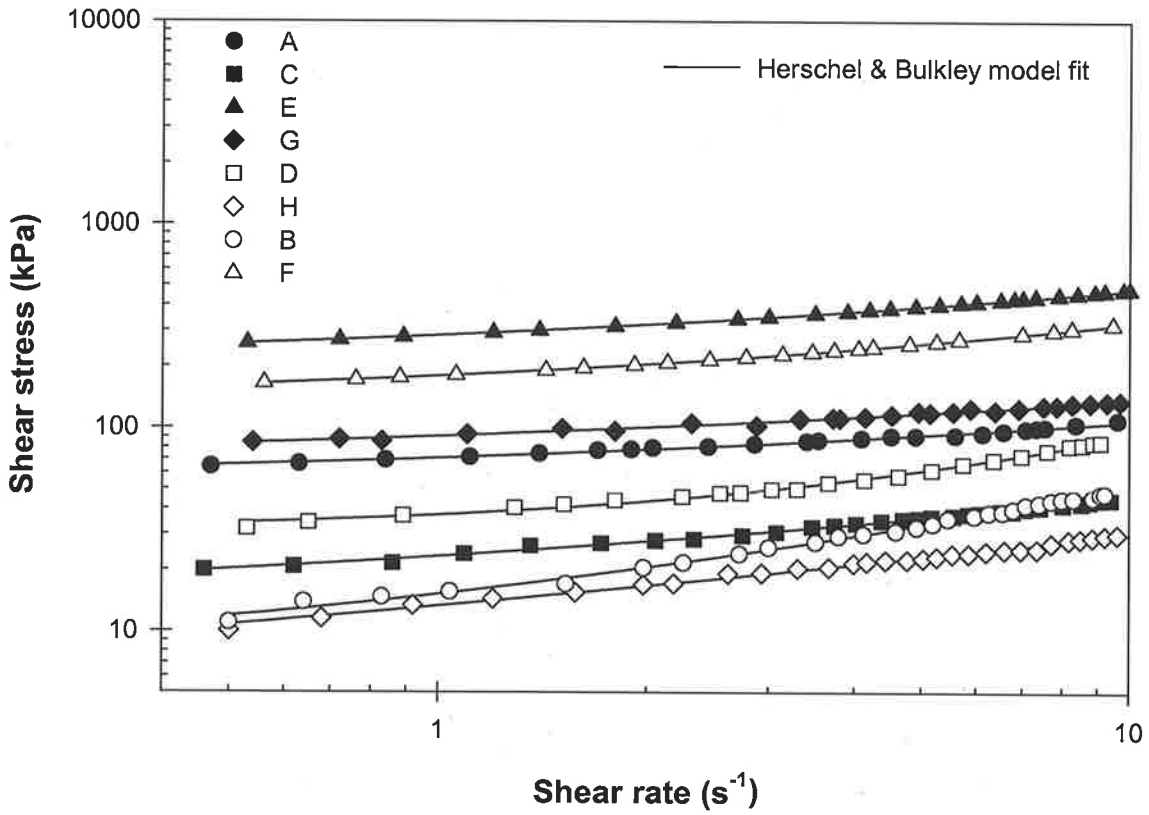

Fig 5.7: Flow curves for the synthetic ash mixtures

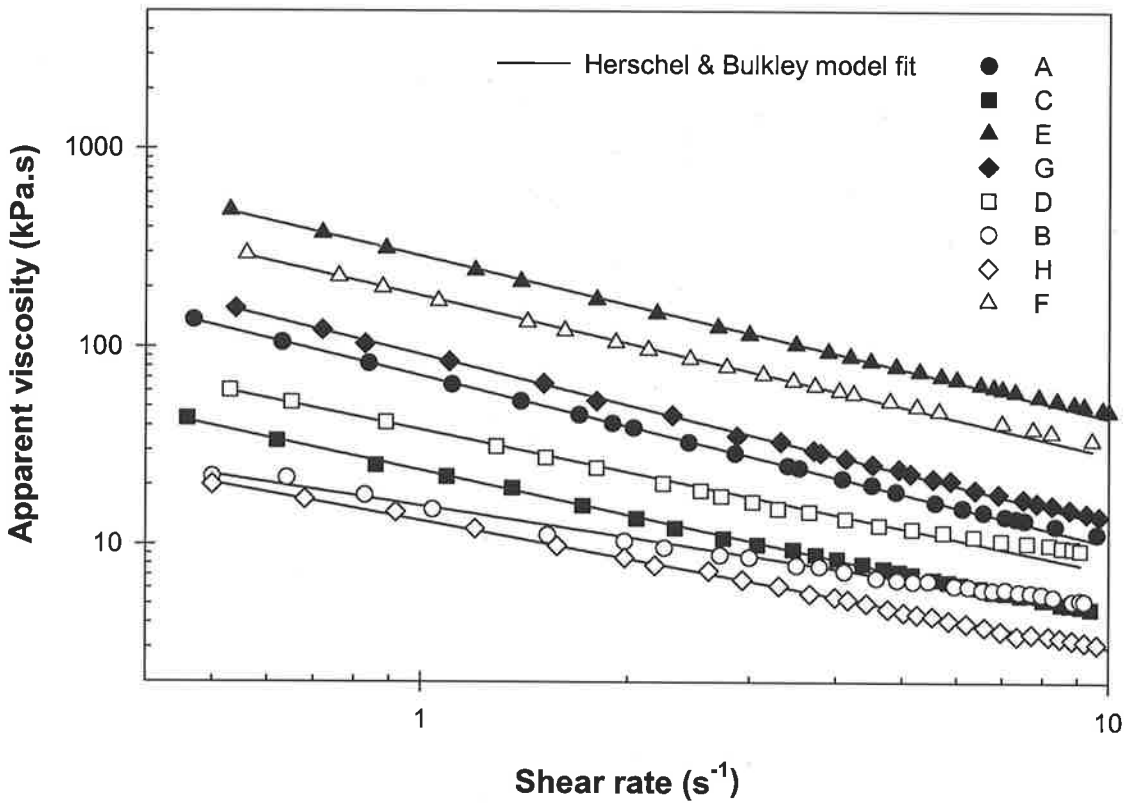

Fig 5.8: Apparent viscosity for synthetic ash mixtures

The data in Fig 5.7 have also been replotted in the form of apparent viscosity (defined as shear stress divided by shear rate) versus shear rate as shown in Fig 5.8. The experimental data has revealed that the viscosity values of the synthetic mixtures are not constant but decrease dramatically with increasing shear rate. This behaviour is known as shear-thinning behaviour, which is commonly found in many industrial fluids.

The rheological data in Fig 5.8 reveals that the mixture E (which is predominantly high in Na_2SO_4) is the most viscous and has the highest yield stress value of all the samples tested. In contrast, mixture B (predominantly high in $CaSO_4$) is the least viscous and has a negligible yield stress. Furthermore, mixtures F, G and A, which all contain high levels of Na_2SO_4, have substantially higher viscosity and yield stress than mixtures A, D, C and B, which are high in either $CaSO_4$ or $MgSO_4$, or a combination of both components. This observation suggests that Na_2SO_4 has a significant effect in increasing the yield stress and viscosity whereas $CaSO_4$ and $MgSO_4$ cause a reduction in the yield stress and the viscosity of the synthetic mixtures.

Effect of chemical compositions

The Herschel & Bulkley model was used to describe the flow data of the synthetic ash mixtures. Details about the selection of a flow model for describing rheological data have already been given in chapter 4, section 4.4.6. The values of the Herschel & Bulkley model parameters for the synthetic ash mixtures obtained in replicates are given in Table V.4

Table V.4: Herschel & Bulkley model parameters for the synthetic ash mixtures tested at 850°C under a rich air atmosphere

Synthetic mixture	τ_y^{H-B} (kPa)		K (kPa.s^n)		n	
	1	2	1	2	1	2
A	51.4	47.7	19.27	22.16	0.4	0.4
B	1.63	1.49	12.08	15.62	0.6	0.6
C	10.7	12.8	8.81	10.63	0.5	0.6
D	13.3	14.6	24.55	18.01	0.6	0.6
E	194.8	197.6	89.11	85.47	0.4	0.5
F	129.7	123.1	49.3	47.57	0.6	0.64
G	64.6	59.0	30.11	27.4	0.5	0.5
H	3.9	4.4	9.45	10.02	0.5	0.5

A comparison of the results in Table V.4 for sample E, F and G clearly indicates the significant effects of the mixture composition on the rheological properties. The highest yield stress and viscosity of mixture E (high Na_2SO_4) were reduced by a factor of 1.5 and 2, respectively, by adding $CaSO_4$ to this mixture as seen in sample F (high $CaSO_4$ and Na_2SO_4). However, when $MgSO_4$ was added, a greater reduction, by factors of 3.5 (yield stress) and 4 (viscosity), was obtained as shown for sample G (high $MgSO_4$ and Na_2SO_4). Similar effects can be found from comparisons with the other samples. These results also demonstrate that Na_2SO_4 effectively increases the yield stress and viscosity of the eutectic mixture, whereas $MgSO_4$ has the opposite effect. Furthermore, it is interesting to note that the flow behaviour index (n) ranges from 0.4 to 0.6 and appears to be dependent on the mixture composition. This indicated that chemical compositions also have an effect on the sensitivity of viscosity to shear rate. That is, for a sample low in flow behaviour index value, viscosity of the sample becomes more shear sensitive. Data in Table V.4 show that the value of the flow behaviour index in sample A was the lowest among the

synthetic mixtures tested. This indicates that the viscosity of the sample A changes rapidly with shear rate compared to the other samples.

Comparisons between sample H (predominantly low in $CaSO_4$, $MgSO_4$ and Na_2SO_4) and sample E (predominantly high in Na_2SO_4) found that the yield stress and consistency increased by 40 and 11 times, respectively. This demonstrated that the values of the yield stress and consistency parameters are increased by increasing the concentration level of the Na_2SO_4 compound. The effect of Na_2SO_4 on flow behaviour index parameter appears to be minimal as the value of this parameter was only slightly changed, from 0.5 to 0.4. Between sample C (high in concentration of $MgSO_4$) and sample H, the yield stress and the consistency index parameters were also increased. The yield stress increased by a factor of 3, and the consistency increased by a factor of 1. Comparisons between samples C and H found that the yield stress and the viscosity of the synthetic mixture increased with increasing concentration of $MgSO_4$. However, $MgSO_4$ has no effect on the shear sensitivity of the viscosity of the synthetic mixture, as values of the flow behaviour index appear to be similar between the samples H and C. Increasing concentration levels of $CaSO_4$ in the mixture found that the yield stress was decreased, but the viscosity and flow behaviour index were increased. This suggests that increasing the concentration of $CaSO_4$ decreases the yield stress value of the mixture, but $CaSO_4$ produces a viscosity mixture with high viscosity and lower shear sensitivity.

The analysis of variance

To determine the level of significance of the concentration of the chemical compounds on the Herschel & Bulkley model parameters, the experimental results were also statistically analysed using the analysis of variance. The analysis of variance is a useful tool to identify or determine the level of significance the different factors (independent variables) have on the response (the dependent variable). In this study, the factors are chemical compounds and their interactions and the responses are the empirical constants in the Herschel & Bulkley model (the τ_y^{H-B}, the K and the n parameters).

To perform an analysis of variance, six initial values are required. They are **i)** the average effect of a factor, **ii)** a sum of squares (SS), **iii)** the number of degrees of freedom (df), **iv)** a mean square (MS) value, **v)** an F value and **vi)** a Prob-F value. The level of significance of a factor is determined based on its probability of distribution value (Prob-F). It is generally accepted that a significant factor has a Prob-F value less than or equal to 0.05 ($0.01 \leq$Prob-F≤ 0.05) (Montgomery, 1991).

The average effect of a factor is the difference between the average response at the first level of that factor and the average response at the second level of that factor. In this work, the first level is referred to as the low concentration level, and the second level is referred to as the high concentration level. The average factor effect is also known as the 'contrast' (Montgomery, 1991). The SS shows the distribution of a factor. Montgomery (1991) has suggested that for a factorial design experiment (2^3) with two replicates, the SS value can be calculated as the square of the contrast value of that factor divided by 8n, where n is the number of replicates. The number of degrees of freedom for each factor is equal to (n-1). The MS value is equal to the SS value for each factor divided by the number of degrees of freedom. The F value is the MS value of that factor divided by the number of degrees of freedom.

The contrast values for the significant factors can be either a positive or negative value. Montgomery (Montgomery, 1991) suggested that a positive value means if the level of that variable is increased from the first level to the second level this will result in an increase in the response value. A negative value (-) means if the level of the variable increases, the response value will be decreased.

Results of the analysis of variance on the effect of chemical compounds on the Herschel & Bulkley model parameters are given in Table V.5.

Table V.5: Analysis of variance on the Herschel & Bulkley model parameters: **a**-the yield stress (τ_y^{H-B}); **b**-the consistency index (K); **c**-the flow behaviour index (n)

Source of variation	Factor effect	Sum of square (SS)	Degree of freedom (df)	Mean square (MS)	F-value	Prob-F
$CaSO_4$ (A)	-21.44	1837.41	1	1837.41	297.43	<0.0001
$MgSO_4$ (B)	-47.06	8861.40	1	8861.4	1434.44	<0.0001
Na_2SO_4 (C)	99.82	39852.14	1	39852.14	6451.06	<0.0001
AB	14.82	878.83	1	878.83	142.26	<0.0001
AC	-19.60	1536.64	1	1536.64	248.74	<0.0001
BC	-58.58	13721.78	1	13721.78	2221.21	<0.0001
ABC	13.94	777.85	1	777.85	125.91	<0.0001

(a)

Source of variation	Factor effect	Sum of square (SS)	Degree of freedom (df)	Mean square (MS)	F-value	Prob-F
$CaSO_4$ (A)	17.40	1212.08	1	1212.8	21.95	0.0016
$MgSO_4$ (B)	-21.68	1878.79	1	1878.79	34.02	0.0004
Na_2SO_4 (C)	33.36	4452.89	1	4452.89	80.63	<0.0001
AB	-13.64	745.02	1	745.02	13.49	0.0063
AC	8.82	311.14	1	311.17	5.63	0.045
BC	-26.14	2731.11	1	2731.11	49.46	0.0001
ABC	-16.62	1104.90	1	1104.90	20.01	0.0021

(b)

Source of variation	Factor effect	Sum of square (SS)	Degree of freedom (df)	Mean square (MS)	F-value	Prob-F
$CaSO_4$ (A)	0.53	0.025	1	0.025	34.51	0.0004
$MgSO_4$ (B)	0.039	5.6E-05	1	5.6E-05	0.078	0.7868
Na_2SO_4 (C)	1.8E-05	2.2E-03	1	2.2E-03	3.14	0.1144
AB	-0.013	0.020	1	0.020	28.25	0.0007
AC	-0.036	7.56E-04	1	7.5E-04	1.05	0.3350
BC	-6.8E-03	6.0E-03	1	6.0E-03	8.36	0.0202
ABC	-0.022	7.6E-03	1	7.6E-03	10.65	0.0115

(c)

The data in Table V.5 (**a**, **b**) show that $CaSO_4$, $MgSO_4$, Na_2SO_4, and their interactions are significant factors on the yield stress and the consistency index properties of the synthetic mixtures. It was found that the contrast of $CaSO_4$ and $MgSO_4$ are negative values (-), while the contrast of Na_2SO_4 is a positive value (+). This means that if the concentration of Na_2SO_4 is increased from the minimum concentration level to the maximum concentration level then the value of the yield stress will be increased by a factor of 100 and the consistency index will be increased by a factor of 34. If the concentration of $CaSO_4$ is increased, values of the yield stress will be decreased by 20 times, but the consistency index will be increased by 34 times. Similarly, when the concentration of $MgSO_4$ is increased, the yield stress and the consistency index will be decreased by 47 and 21 times, respectively.

The contrast values for the interactions of $CaSO_4$-$NaSO_4$ and $MgSO_4$-Na_2SO_4 of the yield stress parameter have found to be in negative values suggesting that by adding either the $CaSO_4$ compound or the $MgSO_4$ compound into a sample predominantly high in Na_2SO_4, will decrease the value of the yield stress parameter by factors of 20 and 60 , respectively. For the consistency index parameter, it was found that the interaction of $CaSO_4$-$NaSO_4$ is positive and the interaction of $MgSO_4$-Na_2SO_4 is negative. This indicates that the consistency index will be increased by 8 times when $CaSO_4$ is added to a predominantly high in Na_2SO_4 sample, while the consistency index will be decreased by 26 times when $MgSO_4$ is added.

Table V.5 **c** shows that for the flow behaviour index parameter (n), it was found that $CaSO_4$ and the interactions of $CaSO_4$: $MgSO_4$, $MgSO_4$: Na_2SO_4 and $CaSO_4$:$MgSO_4$:Na_2SO_4 are significant factors. It was also found that the value of the flow behaviour index parameter will be decreased if the concentration of $CaSO_4$ is increased, as the contrast values of this composition are negative.

In order to demonstrate explicitly how the interactions of chemical compounds affect the rheological properties of the synthetic mixtures, plots showing the effects of differing levels of concentration of the significant factors on the rheological properties of the mixtures are shown in Figs 5.9-5.11 for the yield stress, the consistency index and the flow behaviour index parameters , respectively.

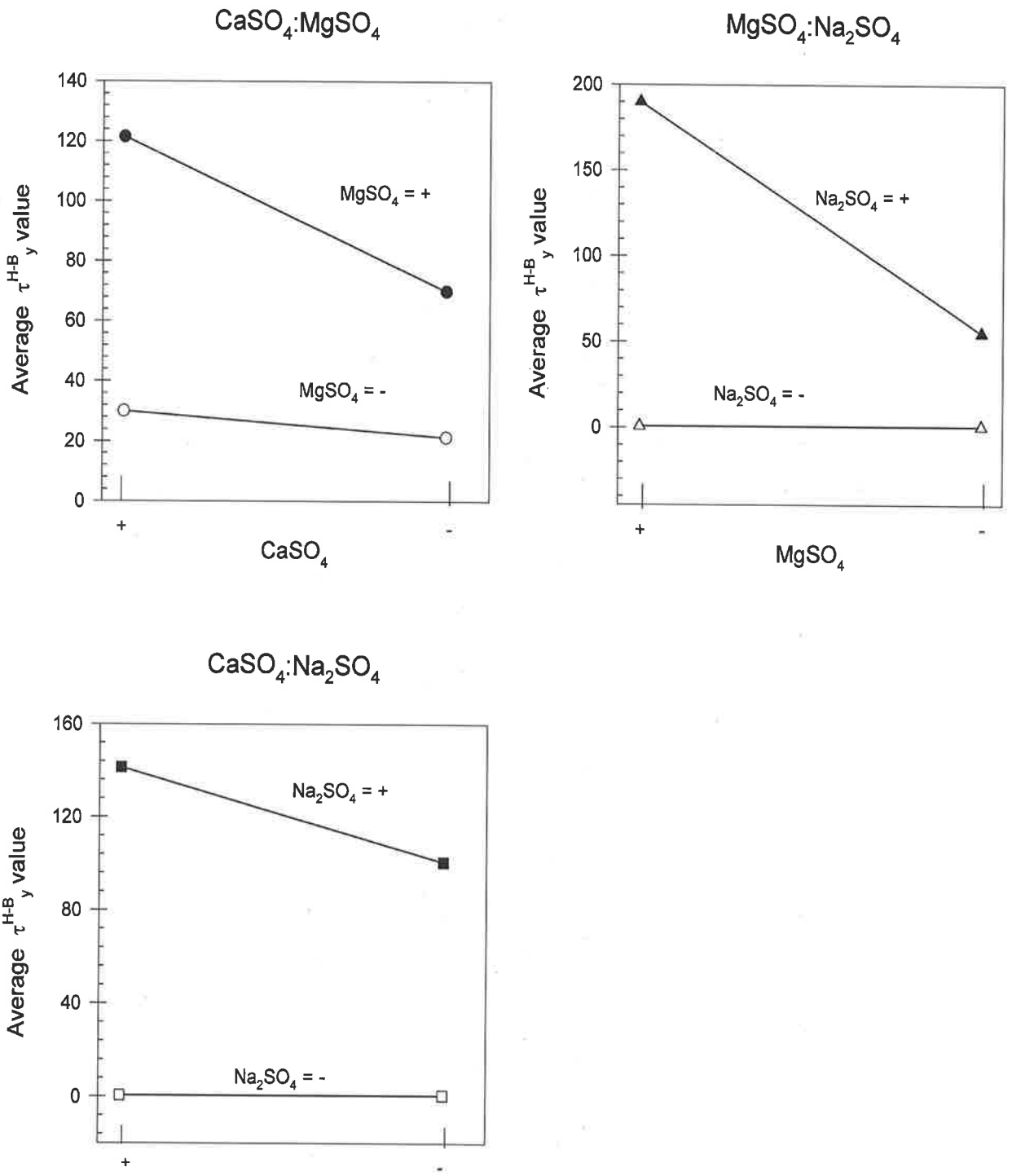

Fig 5.9: Effects of interaction of chemical compounds on the yield stress (τ_y^{H-B})

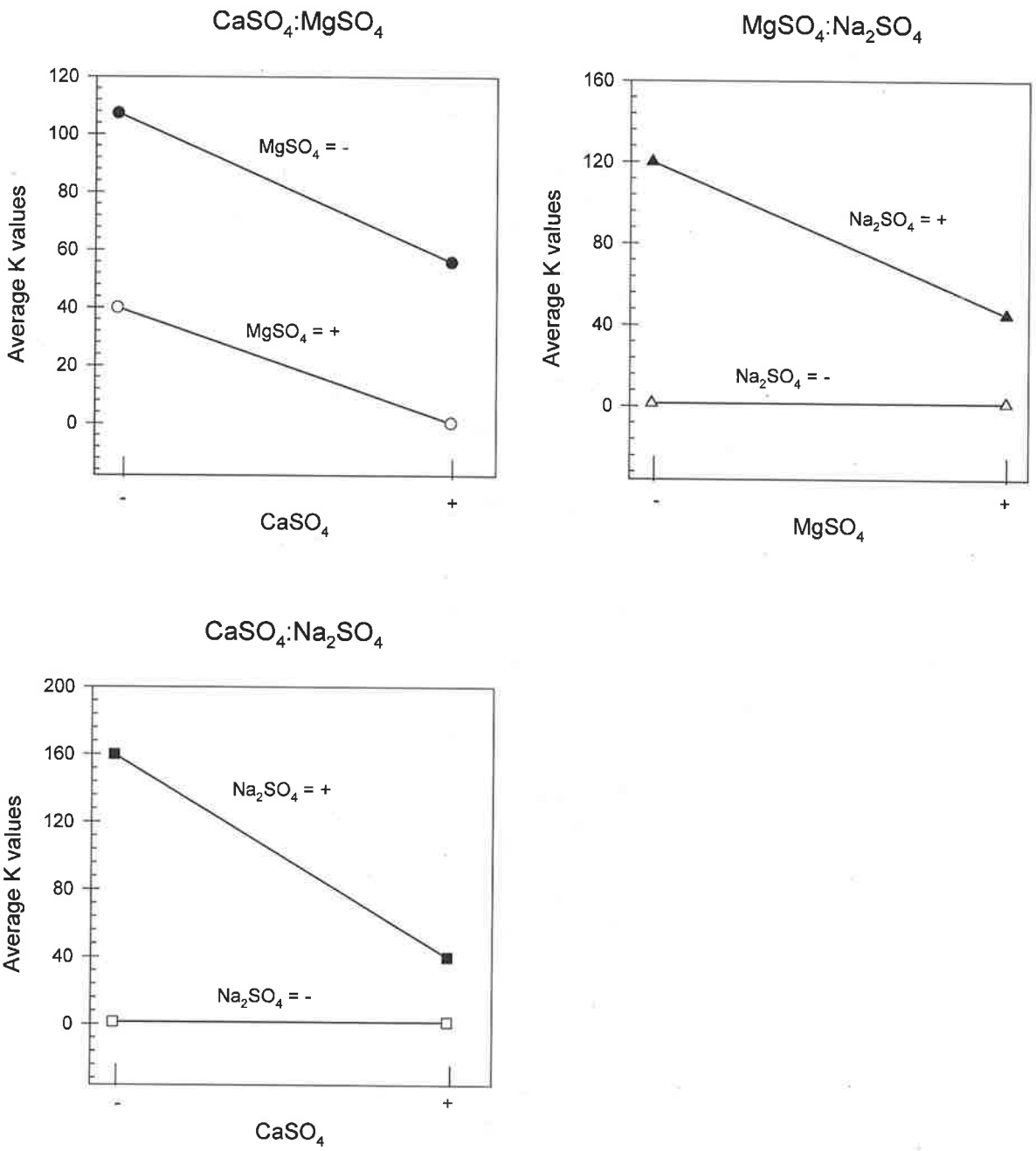

Fig 5.10: Effects of interaction of chemical compounds on the consistency index (K)

The $CaSO_4$:$MgSO_4$ interaction plots in Figs 5.9 and 5.10 show that $CaSO_4$ has a large effect on the yield stress and the consistency index when $MgSO_4$ is at its high concentration level. Note from the $CaSO_4$: Na_2SO_4 and $MgSO_4$:Na_2SO_4 interactions that Na_2SO_4 has a large effect on increasing values of the yield stress and the consistency index when both $CaSO_4$ and $MgSO_4$ are at their low concentration level.

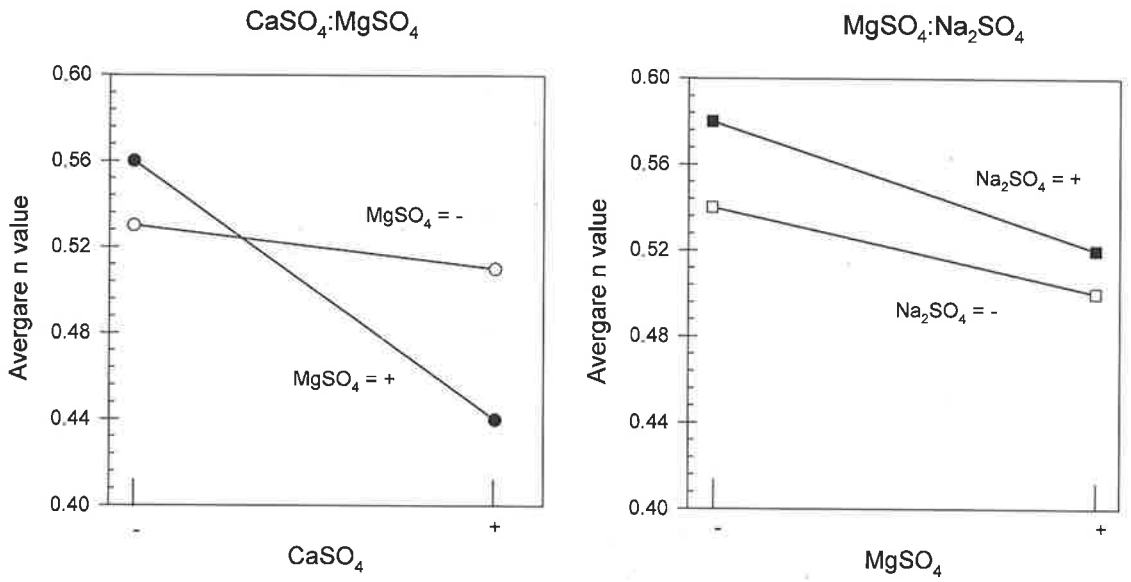

Fig 5.11: Effects of interaction of chemical compounds on the flow behaviour index (n)

Fig 5.11 shows that the average n value decreased more rapidly when either $CaSO_4$ or $MgSO_4$, or a combination of both are at their high concentration level. When investigating the interaction of $MgSO_4$:Na_2SO_4 it was found that Na_2SO_4 has a greater effect on the flow behaviour index when $MgSO_4$ is at a low concentration level.

Before the conclusions from the analysis of variance are accepted, the adequacy of the analysis of variance needs to be examined. A useful technique is a normal probability plot (Pk) of the factor effect value (Montgomery, 1991). To calculate the normal probability (Pk) the experimental data must be sorted from largest to smallest. Then values of the normal probability can be calculated using the formula Pk = (j-0.5)/N (Montgomery, 1991). J is the number of sorted data and N is the number of experiments, and in this work j is equal to 8. The factor effect value is placed on the x-axis, and the normal probability is placed the y-axis. Normal probability plots showing the effects of chemical compounds on the τ_y^{H-B}, the consistency index parameter (K) and the flow behaviour index parameter (n) are shown in Figs 5.12-5.14 , respectively.

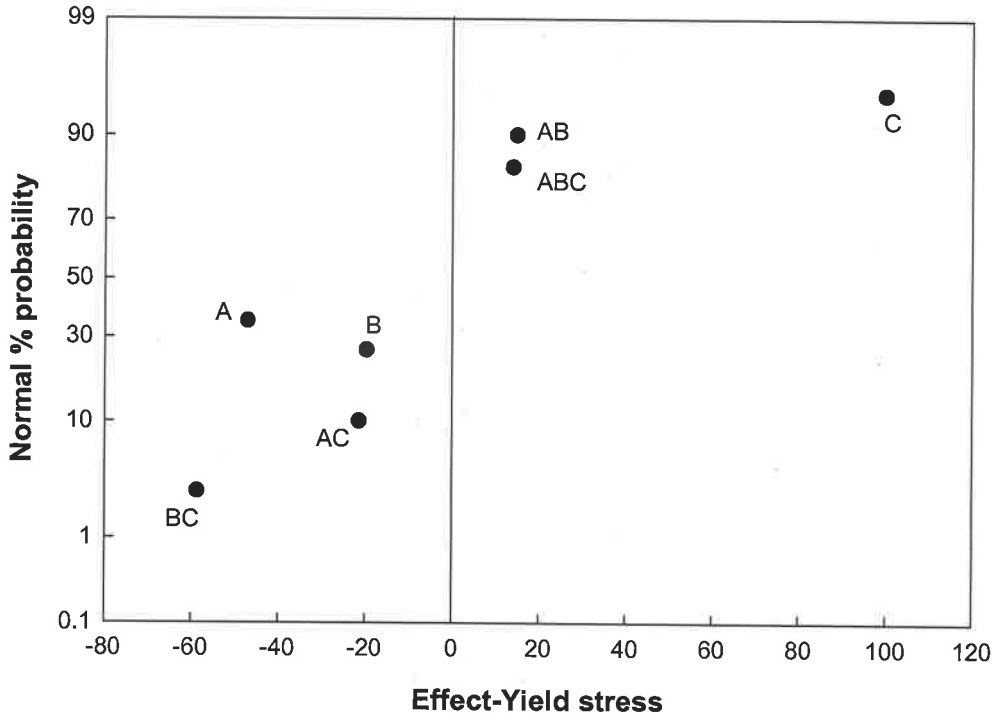

Fig 5.12: Normal probability plot shows the effects of chemical compounds on the yield stress (τ_y^{H-B})

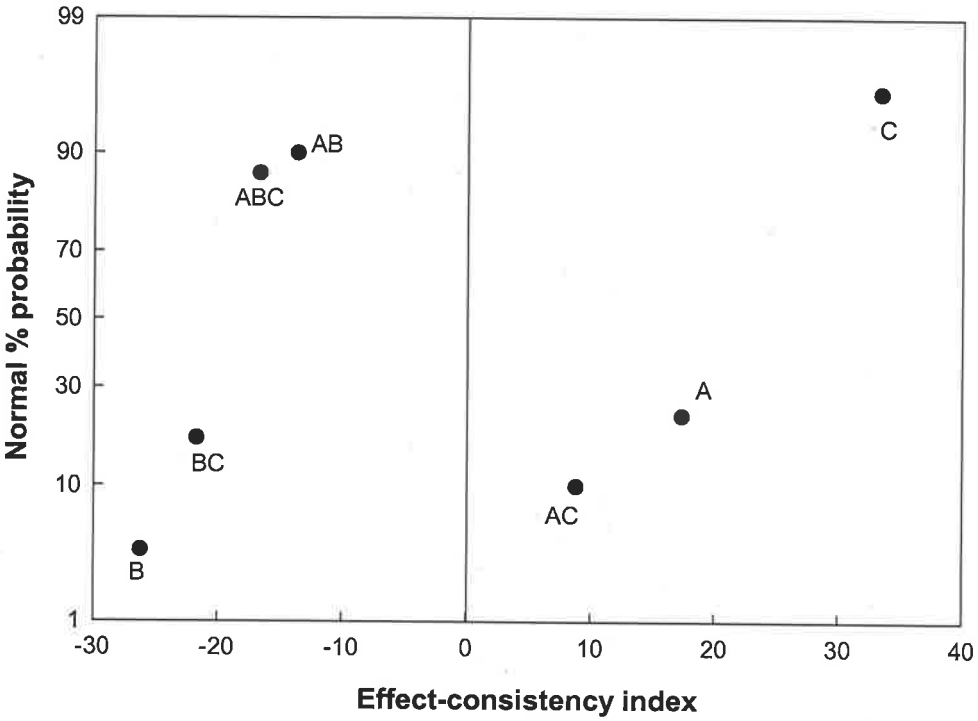

Fig 5.13: Normal probability plot shows the effects of chemical compounds on the consistency index parameter (K)

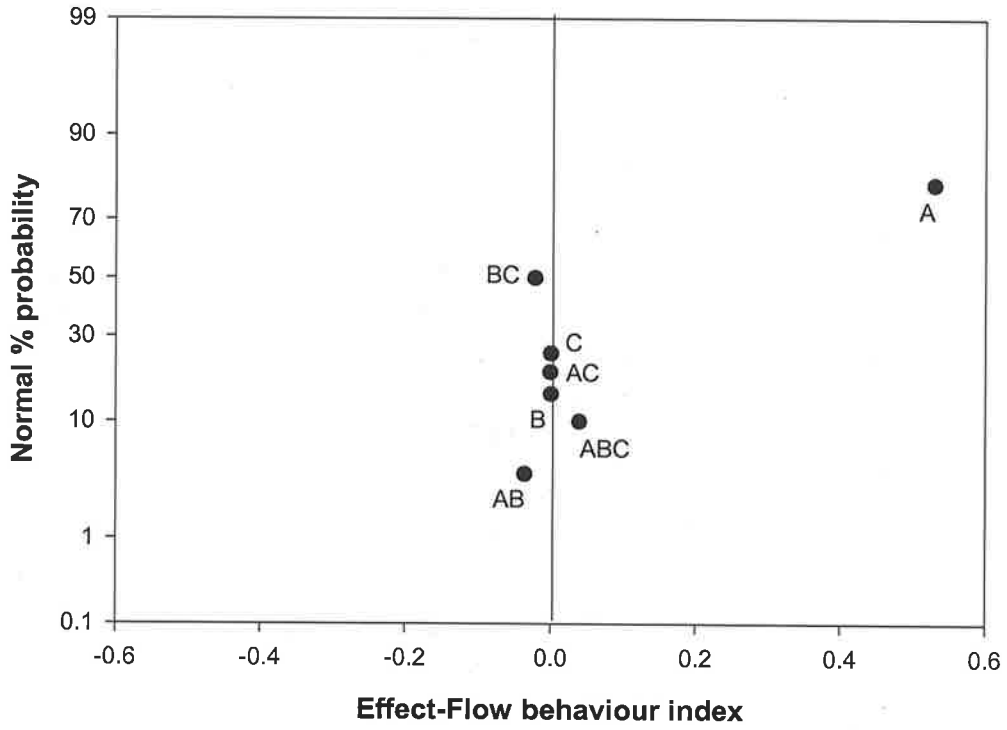

Fig 5.14: Normal probability plot shows the effects of chemical compounds on the flow behaviour index parameter (n)

The straight line in Figs 5.12-5.14 is a line of the zero effect, which drawn through the zero effect factors (points). Factors (points) that are not on the line are the significant factors. Fig 5.12 shows that there are seven factors that have a significant effect on the time dependent properties. They are $CaSO_4$ (A), $MgSO_4$ (B), Na_2SO_4 (C), $CaSO_4$-$MgSO_4$ (AB), $CaSO_4$-Na_2SO_4 (AC), $MgSO_4$-Na_2SO_4 (BC) and $CaSO_4$-$MgSO_4Na_2SO_4$ (ABC). The results obtained from the normal probability plot in Figs 5.13 and 5.14 also confirmed that the results of the analysis of variance on the effect of chemical compositions on the consistency index (K, a measure of viscosity) and flow behaviour index parameters (n) are correct.

It can be concluded based on the analysis of variance that $CaSO_4$ and $MgSO_4$ are the key chemical compounds that decrease the yield stress, the consistency index and the flow behaviour index parameters, while the Na_2SO_4 composition increases values of these three parameters. These experimental results offer a reasonable explanation for the observation of low values of the Herschel & Bulkley model parameters of the Victorian coal ashes, and high values of these three parameters of the South Australian ashes.

Effect of temperature on equilibrium rheological properties

Fig 5.15 **a** shows flow curves of the synthetic mixture number E tested at five different temperatures ranging from 850 to 1250°C. The non-linear characteristic of the flow curves indicates that the synthetic ash mixture is a non-Newtonian fluid within the range of shear rates and temperatures tested. Fig 5.15 **b** shows that the viscosity of the sample decreased as temperature increased over the temperature range tested. This behaviour suggests that the sample is a shear thinning material. Although the experimental results presented here are only for sample E, similar rheological characteristics were also found with the other samples.

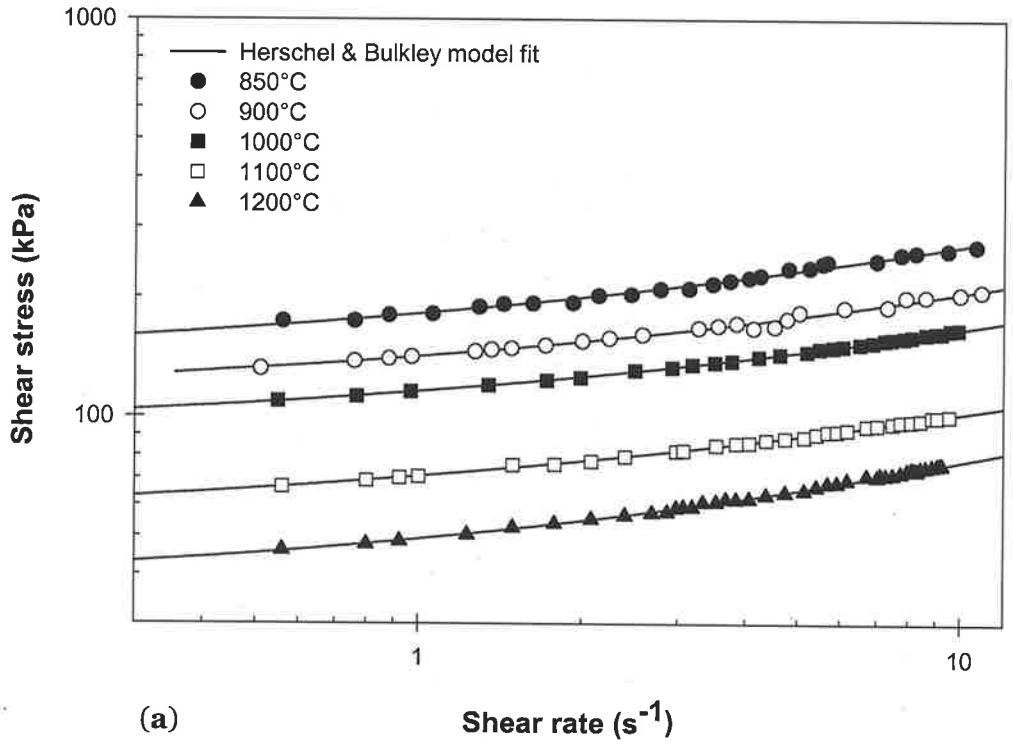

(a)

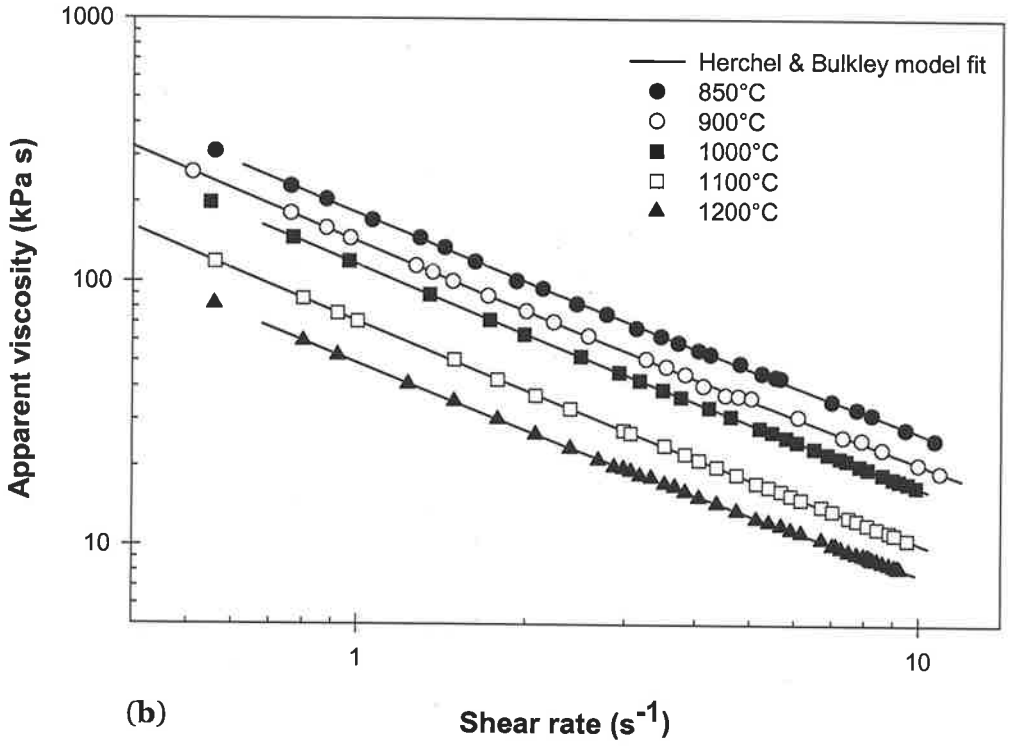

Fig 5.15: (**a**)-Flow curves of the sample E tested at five different temperatures; (**b**)-Apparent viscosity of the sample E tested at five different temperatures

Table V.6: Values of the empirical parameters: **a**-the yield stress (τ_y^{H-B}); **b**-the consistency index (K); **c**-the flow behaviour index (n)

Sample Number	Temperature (°C)									
	850		900		1000		1100		1200	
	1	*2*	*1*	*2*	*1*	*2*	*1*	*2*	*1*	*2*
A	51.41	47.65	44.66	47.05	37.18	39.03	23.24	35.02	17.77	15.36
B	1.63	1.49	1.25	1.8	0.93	1.12	0.64	0.98	0.27	0.76
C	10.7	12.8	14.59	13.6	10.66	12.76	8.73	9.52	4.79	5.05
D	13.25	14.63	10.6	11.7	8.73	10.3	6.42	8.03	5.38	4.03
E	194.8	197.6	131.9	134	104.5	112.6	74.75	67.53	51.23	62.42
F	129.7	123.1	106.3	117	87.76	80.42	50.74	55.63	34.61	42.3
G	64.56	59.03	57.12	63.59	28.48	32.69	14.99	17.63	3.02	3.76
H	3.91	4.63	2.56	2.3	2.04	2.32	0.67	0.96	0.49	0.67

(a)

Sample Number	Temperature (°C)									
	850		900		1000		1100		1200	
	1	*2*	*1*	*2*	*1*	*2*	*1*	*2*	*1*	*2*
A	19.27	22.16	17.64	16.93	14.07	15.06	10.77	13.17	5.91	8.03
B	12.08	15.62	10.06	13.01	6.41	9.63	6.08	5.02	3.99	4.62
C	8.81	10.63	7.83	8.01	6.29	6.97	5.43	5.02	5.05	4.83
D	24.55	18.01	20.35	19.08	15.77	16.72	10.11	14.01	5.5	8.35
E	89.11	85.4	37.03	28.07	25.71	20	18.63	14.4	15.12	14.12
F	49.3	47.57	36.52	34.76	30.03	29.92	25.62	19.43	20.41	19.4
G	30.11	19.4	22.43	14.43	15.71	10.7	11.63	8.32	10.12	8.7
H	9.45	10.02	5.57	8.57	2.73	4.03	1.49	2.09	0.97	1.07

(b)

Sample Number	Temperature (°C)									
	850		900		1000		1100		1200	
	1	*2*	*1*	*2*	*1*	*2*	*1*	*2*	*1*	*2*
A	0.42	0.47	0.47	0.49	0.48	0.5	0.44	0.46	0.46	0.48
B	0.57	0.6	0.57	0.59	0.58	0.5	0.54	0.56	0.56	0.58
C	0.52	0.51	0.59	0.62	0.54	0.57	0.59	0.62	0.53	0.56
D	0.58	0.62	0.56	0.58	0.57	0.59	0.5	0.63	0.63	0.66
E	0.43	0.41	0.45	0.49	0.45	0.49	0.41	0.45	0.47	0.51
F	0.62	0.61	0.65	0.69	0.65	0.69	0.61	0.65	0.67	0.61
G	0.5	0.48	0.43	0.49	0.48	0.54	0.52	0.58	0.51	0.57
H	0.5	0.48	0.43	0.46	0.43	0.46	0.41	0.44	0.48	0.51

(c)

Data in Table V.6 (**a, b**) show both the yield stress and the consistency index values of the synthetic mixtures decreased as temperature increased. In contrast, it was found that flow behaviour changed only slightly with temperature. It may therefore be considered that the flow behaviour index of the synthetic mixtures is independent of temperature.

Over the temperature range tested, it was found that sample E was the most viscous and had the highest yield stress of all samples tested. In contrast, sample B was the least viscous and lowest in yield stress. To demonstrate the effects of temperature on the rheological properties of the synthetic mixture E, each empirical parameter in the Herschel & Bulkley model has been plotted against temperature as shown in Figs 5.16 - 5.18.

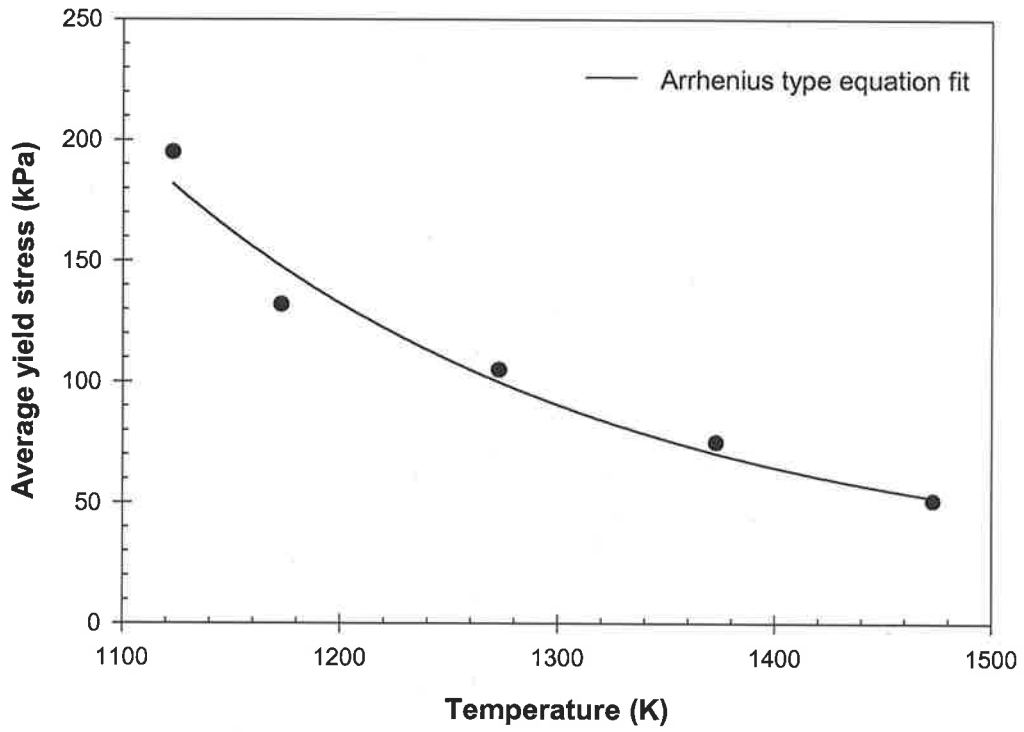

Fig 5.16: Effect of temperature on the average yield stress of the synthetic mixture E

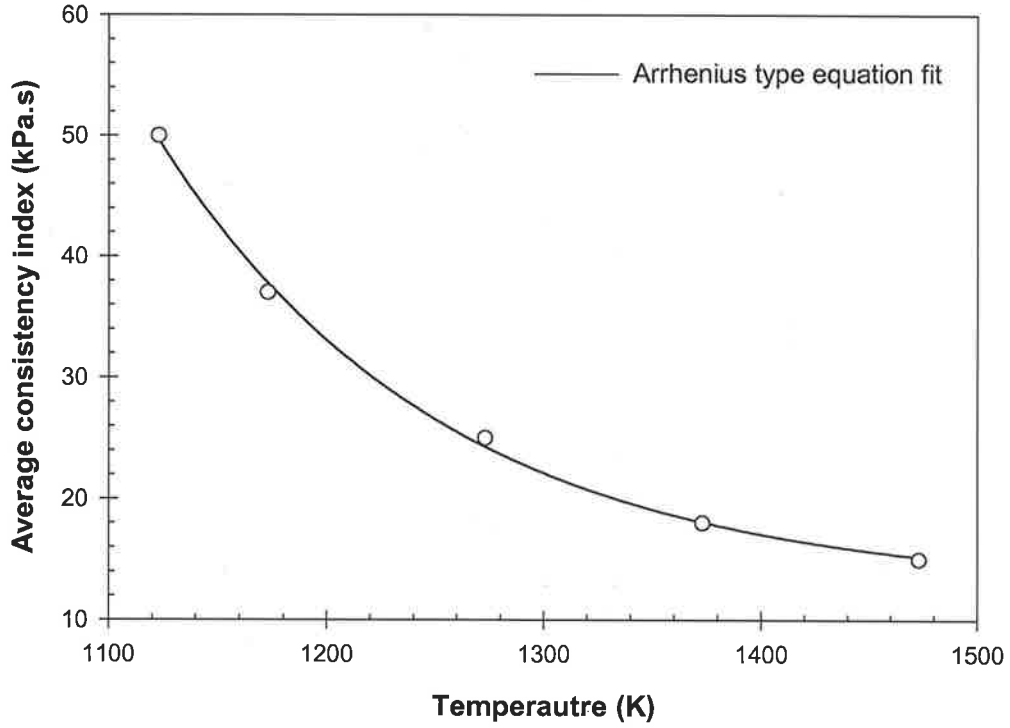

Fig 5.17: Effect of temperature on the average consistency index of the synthetic mixture E

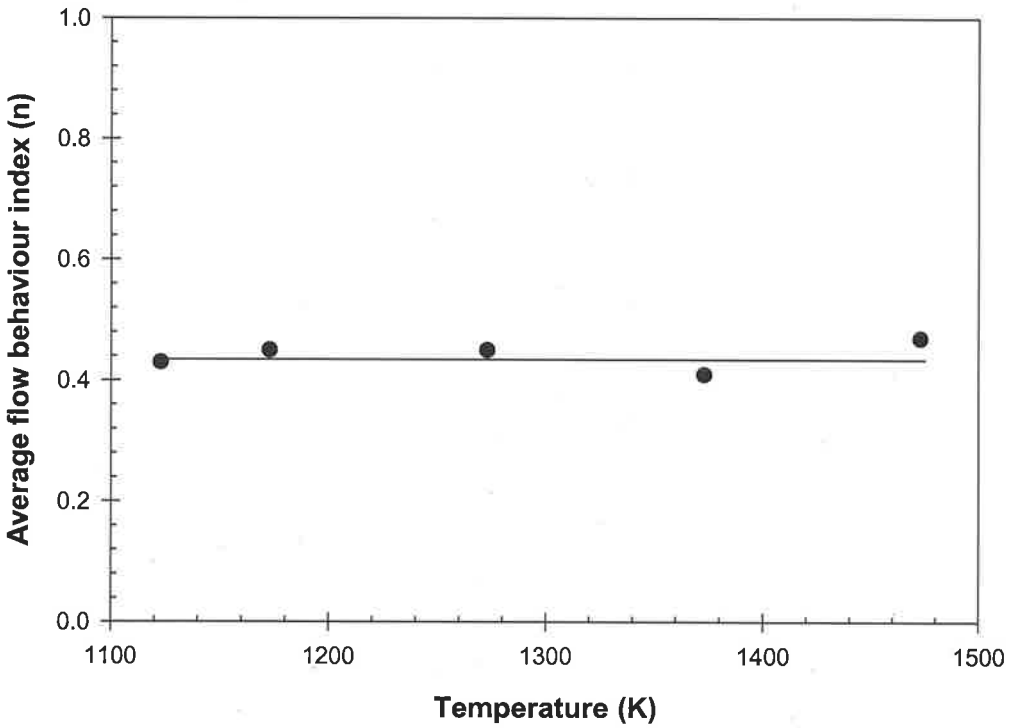

Fig 5.18: Effect of temperature on the average flow behaviour index of the synthetic mixture E

It can be seen in Figs 5.16 and 5.17 that the yield stress (τ_y^{H-B}) and the consistency index (K) decreased with increasing temperature. This demonstrates clearly the dependency of the yield stress, and the consistency index parameters, on the operating temperature. However, it was found from Fig 5.18 that the flow behaviour index (n) was constant over the range of temperatures tested.

It was found that the relationship of the yield stress parameter and the consistency index parameter with temperatures can also be described using an Arrhenius type equation (see section 4.5.1 for details about the Arrhenius equation), and values of the constant parameters in the Arrhenius type equation for all the synthetic mixtures tested are given in Table V.7.

Table V.7: Values of the constant parameters in the Arrhenius type equation

Synthetic mixture	τ_y^{H-B} (kPa)		K (kPa s^n)	
	A (kPa)	$\mathbf{E_a}$ (kJ/mol)	**A** (kPa)	$\mathbf{E_a}$ (kJ/mol)
A	0.928	21.3	3.76	21.5
B	0.47	25.27	7.13	25.8
C	2.66	20.99	9.67	18.7
D	3.01	22.86	4.45	22.1
E	118	28.34	19.3	26.12
F	53.6	27.5	13.5	28.92
G	16.4	28.12	8.72	26.71
H	22.9	27.81	6.42	23.86

It was found from Table V.7 that the parameter **A** (the pre exponential parameter) in the yield stress equation varies from mixture to mixture. It was found that sample E has the highest value of the **A** parameter of all samples tested. This indicates that, at the same temperature, the yield stress of a mixture predominantly high in Na_2SO_4 is higher than that of a mixture predominantly high either in $CaSO_4$ or $MgSO_4$. Moreover, it was found that values of the $\mathbf{E_a}$ parameter (the activation energy parameter) were similar in all of the synthetic mixtures tested. This indicates that the sensitivity of the yield stress to temperature for the synthetic mixtures was similar.

Regarding the effect of temperature on the consistency parameter, it was found that, at the same temperature, the value of the **A** parameter of the sample E is the highest. This indicates that a mixture high in Na_2SO_4 is more viscous than a mixture either high in $CaSO_4$ or $MgSO_4$, or a combination of both. Furthermore, it was also found that increasing the concentration of either $CaSO_4$ or $MgSO_4$ in a mixture high in Na_2SO_4 caused the value of the **A** parameter to decrease. This indicates that the viscosity of the synthetic mixture decreases with an increase in either the $CaSO_4$ or the $MgSO_4$ concentration. However, it was found that the sensitivity of the viscosity to temperature was similar for all synthetic mixtures tested. The value of the $\mathbf{E_a}$ parameter was similar in all mixtures tested.

Based on the quantitative comparisons above, it shows that the chemical compounds affect mainly the pre exponential parameter (**A**), while the activation energy parameter ($\mathbf{E_a}$) is less effected. Thus, the analysis of variance on the effects of chemical compounds on temperature dependent parameters for the yield stress and consistency index parameters is performed only for the pre-exponential parameter (**A**). Results of the analysis of variance on the effect of chemical compounds on the pre-exponential parameter (**A**) is shown in Table V.8

Table V.8: Analysis of variance on the effect of chemical compositions on the pre-exponential parameter (**A**). **a**-the yield stress (τ_y^{H-B}); **b**-the consistency index parameter (K)

Source of variation	Factor effect	Sum of square (SS)	Degree of freedom (df)	Mean square (MS)	F-value	Prob-F
$CaSO_4$ (A)	-25.72	2646.07	1	2646.07	1873.67	< 0.0001
$MgSO_4$ (B)	-42.68	7286.33	1	7286.33	5159.42	< 0.0001
Na_2SO_4 (C)	39.9	6368.84	1	6368.84	4509.75	< 0.0001
AB	-18.54	1373.44	1	1373.44	973.53	< 0.0001
AC	-15.3	937.28	1	937.28	663.68	< 0.0001
BC	-34.4	4732.75	1	4732.75	3351.24	< 0.0001
ABC	7.6	230.58	1	230.58	163.28	< 0.0001

(a)

Source of variation	Factor effect	Sum of square (SS)	Degree of freedom (df)	Mean square (MS)	F-value	Prob-F
$CaSO_4$ (A)	-3.78	56.93	1	56.93	526.07	< 0.0001
$MgSO_4$ (B)	-4.92	92.26	1	92.26	852.54	< 0.0001
Na_2SO_4 (C)	4.22	70.9	1	70.9	655.16	< 0.0001
AB	-1.28	6.5	1	6.5	60.09	< 0.0001
AC	-1.56	9.7	1	9.7	89.67	< 0.0001
BC	-5.06	102.72	1	102.72	949.23	< 0.0001
ABC	1.70	11.49	1	11.49	106.2	< 0.0001

(b)

Table V.8 (**a, b**) reveals that the Prob-F values of all chemical compositions and their interactions are all less than 0.05, indicating that these factors have a significant effect on pre-exponential parameters for both the yield stress and consistency index parameters. Based on the contrast values for the significant factors, it was found that the effect of Na_2SO_4 is a negative value, and the factor effect of $CaSO_4$ is positive. The results in Table V.8 (**a**) suggest that increasing the concentration of Na_2SO_4 will increase the value of the pre-exponential of the yield stress parameter by 40 times. If the concentration of $CaSO_4$ is increased, the **A** parameter will be decreased by 25 times. For the consistency index parameter (Table V.8, **b**), it was found that if the concentrations of either $CaSO_4$ or $MgSO_4$ were increased the pre exponential parameter would be decreased by approximately 4 times. However, if the concentration of Na_2SO_4 is increased the rate of breakdown will be increased by 4 times.

5.6 RELEVANCE OF SYNTHETIC ASH RHEOLOGY TO COAL ASH RHEOLOGY

The present statistical analyses of the rheological data for synthetic ash mixtures has clearly demonstrated that Na_2SO_4 is the key chemical compound causing high rheological properties, especially the yield stress and consistency index parameters, of the synthetic mixtures. $CaSO_4$ and $MgSO_4$ are found to decrease the yield stress and consistency of the mixtures. The information obtained in this chapter can also be used to describe how chemical compositions affect rheological properties of actual low-rank Australian coal ash samples. South Australian ashes (Bowman-**A**, Lochiel-**A** and Lochiel-**B)** are higher in yield stress and consistency index parameter (a measure of viscous property) than Victorian ashes (Loy Yang-**A**, **B** and Morwell-**B**) because the South Australian ashes are higher in the concentration of Na_2SO_4 compound than the Victorian ashes. Comparing between Lochiel-**A** and Lochiel-**B**, these two ash samples are similar in concentration of Na_2SO_4 compounds, the Lochiel-**A** is higher in yield stress and more viscous than the Lochiel-**B**. This is because of the concentration level of $CaSO_4$ which is higher in Lochiel-**B** than in Lochiel-**A**. For the Loy Yang-**A** and Loy Yang-**B**, the Loy Yang-**B** is lower in yield stress and viscosity than the Loy Yang-**A** because the concentration of $MgSO_4$ compound in the Loy Yang-**B** was higher than that found in the Loy Yang-**A** ash.

The effects of chemical compositions on time dependent properties of the synthetic mixtures show that $CaSO_4$ and $MgSO_4$ are chemical compositions that cause a high degree of thixotropy, a high rate of thixotropic breakdown (k) and viscosity ratio (η_0/η_α), while the Na_2SO_4 compound has the opposite effects. The information obtained also describes why the Loy Yang-**A** was higher in degree of thixotropy and has a faster rate of thixotropic structure breakdown than the Bowman-**A** and Lochiel-**A** ashes. This is due to the Loy Yang-**A** having a lower in concentration of Na_2SO_4 than the Bowman-**A** and Lochiel-**A** ashes.

5.7 CONCLUSIONS

Investigations into the effect of $CaSO_4$, $MgSO_4$ and Na_2SO_4 on the rheological properties of synthetic ash mixtures have been carried out using a factorial design experiment. The effects of $CaSO_4$, $MgSO_4$ and Na_2SO_4 concentrations on the time dependent properties and equilibrium flow properties of the mixtures have been studied systematically. The experimental findings allow the following conclusions to be drawn:

- The synthetic ash mixtures are viscoplastic materials characterised by time dependent, thixotropic characteristics.

- Mixtures predominantly high in $CaSO_4$, and $MgSO_4$ have a high degree of thixotropy, while a mixture predominantly high in Na_2SO_4 has a low degree of thixotropy.

- Na_2SO_4 was found to be a significant compound that causes high values of yield stress and the consistency index (a measure of the viscous property) parameter in the synthetic mixtures.

- $CaSO_4$ and $MgSO_4$ compounds were found to decrease the yield stress and the consistency index parameters.

- Information obtained in this work can be used to satisfactorily describe the rheological characteristics of the coal ash samples that were studied in chapter four.

CHAPTER SIX

Modelling the Rheological Behaviour of Low Rank Coal Ash

6.1 INTRODUCTION

In chapter 5, the equilibrium flow properties of synthetic ash mixtures have been presented and statistically analysed. By means of the statistical analysis, it is now possible to develop a statistical model for equilibrium flow data to predict the equilibrium flow properties of low-rank Australian coal ashes under fluidised bed combustion conditions. The objectives of this chapter are:

1. What is the relationship between chemical composition and the flow properties of the synthetic ash mixtures?
2. Can the statistical model developed based on only 3 alkali sulphates as liquid phase, with silica representing solid phase predict flow properties of actual coal ash samples?

This chapter contains three sections. The first section presents an overview on the effects of chemical composition and temperature on the equilibrium flow properties of synthetic ash mixtures. Development of statistical models correlating the significant compositions to the equilibrium flow properties is presented in the second section. Validation of the statistical model is also performed by using the model to predict flow properties of new mixtures, whose rheological properties were not used in the development of the model. The third section deals with predicting the flow properties of actual coal ash samples using the statistical model. In addition, few typical models developed for predicting viscosity of brown coals are also used to calculate the viscosity of the low-rank Australian ashes. Comparisons between the statistical model developed in this work and the existing models are also made. Finally, conclusions on the capabilities of the statistical model developed in this work are given.

6.2 OVERVIEW

Chapter 5 has demonstrated how $CaSO_4$, $MgSO_4$, Na_2SO_4 and their interactions affect the time dependent and equilibrium flow properties of synthetic ash mixtures. It was found that Na_2SO_4 is the key chemical compound that causes high initial viscosity (η_o) and equilibrium viscosity (η_α) of the mixtures, while $CaSO_4$ and $MgSO_4$ were found to decrease the initial and equilibrium viscosity of the mixtures. Chapter 5 also showed that the rate of thixotropic structure breakdown (k) of samples predominantly high in either $CaSO_4$ or $MgSO_4$, or a combination of both was faster than samples predominantly high in Na_2SO_4 composition. The time dependent flow properties were strongly dependent on shear rate and operating temperature.

It was found that Na_2SO_4 is the key compound that increases the value of the yield stress (τ_y^{H-B}) and consistency index (K), and vice versa for $CaSO_4$ and $MgSO_4$ compounds. Viscosity of the synthetic mixtures became more sensitive to shear rate, as concentration of Na_2SO_4 increased. The τ_y^{H-B} and K were strongly dependent on temperature, and temperature dependence of τ_y^{H-B} and K could be satisfactorily described by an Arrhenius equation. The flow behaviour index parameter (n), however, was independent of temperature.

Comparing values of the pre-exponential parameter (**A**) found that samples predominantly high in Na_2SO_4 had the highest **A** values. This implied that over the temperature range tested, a sample high in Na_2SO_4 is also highest in the yield stress and consistency index parameters. Values of the activation energy parameter (**Ea**) were similar for all of the synthetic mixtures tested, indicating the comparable temperature sensitivity of the synthetic mixtures. The analysis of variance indicated that the values of **A** increased with increasing concentration of Na_2SO_4. The value of **A** was decreased with increased concentration of either $CaSO_4$ or $MgSO_4$ compounds.

6.3 DEVELOPMENT OF STATISTICAL MODELS

From a two levels factorial design experiment, it is possible to develop a linear correlation that relates the significant chemical compounds to the equilibrium flow properties. The relationship can be characterised by using a linear regression equation, which is fit to a set of experimental data.

The analysis of variance in chapter 5 (see Table V.5 for the results) revealed that the flow properties of the synthetic ash mixtures are affected by the concentration of more than one significant chemical compound. The yield stress and consistency index parameters were controlled by $CaSO_4$, $MgSO_4$, and Na_2SO_4 and the interactions of $CaSO_4$:$MgSO_4$, $CaSO_4$:Na_2SO_4, $MgSO_4$:Na_2SO_4 and $CaSO_4$:$MgSO_4$:Na_2SO_4 compounds. This means, the regression equation for the τ_y^{H-B} and K must contain these seven significant variables. The flow behaviour index parameter (n) was strongly dependent on $CaSO_4$, and the interaction of $CaSO_4$:$MgSO_4$, $MgSO_4$:$MgSO_4$ and $CaSO_4$:$MgSO_4$:Na_2SO_4. Thus, the relationship between the flow behaviour index parameter and chemical compounds must contend with these 4 significant factors.

The linear regression relating the yield stress (τ_y^{H-B}) to the significant compounds is given in equation 6.1. Equation 6.2 shows the relationship of the consistency index parameter (K) with the significant chemical compound. The relationship of the flow behaviour index (n) parameters is shown in equation 6.3.

$$\tau_y^{H-B} = \beta_0 + \beta_1 x_A + \beta_2 x_B + \beta_3 x_C + \beta_4 x_A x_C + \beta_5 x_B x_C + \beta_6 x_A x_B + \beta_7 x_A x_B x_C \qquad 6.1$$

$$K = \alpha_0 + \alpha_1 x_A + \alpha_2 x_B + \alpha_3 x_C + \alpha_4 x_A x_C + \alpha_5 x_B x_C + \alpha_6 x_A x_B + \alpha_7 x_A x_B x_C \qquad 6.2$$

$$n = \chi_0 + \chi_1 x_A + \chi_2 x_A x_B + \chi_3 x_B x_C + \chi_4 x_A x_B x_C \qquad 6.3$$

where x_A, x_B and x_C are code factors that represent relative concentrations of $CaSO_4$, $MgSO_4$, and Na_2SO_4 , respectively. β_i, α_i, χ_i are the regression coefficients for the yield stress, consistency index and flow behaviour index parameters. β_0, α_0, χ_0 are the regression coefficient, which is obtained from the average responses, β_1, α_1, χ_1 are the regression coefficient when $CaSO_4$ is at the high level, β_2, α_2, χ_2 are the regression coefficient when $MgSO_4$ is at the high level, and β_3, α_3, χ_3 are the regression coefficient when Na_2SO_4 is at the high level. β_4, α_4, χ_4; β_5, α_5, χ_5; β_6, α_6, χ_6 are the regression

coefficient of the interaction of $CaSO_4$: Na_2SO_4, $MgSO_4$:Na_2SO_4 and $CaSO_4$: $MgSO_4$, , respectively. β_7, α_7, χ_7 are the regression coefficient for the interaction of $CaSO_4$:$MgSO_4$:Na_2SO_4.

The code factor is a common scale ranging between -1 and +1 for each factor. Typical coding has -1 as the minimum or low level of a factor, +1 as the maximum or high level of a factor (Montgomery, 1991). For example, if code variable of $CaSO_4$ equal to −1 means $CaSO_4$ is at its low concentration level, which is 11 mol %.

The code factor offers an easier way to describe the effects of significant factors when the level of significant factors was changed from low to high level than describing in their actual values, especially when describing the effects of interactions of the factor. The code factors for each chemical compounds are expressed in equations below:

$$x_{CaSO_4} = \frac{Conc_{CaSO_4} - (Conc_{CaSO_4,low} + Conc_{CaSO_4,high})/2}{(Conc_{CaSO_4,high} - Conc_{CaSO_4,low})/2} \quad 6.4$$

$$x_{MgSO_4} = \frac{Conc_{MgSO_4} - (Conc_{MgSO_4,low} + Conc_{MgSO_4,high})/2}{(Conc_{MgSO_4,high} - Conc_{MgSO_4,low})/2} \quad 6.5$$

$$x_{Na_2SO_4} = \frac{Conc_{Na_2SO_4} - (Conc_{Na_2SO_4,low} + Conc_{Na_2SO_4,high})/2}{(Conc_{Na_2SO_4,high} - Conc_{Na_2SO_4,low})/2} \quad 6.6$$

where $Conc_{CaSO_4}$, $Conc_{MgSO_4}$ and $Conc_{Na_2SO_4}$ represent actual concentration of $CaSO_4$, $MgSO_4$ and Na_2SO_4 in the mixture, respectively. $Conc_{CaSO_4,low}$, $Conc_{MgSO_4,low}$ and $Conc_{Na_2SO_4,low}$ are the concentration of $CaSO_4$, $MgSO_4$ and Na_2SO_4 at their low level, and $Conc_{CaSO_4,high}$, $Conc_{MgSO_4,high}$ and $Conc_{Na_2SO_4,high}$ are the concentration of $CaSO_4$, $MgSO_4$ and Na_2SO_4 at their high level. For example x_{CaSO_4}, can be calculated as:

$$x_{CaSO_4} = \frac{Conc_{CaSO_4} - (26+11)/2}{(26-11)/2} \quad 6.7$$

$$= \frac{Conc_{CaSO_4} - 18.5}{7.5} \quad 6.8$$

Thus, if the concentration of $CaSO_4$ is at 26 mol%, then x_{CaSO_4} equals +1. This indicates that the concentration of $CaSO_4$ is at the high level. If the concentration of $CaSO_4$ is at 11

mol%, then x_{CaSO_4} equals -1. The code variables for $MgSO_4$ and Na_2SO_4 can be calculated using the following equations:

$$x_{MgSO_4} = \frac{Conc_{MgSO_4} - (21+5)/2}{(21-5)/2} \qquad 6.9$$

$$x_{Na_2SO_4} = \frac{Conc_{Na_2SO_4} - (19+10)/2}{(19-10)/2} \qquad 6.10$$

If the concentration of $MgSO_4$ is at 21 mol% then the code variable (x_{MgSO_4}) of this compound has a value of +1. If the concentration of $MgSO_4$ is at 10 mol%, then the code variable of $MgSO_4$ equals -1. The code variable for the Na_2SO_4 compound is also calculated in a similar manner.

The regression coefficient value is defined as the average response of a factor as the change in response produced by a change in the level of that factor, over the levels of the other factor (Montgomery, 1991). For the 2^3 factorial design, there are seven degrees of freedom (2^3-1) between the eight experiments associated with the main effects of $CaSO_4$, $MgSO_4$, and Na_2SO_4, the two factor interactions $CaSO_4$:$MgSO_4$, $CaSO_4$:Na_2SO_4, $MgSO_4$:Na_2SO_4 and the three factor interaction $CaSO_4$:$MgSO_4$:Na_2SO_4. For example, the regression coefficient of the main effect $CaSO_4$ can be calculated from the difference between the response when $CaSO_4$ is at the high level (samples A, B, D and F) and when $MgSO_4$, and Na_2SO_4 are at the low level divided by the number of observations. Equations used to calculate the regression coefficient for each factor are given below:

For the $CaSO_4$

$$\beta_1, \alpha_1, \chi_1 = \frac{1}{4n}[A + B + D + F - C - E - G - H] \qquad 6.11$$

where A to H are responses of sample A to H (see Table V.2 for more details), which can be either the yield stress or the consistency index, or the flow behaviour index. In a similar manner, the effect of $MgSO_4$, and Na_2SO_4 can also be calculated using equations 6.12 and 6.13.

For $MgSO_4$

$$\beta_2, \alpha_2, \chi_2 = \frac{1}{4n}[A + C + D + G - B - E - F - H] \qquad 6.12$$

For Na_2SO_4

$$\beta_3, \alpha_3, \chi_3 = \frac{1}{4n}[A + E + F + G - B - C - D - H] \quad 6.13$$

The regression coefficient of the interaction $CaSO_4$:$MgSO_4$, $CaSO_4$:Na_2SO_4, $MgSO_4$:Na_2SO_4 can be calculated as:

For the interaction of $CaSO_4$:Na_2SO_4

$$\beta_4, \alpha_4, \chi_4 = \frac{1}{4n}[A + D + E + H - B - C - F - G] \quad 6.14$$

For the interaction of $MgSO_4$:Na_2SO_4

$$\beta_5, \alpha_5 = \frac{1}{4n}[A + B + G + H - C - D - E - F] \quad 6.15$$

For the interaction of $CaSO_4$:$MgSO_4$

$$\beta_6, \alpha_6 = \frac{1}{4n}[A + C + F + H - B - D - E - G] \quad 6.16$$

For the interaction of $CaSO_4$:$MgSO_4$: Na_2SO_4

$$\beta_7, \alpha_7 = \frac{1}{4n}[A + B + C + E - D - F - G - H] \quad 6.17$$

Values of the response to the yield stress (β_i), consistency index (α_i) and flow behaviour index (χ_i) for each sample could be found in Table V.6. The regression coefficients that were calculated from equations 6.11 to 6.17 for the yield stress (β_i), consistency index (α_i) and flow behaviour index (χ_i) are shown in Table VI.1.

Table VI.1: Values of the regression coefficients: (**a**)-Yield stress (τ_y^{H-B}); (**b**)-Consistency index (K); (**c**)-Flow behaviour index (n)

Temp (°C)	β_0	β_1	β_2	β_3	β_4	β_5	β_6	β_7
850	57.83	-9.98	-24.23	50.64	8.12	-10.53	-28.57	6.27
900	47.99	-5.45	-17.42	43.45	3.38	-7.24	-20.92	2.06
1000	34.42	-1.23	-14.05	30.92	4.67	-3.01	-16.94	3.32
1100	22.6	-0.02	-8.66	19.8	4.25	-1.23	-11.03	3.41
1200	16.15	-1.09	-7.97	14.15	3.54	-1.70	-9.35	2.84

(**a**)

Temp (°C)	α_0	α_1	α_2	α_3	α_4	α_5	α_6	α_7
850	30.07	-4.40	-9.34	15.23	1.30	-14.02	-8.71	3.85
900	21.3	-2.88	-6.42	12.68	1.67	-9.01	-6.82	2.64
1000	16.66	-2.62	-5.63	8.23	1.24	-7.15	-5.29	2.26
1100	10.17	-1.75	-3.65	5.02	1.02	-4.95	-4.02	1.86
1200	7.96	-1.37	-2.78	3.69	0.82	-4.05	-3.62	1.09

(**b**)

Temp (°C)	χ_0	χ_1	χ_2	χ_3	χ_4
850	0.54	-0.039	-0.036	-0.019	-0.02
900	0.54	-0.004	-0.015	-0.015	-1.3E-3
1000	0.52	-0.027	-5.6E-3	-6E-4	-8.2E-3
1100	0.53	-0.023	-0.011	-1.9E-3	-0.017
1200	0.55	-0.032	-0.014	-0.012	-0.031

(**c**)

Values of the yield stress, the consistency index and the flow behaviour index at a given temperature can be calculated by substituting the regression coefficients listed in Tables VI.1 (**a**, **b** and **c**) into equations 6.1, 6.2 and 6.3. After the value of each Herschel-Bulkley model parameter has been calculated, the rheological properties of a sample can be estimated as a function of shear rate at a given temperature. For example, at temperature 850°C a synthetic mixture has a concentration level of $CaSO_4$ at 26 mol%, $MgSO_4$ at 5

mol%, and Na_2SO_4 at 10 mol%. The yield stress, the consistency index, and the flow behaviour index can be calculated as below:

$$\tau_y^{H-B} = 57.83+(-9.98*1)+(-24.23*-1)+(50.64*-1)+(8.12*1*-1)+(-10.53*1*-1)$$
$$+(-28.57*-1*-1)+(6.27*1*-1*-1)$$
$$= 1.43 \text{ kPa}$$

$$K = 30.07+(-4.40*1)+(-9.38*-1)+(15.23*-1)+(1.30*1*-1)+(-14.02*1*-1)$$
$$+(-8.71*-1*-1)+(3.85*1*-1*-1)$$
$$= 25.73 \text{ Pa s}$$

$$n = 0.54+(0.039*1)+(-0.036*1*-1)+(-0.019*-1*-1)+(-0.02*1*-1*-1)$$
$$= 0.57$$

Then, formula of the Herschel & Bulkley model representing this mixture equals $\tau_y = 1.25 + 25.73\dot{\gamma}^{0.57}$.

6.4 VALIDATION OF THE MODEL

In order to validate the model developed, five additional mixtures also containing $CaSO_4$, $MgSO_4$, Na_2SO_4 and SiO_2 were prepared with a different concentration level of these 3 alkali sulphate compounds from those previously used in the development of the model. The melting points of the new mixture were obtained from a phase diagram and found to be at 850°C. The compositions of the new samples in mol percent are shown in Table VI.2.

Table VI.2: The testing model mixture in mol percent

Sample number	$CaSO_4$	$MgSO_4$	Na_2SO_4	SiO_2
I	11.75	14.08	18.21	55.96
II	27.0	12.45	21.81	30.19
III	12.33	20.83	20.4	46.44
IV	22.95	27.6	18.3	31.15
V	26.09	22.14	18.65	33.12

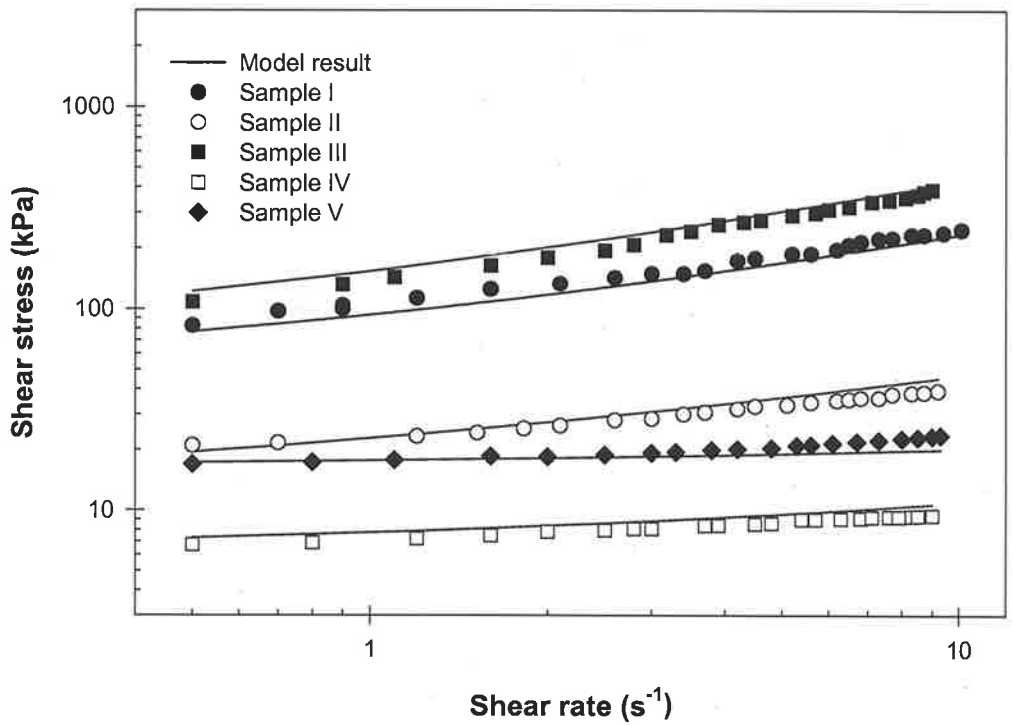

Fig 6.1: Validation of the statistical model developed at temperature 1000°C

Fig 6.1 shows a comparison between experimental data obtained for the new mixture and the predicted results that were obtained using the statistical model. The experiments were performed at a temperature of 1000°C under a rich air atmosphere. Small deviations between the model and the experimental data were observed for samples II and III. The model appears to correlate well with the experimental results at $\dot{\gamma} \leq 3s^{-1}$, however the model either over predicts or under predicts the flow properties at $\dot{\gamma} \geq 3s^{-1}$ for the samples II and III, , respectively. This may be due to the slipping of theses samples during their rheological measurements. To demonstrate explicitly how accurate the developed statistical model is, the relative error is used to compare the difference between the model prediction and the experimental data. The relative error is defined in the equation below:

$$\text{Relative error} = \frac{(\text{Model} - \text{Experimental})}{\text{Experimental}} = (\text{Model predicted-experimental})\text{-}1 \qquad 6.18$$

The relative error has absolute value, and ranges between 0 and 1. 0 is perfect agreement and 1 is total disagreement. Values of the relative error for the samples I to V tested at temperature 1000°C are given in Table VI.3.

Table VI.3: Values of the relative error: (**a**)- Yield stress τ_y^{H-B}; (**b**)- Consistency index (K); (**c**)- Flow behaviour index (n)

	Sample number	Model	Experimental	Relative error
$\dot{\gamma} = 0.5s^{-1}$	I	79.61	82.4	0.03
	II	89.73	90.92	0.01
	III	51.73	54.1	0.04
	IV	17.18	15.48	0.1
	V	38.89	37.81	0.02

(**a**)

	Sample number	Model	Experimental	Relative error
$\dot{\gamma} = 3.0s^{-1}$	I	109.03	124	0.12
	II	105.93	108.5	0.02
	III	75.0	81.7	0.08
	IV	20.14	18.57	0.08
	V	44.86	42.97	0.04

(**b**)

	Sample number	Model	Experimental	Relative error
$\dot{\gamma} = 10.0s^{-1}$	I	149	177	0.15
	II	127.8	119.1	0.07
	III	101.3	114.1	0.11
	IV	23.46	21.64	0.08
	V	51.92	52.46	0.01

(**c**)

Table VI.3 (**a**, **b** and **c**) show that over shear rate range tested, values of the relative error of samples I to V are all close to 0, indicating the good agreement between the experimental data and the developed statistical model. In addition, comparisons between the model and rheological properties of the mixture I at temperature ranging from 850°C

to 1200°C were also made, and the relative error was also analysed as shown in Fig 6.2 and Table VI.4, respectively.

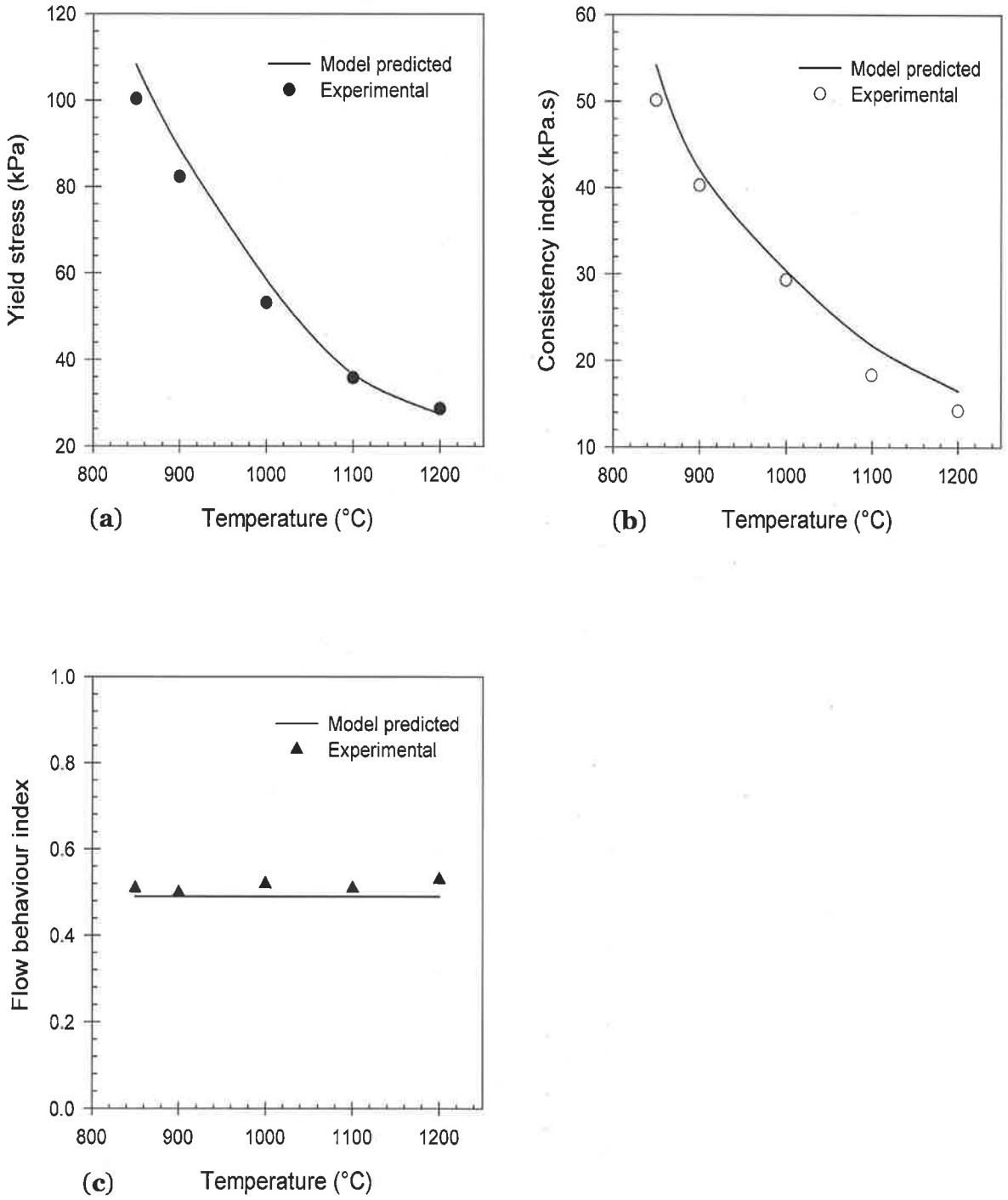

Fig 6.2: Comparison between the regression model and flow properties of the synthetic mixture F over the range of temperature tested, (**a**)-the yield stress (τ_y^{H-B}); (**b**)-the consistency index (K); (**c**)-the flow behaviour index (n)

Fig 6.2 shows that over the temperature range tested, the model agrees very well with the experimental data. However, some deviations are observed from the prediction of the yield stress and consistency index properties. It was found that the model slightly over predicts the yield stress and consistency index properties at temperatures between 850°C and 1000°C. This may be due to at these temperature range, the sample may contain too little of the sulphates to form enough molten phase and hold the silica particles together, resulting in slipping of the silica particles during shearing process. Thus, this may be the reason why the model slightly over predict the τ_y^{H-B} and K of the mixture I at temperatures between 850°C and 1000°C. However, Table VI.4 shows that values of the relative error of the τ_y^{H-B}, K and n are comparatively close to 0, indicting the good prediction of the statistical model for these three rheological properties over temperature range tested. Although the comparisons have been made with only the mixture I over the temperature range tested, the same conclusions apply to all other synthetic mixtures investigated.

Table VI.4: Values of the relative error for each of the Herschel & Bulkley model parameters at temperature ranging from 850°C to 1200°C

	Temperature (°C)	Model	Experimental	Relative error
τ_y^{H-B} (kPa)	850	108.31	100.3	0.08
	900	88.8	82.3	0.07
	1000	58.57	53.14	0.10
	1100	36.62	35.81	0.02
	1200	27.4	28.7	0.04
K (kPa.s^n)	850	54.2	50.1	0.08
	900	42.10	40.3	0.04
	1000	30.4	29.34	0.03
	1100	21.74	18.31	0.18
	1200	16.53	14.27	0.15
n	850	0.49	0.5	0.02
	900	0.49	0.51	0.04
	1000	0.49	0.52	0.05
	1100	0.49	0.51	0.04
	1200	0.49	0.53	0.07

The validation of the statistical model developed in this work has demonstrated that the statistical model developed in this work has the capability of predicting rheological properties of synthetic mixtures that have concentration between 11 to 26 mol% for $CaSO_4$, 5 to 21 mol% for $MgSO_4$, and 10 to 19 mol% for Na_2SO_4 very accurately over shear rate of 0.5 to 10 s^{-1} at temperature ranging from 900 to 1000°C. Based on the validation of the statistical model, it is now in the good position to use the statistical-rheological model developed to predict the flow properties of the low-rank Australian coal ash samples under fluidised bed combustion conditions.

6.5 PREDICTING THE FLOW PROPERTIES OF COAL ASH SAMPLES WITH THE STATISTICAL MODEL DEVELOPED

After the statistical model has been developed and validated, it is now possible to predict the equilibrium flow properties of the low-rank Australian coal ash samples. It is important to mention here that the statistical models are developed based on the synthetic ash mixtures containing only a few key chemical compounds, which $CaSO_4$, $MgSO_4$, Na_2SO_4 compounds represent in the liquid phase found in the coal ash sample, with SiO_2 representing the solid phase. Thus, before the model can be applied to predict flow properties of the actual coal ash samples, concentration levels of $CaSO_4$, $MgSO_4$ and Na_2SO_4 compounds in each ash sample need to be calculated.

In order to calculate the concentration level of these three alkali sulphate compounds of the low-rank Australian ash samples, chemical analysis of the ash samples was used. Based on the mass balance of all chemical species in each ash sample, approximate concentration of $CaSO_4$, $MgSO_4$ and Na_2SO_4 compounds in each coal ash sample can be calculated. Concentration levels of $CaSO_4$, $MgSO_4$ and Na_2SO_4 compounds in the low-rank Australian coal ash samples studied in this work are shown in Table VI.5.

Table VI.5: Concentration levels in mol percent of $CaSO_4$, $MgSO_4$ and Na_2SO_4 compounds of the low-rank Australian ash samples studied

Coal ash sample	$CaSO_4$	$MgSO_4$	Na_2SO_4
Loy Yang-**A**	11.0	7.3	11.6
Lochiel-**A**	12.0	14.8	18.3
Bowman-**A**	11.3	11.6	19.0
Loy Yang-**B**	15.4	16.4	9.6
Lochiel-**B**	16.9	8.2	15.8
Morwell-**B**	26.0	21.0	12.7

Concentration level of $CaSO_4$, $MgSO_4$ and Na_2SO_4 compounds for each coal ash sample are firstly placed into equations 6.4 to 6.6 to obtain the code factor of each chemical compound. Then the code factors are placed in equations 6.1 to 6.3 for calculating the τ_y^{H-B}, K and n at a desire temperature, , respectively. Figs 6.3 to 6.5 show the comparison between the statistical model and the experimental data of the Bowman-**A**, Lochiel-**A** and Lochiel-**B** ashes.

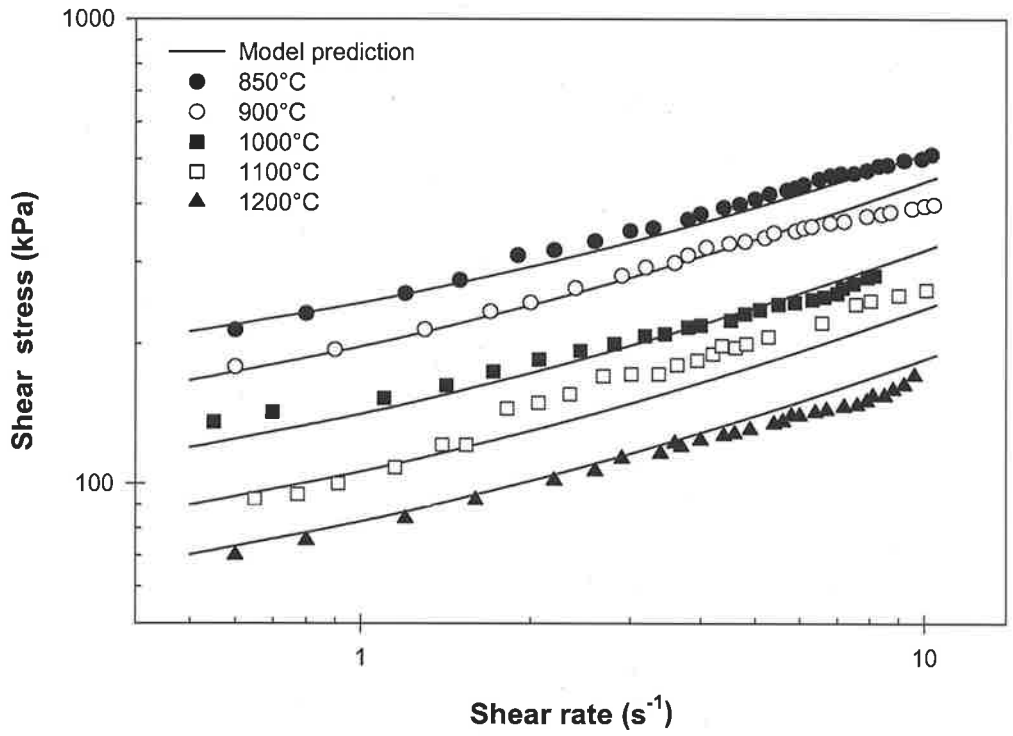

Fig 6.3: Comparisons of the experimental data and the model prediction for the Bowman-**A** ash

Fig 6.3 shows that the statistical model developed can excellently predict the flow properties of the Bowman-**A** ash over the temperature range tested. A small deviation between the model and experimental data were found at $\dot{\gamma} \geq 4s^{-1}$ and at temperature above 850°C, where the model either over predicts or under predicts the flow properties of the ash sample. This may due to at $\dot{\gamma} \geq 4s^{-1}$ the ash sample was pushed out off the cone and plate system, resulting in the deviation between the model and experimental data. However, overall the model can predict the flow properties of the Bowman-**A** ash very well over shear rate and temperature range tested.

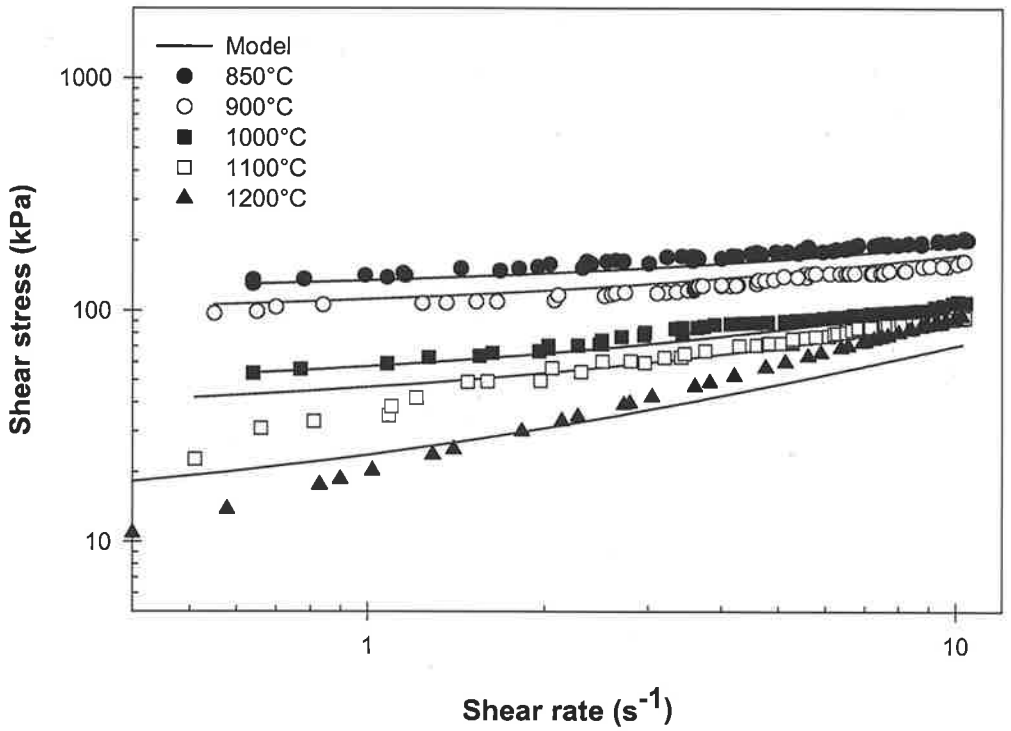

Fig 6.4: Comparisons of the experimental data and the model prediction for the Lochiel-**A** ash

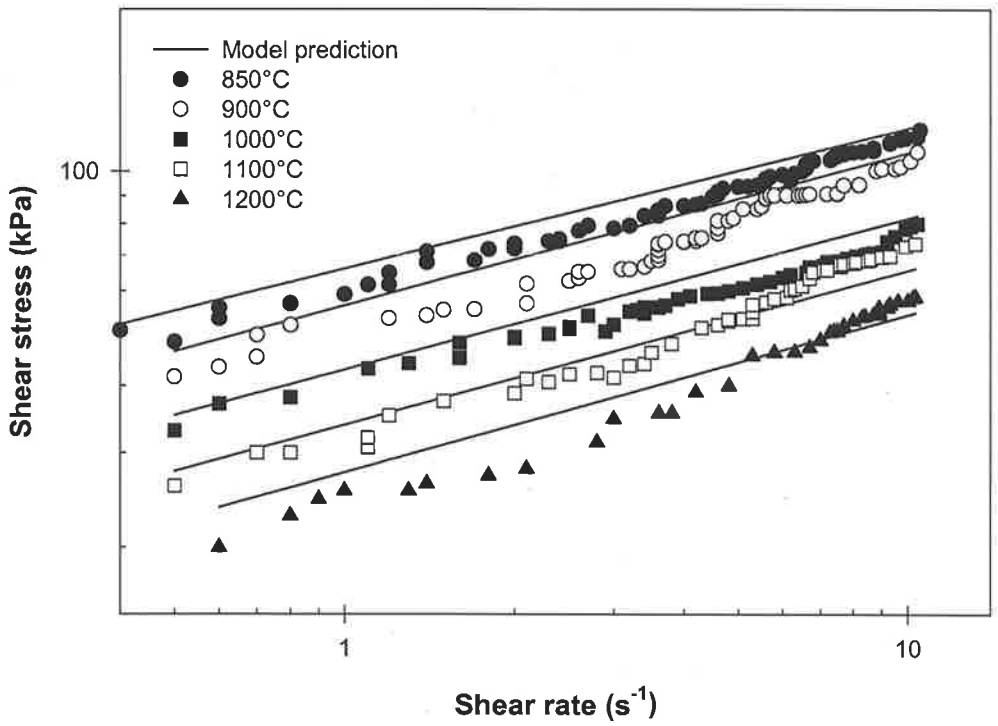

Fig 6.5: Comparisons of the experimental data and the model prediction for the Lochiel-**B** ash

Figs 6.4 and 6.5 show the comparisons of the statistical model and the experimental data for the Lochiel-**A** and Lochiel-**B** ashes. It was found that at temperatures between 850°C and 1000°C, the model correlates well with the experimental data of these ash samples over shear rate range tested. However, at temperatures above 1000°C the model over predicts, especially at $\dot{\gamma} \leq 1 s^{-1}$, the flow properties of the Lochiel-**A** and Lochiel-**B** ash samples. The difference between the statistical model and experimental data at low shear rate regime may be due effects of other chemical compounds that are not considered in the model.

From the chemical analysis in chapter 4 (Table IV.1), it was found that the concentration level of the Al_2O_3 compound was also high in the Lochiel-**A** and Lochiel-**B** ash samples. Furthermore, it was found from a phase diagram book (Hall, 1947) that Al_2O_3 reacts with Na_2O, SiO_2 and SO_3 compounds, and they form a eutectic mixture of aluminosilicate ($Na_2AlSi_3O_8$), which melts at a temperature of 1000°C. Thus, it is reasonable to assume that Al_2O_3 is the chemical compound that causes the difference between the statistical model and the flow properties of the Lochiel-**A** well and Lochiel-**B** at temperatures above 1000°C.

To qualitatively demonstrate the accuracy of the statistical model for predicting rheological properties of the South Australian ashes, the relative error between model and experimental data was calculated. Table VI.6 shows typical results of the relative error calculated for the Lochiel-**A** ash over temperature range tested.

Table VI.6: Values of the relative error of the Lochiel-**A** ash

	Temperature (°C)	Model	Experimental	Relative error
τ_y^{H-B} (kPa)	850	104.5	113.6	0.08
	900	93	81.2	0.15
	1000	48	50.3	0.04
	1100	34	28.1	0.2
	1200	19.1	13.1	0.45
K (kPa.s^n)	850	52.4	65.3	0.19
	900	72.4	62.3	0.16
	1000	58.7	52.1	0.13
	1100	47.8	33.0	0.45
	1200	36.6	20.2	0.81
n	850	0.44	0.42	0.04
	900	0.56	0.54	0.04
	1000	0.42	0.4	0.05
	1100	0.44	0.45	0.02
	1200	0.43	0.41	0.05

Table VI.6 shows that value of the relative error increases with increasing temperature. This means that the accuracy of the model to predict rheological properties of the Lochiel-**A** ash decreased as temperature increased. At temperatures between 850°C and 1000°C, it was found that the relative error of the τ_y^{H-B} and n are ranging between 0.04 and 0.15, while the relative error of the K is between 0.13 to 0.19. The relative error demonstrated that the model excellent predicted values of the τ_y^{H-B}, K and n of the Lochiel-**A** ash at temperature ranging from 850°C and 1000°C.

At temperatures above 1000°C, it was found that the value of the relative error of the yield stress parameter is between 0.2 and 0.45. This indicated that the model fairly predicts the yield stress of the Lochiel-**A** at this temperature range. Furthermore, the relative

error of the consistency index parameter was between 0.45 and 0.81 at the temperatures between 1100°C and 1200°C. This means that the model inadequately predicts value of the consistency index parameter at these temperature ranges. The reason of the poor prediction of the model may due to at this temperature range other chemical compounds becomes dominate factor and controls viscosity of the ash sample. On the other hand, the model still gives the good prediction for the flow behaviour index parameter. The good prediction of the flow behaviour index parameter is important as it confirms that the flow behaviour index parameter is independent on temperature, but rather on the chemical compositions.

The information obtained from Figs 6.3 to 6.5 and from Table VI.6 is very important in the sense that it confirms the hypothesis that the rheological properties of the South Australian ashes are basically controlled by $CaSO_4$, $MgSO_4$ and Na_2SO_4 compounds and their concentration levels. Although, there are possible effects of other chemical compounds, especially Al_2O_3, on the rheological properties of the Lochiel-**A** and Lochiel-**B** ashes, but the statistical model can reasonably predict the flow properties of the two ash samples. Further work about effects of Al_2O_3 on rheological properties of coal ash is necessary.

Predictions of the flow properties of Victorian ashes have also been made using the statistical model. The comparison of the predictions and experimental results over the tested temperature range for Victorian ashes are shown in Figs 6.6 to 6.8.

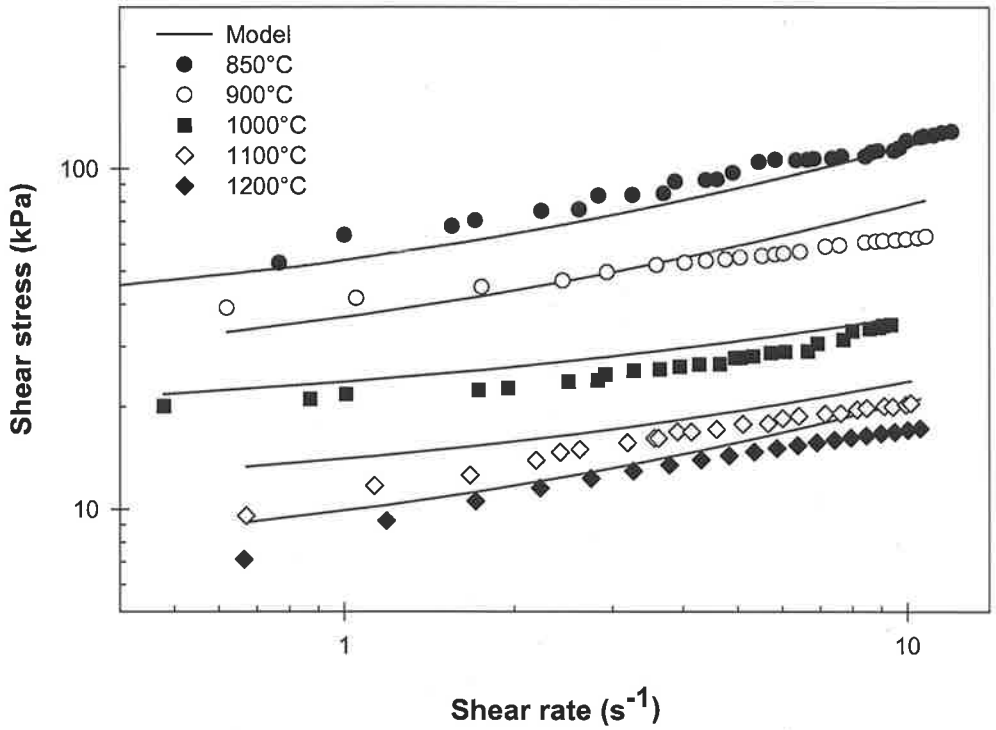

Fig 6.6: Comparisons of the experimental data and the model prediction for the Loy Yang-**A** ash

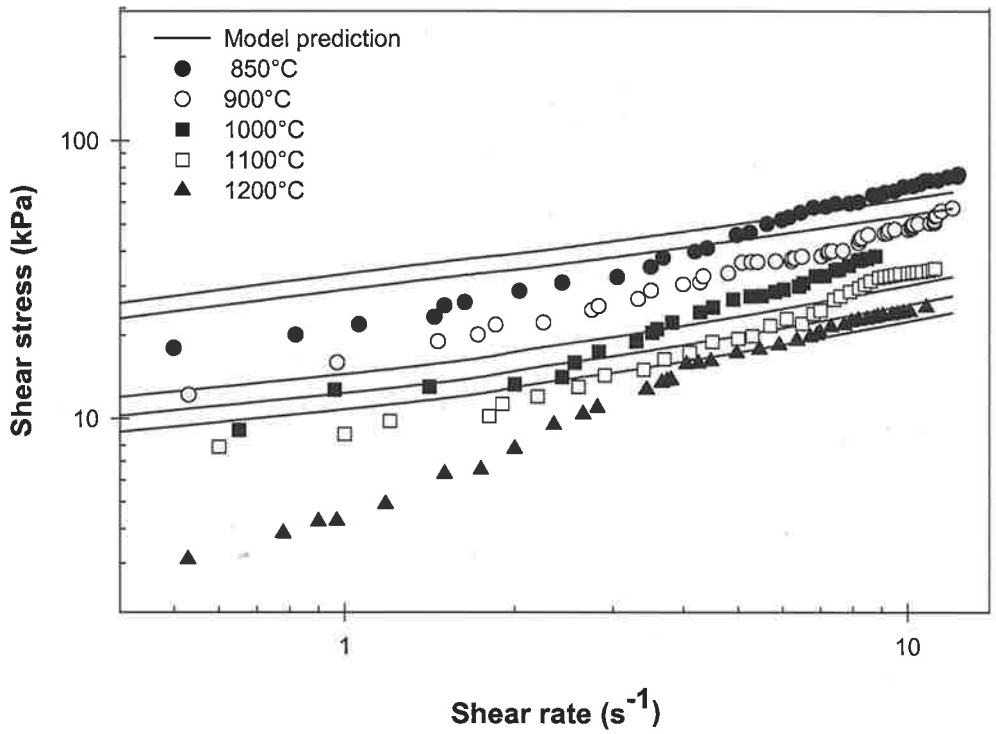

Fig 6.7: Comparisons of the experimental data and the model prediction for the Loy Yang-**B** ash

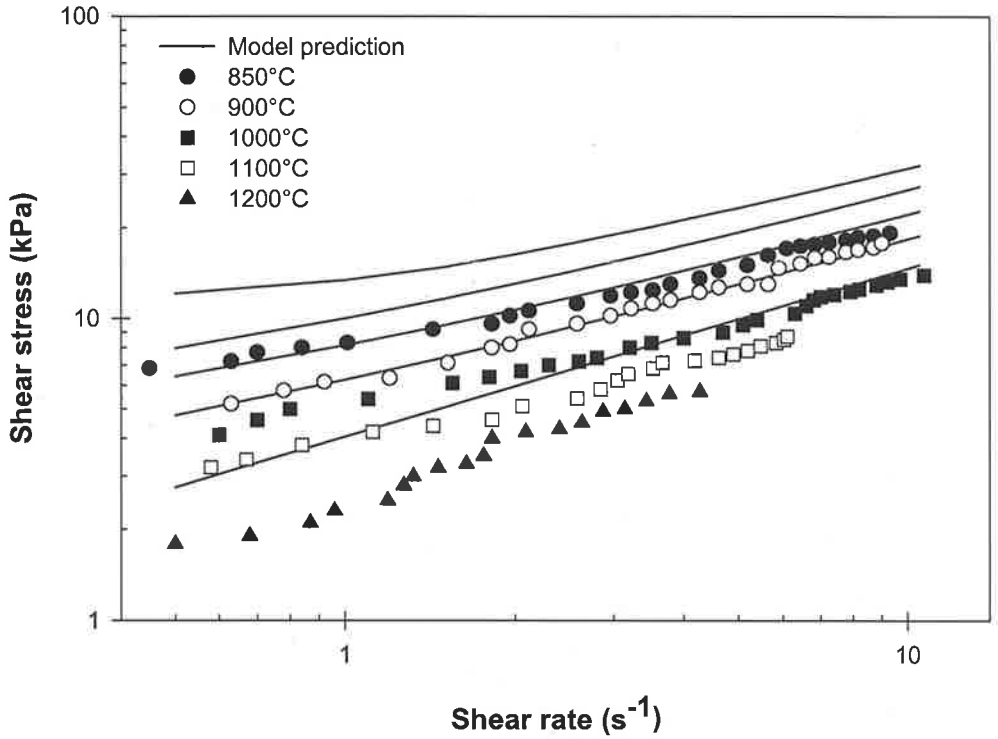

Fig 6.8: Comparisons of the experimental data and the model prediction for the Morwell-**B** ash

Figs 6.6 to 6.8 show that the model can satisfactorily predict the flow properties of the Loy Yang-**A** ash, but the model gives the poor prediction of the flow properties of the Loy Yang-**B** and Morwell-**B** ashes. The model over predicts of the flow properties for the Loy Yang-**B** and the Morwell-**B** ash samples for all the temperature range tested. The poor prediction of the statistical model for the Loy Yang-**B** and Morwell-**B** ashes is very interesting in the sense that the model cannot predict the rheological properties of the ash samples that came from the same coal but obtained differently. This may simply because of the concentration levels of $CaSO_4$, $MgSO_4$ and Na_2SO_4 compounds in the Loy Yang-**B** ash are outside the model range. In addition, it may due to there is not enough amount of $CaSO_4$, $MgSO_4$ and Na_2SO_4 compounds to form a molten layer within the ash sample, which results in failure of the model for predicting the rheological properties of the Loy Yang-**B** ash.

In regard to the Morwell-**B** ash, the failure of the model may not only due to not enough amount of $CaSO_4$, $MgSO_4$ and Na_2SO_4 compounds to form the molten phase in the ash sample, but also effects of other chemical components. The bulk chemical and XRD analyses showed that the Morwell-B ash is also high in concentration level of Al_2O_3 and Fe_2O_3 components. The Al_2O_3 compound can react with Na_2O and SiO_2 and form a

mixture of $Na_2AlSi_3O_8$ (aluminosilicate), which has melting point temperature at 1000°C (Hall, 1947). Furthermore, a phase diagram book has suggested that there is a possibility for Fe_2O_3 to react with Na_2O and Al_2O_3 compounds and form a mixture of Fe_2O_3-Na_2O-Al_2O_3, which has its melting temperature at 650°C (Hall, 1947). These may be the reasons that why the flow properties of the Morwell-**B** ash could not be predicted by the statistical model. The observations on effects of Al_2O_3 and Fe_2O_3 suggest that further work is necessary in this area.

6.6 COMPARING THE VISCOSITY PREDICTION OF THE STATISTICAL MODEL WITH OTHER EXISTING MODELS

A review of the open literature has found that models proposed by Watt and Fereday (1963) and Streeter (1981) are the most relevant to low rank Australian ashes. This is due to the fact that these two models were developed to predict the viscosity of British ashes (Watt and Fereday) and US lignite ashes (Streeter) that had concentrations of the specific chemical compositions similar to those found in low-rank Australian ashes. Details about the Watt and Fereday model can be found in section 2.4.4. The comparison has been made for the apparent viscosity (η), which determined at constant shear rates, of the Bowman-**A** and Morwell-**B** ashes.

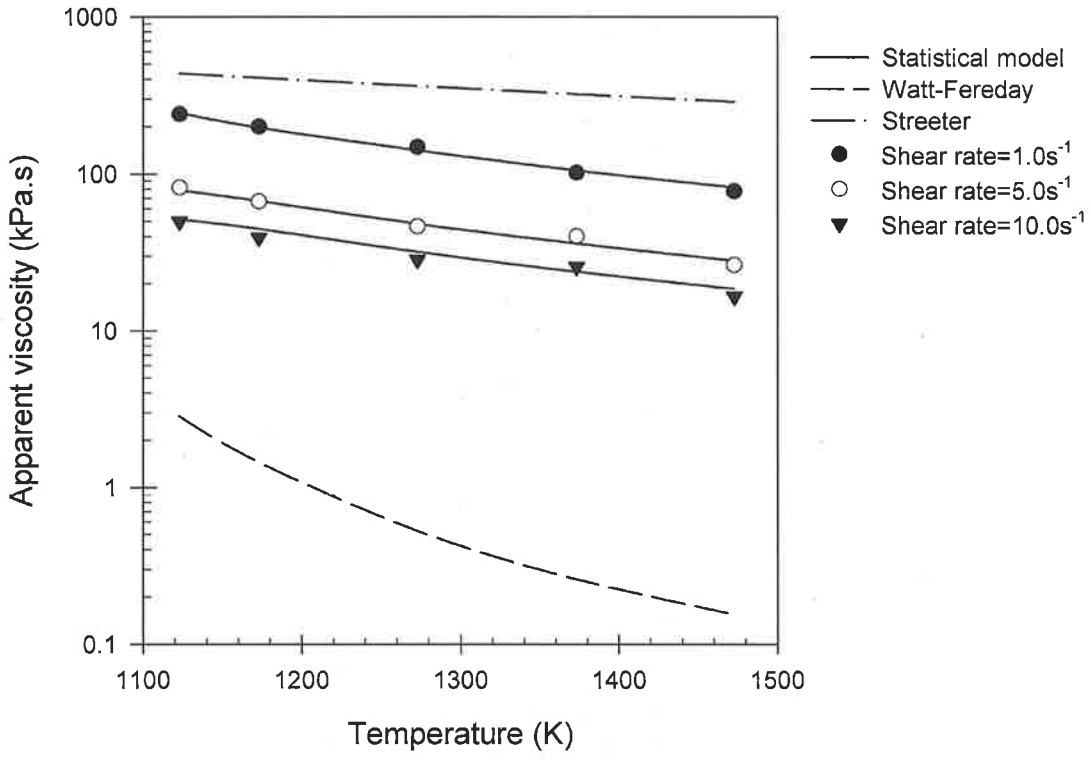

Fig 6.10: Comparison of the statistical, Watt and Fereday and Streeter models tested for correlating viscosity of Bowman-**A** ash

Fig 6.10 shows the prediction results of the apparent viscosity of the Bowman-**A** ash, which determined at shear rate of 1, 5 and 10 s^{-1}, that were obtained from the Watt-Fereday, the Streeter and the statistical model developed in this work. The comparison reveals that the Watt and Fereday and the Streeter models generate the poor prediction of the apparent viscosity (η) of the Bowman-**A** ash over the desired shear rate and the temperature ranges tested. The Watt and Fereday under predicted the apparent viscosity of the ash sample and vice versa for the Streeter model. On the other hand, the apparent viscosity of the Bowman-**A** ash could be predicted very well by the statistical model developed in this work.

The comparison in Fig 6.10 is very important as it demonstrated explicitly the superior of the statistical model to the other two existing models. The comparison also confirms that rheology of the Bowman-**A** ash, also the Lochiel-**A**, **B** and the Loy Yang-**A** ashes, is basically controlled by $CaSO_4$, $MgSO_4$ and Na_2SO_4 compounds. Furthermore, from the unique ability of the statistical model developed in this work, it has suggested that rheological properties of low-rank Australian ashes can now be predicted by using only the concentration of $CaSO_4$, $MgSO_4$ and Na_2SO_4 compounds and temperature.

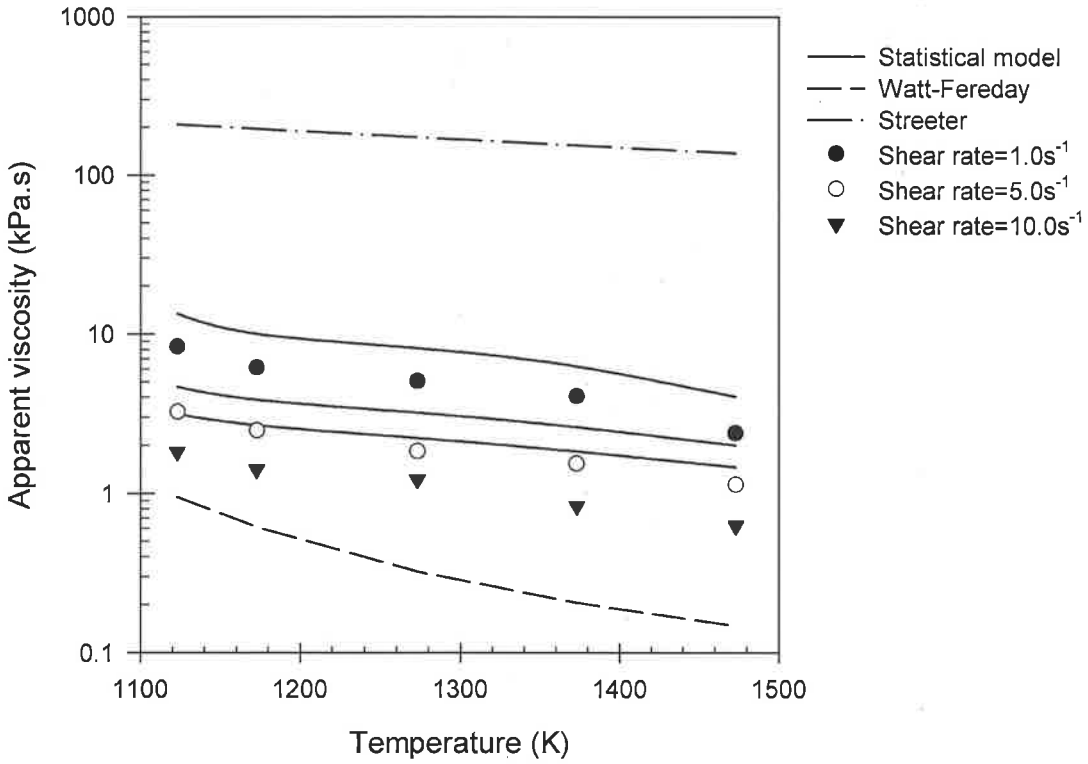

Fig 6.11: Comparison of the statistical, Watt and Fereday and Streeter models tested for correlating viscosity of Morwell-**B** ash

Fig 6.11 shows the prediction results of the apparent viscosity of the Morwell-**B** ash obtained from the Watt and Fereday, the Streeter and the statistical models. It was found

that for the Morwell-**B** ash, the Watt and Fereday, Streeter and statistical models are not be able to predict the apparent viscosity of this ash sample. It was observed that the Watt and Fereday and statistical models under predicted, while the Streeter model over predicted the viscosity of the Morwell-**B** ash sample.

The poor prediction of the statistical model on the η of the Morwell-**B** ash must come from the effects of Fe_2O_3 and Al_2O_3 compounds on the η of the ash sample. These two chemical compounds were not included in the statistical model developed in this work. It is possible that the Fe_2O_3 and Al_2O_3 impede the formation of $CaSO_4$, $MgSO_4$ and Na_2SO_4 compounds to form resulting in too little of these chemical compounds in the ash sample. Thus, the rheological properties of the Morwell-**B** ash could not be adequately described by the statistical model.

Furthermore, the poorly predicting of the two existing models for the apparent viscosity of the Morwell-**B** ash is very interesting as these two models had incorporated Fe_2O_3 and Al_2O_3 compounds into their models; but yet could not predict the apparent viscosity of the Morwell-**B** ash. This may be simply because of the concentration levels of these two chemical components are outside the Watt and Fereday, and the Streeter models range.

Based on the unsatisfactory performance of the statistical model developed in predicting rheological properties of high concentration of Fe_2O_3 and Al_2O_3 compounds ashes suggests that further work in this area is necessary.

6.7 CONCLUSIONS

In this chapter, models for predicting the flow behaviour of synthetic ashes based on a linear regression method have been developed. The regression models relate the flow properties to the concentrations of significant chemical compounds for each tested temperature. The regression model has also been tested for its adequacy and reliability. The model has been used to predict the flow properties of low-rank Australian coal ashes over the tested temperature range. The following conclusions can be drawn from the studies described in this chapter:

- The relationship between the significant chemical compounds and the flow properties of the synthetic ash mixtures can be related using a linear regression equation, which correlate the rheological properties to significant chemical compounds.

- The statistical model developed in this work successfully predicts the flow properties of South Australian coal ashes (the Bowman-**A**, the Lochiel-**A** and the Lochiel-**B** ash) and the Loy Yang-**A** ash (a Victorian ash sample). The observation has confirmed that rheology of low-rank Australian ashes is controlled by $CaSO_4$, $MgSO_4$ and Na_2SO_4 compounds. However, the model fails to predict the flow properties of the Loy Yang-**B** and the Morwell-**B** ashes. Based on the chemical and mineralogical analyses of these two ash samples, it is assumed that there are other chemical compounds especially Fe_2O_3 and Al_2O_3 controlling the rheological properties of the Loy Yang-**B** and the Morwell-**B** ashes. Further work is necessary in this area.

- Comparisons between the viscosity prediction of the statistical model developed in this work with two other existing models proposed by Watt and Fereday (1964), and Streeter (1981) has also been performed in this work. It is found that these two existing models cannot predict the apparent viscosity of the Bowman-**A** and the Morwell-**B** ashes over temperature range tested. Based on the comparisons, it appears that the statistical model developed in this work is superior to the existing model for predicting the rheological properties of low-rank Australian coal ash. Moreover, it is found that the rheology of low-rank Australian ashes can be predicted by using the concentration of key chemical compounds and the temperature.

CHAPTER SEVEN

Relationship between Ash Rheology and Fluid Bed Agglomeration

7.1 INTRODUCTION

The current research investigates rheological characteristics of low-rank Australian coal ashes in oxidising conditions for temperatures ranging from 850°C to 1200°C. The experimental results showed that coal ash samples are viscoplastic and time-dependent materials. The rheology of coal ash was found to be complex but is controlled by a few key chemical species, which are calcium sulphate ($CaSO_4$), magnesium sulphate ($MgSO_4$) and sodium sulphate (Na_2SO_4). The experimental results with synthetic ash mixtures containing $CaSO_4$, $MgSO_4$, Na_2SO_4 and solid silica as models for coal ash have shown how these alkali sulphate components affect the flow properties of the mixtures. Moreover, the synthetic ash's results have been used to develop a statistical model, which satisfactorily predicts rheological properties of low-rank Australian coal ashes at temperatures ranging from 850°C to 1200°C.

This chapter has been divided into four sections, and is aimed at determining what relationship there is between the rheological properties of coal and the problem of agglomeration in fluidised bed combustion. The first section presents observations on fluidised bed combustion behaviours of Australian brown coals and lignite. The current understanding of fluid bed agglomeration and its mechanisms is also given. The information obtained from this section improves the understanding of how coal ashes, chemical components and operating conditions affect fluid bed agglomeration. Moreover, by comparing the experimental observations with the rheological experiments, rheological properties that may cause agglomeration can also be identified. The second section presents the relevance of ash rheology to agglomeration of fluid bed particles. Effects of yield stress, the consistency index parameter and the flow behaviour index on fluid bed agglomeration are considered and discussed in the thrid section. The section three deals with how the existing mathematical models for agglomeration can be

improved with the knowledge about the ash rheology obtained in this work. Finally, conclusions are given in the last section.

7.2 BEHAVIOUR OF ASH DURING FLUIDISED BED COMBUSTION OF AUSTRALIAN BROWN COALS AND LIGNITE

A small number of publications on agglomeration of bed particles during fluidised bed combustion and gasification of low-rank coals are currently available. These include the work of Manzoori (1990), Linjewile et al (1994), Skrifvars et al (1994), Benson et al (1998) and Bhattacharya et al (2000).

The Ph.D. work by Manzoori (1990) may be considered as the first attempt to investigate the mechanisms involved in the agglomeration of fluid bed particles when utilising low-rank Australia coals in fluidised bed combustors. The investigations were performed in a spouted bed fluidising unit with an inside diameter of 77 mm. Silicate sand material, with particle sizes ranging from 0.85 to 1.0 mm, was used as the fluid bed material. The combustion experiments were performed at a fixed temperature of 800°C. During the experiment, pressure drops across the fluidised bed unit were closely monitored. Four different low-rank Australian coals were used, two Victorian coals (Loy Yang and Morwell coals) and two South Australian coals (Lochiel and Bowmans coals).

Manzoori (1990) found that the experiment with Victorian coals went smoothly without a significant pressure loss problem. In contrast, the experiments with South Australian coals were difficult, as the experiments were suffering from a drastic pressure drop problem. Manzoori (1990) reported that pressure in the fluidised bed column dropped within the first two hours of the experiment and approached a complete loss of pressure after approximately three hours. He suggested that the pressure drop could be used as an indication of the number of particles being fluidised. A high drop in pressure means fewer particles are fluidised. Visual inspection of the fluidised bed column interior revealed that with South Australian coals there were a number of particles, which resided in the bottom section of the fluidised bed column. When the fluid bed particles were withdrawn large agglomerated bed particles were found. The largest agglomerated particle found from South Australian coals (Bowmans coal) was 60 mm in diameter, while the largest for Victorian coals (Loy Yang) was 3 mm. Chemical analyses, using the SEM-EDX and XRD methods, of these agglomerated bed particles showed that deposition of a molten ash layer had bound the fluid bed particles together. It was found that the molten ash was rich in $CaSO_4$, Na_2SO_4, $MgSO_4$ and a mixture of SiO_2-Al_2O_3-Na_2O compounds.

Bhattacharya (2000) studied fluid bed agglomeration and deposition of coal ash as functions of operating temperature and processing time. They performed fluidised bed experiments in a Circulating Fluidised Bed Combustion unit (CFBC) with an inside diameter of 1500 mm. Silica sand was used as fluid bed particles. Four Australian lignite coals were used - one South Australian (Lochiel coal) and three Victorian coals (Loy Yang, Morwell and Yallourn coals). The combustion experiments with Victorian coals were performed at temperatures ranging from 800°C to 900°C. It was reported that there were no bed agglomeration problems during the combustion of Victorian coals, allowing the fluidised bed experiments to be operated for up to 96 hours. The experiments with Lochiel coal were performed at temperatures ranging from 800°C to 850°C. It was found that with the South Australian coal, the fluidised bed experiment could only be operated for up to 36 hours before the process was interrupted by problems associated with fluid bed agglomeration. The largest size of agglomerated bed particles found in the chamber was 50 mm. Chemical analyses, again using the SEM and XRD methods, of the agglomerated particles revealed that the fluid bed particles were bound together with a rich layer of solium sulphate and calcium sulphate and a complex silicate mixture containing sodium and aluminium.

Linjewile et al (1994) and Bhattacharya (2000) investigated the effects of additive materials on the occurrence of fluid bed agglomeration. Four different substances were used as additive materials, dolomite, a kaolin/sillimanite rich clay, aluminium hydrate and silica. The experiment with additive materials was performed with Lochiel coal. It was found that the fluidised bed experiment using the aluminum hydrate and the kaolin/sillimanite could be operated longer than with the dolomite and the silica experiments. Based on the SEM-EDX and XRD analyses, Linjewile and Bhattacharya have found that the coating thickness of molten ash on the surface of the fluid bed particles decreased when either the aluminum hydrate or the kaolin/sillimanite were mixed with the coal sample. They suggested that the additive material may cause a physical dilution and affect the chemical reactions that occur between the additives and the inorganic constitutes in coal.

These observations on the behaviour of fluidisation during the combustion of low-rank Australian coals showed that the agglomeration of bed particles in a fluidised bed combustor mainly involves the deposition of a molten ash on the surface of the bed particles. Over temperature ranges of 800°C to 850°C, Victorian coals are far superior than South Australian coals in terms of fluidisation characteristics. The experiments with Victorian coals found that a fluidised bed combustor can be operated for longer periods

with these coals than with South Australian coals. This is because the Victorian coals are low in total ash content and have lower concentrations of the chemical species that form the molten ash layer. No agglomeration or defluidisation was observed during the combustion of any of the Victorian coals that were tested. As far as the combustion behaviour is concerned, fluidised bed technology is suitable for power generation using Victorian brown coals.

Based on these experimental findings, Manzoori (1990), Linjewile et al (1994) and Bhattacharya (2000) have developed a hypothesis to describe behaviours of low-rank Australian ashes during fluidised bed combustion process. They suggest that during fluidised bed combustion process, a molten ash layer is formed and initially entrapped inside the ash structure leading to form the structure of the ash itself. As the fluidised bed process continues, the structure of the ash particles is broken down mainly by the hydrodynamic force and the molten ash is dispersed onto surface of the ash particles. When the ash particles coated with the molten ash layer come into contact with the fluid bed particles, the molten ash is transferred onto the surface of the bed particles.

Furthermore, Manzoori (1990), Skrifvars et al (1994), Linjewile et al (1994) and Bhattacharya (2000) found that the molten ash layer, which deposited on the surface of the bed particles, acts like an adhesive layer holding the fluid bed particles together after collisions. As the fluidised bed processes, collisions between the fluid bed particles coated with the molten ash occur and the momentum of the collided particles is dissipated into the molten ash layer causing a reduction in the total energy. Simultaneously, the rheological properties of the molten ash layer control the mobility and tendency of the collided particles, making them to adhere together. If the momentum required for the particles to rebound is less than the adhesive force (or viscous force), agglomeration of fluid bed particles occurs.

7.3 RELEVANCE OF ASH RHEOLOGY TO AGGLOMERATION OF FLUID BED PARTICLES

Manzoori (1990) and Linjewile et al (1994) performed fluidised bed combustion experiments with the Bowmans, Lochiel, Loy Yang and Morwell coals at the average fluid bed temperature of 850°C and at fluidised bed velocity of 20 m/s. They found that agglomeration of fluid bed particles occurred when fluidising Bowmans and Lochiel coals. No fluid bed agglomeration was observed with the Loy Yang and Morwell coals. Manzoori and Linjewile also reported that defluidisation of the fluidised bed unit occurred within 1.2 and 10 hours of operation with the Bowmans and Lochiel coal, respectively. The

fluidised bed experiments with the Loy Yang and Morwell coals could be operated up to 18 hours without the defluidisation.

From the rheological studies of low-rank Australian coal ashes, it was observed that the coal ash samples exhibit non-Newtonian flow behaviour, characterised by a yield stress and a shear rate dependent viscosity. The rheological experiments indicated that yield stress of the Bowmans and Lochiel ashes are higher than the Loy Yang and Morwell ashes in which the Bowman ash has the highest yield stress of all the samples tested. Rheology of coal ash in chapter four showed that at the temperature of 850°C, the yield stress values of the Bowmans and Lochiel ashes are at 163.5 and 113.6 kPa, while the yield stress values of the Loy Yang-A and Morwell-B ashes are at 38.1 and 6.2, respectively. This indicates that agglomeration of fluid bed particles is likely to occur at an operating temperature of 850°C, when yield stress value is above 100 kPa. Comparing the yield stress of these ash samples found that the yield stress of the Bowmans is 4.5 and 26 times higher than the Loy Yang and Morwell ashes. The yield stress of Lochiel ash is 3 and 18 times higher than the Loy Yang and Morwell ashes, respectively.

Bhattacharya and co-workers (2000) used a CFBC unit to perform combustion experiments at the fluidised bed temperature of 800°C and 850°C with the Lochiel, Loy Yang, Morwell and Yallourn coals. They found that with Lochiel coal, agglomeration of the fluid bed particles occurred within 10 hours of operation and the CFBC unit was unexpectedly stopped after approximately 26 hours of the coal firing process due to defluidisation of the fluid bed particles. The largest size of agglomerated bed particles found in the chamber was 50 mm. In contrast, no fluid bed agglomeration was found during coal firing process of the Loy Yang, Morwell and Yallourn coals. The CFBC unit could be operated continuously for up to 90 hours without defluidisation.
The presence of a high yield stress of the ash samples in the range of temperature of interest may have significant impact on agglomeration of fluid bed particles. Since the yield stress is the critical shear stress that must be overcome to start viscous flow, its magnitude determines the tendency of the molten ash to adhere to the surface of fluid bed particles following the transfer of the ash from the burning char. It is thus desirable to have a lower yield stress in order to reduce the degree of *'stickiness'* of the molten ash matter depositing on a solid surface.

It is now possible to quantitatively explain why the tendency of fluidised bed agglomeration is high with the Bowmans and Lochiel coals, but low with the Loy Yang and Morwell coals by using the information about the yield stress. After collisions of fluid

bed particles coated with a molten ash layer, a certain stress is required to separate the collided particles, which implies the yield stress of the molten layer. If the yield stress is high enough, the particle will adhere together rather than bouncing off each other resulting in agglomeration of the fluid bed particles. Since the yield stress of the Bowmans and Lochiel coals are higher than the yield stress of Loy Yang and Morwell coals, it is reasonably concluded here that the tendency of particles to stick together after their collisions is in the descending order of Bowmans>Lochiel>Loy Yang>Morwell.

Although, the yield stress illustrates the tendency of stickiness of the fluid bed particles after collisions, but using only the yield stress property may be insufficient to cause agglomeration of the fluid bed particles. This is because in the fluidised bed unit, the hydrodynamic force is sufficiently high and the ash particles are moving around. This means the stuck particles can still be broken by the hydrodynamic force. Viscosity of the molten ash layer is another physical property that may be significant in controlling the behaviours of agglomeration. Since the viscosity is the physical property controlling flow ability and mobility of fluids, its magnitude determines the tendency of the molten ash to hold the particles together after a collision- high viscosity is able to hold the particles together longer than low viscosity after a collision.

Chapter four has demonstrated that the viscosity levels of the Bowmans and Lochiel ashes are higher than those of the Loy Yang and Morwell ashes. The Bowmans is the most viscous sample of all the ashes tested. Knowing the ash rheology will provide a better understanding of why the agglomeration of fluid bed particles is a serious problem when the Bowmans and Lochiel ashes are used. This is because the Bowmans and Lochiel ashes not only produce a sticky molten ash layer but also produce a very viscous molten ash layer that is able to hold the fluid bed particles together after collisions for a longer period of time. As the fluidisation progresses, the size of the agglomerated particle is increased leading to defluidisation of the fluidised bed unit. Unlike the Loy Yang and Morwell ashes, which are low in the tendency of particles to stick together after collisions. This may be the reason why agglomeration and defluidisation are not serious problems when fluidising the Loy Yang and Morwell coals.

The shear thinning characteristics of the molten ash imply that the viscosity of coal ash deposits changes with the local particle and gas velocities in a fluidised bed- higher velocity means higher shear rate leading to low ash viscosity. The meaning of shear thinning characteristics of low-rank Australian ash samples may suggest that problems associated with agglomeration and defluidisation could be reduced by operating a

fluidised bed unit at a high gas velocity. Furthermore, the ash rheology in chapter four has revealed that the viscosity of the Loy Yang ash is more sensitive to shear rate than the viscosity of the Bowmans and Lochiel ashes. This means that not only viscosity of the Loy Yang ash decreases with increasing shear rate (or gas velocities) but it also decreases more rapidly than the viscosity of the Lochiel and Bowmans samples. This implies that after collisions of bed particles when the Loy Yang coal is used, viscosity of the molten layer decreases rapidly and results in decreasing the ability of the molten layer to hold the collided particles together. This may be the main reason why fluid bed agglomeration and defluidisation are not serious issues with the Loy Yang coal. For the Morwell ash, it was found that the viscosity of this ash is not sensitive to shear rates comparable to those found in the Bowmans, Lochiel and Loy Yang ashes. However, values of yield stress and viscosity of the Morwell ash are relatively too small to stick and to hold the fluidised bed particles together after their collisions.

7.4 IMPLICATION OF ASH RHEOLOGY TO MATHEMATIC MODELS DEVELOPED FOR FLUID BED AGGLOMERATION

A survey of the open literature has revealed that there are three different categories of models developed for predicting particles' agglomeration. The first category was developed based on the assumption of energy balance, which is that the energy required to stick fluid bed particles together after a collision must be greater than the energy required to separate the collided particles. The second category model developed for calculating the rate of agglomeration in the fluidised bed column by using collision frequency and population balance methods. For the third category, the model was developed for predicting the size distribution of agglomerated particles by using the population balance approach. Of these three model categories, it was found that the fist category model could be used to determine whether agglomeration would occur in a fluidised bed coal combustion/gasification (He, 1997; McLaughlin, 1999).

According to a concept of force balance, the fluid bed particles would be agglomerated if separation force were less than adhesive force. The separation force was found to be centrifugal force, which is generated by particles rotating during fluidisation process, and adhesive force is mainly a combination between drag force and viscous force (Mazzone, 1986; Kang et al, 1991; He, 1997; McLaughlin, 1999). Thus, based on the concept of force balance, relationship between separation's forces and agglomeration' forces can be expressed in equation 7.1.

$$\left\{\begin{array}{c}\text{Kinetic}\\ \text{energy for}\\ \text{separation}\end{array}\right\} \leq \left\{\begin{array}{c}\text{Energy}\\ \text{dissipation due to}\\ \text{friction}\end{array}\right\} + \left\{\begin{array}{c}\text{Energy due to}\\ \text{force of liquid}\\ \text{layer}\end{array}\right\} \qquad 7.1$$

Some works have suggested that the energy due to the friction could be neglected (Orr et al, 1975; Adams an Perchardm, 1984; Mazzone, 1986; Kang et al, 1991). This is because effects of gravity force in fluidised bed unit are very minimal. Thus, agglomeration of fluid bed particles will occur when the separation force is greater than force due to liquid layer only. Furthermore, a survey of the open literature has revealed that the force of liquid layer can be further classified into two types (Adams and Perchard, 1984; Ennis et al, 1990). They are the force due to the surface curvature of the liquid bridge (surface tension) and the force due to the viscous effect of the liquid in mobile bridges. It appears that ash rheology would have significant effects on the force due to the viscous effect of the liquid layer only. Fig 7.1 shows a summary of the forces balanced on two collided particles coated with a liquid layer.

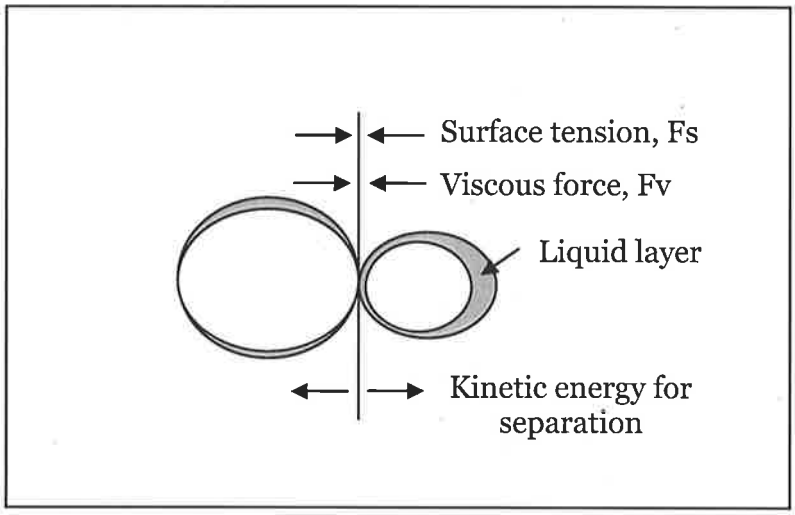

Fig 7.1: A schematic diagram of collision between two particles

Force due to viscous effects

In a dynamic system such as fluidised bed, the magnitude of a viscous force is a function of the viscosity of the binding agent (molten ash layer for this work). Based on the approach developed by Adams and Perchard (1985) for calculating viscous force of Newtonian fluids, the viscous force can be expressed as:

$$F_v = 3\pi R^2 \mu \frac{v_s}{2h_0} \qquad 7.2$$

where μ is the viscosity of fluid. R is radius of contact area, v_s is separation velocity and h_o is a minimum separation distance.

It was found from a system contained with two identical size spheres that a minimum separate distance was approximately at $4x10^{-10}$ m (Tabor, 1977; Dahneke, 1971). Adams an Perchardm, (1984), Mazzone, (1986) and Kang et al (1991) suggested that as soon as particles collided and are bouncing away from each other, due to the force of impact, the binding force becomes activated and increases with the separation velocity. From equation 7.2, it can be seen that for systems having the same values of R, v_s and h_o, the viscous force is strongly dependent on viscosity of the coated layer (molten ash in this work). For example, at shear rate of $3s^{-1}$ and operating temperature of 850°C, viscosity of the Bowmans-**A**, Lochiel-**A** and Loy Yang-**A** are at 125, 60 and 25 kPa.s, respectively. This means that the viscous force of the Bowmans-**A** is 2.5 and 5 times higher than the viscous force formed by the Lochiel-**A** and the Loy Yang-**A** ashes. Based on the value of the viscous force, it may be one of the reasons why agglomeration of fluid bed particles is the serious problem when the Bowmans and Lochiel coals are used.

Knowing only the viscosity of a liquid layer coated on the surface of fluid bed particles may be satisfactory for calculating the viscous force of a system given that the coated fluid is a Newtonian fluid (Adams an Perchardm, 1984; Mazzone, 1986; Kang et al, 1991; He, 1997), but can produce serious errors when the coated fluid exhibit non-Newtonian fluids. Based on the series of experimental observations presented in this work, it is found that the low-rank coal ash samples are a non-Newtonian fluid characterised by a yield stress and shear thinning viscous behaviours. In addition, from the recently established relationship between ash rheology and fluid bed agglomeration, it has been found that yield stress and shear thinning viscosity behaviour have significantly affected the agglomeration characteristics of fluid bed particles. Thus, it is necessary to incorporate the non-Newtonian properties of the molten ash layer into the existing

equation developed for calculating viscous force. By means of incorporating, the equation 7.1 can be rewritten as:

$$F_v = 3\pi R^2 \eta \frac{v_s}{2h_0} \qquad 7.3$$

where η is the non-Newtonian viscosity (apparent), which is a function of temperature, shear rate and chemical composition.

At the present, the new equation proposed for calculating the viscous force has not yet been incorporated into the model developed to predict agglomeration of fluid bed particles. Future experimental verifications for the model as well as the new proposed equation are necessary and need to be carried out.

It can be seen that the non-Newtonian nature of molten low-rank coal ash would complicate the modelling of particles agglomeration, especially for calculating the adhesive force. Nevertheless, a good understanding of ash rheology and the rheology of key chemical compositions have improved our understanding of the mechanisms of ash deposition and subsequent particle agglomeration and bed defluidisation.

7.5 CONCLUSION

Based on comparisons between rheology of coal ashes and synthetic mixtures and experimental observations on behaviour of fluid bed agglomeration, the following conclusions can be drawn:

- Yield stress property of molten ash layer controls the stickiness of the collided particles. The collided particles tend to stick together easier with high yield stress fluids than with low yield stress fluids. Apparent viscosity is the physical property controlling flow ability and mobility of fluids, its magnitude determines the tendency of the molten ash to hold the particles together after a collision - high viscosity is able to hold the particles together longer than low viscosity after a collision.

- The shear thinning characteristics of the molten ash imply that the viscosity of coal ash deposits changes with the local particle and gas velocities in a fluidised bed - higher velocity means higher shear rate leading to low ash viscosity. The meaning of shear thinning characteristics of low-rank Australian ash samples may suggest

that problems associated with agglomeration and defluidisation could be reduced by operating a fluidised bed unit at a high gas velocity.

- Of the models developed fro predicting agglomeration of fluid bed particles in fluidised bed systems, the model developed based on the concept of energy balance is found to be the most relevant. At the present, the model developed based on the initial assumption that the molten ash is a Newtonian fluid, and take into account ash rheology as a single viscosity parameter. This may cause serious errors when coal ash exhibits non-Newtonian behaviours. A good understanding of the rheology of coal ash and synthetic mixtures lead to the improvement of a mathematical equation used for calculating the viscous force, and hence improving accuracy of the agglomeration model. However, at the present the model proposed in this work has not yet been incorporated into agglomeration models. Further experimental verifications are essentially required.

CHAPTER EIGHT

Conclusions and Recommendations

8.1 CONCLUSIONS

A unique high temperature rheometer has been developed based on the principal concepts of viscometric and fluid mechanics. The development of the new ash rheometer is very important as the shear rheology of low-rank coal ash can be completely characterised for the first time. With the development of the ash rheometer, various aspects of flow behaviours and properties of low-rank coal ashes have been studied. It was found that low-rank Australian ashes are non-Newtonian fluids and their rheological properties are strongly affected by chemical compounds; shear rate, temperature and operating atmosphere. In this work, rheology of synthetic ash mixtures containing only a few key chemical compounds has also been studied. The synthetic mixtures' experimental data were used to develop statistical models, which later used to predict rheological properties of the coal ash samples. The model successfully estimated the equilibrium flow properties of high alkali sulphate ash samples, however, the model failed to predict rheological properties of low alkali sulphate ash samples. In this work, relevance between ash rheology and fluid bed agglomeration has been established based on the quantitative scientific evidences. Implication of ash rheology on models developed for predicting fluid bed agglomeration is also discussed. The major conclusions include:

1. A unique high temperature rheometer is designed based on the principal concepts of shear flow rheometry and fluid mechanics. The developed rheometer allows fundamental shear rheological properties, such as shear stress and shear rate, to be obtained without relying on calibrations with materials of known properties. The rheometer has the capability to measure the rheological properties of materials at temperatures ranging from 500°C to 1300°C under a controlled operating condition. A cone-plate system has been used as the rheometer's measuring geometry. The suitability and accuracy of the rheometer has also been extensively tested with a known viscosity Newtonian fluid (borosilicate glass) and

with a know viscosity material (a ternary oxide mixture of 38%CaO, 20%Al_2O_3 and 42%SiO_2), without using any calibrations.

2. Rheological properties of six low–rank Australian coal ashes have been characterised and measured. The rheological data have shown that at equilibrium state, the coal ash samples are highly non-Newtonian and characterised by shear thinning behaviour with a yield stress. Thixotropy characteristics of the ash samples are also observed. It was found that time dependent and equilibrium flow properties of the coal ash samples depend strongly on shear rate, temperature and coal type. The rheological results revealed that at equilibrium state, the South Australian ashes are more viscous and higher in yield stress than the Victorian ashes at the same temperature. Chemical analyses of ash samples identified that $CaSO_4$, $MgSO_4$ and Na_2SO_4 are the key chemical compounds controlling rheological properties of the ash samples. These three alkali sulphate compounds react together and form a low melting point eutectic mixture. The values of the yield stress, the viscosity and the shear thinning behaviours are strongly dependent on concentration levels of these three alkali sulphate compounds. Operating atmospheres have also affected rheological properties of coal ash samples; yield stress, viscosity and shear thinning behaviours all change corresponding to changes in the operating atmosphere. However, only qualitative information has been obtained in this work. Further investigations in this area are necessary.

3. Rheological properties of synthetic ash mixtures, which contain only a few key chemical compounds are also measured and characterised. The synthetic mixture contained $CaSO_4$, $MgSO_4$, Na_2SO_4 and SiO_2 compounds in which SiO_2 represents the unmelted solid particles. Based on the experimental findings, it was found that either $CaSO_4$ or $MgSO_4$ or a combination of both are key compounds causing a high degree of thixotropy, and vice versa for Na_2SO_4 compound. Na_2SO_4 is a significant compound that causes high values of yield stress and the consistency index (a measure of the viscous property) parameter in the synthetic mixtures. $CaSO_4$ and $MgSO_4$ compounds were found to decrease the yield stress and the consistency index parameters.

4. Based on the work on synthetic ash mixture, a regression model that relates the flow properties to the concentrations of significant chemical compounds for each tested temperature has been developed in this work. The regression model has

also been tested for its adequacy and reliability. The model has been used to predict the flow properties of low-rank Australian coal ashes over the tested temperature range. With the development of the regression model, it allows, for the first time, the rheology of a complex material such as coal ash to be predicted. In this work, the statistical model developed was used to predict rheological properties of the low-rank Australian coal ashes. It was found that the model successfully predicts flow properties of the South Australian ashes, while the model fails to predict flow properties of the Victorian ashes. This is due to other chemical compounds, especially Fe_2O_3 and Al_2O_3, that also have an effect on flow properties of the Victorian ashes. Further work is necessary in this area. In addition, comparisons between the viscosity prediction of the statistical model developed in this work with two other existing models proposed by Watt-Fereday (1964), and Streeter (1981), found that the model developed in this work is superior to the two listed models.

5. Relationships between ash rheology and fluid bed agglomeration have been established based on the experimental observation by Manzoori (1990), Linjewile et al (1994) and Bhattacharya et al (2000). It was found that the magnitude of the yield stress of molten ash determines the degree of stickiness of the molten ash layer - high yield stress means that there is also a high degree of stickiness. As a consequence, a high yield stress ash layer has a higher tendency to stick the fluid bed particles together after collisions. The apparent viscosity is the physical property controlling flow ability and mobility of fluids, its magnitude determines the tendency of the molten ash to hold the particles together after a collision - high viscosity is able to hold the particles together longer than low viscosity after a collision. The shear thinning characteristics of the molten ash imply that the viscosity of coal ash deposits changes with the local particle and gas velocities in a fluidised bed - higher velocity means higher shear rate leading to low ash viscosity. The meaning of shear thinning characteristics of low-rank Australian ash samples may suggest that problems associated with agglomeration and defluidisation could be reduced by operating a fluidised bed unit at a high gas velocity. In addition, implication of ash rheology on models developed from predicting fluid bed agglomeration has also been described. It was found that non-Newtonian properties of molten ash complicate the modelling of particles agglomeration, especially for calculating the adhesive force. Nevertheless, a good understanding of ash rheology and the rheology of key chemical compositions has improved our

understanding of the mechanisms of ash deposition and subsequent particle agglomeration and bed defluidisation.

8.2 RECOMMENDATIONS

The following is an outline of the recommendations for further works based on this study:

- In the current study, yield stress values of the coal ashes and the synthetic mixtures are determined by extrapolations of the flow data using a viscous flow model (Herschel & Bulkley model). The yield stress values obtained from this method, however, should be used with care. This is because of the reliability of the yield stress value is restricted within the range of shear rates tested. It is, therefore, recommended that for each coal ash sample a complete yield stress measurement should be performed as a function of time and temperature. The stress controlled measurements with a cone and plate geometry are strongly recommended for the yield stress measurements of the coal ash sample since direct stress-controlled measurements can be performed and true yield stress can be determined. The main reason for suggesting the cone and plate system is due to the fact that a small amount of coal ash sample is required for each test. The rotating cup in a stationary vane is also recommended.

- In this work, the focus of rheological measurements has been placed onto the combustion atmosphere. However, it was found in chapter 4 that the operating atmosphere has also affected rheological properties of coal ash. Under a neutral environment (the rich N_2), the coal ash seem to be higher in yield stress and viscosity, and viscosity is more shear sensitive than under oxidising and combustion atmospheres. At the present, it is assumed that changing operating atmosphere also changes reactions of chemical compositions. As a consequence, different chemical formations are formed within a coal ash sample. It is possible that in a neutral atmosphere, $CaSO_4$, $MgSO_4$ and Na_2SO_4 are not key chemical compounds controlling rheological properties of a coal ash sample, but become a mixture of aluminosilicate that really controls rheological properties of coal ash. Thus, it is strongly recommended to perform quantitative studies on effects of operating atmosphere on rheological properties of low-rank coal ash sample. In addition, effects of pressure on rheological behaviours and properties of coal ash are also encouraging to study. This is because the information obtained will be very useful for understanding the mechanisms of coal ash depositions and

agglomeration in fluidised bed gasification and in the pressurised fluidised bed unit.

- Further development of the model for ash rheology based on the fundamental study of a synthetic ash mixture containing more chemical components especially Fe_2O_3 and Al_2O_3 in addition to the alkali sulphate and silica is also recommended. It has been found that the regression model developed in this work fails to predict rheological properties of a rich in Fe_2O_3 and Al_2O_3 compounds ash. This is because these two chemical compounds react with SiO_2 and Na_2SO_4 during high temperature rheological measurements and form a new mixture that also has effects on rheological properties of the ash sample. Thus, in order to improve the capability of the regression model for predicting rheological properties of other coal ash samples that are high in Fe_2O_3 and Al_2O_3 compounds, further development of the model is necessary.

- In the development of the modelling of agglomeration, only quantitative investigation has been performed. A more realistic extension of development of the model would be to include the non-Newtonian rheology of coal ash into the model. When incorporating the non-Newtonian properties, the model would become more accurate for predicting viscous force than the existing model, which considers a molten ash as a Newtonian fluid. As a result, the model developed for predicting fluid bed agglomeration would be significantly improved.

References

Abbott, M.F. and Moza A.K., (1981). "Studies on slag deposit formation in pulverized coal combustors. 2. Results on the wetting and adhesion of synthetic ash drops on different steel substrates." Fuel **60**: 1065-1072.

Adams, M.J. and Perchard. V., (1985). "The cohesive forces between particles with interstitial liquid." I. Chem. E. Symposium Series **91**: 147-160.

Arstoopour, H. and Huang, C.S., (1988). "Fluidisation behaviour of particles under agglomeration conditions." Chemical Engineering Science **43**: 3063-3075.
Atlas, S. (1995). Slag Atlas.

Belyankin, D.S. and Lapin, V.V., (1954). Physico-chemical Systems of Silicate Technology. Moscow, Moscow: Promstroyizdat.

Benson, S.A. and Sondreal, E.A., (1995). "Status of coal ash behaviour research." Fuel Processing Technology **44**: 1-12.

Bhattacharya, P.S. (2000). "Private communication."

Bhattacharya, P.S. and Vuthaluru, H.B., (1997). Preliminary results from CFBC pilot plant trials at Osborne. CRC internal conference.

Bingham, E.C. and Green. H., (1920). "Paint, a plastic material and not a viscous liquid; the measurement of its mobility and yield value." Proc. Am. Soc. Test. Mat **20**(II): 640-675.

Bird, R.B., Stewart, E. W. and Lightfoot, S., (1960). Transport Phenomena, Wiely, New York.

Boow, J., (1965). "Viscosity / Temperature Characteristics of some Australian Coal-ash Slags in the Range 1100°C to 1600°C." Journal of The Institute of Fuel: 3-12.

Boow, J., (1969). "Measurement of the viscosity of supercooled slags at 750°C to 1000°C." Fuel **48**: 171-178.

Casson, W. (1959)., A flow equation for pigment-oil suspensions of the printing ink type. Rheology of disperse systems. C. C. Mill. London, Pergamon: 84-104.

Cheng, D. C. H. (1966). "Cone and plate viscometry: Explicit formulae for shear stress and shear rate and the determination of inelastic thixotropic properties." Brit. J. Appl. Phys **17**: 253-263.

Cheng, D. C. H. (1967). "Hysteresis loop experiments and the determination of thixotropic properties." Nature **216**: 1099-1100.

Cross, M. M. (1965). "Rheology of non-Newtonian fluids: a new flow equation for pseudoplastic systems." J. Collid Sci. **20**: 417-437.

Darby, R. (1985). "Couette viscometer data reduction for materials with a yield stress." J. of Rheology **29**: 369-378.

Dean, J. A. (1985). Lange's Handbook of Chemistry. New York, McGraw Hill.

Dietzel, A. and R. Bruckner (1955). "Calibration of an absolute viscometer for high temperature and the measurement of the viscosity of boric oxide." Glastech. Ber **28**: 455.

Durie, R. A. (1991). "The science of Victoria Brown Coal. Structure, Properties and Consequences for Utilisation." (Butterworth-Heinemann Ltd, UK,): 528.

Erickson, T. A., K. D. Ludlow, et al. (1992). "Fly ash development from sodium, sulphur and silica during coal combustion." Fuel **71**: 15 -18.

Falcone, S. (1989). Ash and slag characterisation. Proc. of 9th Annual Gasification and Gas Stream Clean Up System Contractor's Review Meeting, Morgantown, WV, USA.

Frenkel, J. (1945). "Viscous flow of crystalline bodies under the action of surface tension." Journal of Physics **IX**(5): 385-391.

Gibb, W. H. (1986). "The role of calcium in the slagging and fouling characteristics of bituminous coals." J. Institute of Energy **58-60**: 206-212.

Gibb, W. H. (1986). "The slagging and fouling characteristics of coals- I: Ash viscosity measurement for the determination of slagging propensity." Power Industry Res. **1**: 29-42.

Gluckman, M. J., J. Yerushalmi, et al. (1976). "Defluidisation characteristics of sticky or agglomerating beds." Fluidisation Technology (II): 395-422.

Groen, J. C., D. D. Brooker, et al. (1998). "Gasification slag rheology and crystallization in titanium-rich, iron-calcium-aluminosilicate glasses." Fuel Processing Technology **56**: 103-127.

Herschel, H. and R. Bulkley (1926). "Measurement of consistency as applied to rubber-benzene solutions." Proc. Am. Test. Mat. **26**(II): 621-633.

Hough, D. C., A. Sanyal, et al. (1986). "The development of an improved coal ash viscosity/temperature relationship for the assessment of slagging propensity in coal-fired boilers." J. Institute of Energy (June): 77-81.

Huffman, G. P., F. E. Huggins, et al. (1981). "Investigation of the high-temperature behaviour of coal ash in reducing and oxidizing atmospheres." Fuel **60**(July): 585-597.

Hupa, M., B. J. Skrifvars, et al. (1989). "Measuring the sintering tendency of ash by a laboratory method." J. Institute of Energy **September**: 131-137.

Hurst, J. H., F. F. Novak, et al. (1994). Prediction of the amount of calcium carbonate needed for successful slag tapping of some Australian coals in a slagging gasifier. 6th Australian Coal Science Conference, Newcastle.

Hurst, J. H., F. F. Novak, et al. (1999). "Viscosity measurements and empirical predictions for fluxed Australian bituminous coal ashes." Fuel **78**: 1831-1840.

Hurst, J. H., F. F. Novak, et al. (1994). "Viscosity measurements on melts from some NSW coal ashes". Tewnty Eighth Newcastle symposium.

Hurst, J. H., P. J. Patterson, et al. (2000). "Viscosity measurements and empirical predictions for some model gasified slags II." Fuel **79**: 1797-1799.

Jones, E. E. and S. J. Lindsey (1987). "Viscosity studies of the slags of Southern lignites." Minerals and Metallurgical Processing(February): 60-64.

Kalmanovitch, D. P., A. Sanyal, et al. (1986). "Slagging in boiler furnaces-prediction technique based on high-temperature phase equilibria." J. Institute of Energy **March**: 20-23.

Kang, S. W., A. F. Sarofim, et al. (1991). "Agglomeration formation during coal combustion: A mechanistic Model." Combustion and Flame **86**: 258-268.

Kosminski, A. (2000). Private Communication.

Krieger, I. M. and H. S. Maron (1952). "Direct determination of flow curves of non-Newtonian fluids." J. Applied Physics **23**: 147-149.

Krieger, W. D. and H. Elrod (1953). "Direct determination of the flow curves of non-Newtonian fluids. II. Shear rate in the concentric cylinder viscometer." J. Applied Physics **24**: 131-136.

Levin, E. M., R. C. Robbins, et al. (1979). Phase diagrams for ceramists.

Lindsay, J. (1993). Slagging investigations at Callide 'B' Power station. Combustion News.

Machin, J. S. and D. L. Hanna (1945). "Viscosity studies of system CaO-MgO-Al_2O_3-SiO_2." J. American Ceramic Society **28**(11): 310-316.

Macosko, C. (1994). Rheology Principles measurements and applications. New York, Wiley-VCH.

Manzoori, A. (1992). "The fate of organically bound inorganic elements and sodium chloride during fluidised bed combustion of high sodium high sulphur low rank coals." Fuels **71**(May): 513-522.

Manzoori, A. R. (1990). Role of the inorganic matter in agglomeration and defluidisation during CFBC of low-rank coals. Department of chemical engineering. Adelaide, Adelaide University.

Manzoori, A. R., T. M. Linjewille, et al. (1994). The effect of additives on agglomeration and defluidisation during FBC of low-rank coals. Melbourne, CRC- New Technologies for Power Generation from Low-Rank Coal.

Mason, D. M. and J. G. Patel (1992). "Chemistry of ash agglomeration in the U-Gas process." Fuel Processing Technology **30**: 215-226.

Metzner, A. B. and J. C. Reeds (1955). "Flow of non-Newtonian fluids correlation of the laminar, transient and turbulent-flow regions." A.I.Ch.E. J. **1**(4): 434-440.

Miah, S. A. and D. Q. Nguyen (1996). A review on the rheology and rheological measurement of molten coal ash. Adelaide, CRC. New Technologies for Power Generation from Low-Rank Coal**:** 1-45.

Mills, K. C. (1986). "Estimation of Physicochemical Properties of Coal Slags and Ashes." American Chemical Society: 195-214.

Mills, K. C. and J. M. Rhine (1989). "The measurement and estmation of the physical properties pf slags formed during coal gasification. I: Properties relevant to fluid flow." Fuel **68**: 193-200.

Moilanen, A., S. Kline, et al. (1991). "The effect of ash viscosity on the sintering of peat fly ash." J. Institute of Energy **64**: 21-25.
Moilanen, A., B. J. Skrifvars, et al. (1989). The effect of temperature, chemical composition and gas atmosphere on sintering of peat fly-ash. Proc. International Conference on coal science, Tokyo, Japan.

Montgomery, D. C. (1991). Desgin and analysis of experiments, 2nd, John Wiley & Sons.

Morrison, F. A. (2001). Understanding Rheology, Oxford University Press.

Nguyen, Q. D. (1983). Rheology of concentrated suspensions. Department of Chemical Engineering. Melbourne, Monash University.

Nguyen, Q. D. and D. V. Boger (1992). "Measuring the flow properties of yield stress fluids." Annual Review of Fluid Mechanics **24**: 47-88.

Nicholls, P. and W. T. Reid (1940). "Viscosity of coal ash slags." Transaction of the A.S.M.E.(February): 141-153.

Nowork, J. W., S. A. Benson, et al. (1993). "The effect of surface tension/viscosity ratio of melts on the sintering propensity of amorphous coal ash slags." Fuel **72**(7): 1055-1061.

Oh, M. S., D. D. Brooker, et al. (1993). "Effect of crystalline phase formation on coal slag viscosity." Fuel Processing Technology **44**: 191-199.

Oldroyd, J. G., D. J. Strawbridge, et al. (1951). A coaxial-cylinder elastoviscometer. Proc. Phys. Society.

Patterson, W. C. (1990). "The energy alternative: Changing the way the world works."

Raask, E. (1966). "Slag-coal interface phenomena." Trans of ASME **88-89**: 40-44.

Raask, E. (1985). Mineral Impurities in coal combustion; Behaviour problems and remedial measures, Hemisphere Publish Corporation, Washington.

Readett, D. J. and K. B. Quast (1985). South Australian Lignite- Lignite/Water System, S.A. Institute of technology, School of Mining and Metallurgy.

Reid, W. T. (1974). Corrosion and deposits in combustion systems. Combustion technology: Some Modern Developments. H. B. a. B. Palmer, J. M.: 35-59.

Reid, W. T. (1984). The relation of mineral composition to slagging fouling and erosion during and after combustion. Prog. Energy Combustion Science.

Reid, W. T. and P. Cohen (1944). "The flow characteristics of coal ash slags in the solidification range." Trans of ASME **66**: 685-690.

Robinson, H. A. and C. A. Peterson (1944). "Viscosity of recent container glass." The Journal of The American Ceramic Society **27**(May, 1): 129-138.

Sage, W. L. and J. B. McIlroy (1960). "Relationship of coal ash viscosity to chemical composition." Trans of ASME **82**: 148-155.

Schobert, H. H., R. C. Streeter, et al. (1985). "Flow properties of low-rank coal ash slag: Implications for slagging gasification." Fuel **64**: 1611-1617.

Schobert, H. H. and C. Witthoeft (1981). "The petrochemisty of coal ash slags. Part 3. Behaviour of the rosebud slag- Limestone system." Fuel Processing Technology **5**: 157-164.

Senior, C. L. and S. Srinivasachar (1995). "Viscosity of Ash Particles in Combustion Systems for Prediction of Particle Sticking." Energy & Fuels **9**: 277-283.

Sergeant, G. D., R. Leung, et al. (1994). "The effect of aging on the viscosity of bitumen produced from shale oil." Fuel Processing Technology **37**: 67-72.

Siegell, J. H. (1984). "High-Temperature defluidisation." Powder Technology **38**: 13-22.

Skrifvars, B. J., M. Hupa, et al. (1994). "Sintering mechanisms of FBC ashes." Fuel **73**: 171-176.
Skrifvars, B. J., M. Hupa, et al. (1992). "Sintering of ash during fluidised bed combustion." Ind. Eng. Chem. Res. **31**: 1026.

Souto, M. A., J. C. Rodriguex, et al. (1996). "Formation of solid deposits in the gas circuit of a pressurised fluidised-bed combustion plant." Fuel **75**: 675-680.

Standard, A. (1996). Coal and Coke- Sampling procedures. Australia, Standards Australia**:** 37-42.

Steenari, B. M., O. Lindqvist, et al. (1998). "Ash sintering and deposit formation in PFBC." Fuel 77(5): 407-417.

Steenari, B. M., S. Schelander, et al. (1999). "Chemical and leaching characteristics of ash from combustion of coal, peat and wood in a 12 MW CFB-a comparative study." Fuel **78**: 249-258.

Tardos, G., D. Mazzone, et al. (1985). "Destabilization of fluidised bed due to agglomeration Part II: Experimental Verification." Can. J. Chem. Eng **63**(June): 384-388.

Tiu, C. and D. V. Boger (1974). "Complete rheological characterisation of time-dependent food products" J. Text.Studies. 5, 329-338.

Tiu, C. (2000). "Private Communication."

Urbain, G., F. Cambier, et al. (1981). "Viscosity of silicate melts." Trans. J. Britsh. Ceram. Soc. **80**: 139-141.

Vaisburd, S. and D. G. Brandon (1997). "A combined unit for viscosity, surface tension and density measurements in oxide melts." Meas. Sci. Technol **8**: 822-826.

Van Wazer, J. R., J. W. Lyons, et al. (1963). Viscosity and flow measurement- A laboratory handbook of rheology. New York.

Vorres, K. S., S. Greenberg, et al. (1986). "Viscosity of synthetic coal ash slags." J. Am. Chem. Soc: 157-169.

Vuthaluru, B. H. (1999). "Remediation of ash problems in pulverised coal-fired boilers." Fuel **78**: 1789-1803.

Vuthaluru, B. H. (1999). Role of Ca and Mg During Fluidised-Bed Combustion of a South Australian Lignite. Adelaide, CRC Clean Power from lignite**:** 1-13.

Vuthaluru, B. H. and T. F. Wall (1998). "Ash formation and deposition from a Victorian brown coal-modelling and prevention." Fuel Processing Technology **53**: 215-233.

Vuthuluru, B. H. and D. K. Zhang (1997). Ash characteristics of low-rank coals during fluidised bed combustion. CRC Power Generation for New technologies from low-rank coal.

Wall, T. F. (1992). Mineral matter transformations and ash deposition in pulverised coal combustion. Twenty-fourth Symposium (International) on Combustion., The Combustion Institute.

Watt, J. D. (1969). "The flow properties of British coal ash: II The crystallising behaviour of the slags." J. Institute of Fuel **42**: 131-134.

Watt, J. D. and F. Fereday (1969). "The flow properties of slag formed the ashes of British coals: Part 1. Viscosity of homogeneous liquid slags in relation to slag composition." J. Institute of Fuel **March**: 99-103.

Watt, J. D. and F. Fereday (1969). "The flow properties of slags formed from the ashes of British coals: I Viscosity of homogeneous liquid slags in relation to slag composition." J. Institute of Fuel **42**: 99-103.

Weymann, H. D. (1962). "Colloid." **181**: 131.

Yan, H. (2000). "Private Communication."

Yang, T. M. T. and I. M. Krieger (1978). "Comparison of methods for calculating shear rate in coaxial viscometer." J. of Rheology **22**(4): 413-421.

Yoshimura, A. S. and R. K. Prud'homme (1988). "Wall slip correlations for couette and parallel disk viscometer." J. of Rheology **32**: 69-92.

Zhang, K. D., J. P. Jackson, et al. (1997). "Low-Rank Coal and Advanced Technologies for Power Generation." Engineering Foundation Conference, Hawaii.

Zhang, L. and S. Jahanshahi (1998). "Review and Modelling of Viscosity of Silicate Melts: Part I. Viscosity of Binary and ternary Silicates Containing CaO, MgO and MnO." Metallurgical and Materials Transactions B **29B**(February): 177-185.

Zhou, J. and Q. D. Nguyen (1998). Rheological characterisation of coal ash at high temperatures. Adelaide, CRC. New Technologies for Power Generation from Low-Rank Coals: 1-35.